The Role of Regulator of Calcineurin 1 (RCAN1) in the Adipose Tissue and Pancreatic β-cells

by

Pauline Yap

Thesis
Submitted to Flinders University
for the degree of

Master of Science by Research (MSc)

College of Medicine and Public Health

May 2020

DEDICATION

This thesis is dedicated in loving memory of both my late grandmothers Molly (1926-1999) and Rosy (1935-2010) both suffers of Type 2 diabetes. Thank you for your love. I am hopeful that a cure will be found one day to help others with Type 2 diabetes.

.

ABSTRACT

Obesity, characterised by excess fat, is a huge risk factor for both insulin resistance and Type 2 diabetes (T2D). Current treatments are only partially effective. Regulator of Calcineurin 1 (*RCAN1*), a gene on chromosome 21, is highly expressed in the brain, heart and metabolic tissues such as the adipose tissue and pancreatic β-cells. RCAN1 is an endogenous inhibitor of the protein phosphatase, calcineurin, in the calcineurin-NFAT pathway. Recently, it was shown that RCAN1 was a candidate driver of β-cell dysfunction in T2D (Peiris et al., 2012, Peiris et al., 2016) and was increased with obesity. *Rcan1*$^{-/-}$ mice on a high fat diet (HFD) exhibited a lean phenotype and had increase browning of white adipose tissue (WAT) (Rotter et al., 2018). However, it is unknown if other mechanisms, apart from thermogenesis, are responsible for this phenotype. The recent discovery of a novel suite of drugs that inhibits RCAN1 could be a potential therapeutic for obesity and T2D. This is possible if the drugs are successful in decreasing lipid storage in adipocytes, increasing proliferation and decreasing apoptosis in pancreatic β-cells.

Therefore, the aims of this research include determining the minimum concentration of five inhibitors of RCAN1-calcineurin association (IRCA) drugs that were not lethal to cells and are effective in reducing fat storage in adipocytes, increase proliferation and decrease apoptosis in β-cells. Additionally, to extend our understanding of mechanisms in the adipose tissue that could drive the anti-obesity effects in *Rcan1*$^{-/-}$ mice, we aimed to investigate gene expression changes associated with lipolysis, adipogenesis and lipogenesis in the WAT of *Rcan1*$^{-/-}$ mice compared to wild-type. To investigate possible factors that might induce RCAN1 expression, several factors were investigated in adipocytes.

The results of this study showed an increase in fat storage in adipocytes, instead of a reduction, when the effective minimum concentration of IRCA drugs were determined. This was observed only in more diluted concentrations of the IRCA drugs used, suggesting possible off-target effects not specific to RCAN1-calcineruin interaction. The effective minimum concentration of IRCA drugs on β-cells were determined and their effects on proliferation and apoptosis-associated gene expression were tested. Whilst no expression changes were found, a significant increase in real-time proliferation was found when IRCA1 was used to treat β-cells compared to control. Furthermore, there were gene expression changes associated with lipolysis, lipogenesis and adipogenesis in WAT from *Rcan1*$^{-/-}$ mice and WT mice fed a low-fat diet (LFD) and a HFD. These novel pieces of data add to our understanding of the lack of HFD-induced obesity phenotype seen in our *Rcan1*$^{-/-}$ mice in a recent publication (Rotter et al., 2018). Moreover, the use of several factors significantly increased gene expression of RCAN1 isoforms, *Rcan1.1* and *Rcan1.4*, in adipocytes. Overall, the findings of this research provide exciting and new insights into possible mechanisms involved in *Rcan1*$^{-/-}$ mice adipocyte function. We have also identified

a potential new therapeutic that increases the proliferation in β-cells and we now have a broad overview of factors that could upregulate or downregulate RCAN1 gene expression in adipocytes.

TABLE OF CONTENTS

LIST OF FIGURES

LIST OF TABLES

COMMONLY USED ABBREVIATIONS

μM	Micromole
3T3-L1	Adipocyte cell line
5-HT	5-hydroxytryptamine
AC	Adenylate cyclase
ACC1	Acetyl-CoA carboxylase 1
ACC2	Acetyl-CoA carboxylase 2
ACL	ATP-citrate lyase
AD	Alzheimer's disease
ATGL	Adipose triglyceride lipase
β-TC6	Beta-TC6 cell line
Ca^{2+}	Calcium
cAMP	Cyclic adenosine monophosphate
C/EBPα	CCAAT/enhancer-binding protein alpha
CGI-58	Comparative gene identification 58
ChIP	Chromatin immunoprecipitation assay
ChREBP	Glucose-responsive transcription factor
CI	Cell index
CN	Calcineurin
CsA	Cyclosporin A
CREB	cAMP-response element binding
DNL	*de novo* lipogenesis
DS	Down Syndrome
eWAT	Epididymal white adipose tissue
FAS	Fatty acid synthase
Fsk	Forskolin
FK506	Tacrolimus

G0s2	G0/G1 switch gene 2
H_2O_2	Hydrogen Peroxide
HFD	High fat diet
HSL	Hormone sensitive lipase
IL6	Interleukin 6
IRCA	RCAN1-calcineurin association
KH7	2-(1H-benzimidazol-2-ylthio)-2-[(5-bromo-2 hydroxyphenyl)methylene]hydrazide,propanoic acid
K_i	Inhibition constant
LFD	Low fat Diet
NFAT	Nuclear factor of activated T-cells
PGC1-α	Peroxisome proliferator-activated receptor gamma Coactivator -1 alpha
PKA	Protein kinase A
PLIN1	Perilipin 1
Pparg	Peroxisome proliferator-activated receptor gamma
RCAN1	Regulator of Calcineurin 1
RCAN1.1	Isoform 1 of Regulator of Calcineurin 1
RCAN1.4	Isoform 4 of Regulator of Calcineurin 1
sAC	soluble Adenylyl Cyclase
SREBP-1	Sterol regulatory element binding transcription factor 1
sWAT	Subcutaneous white adipose tissue
T2D	Type 2 Diabetes
TNFα	Tumour Necrosis Factor alpha
UCP-1	uncoupling protein-1

DECLARATION

I certify that this thesis does not incorporate without acknowledgment any material previously submitted for a degree or diploma in any university; and that to the best of my knowledge and belief it does not contain any material previously published or written by another person except where due reference is made in the text.

Pauline Yap

13th May 2020

ACKNOWLEDGEMENTS

Professor Damien Keating My supervisor thank you for your guidance and supervisorship. Thank you for building resilience, perseverance and tenacity in me – essential qualities required to succeed in the uphill learning journey in research and in life. Thank you for setting high standards and for expecting nothing but the best. Your drive for excellence is both exemplary and admirable. Thank you for the opportunity to embark on this Masters project.

Dr Darling Rojas-Canales My co-supervisor thank you for your expertise in islet isolation surgery technique and for your invaluable advice. Thank you for being a great listening ear, for helping me prepare for my talks and for looking at my drafts. Thank you especially for positive words of encouragement during difficult days.

Dr Claire Jessup My co-supervisor thank you for teaching cell culture techniques to me and for looking through cell counting troubleshooting in the early days.

My Colleagues (*past and present*) Thank you for your help big and small.

Father, Mother, Phoebe and Petrina My family thank you for your love, care, prayers and support in so many ways especially on difficult days. I could not have made it this far without you.

My Church community and friends at TYW My second family, thank you for sharing life with me, for your friendship, prayers, love and support.

Jennifer, Joyce, Phoebe, Esther, Sharon, Krystle, Suetyen and Michelle My dearest friends, thank you for your heart-felt friendship and prayers.

My heavenly Father Soli Deo Gloria! Thank You for Your grace, Your love and for carrying me through the hardest days, for being the Prince of peace, my saviour and my Lord.

The Australian Government Thank you for providing the Australian Government Research Training Program Scholarship which enabled fees offset that was helpful in helping me undertake this Masters degree.

Chapter 1. INTRODUCTION

1.1 General Introduction

Diabetes, defined by hyperglyemia (Bouret et al., 2015) due to partial or full decline in β-cell mass and insulin insufficiency (Heit, 2007, American Diabetes, 2010), is a multifactorial and severe metabolic disorder projected to be the 7th leading cause for death globally by 2030 (World Health Organisation, 2016). Comorbidities associated with diabetes also contribute to increasing health and healthcare cost. There are several types of diabetes (Table 1.1). An estimated 1 million Australians have clinical diabetes and 3 million are expected to have diabetes by 2025. In Australia, the annual cost estimates to be 14.6 billion and Type 2 diabetes (T2D) constitutes 90% of all types (Diabetes Australia, 2015).

Table 1.1 Diabetes types (Diabetes Australia, 2015)

Types	Information
Type 1 (T1D)	• 5% incidence • Immune destruction of β-cells
Type 2 (T2D)	• 90% incidence • Typically late onset • Increasingly developing in children • Obesity (↑ fat mass) is a risk factor
Other types	• Gestational diabetes mellitus (GDM) • Monogenic diabetes e.g. Maturity onset diabetes of the young (MODY) • Pharmacologically-induced diabetes • Neonatal diabetes mellitus (NDM) - temporary/ permanent

Type 1 diabetes (T1D), immune-mediated diabetes, account for approximately 5% of all cases. T1D usually occurs in children and arises from the autoimmune destruction of β-cells in the pancreas due to CD4+ and CD8+ T cells and macrophages targeting β-cell antigens leading to insulin secretion deficiency and hypoinsulinemia (Gillespie, 2006). It is currently held that both T1D and T2D have underlying genetic predisposition outlining its etiology (Dotta et al., 2005, Peiris et al., 2016).

Globally, T2D a poorly understood disease, is constantly on the rise and driven by increased rates of obesity, which often occurs together (Bouret et al., 2015, World Health Organisation, 2016). The pathology of T2D will be discussed in further sections. Obesity, a global epidemic (Gesta et al., 2007), is a chronic condition that affects all age groups and is associated with mortality and morbidity, decreasing life expectancy by 6-20 years (Bouret et al., 2015). Old age, obesogenic side-effects of drugs, disease (e.g. hypothyroidism), increased food consumption, lifestyle and genetic predisposition (Caterson and Gill, 2002) can result in obesity. Body mass index (BMI), an anthropometrical standard measure of overweight and obesity (National Insitutes of Health, 1998, World Health Organisation,

2000), is weight in kilograms divided by height in meters squared (Deurenberg et al., 1991). Obesity is determined by a high BMI of ≥30kg/m^2 (Bouret et al., 2015). Having excess body fat is associated with cardiac and metabolic conditions and peripheral insulin resistance (Despres, 1993) – all hallmarks of T2D and its complications. This risk is heightened with an increased distribution of visceral fat (Gesta et al., 2007). The dysregulation of energy metabolism is central to both obesity and T2D. Therapies for obesity-associated T2D must ameliorate its pathophysiology, however, no cure has been found to treat both. Current treatments are successful to a certain degree, however, off-target effects prevail. Exploring both long-lasting drugs and genes responsible for β-cell dysfunction in T2D are essential in furthering our understanding of the pathophysiology of obesity-related T2D.

1.2 Physiological Glucose Homeostasis

Essential for survival, glucose concentrations in the blood are tightly regulated within a narrow range to maintain glucose homeostasis as blood glucose fluctuate in states of fasting and after consumption of food (Czech, 2017). Key tissues in glucose homeostasis are the liver, adipose tissue, skeletal muscle (Carnagarin et al., 2015), brain and pancreas (Roder et al., 2016). Nutrients are regulated and metabolised according to the requisite needs of individual tissues, achieving a balance between regulatory (insulin) and counter-regulatory (glucagon) hormones secreted by the pancreas regulating fuel storage and mobilization (Nolan et al., 2011) (Figure 1.1). In healthy adults, normoglycemia is maintained at a range of 80 to 100mg (Geva et al., 2019) and fluctuates after a meal and in-between meals. Figure 1.1 summarises glucose homeostasis in the body. In particular, hyperglycemia (high blood glucose) occurring in T2D, involves the dysregulation of glucose homeostasis due to insulin resistance in metabolic tissues (Samuel and Shulman, 2012). Overall, obesity, insulin resistance and T2D contributes to the dysregulation of glucose homeostasis and metabolism observed in obese-induced T2D patients (Bouret et al., 2015). These will be discussed in further sections of this introduction.

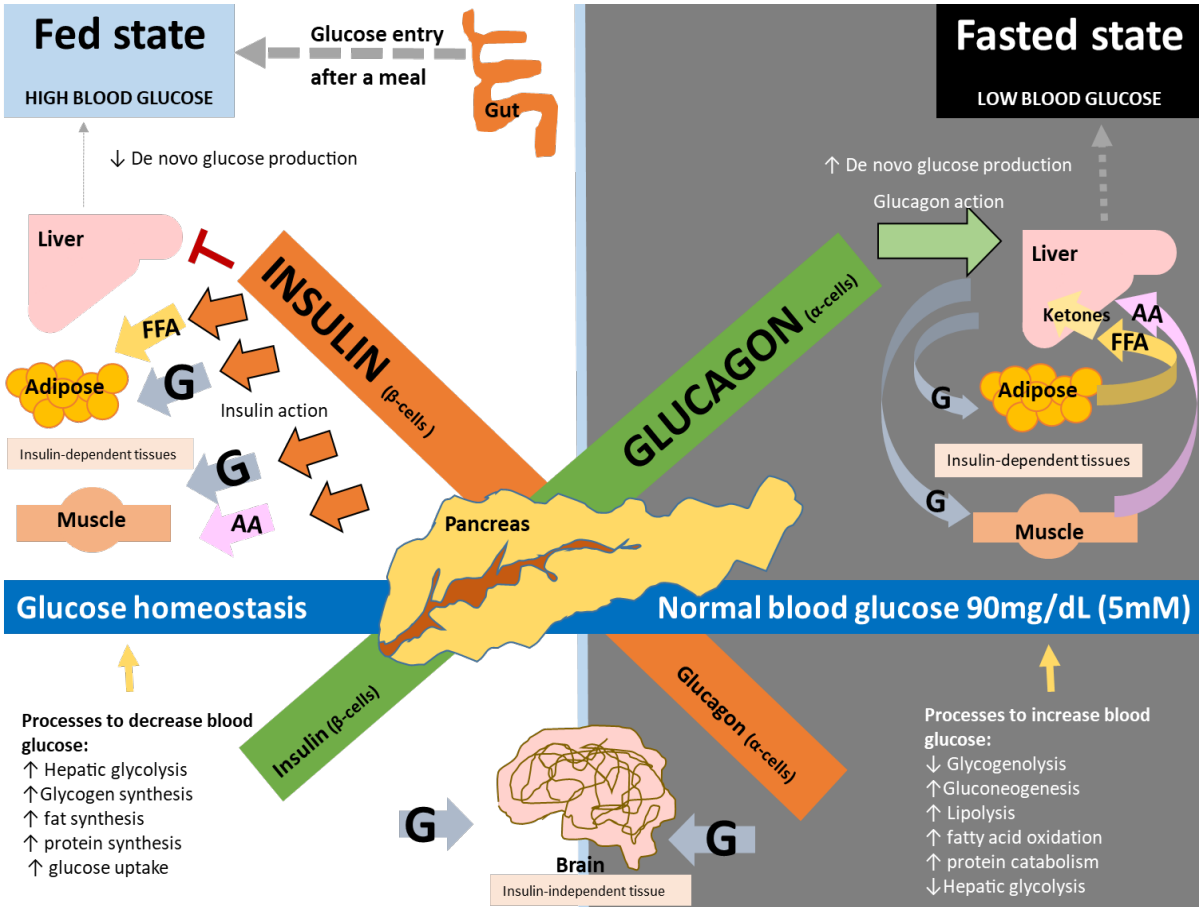

Figure 1.1 Glucose homeostasis by actions of various organs and maintained differently in fasting and fed states. *'G' indicates glucose, 'FFA' indicates free fatty acids and 'AA' indicates amino acids. Arrows of different sizes indicate amount of glucose received*. In the fasted state, the predominant hormone is glucagon (secreted by α-cells) that acts on the liver. Hepatic glycogenolysis and gluconeogenesis produces endogenous glucose (Czech, 2017). Some of this glucose is delivered to insulin-dependent tissues (e.g. muscle and adipose tissues) for self-utilisation and these tissues will undergo protein catabolism and fatty acid oxidation (Dean, 2004). In the fed state, the predominant hormone is insulin (secreted by β-cells) that inhibit the actions of glucagon. Pancreatic β-cells are able to detect changes in the blood glucose (Sharabi et al., 2015). Insulin acts on the liver to inhibit *de novo* glucose production to achieve glucose homeostasis. This glucose is also transported to the brain for utilisation and to adipose tissue and muscle for storage (Nolan et al., 2011).

1.3 Pancreas

The pancreas is a key organ in managing metabolism and glucose homeostasis throughout the body. The pancreas functions as an exocrine organ (secreting pancreatic juices and digestive enzymes into the duodenum) (Husain and Thrower, 2009) and as an endocrine organ (producing insulin, glucagon, and somatostatin) within different cell types in the islets of Langerhans (Jouvet and Estall, 2017) (Figure 1.2). Within the islets of Langerhans, pancreatic β-cells make up the majority of islet cells (65-80%). These β-cells, the only source of endogenous insulin in the body (Bouret et al., 2015), releases insulin in response to high blood glucose as part of the glucose homeostatic mechanism. Insulin is released through the process of glucose-stimulated insulin secretion (GSIS) (Herman and Kahn, 2006), discussed in the next section.

Image removed due to copyright restriction.

Figure 1.2 Anatomy of a human pancreas (Roder et al., 2016). Islet cells include the α-cells (secretes glucagon), δ-cells (secretes somatostatin), γ-pancreatic polypeptide-cells (produce pancreatic polypeptide to auto-regulate endocrine and gastrointestinal secretion, ε-cells (that produces ghrelin) and the pancreatic β-cells (secretes insulin) (Bouret et al., 2015).

1.3.1 Insulin and Glucose-Stimulated Insulin Secretion (GSIS)

The *insulin* gene encodes pre-proinsulin, a precursor of insulin, synthesized by the ribosomes of the rough endoplasmic reticulum (rER). Pre-proinsulin undergoes a sorting process in the rER and the Trans-Golgi Network (Halban, 1991), necessary to enable formation of dense-core secretory granules upon glucose stimulation (Hou et al., 2009). Insulin activates protein and lipid synthesis and storage of glucose as glycogen in the liver and the muscle (Michael et al., 2000). In the adipose tissue, insulin also induces fatty acid storage (Sharabi et al., 2015). Insulin also has roles in the central nervous system, impacting food intake and satiety by regulation gut hormones such as leptin (Banks et al., 1997).

Circulating insulin binds to heterotetrameric insulin receptors located on cell membranes of target tissues (e.g. liver, muscle and adipose cells) to store or to take up glucose (Jouvet and Estall, 2017). The insulin receptors are made up of two extracellular α-subunits, forming the insulin-binding site and linked to two β-subunits via disulfide bonds (De Meyts, 2004). The binding of insulin brings about a conformational change in receptor α-subunits, allowing for the entry of ATP that binds to β-subunits, auto-phosphorylating the receptor and inducing a cascade of intracellular phosphorylation. The insulin-receptor substrate (IRS) 1 and 2 are phosphorylated and downstream phosphorylation with intracellular molecules eventually results in an increase in glycogen, lipid and protein synthesis and the translocation of the GLUT2, the sole glucose transporter in β-cells (Sharabi et al., 2015), to the plasma membrane (Shepherd and Kahn, 1999, Youngren, 2007).

Insulin secretion is regulated by exocytosis in β-cells. Synaptic proteins such as soluble N-ethylmaleimide-sensitive fusion (NSF) protein and the attachment protein of NSF, communicates with the membrane bound receptor SNARE proteins, essential in the regulation of exocytosis of insulin and the fusion of synaptic vesicles with the plasma membrane prior to the release of insulin from vesicles (Wheeler et al., 1996). Synaptobrevin and pre-synaptic plasma membrane proteins, namely synaptosome-associated protein 25 (SNAP-25) and syntaxin (Sudhof, 1995), are SNARE proteins essential for granule fusion and acts to couple Ca^{2+} channels to secretory granules (Meldolesi and Chieregatti, 2004), exposing a subset of release-competent granules (readily releasable pool; RRP) in response to high Ca^{2+} levels (Rorsman et al., 2000). The process of GSIS is summarised in Figure 1.3. Insulin exocytosis of insulin granules from islet β-cells are tightly regulated to maintain glucose homeostasis and is stimulated in the presence of the rise in ATP, due to ATP synthesis by mitochondrial oxidative phosphorylation, in the cytoplasm (Koster et al., 2005) (Figure 1.3 ❷). The entry of divalent cation calcium (Ca^{2+}) acutely increase intracellularly and triggers exocytosis in β-cells through full vesicle fusion or "kiss and run" partial fusion pore (Rorsman and Renstrom, 2003) (Figure 1.3 ❻, ❼). Short-term induction (seconds to minutes) of Ca^{2+} is essential for normal function such as cytoprotection, proliferation, insulin synthesis and secretion. However, long-term induction of Ca^{2+}

signalling increases ER stress, apoptosis and affects differentiation in β-cells, resulting in loss of β-cells as observed in T2D (Sabatini et al., 2018).

Image removed due to copyright restriction.

Figure 1.3 Pancreatic β-cell glucose uptake and insulin release. Image adapted from (Lowell and Shulman, 2005). Increase in blood glucose increases glycolysis (❶) to metabolise glucose in pancreatic β-cells. This increases intracellular ATP to ADP ratio (❷) which sends a metabolic signal that closes the K_{ATP} channels (❸) inducing a membrane depolarization (❹), activating voltage-gated Ca^{2+} channels (VDCC) (❺), allowing Ca^{2+} influx (❻) that signals for insulin exocytosis (❼) thereby releasing insulin (Koster et al., 2005).

1.4 Adipose tissue

1.4.1 Adipose tissue structure and function

The adipose tissue functions to provide protection to internal organs and thermal regulation. The adipose tissue, the largest energy store in the body (Ramsay, 1996, Jensen, 1997), also functions as an endocrine organ and is a key player in whole body energy and glucose homeostasis that directly and indirectly modulates appetite, insulin sensitivity and immunological responses (Spiegelman and Flier, 2001). The adipose tissue consist of two main types; white adipose tissue (WAT) and brown adipose tissue (BAT) (Oikonomou and Antoniades, 2019) (Figure 1.4). Adipocytes, arise from mesenchymal and mesodermal stem cell origin (Gesta et al., 2007). WAT is the most abundant fat form and functions both as an energy store of triacylglycerol and as an endocrine organ that secrete hormones and adipokines. In contrast, brown adipose tissue (BAT), dense with mitochondria, functions to dissipate heat during thermogenesis (Gesta et al., 2007) by utilising and taking up fatty acids and glucose (Bartelt et al., 2011, Rosell et al., 2014). BAT contains the uncoupling protein 1 (UCP1) in the mitochondrial membrane that uncouples energy to produce heat rather than ATP (Cannon and Nedergaard, 2004), disrupting the movement of proton gradient across the inner mitochondrial membrane (Rosen and Spiegelman, 2006). Recently, a third fat type has been discovered: beige adipocytes that arises from multi-locular WAT adipocytes that are different from BAT. These beige adipocytes have decreased UCP1 levels compared to BAT but can induce UCP1 expression and has the ability to expand oxygen usage (Chakkera et al., 2017) which could impact thermogenesis and metabolic regulation.

Image removed due to copyright restriction.

Figure 1.4 Visualisation of all fat depots in mice (de Jong et al., 2015). Fat depots include both subcutaneous depots (anterior and posterior) and visceral depots (perineal, perigonadal, mediastinal, retroperitoneal and mesenteric) (Fantuzzi and Mazzone, 2014). WAT is present in subcutaneous skin around abdominal areas, while BAT is found subcutaneously in inter-scapular, cervical, paravertebral and axillar areas (Rosen and Spiegelman, 2006, Rosell et al., 2014).

Adipocytes, fibrous connective cells of the adipose tissue, are responsible for long-term triglyceride storage. Adipocytes are 25-200μm in diameter (Trujillo and Scherer, 2006, Fruhbeck et al., 2001), depending on how much triglyceride is stored (Spiegelman and Flier, 1996). Approximately half of the content in adipose tissue is made up of other cells such as endothelial cells, fibroblasts, macrophages and the other half contains mature adipocytes (Trujillo and Scherer, 2006, Trayhurn, 2007). The lipid droplet, a 0.1-100μm organelle, makes up majority of the cell body of a mature adipocyte, functions to store triglycerides and plays a role in lipid metabolism. In the central part of the lipid droplet are the lipid esters (Fujimoto and Parton, 2011) used for several processes such as β-oxidation and lipoprotein synthesis (Brasaemle, 2007). Perilipin, a structural protein unique to adipocytes, covers the lipid droplet (Daval et al., 2006) and its function is discussed in further sections of this thesis. Additionally, adipocytes perform an array of functions such as secreting adipokines, lipids, fatty acids (Fruhbeck et al., 2001) and hormones that have a role in immunity, blood pressure, regulation of nutrient uptake, sensitivity to insulin and inflammation. Therefore, adipocytes play a crucial role in the development of obesity-related comorbidities such as insulin resistance and T2D.

1.4.2 Adipose tissue: development and metabolism

Adipose tissue has roles in glucose homeostasis (Figure 1.1). The amount of lipid present depends on processes such as lipoprotein lipase (LPL) hydrolysis, fatty acid uptake, lipid synthesis and esterification (Trujillo and Scherer, 2006). During excess caloric availability, mature adipocytes function to store triacylglycerol for future energy use. As a whole, the adipose tissue mass is balanced by lipolysis, lipogenesis and adipogenesis, regulated by hormones, cytokines and factors related to fuel metabolism (Ramsay, 1996). Gene expression changes related to these pathways will be explored in Chapter 5.

1.4.2.1 Adipocyte cell line

The well-studied (Sarjeant and Stephens, 2012) 3T3-L1 adipocyte cell line is derived from clonal expansion of Swiss mouse embryos 17 to 19 days old (Green and Meuth, 1974, Green and Kehinde, 1976). When confluence is reached, pre-adipocytes transform into adipocytes with accumulation of lipid droplets (Ailhaud et al., 1989). These differentiated adipocytes are morphologically (Novikoff et al., 1980) and biochemically (MacDougald and Lane, 1995) similar to *in situ* adipocytes (Sarjeant and Stephens, 2012) (Figure 1.5), serving as an excellent *in vitro* model for the study of adipocytes in glucose metabolism (Vishwanath et al., 2013).

The 3T3-L1 cell lines require glucocorticoid-supplemented differentiation cocktail to induce adipogenesis and terminal differentiation (Rubin et al., 1978). The differentiation media includes insulin, 3-isobutyl-1-methylxanthine (IBMX), dexamethasone (Dex) and biotin (Rubin et al., 1978). Insulin modules the differentiation process by increasing lipogenesis, stimulating the uptake of glucose, inducing triglyceride synthesis and lipid accumulation thereby promoting the expression of the adipocyte phenotype (Green and Meuth, 1974, Russell and Ho, 1976, Ailhaud et al., 1989). The synthetic glucocorticoid agonist, dexamethasone, aid pre-adipocytes to become mature adipocytes through first activating the expression of transcription factor, such as the CCAAT-enhancer-binding protein (C/EBP)δ protein, and activating the synthesis of chondroitin sulphate proteoglycans (Boone et al., 2000, Cornelius et al., 1994). IBMX, a competitive non-specific phosphodiesterase inhibitor, together with dexamethasone, controls PPARγ activity that induces C/EBPδ and C/EBPβ transcription factors in adipogenesis and differentiation. IBMX increases intracellular cyclic AMP (cAMP) and protein kinase A (PKA) involved in adipogenesis (Pantoja et al., 2008). This is explained in greater detail in Chapter 5 of this thesis. Biotin is added as biotin-dependent enzymes, acetyl-CoA carboxylase (Mackall et al., 1976) and pyruvate carboxylase, are involved in fatty acid synthesis and replenishing of mitochondrial oxaloacetate. High amounts of NADPH are needed for lipogenesis (Mackall and Lane, 1977). Without biotin, fatty acid synthesis (lipogenesis) cannot occur (Kuri-Harcuch et al., 1978).

1.4.2.2 Adipogenesis

Adipogenesis is a bi-phasic process where fibroblast-like pre-adipocytes, precursor stem cells form fibrillar structures, transform into a laminar morphology as the cell move towards being a fully developed triglyceride-containing adipocyte (Mariman and Wang, 2010). During this process, pre-adipocyte change functionally and have increased insulin sensitivity and cell secretion capacity (Lefterova and Lazar, 2009). Surplus fat can be deposited into the adipose tissues via adipogenesis (Mariman and Wang, 2010, Kim and Nam, 2017, Moseti et al., 2016). A fully matured adipocyte is indicated by the presence of peroxisome proliferator-activated receptors 2 (PPARγ2), glucose transporter type 4 (GLUT4) and fatty acid synthase (FAS) (Rosen and MacDougald, 2006).

Early regulators of adipogenesis and adipocyte differentiation include the transcriptional factors peroxisome proliferator-activated receptor gamma (PPARγ), CCAAT/enhancer-binding proteins (C/EBP)α, β and δ and sterol regulatory element binding protein (SREBP)-1 (Spiegelman and Flier, 1996, Fajas et al., 1999, Kim et al., 1998, Farmer, 2006). Other regulators of mature adipocyte synthesis include fatty acid-binding protein 4 (FABP4), adiponectin and fatty acid synthase (Kim et al., 1998). PPARγ, nuclear receptors mainly found in adipocytes, are essential in adipogenesis (Rosen et al., 2002) and maintenance of mature adipocytes (Imai et al., 2004). The adipose- specific deletion of PPARγ in mice decreased size of WAT and caused abnormalities in WAT function (Jones et al., 2005).

In the fibroblast state, PPARγ receptor stimulation induces differentiation, induces expression of genes specific to adipose tissue, morphological alterations and increase in lipid density. PPARγ, the proximal effector of adipogenesis, is essential and sufficient for adipogenesis (Rosen et al., 2000). During adipogenesis, C/EBPβ and δ are responsible for the expression of C/EBPα (Cao et al., 1991). C/EBPβ and C/EBPδ induces PPARγ expression in the early stages of differentiation, while C/EBPα maintains PPARγ expression in later stages of differentiation (Farmer, 2006). Moreover, co-activators such as PPAR-γ-coactivator-1α (PGC-1α), a co-activator of PPARγ and other factors, are also part of the differentiation process (Farmer, 2006). Mature adipocytes are terminally differentiated, are filled with lipids as triacylglycerol synthesis increases, are also able to sense insulin and secrete various adipokines (Shen et al., 2011) (Figure 1.5). The steps for the transformation of 3T3-L1 cells from fibroblast to fully differentiated adipocytes is summarised in Figure 1.5.

Image removed due to copyright restriction.

Figure 1.5 Adipocyte differentiation from fibroblast to pre-adipocytes. Image adapted from (Cowherd et al., 1999, Boone et al., 2000). There are four stages for the transformation of pre-adipocytes into fully mature adipocytes: 1 – pre-confluent proliferation, 2 –confluence-induced growth arrest due to contact inhibition, 3 – growth factors induce clonal expansion and 4 – terminal differentiation and final growth arrest where lipids are loaded (Cowherd et al., 1999). Stage four is controlled by the PPAR family and C/EBP family members, both master regulators of adipogenesis (Farmer, 2006).

1.4.2.3 Lipogenesis

Lipogenesis is the synthesis of fat, including the synthesis of fatty acids and triglycerides within the adipocytes and hepatocytes from either the diet or *de novo* synthesis from non-lipid substrates (Kersten, 2001, Daval et al., 2006). In the fed state, lipogenesis is activated through insulin action on the adipose and liver tissues. Both the sterol regulatory element-binding protein 1 (SREBP1) and carbohydrate-responsive element binding protein (ChREBP) are transcription factors that regulate the expression of *de novo* lipogenesis (DNL) genes and associated enzymes (Brown and Goldstein, 1997, Ruiz et al., 2014). The process of DNL is described in Figure 1.6 and is reviewed extensively (Lafontan, 2009, Chouchani and Kajimura, 2019).

The SREBP1 family controls the expression of enzymes required for endogenous cholesterol, fatty acid, triacylglycerol and phospholipid synthesis (Eberle et al., 2004). SREBP-1a and SREBP-1c are isoforms of SREBP family, alternate splice variants of the *Srebf1* gene. In the absence of sterols, SREBPs release the amino-terminal containing a basic helix-loop-helix leucine zipper domain through site specific proteases and SREBPs translocate into the nucleus to bind to specific sterol response elements in the promoters of target genes (Brown and Goldstein, 1997, Horton et al., 2002). In particular, SREBP-1c activates fatty acid and cholesterol synthesis by binding to sterol regulatory element (SRE) in promoters of lipogenic genes, fatty acid synthase (*FAS*) and ATP-citrate lyase (*ACL*) (Amemiya-Kudo et al., 2002, Shao and Espenshade, 2012). While SREBP-1a has roles in increasing gene expression of acetyl-CoA (ACC), FAS and ACL, components of the lipogenesis pathway (Edwards et al., 2000, Shimano, 2009). These enzymes are present in the cytosol. The alternate isoform of ACC1 enzyme is ACC-beta (ACC2) that is localized to the mitochondrial membrane to limit β-oxidation through malonyl-CoA mediated inhibition of carnitine palmitoyl transferase I (CPT1) which catalyses the transfer of long-chain fatty acyl-CoA into the mitochondrion (Wakil and Abu-Elheiga, 2009).

ChREBP is a glucose responsive transcription factor that upregulate genes responsible for fatty acid synthesis and glycolysis involved in DNL in the adipose tissue (Uyeda et al., 2002, Iizuka et al., 2004). ChREBP binds to the carbohydrate response element (ChoRE) in the promoter regions of transcriptional targets FAS and ACC1 (Towle et al., 1997, Herman et al., 2012). ChREBP is a key determinant of systemic insulin sensitivity and glucose homeostasis. GLUT 4-mediated glucose uptake induces ChREBP which activates DNL in the adipose tissue (Herman et al., 2012). ChREBP-alpha (ChREBP-α) in combination with max-like protein X (MIx) are bound to the carbohydrate response elements in promoters of target genes such as ACL, ACC1, FAS, stearoyl-CoA desaturase-1 (SCD1) and ChREBP-beta (ChREBP-β). Once activated, ChREBP-β activates target genes that synthesises fatty acids (Iizuka, 2013, Song et al., 2018). The function of ACL, ACC1 and FAS are summarised in Figure 1.6 and we will be looking at the gene expression of these lipogenic enzymes in Chapter 5.

Image removed due to copyright restriction.

Figure 1.6 Adipose tissue *de novo* lipogenesis. Diagram adapted from (Song et al., 2018). Glucose first enters the adipocyte via GLUT4 and undergoes glycolysis, generating citrate at the end of the Krebs cycle. In the adipocyte, DNL involves glucose uptake that converts glucose-derived citrate to acetyl-CoA by ACL. Acetyl-CoA is converted to malonyl-CoA, a long-chain fatty acid, by ACC-alpha (ACC1) enzyme (Sullivan et al., 1994). Malonyl-CoA is converted to palmitate by fatty acid synthase (FAS) (Kim et al., 1998, Edwards et al., 2000, Shimano, 2009, Tang et al., 2016). Stearoyl-CoA desaturase (SCD1) converts palmitate into fatty acids. The glucose metabolites from glycolysis induces ChREBP-α activity that joins Mlx to ChORE in the promoter of ACL, ACC1 and FAS, SCD1 and ChREBP-β genes. Shown in the diagram, a HFD inhibits DNL by supressing the activation of ChREBP-β (Song et al., 2018).

1.4.2.4 Lipolysis

Triacylglycerols are the main components of intracellular energy stores in lipid droplets (Kulminskaya and Oberer, 2019). In states of fasting, glucose is low, lipogenesis is perturbed causing reduced triglycerides in white adipose tissue. Lipolysis and glycolysis are activated with the actions of glucagon (Figure 1.1). Glycolysis first breaks glucose down into acetyl-CoA for fatty acid synthesis. Lipolysis is the process where triglycerides are secreted from their lipid droplet storage in adipocytes (Trujillo and Scherer, 2006) and hydrolysed into fatty acids and glycerol that goes into the blood circulation, ensuring that sufficient FFA is maintained to accommodate lipid energy requirements during times of fasting (Jensen, 1997). Lipid droplets within adipocytes function to store and regulate lipolysis of neutral lipids (Greenberg et al., 2011). Lipolysis occurs as both basal and stimulated lipolysis and several enzymes are involved (Duncan et al., 2007) (Figure 1.7). These enzymes were studied during stimulated lipolysis where their function is best demonstrated. Lipolysis can be stimulated by various stimuli such as catecholamines (Langin, 2006).

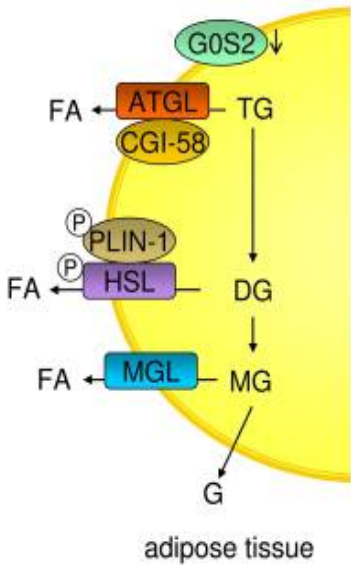

Abbreviations:

Perilipin 1 (PLIN1)

Comparative gene identification-58 (CGI- 58)

Adipose triglyceride lipase (ATGL)

Hormone sensitive lipase (HSL)

Monoglyceride lipase (MGL)

G(0)/G(1) switch gene 2 (G0S2)

Non-esterified fatty acids (NEFA)

Triacylglycerol (TG)

Diacylglycerol (DG)

Monoacylglycerol (MG)

Fatty acid (FA)

Glycerol (G)

Figure 1.7 Lipolysis in adipocyte. Image adapted from (Zechner et al., 2012). PLIN1 functions as a protective barrier that restricts access of TG lipases (ATGL and HSL) to stored TG (in the fed state) and stabilizes lipid droplets (Brasaemle, 2007, Hansen et al., 2017). ATGL is a rate-limiting enzyme for TG hydrolysis in adipocytes, cleaving TG to DG, releasing fatty acids (FA). CGI-58 acts as a co-activator of ATGL (Lass et al., 2006) while G0S2 attenuates ATGL action by selectively inhibiting TG hydrolase activity even in the presence of CGI-58 (Yang et al., 2010). HSL, a cytosolic lipase, mobilises free fatty acids (FFA) from the adipose tissue (Sullivan et al., 1994) by converting DG to MG, releasing FA. Finally, monoacylglycerol lipase (MGL) converts monoglycerol (MG) to glycerol (G).

Once lipolysis occurs, fatty acids in the blood is oxidised to fulfil the fuel requisite of other tissues or re-esterify fatty acids in the adipocyte (Ramsay, 1996). Lipolysis is controlled by the balance of lipolytic, anti-lipolytic hormones and biochemical signals. Inducers of lipolysis includes catecholamines, a pro-lipolytic hormone, binding to β-adrenergic receptors (β1, β2, β3) coupled to G stimulatory proteins that causes an elevated adenylate cyclase (AC) activity. Adenosine triphosphate (ATP) is converted by adenylyl cyclase to cAMP, activating the cAMP-dependent protein kinase A (PKA) pathway (Jaworski et al., 2007). The cAMP/PKA pathway is described in Chapter 6. PKA, a serine/threonine kinase, is involved in phosphorylating and activating lipolysis proteins such as PLIN1(Miyoshi et al., 2007), HSL (Carmen and Victor, 2006, Krintel et al., 2008) and ATGL (Pagnon et al., 2012). The activation of phosphodiesterase 3B in adipocytes inhibit the cAMP/PKA signalling which reduces lipolysis and promotes lipogenesis when insulin is secreted after a meal (Kitamura et al., 1999). ATGL, a member of the family of patatin domain-containing proteins, hydrolyses triglycerides to diacylglycerides in the lipolytic pathway (Figure 1.7). ATGL expression and enzyme activity is complex (Lass et al., 2011); ATGL gene expression is increased by peroxisome proliferator-activator receptor (PPAR) agonist, glucocorticoids and fasting, while food intake and insulin decreases ATGL gene expression (Zechner et al., 2012). ATGL is not regulated by PKA, AMP-activated kinase (AMPK) phosphorylates the S406 serine residue that causes an increase in hydrolytic activity of ATGL. AMPK involvement in lipolysis is controversial (Zechner et al., 2012). CGI-58, co-activates ATGL and enhances ATGL activity up to 20-fold (Lass et al., 2006, Schweiger et al., 2008, Granneman et al., 2009). When hormonally stimulated, PKA phosphorylates PLIN1 at multiple sites releasing CGI-58 which interacts with PLIN1, preventing PLIN1 binding and inducing ATGL activity (Miyoshi et al., 2007, Granneman et al., 2009) (Figure 1.7). G0S2, the most abundant in the adipose tissue and liver, is expressed in high amounts after feeding (Yang et al., 2010) and acts as a potent endogenous inhibitor of ATGL. G0S2 is specific only for ATGL as HSL, MGL, LPL were not inhibited (Cerk et al., 2014). Even in the presence of CGI-58, G0S2 was able to inhibit ATGL activity (Lu et al., 2010, Yang et al., 2010). An interdependent relationship exists between G0S2 and ATGL. G0S2 was translocated to the lipid droplet with ATGL when exposed to β-adrenergic agonists and this translocation was disrupted when ATGL expression was reduced (Yang et al., 2010).

The next lipase in the lipolytic pathway is HSL. Phosphorylation and dephosphorylation regulates HSL activity (Daval et al., 2006). Several kinases can phosphorylate HSL such as PKA (Stralfors and Belfrage, 1983), AMPK and Ca^{2+}/calmodulin-dependent kinase (Lass et al., 2011). When PKA phosphorylates HSL, there is simultaneous phosphorylation of PLIN1, allowing HSL to translocate from the cytosol to the lipid droplet surface (Miyoshi et al., 2007). HSL is involved in converting diacylglycerol (DG) to monoacylglycerol (MG), releasing a single FA. In a healthy person, insulin acts to suppress HSL and adipocyte TG storage is enabled (Lewis et al., 2002). There is a decrease in lipolysis in a dietary-induced obesity model in visceral and subcutaneous adipose tissues. HSL

phosphorylation also downregulated phosphorylation when stimulated with catecholamines (Gaidhu et al., 2010). Finally, MGL breaks down monoacylglycerols (MG) to glycerol (G) in the lipolysis pathway. MGL is ubiquitously expressed and found mostly in the adipose tissue (Zechner et al., 2012). Gene expression of lipolytic proteins are investigated in Chapter 5.

1.4.3 Factors secreted from adipocytes

The adipose tissue, is dynamically involved in an array of cellular functions and secrete various factors (Figure 1.8). Apart from glucose and lipid metabolism, adipocytes are also involved in functions such as immunity, appetite regulation, coagulation and angiogenesis (Coelho et al., 2013). The importance of these factors is highlighted in diseases. For example, leptin, solely an adipocyte-derived hormone, is proportional to the amount of adipose tissue present and has many physiological functions such as signalling to the brain to store fats, regulate appetite and energy expenditure (Coelho et al., 2013). In obese persons, leptin is increased and plays an important role in obesity-induced oxidative stress (Milagro et al., 2006) which is pro-inflammatory in obesity (Ouchi et al., 2011).

Additionally, adiponectin, an important adipocytokine is also secreted exclusively from the adipose tissue (Ghadge et al., 2018), functions to modulate various metabolic processes, such as fatty acid oxidation, acts to inhibit glucose production in the liver (Fang and Judd, 2018) and is an adipose-tissue specific anti-inflammatory protein. In the obesogenic state, adiponectin is dysregulated and expresses inflammatory proteins such as chemokines, cytokines and acute-phase proteins. Macrophages further expel cytokines and chemokines that worsen the inflammation (Trayhurn, 2007). The three major adipokines that adipocytes produce are tumour necrosis factor alpha (TNF-α), interleukins -1β (IL-1β) and -6 (IL-6). TNF-α and IL-6 will be discussed in the context of inflammation in T2D in section 1.5.1. Factors from the adipose tissue, listed in Figure 1.8, will be discussed in Chapter 6.

Image removed due to copyright restriction.

Figure 1.8 The adipose tissue secretes various factors for multiple physiological functions (Coelho et al., 2013). This list of factors in the diagram is non-exhaustive.

1.5 Dysregulation of Glucose Homeostasis leads to T2D and Obesity

1.5.1 Obesity is a risk factor for T2D: insulin resistance

T2D is a complex late onset condition characterised by increased fasting blood glucose >7 mmol/L (>126mg/dl) (American Diabetes, 2019) and is linked to obesity, peripheral tissue insulin resistance and progressively worsening insulin insufficiency due to β-cell dysfunction (Leahy, 2005, Hashimoto and Tanaka, 2017) (Figure 1.9). Age, obesity, lack of physical activity, belonging to a certain ethnic group and having pre-existing health complications, such as hypertension, can increase risk for T2D (Colberg et al., 2010). Obesity, hypertrophy of adipose tissue (increased adipocyte mass), can become diabetogenic with associations to peripheral insulin resistance and contributes to T2D (McLaughlin et al., 2016, Verboven et al., 2018) as well as cancer and other co-morbidities (Fruh, 2017) (Figure 1.9). Insulin resistance is the decline in sensitivity to insulin stimulation in insulin-dependent tissues (skeletal muscle, liver, adipocytes) causing glucose intolerance (Tagi et al., 2019). Following β-cell dysfunction and failure, hypoinsulinemia ensues, leaving no compensatory mechanism for hyperglycaemia and affect organs vital for glucose homeostasis (Poitout and Robertson, 2002). This will be discussed further in the section 1.5.1.2.

Image removed due to copyright restriction.

Figure 1.9 Insulin resistance associated with obesity (Kumar et al., 2014). Adipokines, non-esterified FFA and inflammation due to obesity can induce insulin resistance in adipocytes. Pancreatic β-cell initially counteracts insulin resistance via compensatory hypersecretion of insulin. When β-cells are unable to compensate, β-cell failure and T2D ensues, resulting in lack of insulin secretion and hyperglycemia (Kumar et al., 2014).

Excess adipose tissue in the visceral and deep subcutaneous depots are strongly linked to insulin resistance, reducing insulin action to suppress lipolysis and T2D (Grundy et al., 2004). In obesity, the overloading of lipids in adipocytes induce macrophage recruitment in the adipose tissue (Figure 1.10). Adipokines, TNF-α and IL-6, increases with obesity and act on inflammatory pathways causing macrophages to manufacture large amounts of TNF-α through the IKKβ-NF-kβ (inhibitor of nuclear factor (NF)-κβ (Iκβ) kinase-β-NF-κβ) and the JNK-AP1 (JUN N-terminal kinase-mitogen-activated protein kinases kinase kinase kinase -4-activated protein-1) signalling pathways (Solinas et al., 2007), thereby contributing to obesity-induced insulin resistance (Hotamisligil et al., 1995, Tilg and Moschen, 2008). These pro-inflammatory adipokines can impact β-cell survival (Figure 1.9) directly affecting insulin signalling as adipokines can modulate serine phosphorylation of the insulin receptor substrate (IRS) (Kanety et al., 1995) and affect insulin secretion (Malin and Kashyap, 2016). Moreover, TNF-α also acts to downregulate the gene expression of adiponectin, an anti-inflammatory adipokine (Hector et al., 2007) (Figure 1.9). The chronic inflammation in adipose tissue causes an imbalance between

lipogenesis and lipolysis, the dysregulation of adipogenesis transcriptional factors and impaired lipid oxidation via mitochondria β-oxidation (Boone et al., 2000). The non-esterified fatty acids (NEFA), released from the adipose tissue, is also a huge contributor to insulin resistance when ectopic fatty acids and lipotoxicity ensues (Figure 1.9) and will be discussed in the next section.

Image removed due to copyright restriction.

Figure 1.10 The dysregulation of adipose tissue in obesity (Ghaben and Scherer, 2019). Obesity causes adipocyte to hypertrophy with increased triglyceride storage and accumulate activated macrophages and T-cells. With the expansion of adipose tissue in obesity, adipocytes undergo necrosis due to poorer vascularization (Ouchi et al., 2011).

1.5.1.1 Non-esterified (free) Fatty Acid (NEFA) and Lipotoxicity in Obesity and T2D

When faced with obesity, the adipose tissue can become dysfunctional due to surplus body fat resulting in abnormal adipokine regulation and the misappropriation of non-esterified free fatty acids (NEFA) in non-adipose tissues (Danforth, 2000). Long-chain NEFA leads to ectopic lipid accumulation in these tissues and eventually lipotoxicity and apoptosis ensues (Kusminski et al., 2009). Lipotoxicity occurs due to an imbalance between endogenous lipogenesis and fatty acid oxidation (Poitout and Robertson, 2002). Moreover, plasma free fatty acids (FFA) are indicative of lipolysis of both TG-rich lipoproteins and adipose triglyceride stores, measured against the uptake of re-esterified FFA in the adipose and liver tissues and oxidation in other tissues such as the muscle (Lewis et al., 2002). The mobilization of NEFA from adipocytes into the blood circulation are hallmarks of the classic development of insulin resistance and development of T2D (Lewis et al., 2002). This is confirmed by increased NEFA in the blood of diabetic and pre-diabetic patients in both fasted and postprandial states (Roust and Jensen, 1993, Bergman and Ader, 2000). These pre-diabetic individuals are typically obese. Prolonged high plasma FFA level, lipotoxicity impairs β-cell function and reduces insulin secretion, causing individuals to be in a hyperglycaemic state (Kashyap et al., 2003).

1.5.1.2 β-cell dysfunction and Insulin Resistance causes T2D

T2D is characterised by hyperglycemia and results from insulin resistance and β-cell dysfunction (Figure 1.11) that could occur years prior to the actual diagnosis of T2D (Holman, 1998, Cerf, 2013). Not every obese person acquires T2D (Despres, 1993). Insulin resistance becomes T2D only if insulin-secreting β-cells become dysfunctional and are unable to produce adequate insulin for glycemic homeostasis. Pancreatic β-cell dysfunction is defined by the drop in insulin release when exposed to glucose stimuli (Bagdade et al., 1967, Perley and Kipnis, 1967) or defect in proinsulin to insulin transformation (Kahn and Halban, 1997). The loss of β-cell mass and function leads to β-cell failure in T2D (Butler et al., 2003). This involves a drop in β-cell volume associated with apoptosis (Butler et al., 2003). β-cell dysfunction is linked to glucotoxicity (heightened blood glucose) which induce alterations to β-cell mass due to decreased rate of replacement through neogenesis or replication of β-cells and increased rate of diminishing β-cells due to necrosis or apoptosis (Donath and Halban, 2004). Consequently, there is a reduction in β-cell proliferation and β-cell mass therefore resulting in reduced insulin secretion, β-cell dysfunction and failure. Both hyperglycemia and hyperlipidemia further worsens β-cell dysfunction (Prentki and Nolan, 2006). In *db/db* mice, β-cells display functional alterations in the pre-diabetic state and insulin exocytosis is increased in response to glucose (Do et al., 2016). Several studies alluded to apoptosis, glucotoxicity, oxidative stress and mitochondrial dysfunction as possible contributors to β-cell dysfunction, however, the exact molecular mechanism underlying β-cell dysfunction during insulin resistance in T2D is unknown. These are discussed in the next section.

Image removed due to copyright restriction.

Figure 1.11 T2D is marked by both insulin resistance and β-cell dysfunction. Image adapted from (Leahy, 2005). Worsening insulin resistance correlates to progression from normoglycemia to T2D. The initial compensation phase allows for the maintenance of normoglycemia. A resulting decline in β-cell function occurs with a decrease in β-cell number and mass. Eventually, β-cell failure ensues in T2D (Lowell and Shulman, 2005). Together, both insulin resistance, β-cell dysfunction and gradual decline and eventual failure are characteristic to T2D.

1.5.1.3 Glucotoxicity and Apoptosis in β-cell dysfunction

In the initial stages of hyperglycemia, pancreatic β-cells are able to maintain normal glucose tolerance with a compensatory increase in insulin secretion (Figure 1.9), brought about by increasing β-cells proliferation, insulin synthesis and GSIS (Kahn et al., 1993, Prentki and Nolan, 2006). FLICE inhibitory protein (FLIP) is an inhibitor of the Fas induced-apoptosis (Irmler et al., 1997). In normal conditions, the presence of sufficient FLIP, a caspase 8 inhibitor, induces β-cell proliferation via the Fas pathway (extrinsic apoptosis pathway). This is consistent with the initial compensatory increase of β-cell mass and secretion in hyperglycemic conditions. However, prolonged exposure to hyperglycemia results in glucotoxicity of β-cells. The β-cell number reduces and β-cell function is impaired, marked by an inability to compensate for hyperglycemia and a decrease in β-cell mass by >50% (Rahier et al., 2008).

Apoptosis is a mechanism of cell death summarised in Figure 1.12. Apoptosis results in alterations in β-cell genes or other genes associated with insulin synthesis and secretion (Pick et al., 1998, Federici et al., 2001, Maedler et al., 2001). For example, the downregulation of *insulin* (Robertson et al., 1992) and *Pdx-1* (Marshak et al., 1999) transcripts due to glucotoxicity results in β-cell apoptosis. A reduction in glucose sensitivity (Sako and Grill, 1990, Kaiser et al., 1991) coupled with dysfunctional β-cells eventually leads to β-cells failure (Robertson et al., 1994, Moran et al., 1997) (Figure 1.11). Exposure to chronic hyperglycaemia and cytokines, FLIP switches from proliferation to apoptosis. Glucotoxicity prevents FLIP protein synthesis and activates the Fas signalling pathway to induce β-cell apoptosis (Maedler et al., 2002). This is consistent with the eventual decline in β-cell mass and function in T2D. Genes associated with apoptosis are investigated in Chapter 4.

Image removed due to copyright restriction.

Figure 1.12 General mechanisms of apoptosis pathway (Kumar et al., 2014). Apoptosis involves both the intrinsic pathway and the extrinsic pathway that results in activation of caspases downstream. The mitochondrial pathway BCL2 family of proteins, regulate mitochondrial permeability, becomes imbalanced due to loss of survival signals, DNA damage and other insults, thereby activating BH3-only protein sensors that antagonises anti-apoptotic proteins (BCL2) and activates pro-apoptotic proteins (BAX and BAK). There is subsequent leakage of cytochrome c that activate caspases 9. In the death receptor pathway, plasma membrane receptors (Fas ligands) binds to Fas and activate adaptor proteins that activates caspase 8. Once caspase 8 or caspase 9 are activated, subsequent executioner caspases, such as caspase 3, act to breakdown structural components of the nuclear matrix and cause nuclear fragmentation of nuclei in the downstream apoptosis pathway.

1.5.1.4 Oxidative stress in Obesity and T2D

Oxidative stress can occur from greater exposure to oxidants such as intracellular production of reactive oxygen species (ROS) and endoplasmic reticulum (ER) stress (Riemer et al., 2009) coupled with the downregulation of protective mechanisms against oxidants (Davies, 1999). Oxidative stress is increased in the presence of hyperglycemia which induces the downregulation of *insulin* transcription through upregulation of oxidative stress-induced gene, *Myc*, implicated in both β-cell dysfunction and apoptosis (Kaneto et al., 2002, Pascal et al., 2008). Islets damaged by oxidative stress are unable to repair sufficiently due to poor DNA repair mechanisms (Modak et al., 2009). Oxidants, such as ROS, a resulting by-product of mitochondria oxidative phosphorylation in β-cells glucose metabolism, is

important for normal physiology (Turrens, 2003). However, overproduction of ROS, coupled with the decrease in antioxidants (e.g. superoxide dismutase, glutathione peroxidase 1 and catalase (Lenzen, 2017, Tonooka et al., 2007)) and worsening glucotoxicity and diabetes (Robertson, 2004) leads to diabetic complications such as β-cell dysfunction, lipotoxicity and increased NEFA (Maritim et al., 2003, Robertson et al., 2003). The decline in β-cell function and eventual failure is linked to impaired mitochondria function (Poitout and Robertson, 2002, Tanaka et al., 2002) discussed in the next section. Oxidative stress is derived from various sources (Maritim et al., 2003); ROS is produced by phagocyte-like NADPH oxidases (NOX2) in β-cells that increases ROS production and decreases cAMP production, altering the secretory response (Li et al., 2012). Overall, the mitochondria remain the main source of ROS in T2D β-cells (Marchetti et al., 2004, Robertson, 2004).

The overall effect of oxidative stress is the induction of insulin resistance in peripheral tissues due to ROS overproduction (Furukawa et al., 2004). Obesity induces oxidative stress locally in WAT (Keaney et al., 2003), damaging proteins associated with lipolysis (Curtis et al., 2010) and dysregulating insulin signalling (Demozay et al., 2008). Obesity-induced oxidative stress is strongly linked to T2D defined by hyperglycemia, increased lipid levels (Beltowski et al., 2000), chronic inflammation (Fernandez-Sanchez et al., 2011), decrease in adiponectin levels, increase in inflammatory cytokines (e.g. TNF-α) (Furukawa et al., 2004), overproduction of leptin (Milagro et al., 2006) and mitochondrial dysfunction (Martinez, 2006).

1.5.1.5 Mitochondrial dysfunction and T2D

The mitochondria are essential for metabolic processes such as oxidative phosphorylation, substrate oxidation, generation of ATP and ROS clearance. Mitochondria are necessary for K_{ATP}-dependent GSIS by pancreatic β-cells that utilises mitochondrial generated ATP (Wollheim, 2000, Maechler and Wollheim, 2001) (Figure 1.3). Obesity, insulin resistance and T2D are linked to increased ROS production and when not managed, ROS can cause mitochondrial damage via DNA fragmentation, protein crosslinking and peroxidation of membrane phospholipids and the induction of stress pathways (Fariss et al., 2005). Mitochondrial dysfunction impact negatively on fusion and fission of the mitochondria (Montgomery and Turner, 2015), lowering ATP generation, reducing mitochondrial mass, decreasing responsiveness to glucose and over producing ROS which contributes to insulin resistance (Anello et al., 2005, Montgomery and Turner, 2015). Increased mitophagy results in a reduction in mitochondria number, reducing oxidation via the electron transport chain (Montgomery and Turner, 2015). Moreover, the apoptosis pathway is linked to the mitochondria (Orrenius, 2004) where caspase 3 activation and cytochrome c are exported and are part of mitochondrial-regulation of β-cell mass (Mulder and Ling, 2009) (Figure 1.12). Furthermore, genetic and epigenetic changes can alter both metabolic enzymes and function in β-cell mitochondria. Mitochondrial number is affected by fission of already existing mitochondria and fusion and fission could affect mitochondrial structure that,

in turn, affects proton and protein diffusion (Mulder and Ling, 2009). Basal ATP levels were increased in T2D human islets, however, the increase in ATP did not induce insulin secretion and glucose induction did not hyperpolarize the mitochondrial membrane. These alterations are attributed to changes in the mitochondria of β-cells as there was an increase in expression of complex I and V in these patients (Anello et al., 2005). Additionally, *Tfam* (mitochondrial transcription factor A gene) controls expression of the mitochondrial DNA (mtDNA) and β-cell specific deletion of *Tfam* gene in mice resulted in islets displaying a perturbed respiratory-chain activation and decreased GSIS upon glucose stimulation (Silva et al., 2000). This further highlights the role of mitochondria in β-cells.

Moreover, mitochondria also have a role in WAT that involves the regulation of metabolism and the generation of ATP (Spiegelman and Flier, 2001), energy expenditure, insulin resistance and adipogenesis. Mitochondria is present in low amounts in WAT, compared to BAT and β-cells, and mitochondrial dysfunction in WAT has been understudied. WAT-specific ablation of *Tfam* in mice, upregulated mitochondrial fatty acid oxidation, protected mice from both age- and diet- associated obesity, insulin resistance and liver steatosis (Vernochet et al., 2012). In *db/db* mice adipocytes, decreased mitochondria and dysregulation in mitochondrial respiration were found (Choo et al., 2006). Additionally, obese human sWAT demonstrated a decrease in mtDNA, mitochondrial oxidative genes, oxidative phosphorylation mechanism, fatty acid oxidation was inverse to insulin resistance (Heinonen et al., 2015), increased ROS production and damage linked to decreased mitochondrial antioxidant enzymes, superoxide dismutase and glutathione peroxidase (Chattopadhyay et al., 2015). Overall, mitochondrial dysfunction in WAT could contribute to the insulin resistance in the adipose tissue of obese and T2D patients. Mitochondrial biogenesis and the expression of the thermogenic gene, *UCP1,* is increased, inducing browning of WAT to beige fat with cold exposure, β-adrenergic stimulation (Barbatelli et al., 2010) and being on high caloric diet. The increase in *UCP1* is linked to the decrease in diet-associated obesity. Taken together, the role of mitochondria is important in WAT.

1.5.2 Genetic basis of T2D and obesity

T2D pathology is complex and risk of T2D could arise from both genetic and acquired pre-disposition that are not completely understood (Leahy, 2005). Genome-wide association studies (GWAS) demonstrated that T2D risk is polygenic. A large number of genes are linked to T2D risk loci involved in pancreatic β-cell regulation (Prasad and Groop, 2015). This is critical as pancreatic β-cells are the only source of endogenous insulin produced in the body. Increasingly, new genes are being linked to obesity susceptibility (Bell et al., 2005, Dahlman and Arner, 2007). Furthermore, correlating islet microarray gene expression data with insulin secretion and HbA1c, specific genes (GLR1A, PPP1R1A, PLCDXD3, FAM105A and ENO2) were identified to be implicated in T2D (Taneera et al., 2015). Both DNA methylation studies and epigenetic changes are implicated in the pathology of T2D and obesity (Prasad and Groop, 2015, van Dijk et al., 2015). Obesity-related genes can disrupt energy homeostasis

in the body causing a rise in both adipocyte number and lipid amount (Spiegelman and Flier, 1996, Farmer, 2006). Patients with Down syndrome (DS) often have T2D. Using a Down syndrome screening approach, our lab has recently identified a single gene, regulator of calcineurin 1 (*RCAN1*), implicated in the pathogenesis of T2D (Peiris et al., 2012, Peiris et al., 2016) and plays a role in preventing diet-induced obesity (Rotter et al., 2018). This will be discussed further in section 1.7.

1.6 RCAN1 and the Calcineurin-NFAT pathway

1.6.1 RCAN gene and nomenclature

There are three *RCAN* genes, namely *RCAN1*, *RCAN2* and *RCAN3* found to date and *RCAN1* is the best studied (Davies et al., 2007). This gene is well conserved in mammals (Hilioti and Cunningham, 2003). Previously known as Down syndrome critical region 1 (*Dscr1*), RCAN1 was first identified as a sequence expressed on a yeast artificial chromosome clone which contained a portion of gene known as Down syndrome critical region (DSCR) of human chromosome 21 (Fuentes et al., 1995). It was also known as a myocyte-enriched or modulatory calcineurin interacting protein (*Mcip1*) in mice hearts (Rothermel et al., 2000), neubula (*nla*) in Drosophila melanogaster, Sarah (*sra*) in Drosophila eggs, *Adapt78* in the Chinese Hamster (Crawford et al., 1997), CBP1 and calcipressin-1 (*Csp1* and *CALP1*) (Genesca et al., 2003). To reduce confusion, in 2007, the HUGO Gene Nomenclature Committee (HGNC) and the Mouse Genomic Nomenclature Committee (MGNC) established that the universal nomenclature will be regulatory of calcineruin 1 (RCAN1) (Ermak et al., 2006, Davies et al., 2007). The *RCAN1* gene encode proteins that bind to calcineurin A and inhibit calcineurin-dependent pathways. Calcineurin is a hetermodimeric calcium/calmodulin-activated serine/threonine protein-phosphatase 3 found throughout the body (Musson and Smit, 2011) and is discussed in greater detail in further sections of this thesis.

1.6.1.1 RCAN1 gene/protein structure

In humans, regulator of calcineurin 1 (*RCAN1*) gene is found on chromosome 21 within regions q22.1-q22.2 which encompasses 7 alternatively spiced exons separated by 6 introns (Harris et al., 2005). Differences exist in RCAN1 chromosome between animals and humans; the *Rcan1* gene is found on chromosome 16 in the mouse (Strippoli et al., 2000). Through differential promoter usage (Fuentes et al., 1997), RCAN1 has a unique genomic arrangement resulting in 7 alternative transcripts creating isoforms of RCAN1 (Rothermel et al., 2003) (Figure 1.13). RCAN1.1 and RCAN1.4 are the two predominant isoforms in the mammalian tissue. Each isoform is expressed at different levels in diverse tissues including the brain, liver and skeletal muscle (Fuentes et al., 1997). RCAN1.1, 48kDa long, begins at exon 1 and includes exons 5, 6, 7. RCAN1.1 isoform can be further subdivided into RCAN1.1 short (RCAN1.1S) and RCAN1.1 long (RCAN1.1L) that share exons 5-7 in the C-terminal region, derived from alternative transcription initiation site on exon 1 (Figure 1.13). While RCAN1.4, 24kDA

long, begins at exon 4 and includes exons 4 to 7 (Fuentes et al., 2000, Kingsbury and Cunningham, 2000) . A cluster of 15 NFAT binding sites is present on *RCAN1* within the alternative promoter region of RCAN1.4 where *RCAN1.4* gene expression is regulated by the calcineurin-NFAT (CN/ NFAT) pathway (Harris et al., 2005) (Figure 1.13).

Image removed due to copyright restriction.

Figure 1.13 RCAN1 has two additional isoforms (Harris et al., 2005). All *RCAN1* isoforms share amino acids encoded by exons 5-7 which is a conserved FLISPP sequence which shares homology with the serine poline (SP) boxes found in NFAT protein and contain a putative CN-binding motif. RCAN1.1L has N-terminal amino acids encoded by an elongated version of exon 1, which encodes 26 amino acids in addition to the 29 found in exon 1 of RCAN 1.1S.

The structure of the RCAN1 protein is described in Figure 1.14. The inhibitory actions of RCAN1 involves the direct binding of RCAN1 to the catalytic domain of CN and the SP rich region (Rothermel et al., 2000). Binding of the SP region is neither essential nor sufficient to for CN inhibition (Vega et al., 2002). Two serine residues in the SP region of RCAN1, Ser 112 (Ser^{112}) and Ser 108 (Ser^{108}) respectively, can be phosphorylated by mitogen-activated protein kinase (MAPK) (Abbasi et al., 2006) and one by glycogen synthase kinase 3 (GSK-3) (Genesca et al., 2003), thereby modulating its inhibition activity on CN (Figure 1.14). Furthermore, having the SP repeat from RCAN1 being analogous to NFAT is critical for its role in effecting the CN-NFAT pathway.

Image removed due to copyright restriction.

Figure 1.14 Features of the RCAN1 protein (Rothermel et al., 2003). A family signature Phe-Leu-Ile-Ser-Pro-Pro-Xaa-Ser-Pro-Pro-Pro (FLISPP) of the highly conserved serine-proline (SP) motif (similar to NFAT proteins (Crabtree, 1999)) , CN docking sites (N- and C-terminal domains), N-terminal amphipathic leucine repeat (L) which is a dimerization/protein interacting region, an acidic region (a), a cluster of basic amino acids (b) and a SH2 ligand domain (not shown) (Fuentes et al., 1997, Vega et al., 2002, Mehta et al., 2009).

1.6.1.2 RCAN1 expression and function

RCAN1 is widely distributed throughout the body and has many roles (Rao et al., 1997). RCAN1 is constitutively expressed and is particularly abundant in metabolically active regions such as the skeletal muscle, heart, brain (Fuentes et al., 1997), pancreatic β-cells (Peiris et al., 2012) and in the adipose tissue (Rotter et al., 2018). This presents a unique opportunity for investigation of the role of RCAN1 in T2D and obesity. Both isoforms of RCAN1 are ubiquitously expressed, however, depending on tissue type, RCAN1.1 is more highly expressed. Furthermore, in β-cells, RCAN1.1 is present in more abundance than RCAN1.4 (Peiris et al., 2016).

RCAN1 is also known as a stress-inducible gene activated by multiple stress stimuli that increases intracellular Ca^{2+} (Crawford et al., 1997, Leahy et al., 1999, Davies et al., 2001, Wang et al., 2002). Type of stress-stimuli and extent of RCAN1 activation is variable. Factors that induces RCAN1.1

expression include glucocorticoids and vascular endothelial growth factor (VEGF) (Hirakawa et al., 2009) while Notch signaling pathway downregulates RCAN1.1 expression. Expression of RCAN1.4 is regulated by oxidative stress, Ca^{2+} and calcineurin (Fuentes et al., 2000, Kingsbury and Cunningham, 2000) though the cluster of 15 NFAT binding sites of RCAN1.4 (Yang et al., 2000) (Figure 1.14). Chronic exposure to stress-associated stimuli such as oxidative stress, Ca^{2+} and amyloid-β (Ermak et al., 2001) can be deleterious in neuronal cells. The amount of RCAN1 expression is vitally important for the survival or death of cells, especially in the presence of oxidative stress (Porta et al., 2007b). RCAN1 expression is upregulated in DS and AD (Crawford et al., 1997, Fuentes et al., 2000, Strippoli et al., 2000, Yang et al., 2000). *RCAN1.1* gene expression was also upregulated in the presence of high glucose (Peiris et al., 2012) in human islets, mouse islets and the MIN6 β-cells (Peiris et al., 2016). While *RCAN1.4* expression can be induced by an array of mitogens (Harris et al., 2005) and cytokines involved in inflammation (e.g. ROS (Crawford et al., 1997) and tumour necrosis factor (TNF-α) (Cho et al., 2008, Jang et al., 2011)). Therefore, RCAN1 expression has both a deleterious role in a chronic timeframe (e.g. T2D) and a protective role in an acute time frame (up to days); RCAN1 can protect against transient stressors that increase intracellular Ca^{2+} and internal synthesis of reactive oxygen species (ROS) (Porta et al., 2007b) and oxidative damage (Ermak et al., 2002). In Chapter 6, I investigate factors that could upregulate RCAN1 expression.

RCAN1 is a dual regulator of calcineurin (CN) (Figure 1.15) and RCAN1's best characterized role is as an inhibitor of CN (Fuentes et al., 2000, Kingsbury and Cunningham, 2000, Rothermel et al., 2000, Casas et al., 2001, Ermak et al., 2001). Both isoforms of RCAN1 are similarly potent inhibitors of CN (Rothermel et al., 2000). RCAN1 inhibits CN but also competes with NFAT for the same binding site on CN that usually dephosphorylates NFAT (Martinez-Martinez et al., 2009). Transcript of *Rcan1.4* is induced by Ca^{2+}-dependent NFATc and C/EBP-β transcription factors (Yang et al., 2000, Wu et al., 2007), under the control of CN/NFAT forming an inhibitory (negative) feedback loop (Kingsbury and Cunningham, 2000, Yang et al., 2000) (Figure 1.15). When CN levels are elevated during prolonged Ca^{2+} stimulation (Rothermel et al., 2000), RCAN1 negatively feeds back on the pathway itself, elevating *Rcan1* expression (Fuentes et al., 2000, Yang et al., 2000), resulting in RCAN1 protein inhibition on CN. Overexpression of RCAN1 inhibits CN activity to avoid the harmful effects of CN when there is chronic over activation of Ca^{2+} (Fuentes et al., 2000). Therefore, the negative feedback loop acts as a protective mechanism against unrestrained CN activation that could result in uncontrolled apoptosis (Wang et al., 1999). A positive feedback loop also exists to prevent further cell damage (Ermak et al., 2002) through downstream NFAT transcriptional activity. Upregulating of NFAT proteins in the cytosol creates a positive feedback loop (Crabtree and Olson, 2002).

Image removed due to copyright restriction.

Figure 1.15 Negative feedback and Positive feedback control of NFAT signalling (Crabtree and Olson, 2002). **(A)** NFAT signalling induces RCAN1 gene expression, upregulating *RCAN1* gene expression. Therefore, RCAN1 protein acts to inhibit CN in the CN/NFAT pathway, thereby exerting its negative feedback control. **(B)** Activation of NFAT gene expression upregulates NFAT proteins in the cytosol, creating a positive feedback loop.

1.6.2 The Calcineurin- NFAT pathway

In a given cell, the general CN/ NFAT pathway is depicted in Figure 1.16. Details of this pathway is discussed in the sections to follow.

Image removed due to copyright restriction.

Figure 1.16 Schematic of the calcium-dependent calcineurin-NFAT pathway. Image adapted from (Muller and Rao, 2010). Cellular events start with stress-induced Ca^{2+} entry (❶), Ca^{2+} binds to Calmodulin (CaM) (❷) and the Ca^{2+}/CaM complex binds to Calcineurin (CN) (❸). CN dephosphorylates NFAT (❹), NFAT translocate from the cytosol into the nucleus (❺). NFAT may bind to a transcriptional partner (❻) and together, bind to DNA transcriptional targets (❼). With the absence of Ca^{2+} entry or in the presence of CN inhibitors (e.g. CsA, FK506 or RCAN1), NFAT kinases (e.g. GSK3) phosphorylates NFAT (❽) and induces NFAT nuclear export back into the cytosol (❾). CN/NFAT signalling has a positive feedback loop where NFAT gene expression is induced (*green (+) symbol*) and a negative feedback loop where CN/NFAT signalling induces RCAN1 gene expression and RCAN1 proteins inhibits (*red (-) symbol*) CN action causing it to be inactive (*black arrow*).

1.6.2.1 Intracellular calcium (Ca^{2+}) is induced by stress

There are many stresses that could trigger intracellular calcium (Ca^{2+}) entry, for example, oxidative stress (Davies et al., 2001). Ca^{2+}, essential for survival, is a widely distributed signalling molecule with a wide range of functions within cells, targeting genes and modulating gene expression (Yu et al., 2001). One target of Ca^{2+} is calmodulin. In β-cells, exposure to chronically high glucose (Tang et al., 2007) induces high oxidative stress due to an impaired antioxidant system, triggering Ca^{2+} entry. Ca^{2+} entry in β-cells is essential for insulin production and secretion, β-cells replication and survival and is implicated in T2D (reviewed (Sabatini et al., 2018)). Sources of oxidative stress in T2D have been discussed earlier in this thesis in the section 1.5.1.4.

1.6.2.2 Calcium-Camodulin (Ca^{2+}/CaM) interact with Calcineurin (CN)

Calcineurin (CN) is a heterodimeric calcium/calmodulin-activated serine/threonine protein-phosphatase 3 (PP3) (previously known as protein-phosphatase 2B, PP2B) found throughout the body (Musson and Smit, 2011). Being widely distributed, CN is involved in a raft of different cellular processes and have multiple molecular targets (Asai et al., 1999, Wang et al., 1999, Genesca et al., 2003) including molecules controlled by NFAT members (Mognol et al., 2016). CN is an important enzyme in Ca^{2+}-sensitive signalling cascade and CN regulates the CREB phosphorylation and CREB-dependent transcriptional activation (Kim and Seo, 2011), as well as, the direct dephosphorylation of NFAT triggering gene expression in the nucleus. Moreover, CN has two subunits essential for its function (Crabtree and Olson, 2002) and summarised in Figure 1.17.

Image removed due to copyright restriction.

Figure 1.17 Structure of Calcineurin subunits (Shou et al., 2015). The CN protein has two subunits, calcineurin A (CnA) and calcineurin B (CnB). CnA has three functional domains which includes the N-terminal catalytic region, a regulatory region binding CnB and calmodulin (CaM) and a C-terminus auto-inhibitory domain (AID) that is displaced upon calmodulin binding (Aramburu et al., 2000). CnB has four Ca^{2+}-binding EF-hand motifs which can be recognized by immunosuppressive complexes and competitively binds to CnA.

Calmodulin (CaM) is a ubiquitous multifunctional four domain Ca^{2+}-dependent regulatory protein that mediates many actions of Ca^{2+} (Cheung et al., 1981, Kakiuchi, 1983), regulating gene expression in the CN/NFAT pathway (Klee et al., 1988, Crabtree, 1999, Olson and Williams, 2000). Intracellularly, Ca^{2+} binds to calmodulin forming a calcium-calmodulin complex (Figure 1.18).

Image removed due to copyright restriction.

Figure 1.18 Calcineurin is activated by the binding of calcium and calmodulin (CaM). Image modified from (Rothermel et al., 2003). CnA containing the N-terminal catalytic domain and binding domain for CnB and CaM. The C terminus contains the auto-inhibitory domain that folds to occlude the active site when CaM is not bound. Upregulation of intracellular Ca^{2+} promote binding of Ca^{2+} binding of Ca^{2+}/ CaM to the catalytic subunit of calcineurin (CnA) displacing the auto-inhibitory region upon CN binding to CaM at the CaM binding site (Rothermel et al., 2000).

1.6.2.3 Synthetic and endogenous inhibitors of calcineurin

Liu et al. has helpfully classified endogenous CN binding proteins into four main classes based on their effect (Table 1.2). At high concentrations RCAN1 serves as an inhibitor of CN and an activator at low concentrations (Liu, 2003).

Table 1.2 Classification of calcineurin binding proteins (Liu, 2003)

Protein classes	Main effect	Proteins
Inhibitors	Lead to inhibition of calcineurin	CN-binding protein 1 (Cabin 1/ cain) FKBP38 CHP A238L
Anchoring proteins	Physically associate calcineurin to other signalling proteins	A-kinase anchor protein 79 (AKAP79) FKBP12 Calsarcin BCL-2
Activators	Activate calcineurin	Ca^{2+}/CaM
Dual regulators	Inhibition and activation	RCAN1 CBP1

Endogenous physiological inhibitors of CN include AKAP79 (Coghlan et al., 1995, Klauck et al., 1996, Kashishian et al., 1998), CABIN1 (Sun et al., 1998), CHP and RCAN1 (Rothermel et al., 2000). RCAN1 alters CN under pathological and non-pathological conditions. In the CN-NFAT pathway, inhibitors of RCAN1 inhibits RCAN1 and does not affect CN activity (Chan et al., 2005). This pathway is discussed in a later section "RCAN1 inhibits the Calcineurin-NFAT pathway" and these inhibitors are discussed in section 1.8.

Synthetic CN inhibitors include Cyclosporin A (CsA) and tacrolimus (FK506) which are pharmacological drugs that exert immunosuppressive actions in organ transplant patients. These drugs bind to cytosolic immunophilins and induce a complete and continual inhibition of CN thereby regulating CN enzymatic activity whilst non-competitively binding to CN (Chan et al., 2005) causing negative side effects (Martinez-Martinez and Redondo, 2004) such as weight gain and hyperglycaemia with 15-30% of patients having post-transplant diabetes mellitus (PTDM) (Weir and Fink, 1999). These

side-effects caused further co-morbidities and increased mortality rates (Weir, 2001, Doyle and Egan, 2003, Heisel et al., 2004).

1.6.2.4 Nuclear factor of activated T cells (NFAT)

Nuclear factor of activated T cells (NFAT) are transcriptional regulatory proteins first discovered and studied in activated T cell nuclear samples. There are five identified members in the NFAT family encoded by different genes (Macian, 2005). NFAT1-NFAT4 is regulated by Ca^{2+} where the entry of Ca^{2+} activate enzymes such as CN and dephosphorylate NFAT, inducing NFAT nuclear translocation (Rao et al., 1997, Macian, 2005, Crabtree and Olson, 2002). In this thesis, NFAT 1- NFAT4 proteins will be collectively termed NFAT.

In resting cells, in the cytoplasm, NFAT interacts with CN (CnA and CnB) and resides in the cytoplasm via a complex of proteins. The nuclear localisation sequence and residues in the DNA binding domain that contact with DNA are inaccessible when NFAT is phosphorylated (Rao et al., 1997) due to interactions with the serine-rich region and the SP repeats (Beals et al., 1997). The functions of NFAT are discussed in the next section. Furthermore, obesity is linked to inflammation and transcriptional effectors (e.g. NFAT) that contribute to immune function. NFAT also regulates the *Pparg2* gene transcription, important in adipocyte differentiation (Yang et al., 2006a), therefore, NFAT and its transcriptional activities could be important to the study of obesity and T2D.

1.6.2.5 RCAN1 inhibits the Calcineurin-NFAT pathway

The focus of this thesis is the interaction of RCAN1 with CN that will be discussed in greater detail. On a cellular level, RCAN1 is found in both the nucleus and cytoplasm (Pfister et al., 2002). The amount of RCAN1 in the cell, its localization in the cytosol or nucleus and its phosphorylation status can either inhibit or enhance CN signaling (Pfister et al., 2002, Hilioti et al., 2004, Abbasi et al., 2006). Low RCAN1 facilitate CN signaling (Mehta et al., 2009). While high RCAN1 concentration inhibited CN signaling (Hilioti et al., 2004). Furthermore, phosphorylation by Dual Specificity Tyrosine Phosphorylation Regulated Kinase 1A (DYRK1A), for example, induced RCAN1 to switch from inhibitor to promoter of CN signaling (Jung et al., 2011). Therefore, the amount of RCAN1 expressed is important and key to understanding pathological conditions such as T2D.

RCAN1 interacts directly with CN (Fuentes et al., 2000, Rothermel et al., 2000) (Figure 1.16), binding to the A subunit of CN in a linker region between CnA catalytic domain and CnB binding domain (Fuentes et al., 2000). When RCAN1 auto-inhibitory domain undergoes conformational change, the protein is active. Exon 7 of RCAN1 alone binds to CN with high affinity (Chan et al., 2005). RCAN1 binding to CN did not disrupt formation of CN- CaM binding but disrupted CN binding to NFAT by competing for the same binding site (Vega et al., 2002, Mehta et al., 2009). This is evident in overexpression of RCAN1 inhibiting NFAT translocation to the nucleus, inhibiting CN-NFAT-

mediated gene transcription (Fuentes et al., 2000). When NFAT is in a constitutively active form, RCAN1 does not inhibit its translocation, therefore, RCAN1 specifically targets CN in this pathway (Rothermel et al., 2000). However, the regulatory role of RCAN1 may not be limited to CN inhibition. The presence of low Ca^{2+} levels result in downregulation of CN via hormonal and developmental signals, a reduction in CN inhibition by RCAN1 and RCAN1 would be quickly degraded. When NFAT is activated and translocates into the nucleus, RCAN1.4 protein is synthesized and binds to CN to resume inhibition effect. The positive and negative feedback loop in the CN/NFAT pathway (Figure 1.16) establishes equilibrium among CN activity, NFAT transcription and RCAN1 protein abundance (Rothermel et al., 2003).

The activation of NFAT is regulated by phosphorylation status (Feske et al., 2003) and translocates to the nucleus (Flanagan et al., 1991, Clipstone and Crabtree, 1992) (Figure 1.16). NFAT has many targets and facilitates transcription of these targets once bound to DNA (Wilkins and Molkentin, 2002). In the rat I insulin promoter, *Nfat* binds to three elements and activates insulin gene transcription. Mutations in these sites resulted in significant decreased in the combined effect of glucose and GLP-1 in promoting insulin gene transcription by NFAT via PKA- and CN-dependent pathways in pancreatic β-cells. GLP-1 synergistically increases the effect of glucose on NFAT-mediated gene transcription in β-cells. cAMP directly increases Ca^{2+} release from intracellular stores in β-cells (Lawrence et al., 2002). The CN/NFAT pathway will be discussed further in the context of T2D in the next section.

1.7 RCAN1 in disease

1.7.1 Alzheimer's disease (AD) and Down Syndrome (DS)

RCAN1 is especially well studied in DS where the gene was first discovered on chromosome 21 (Korenberg et al., 1994, Sinet et al., 1994). Expression of RCAN1 is high in some areas of the adult brain (Baek et al., 2009, Kurabayashi and Sanada, 2013) highlighting RCAN1's importance to neuron and normal neuronal function such as apoptosis (Asai et al., 1999, Sun et al., 2011, Porta et al., 2007a), long term potentiation (Hoeffer et al., 2007) and synaptic function (Chang and Min, 2009). People with DS have metabolic defects (e.g. T2D), immunological defects and neurodegenerative conditions (e.g. AD) (Ermak et al., 2001). RCAN1 is a well-known inhibitor of calcineurin in the brain (Varma et al., 2017) involved in pathology of AD by inhibiting CN activity, causing insoluble hyper-phosphorylated (Xie and Johnson, 1998, Garver et al., 1999) tau and neurofibrillary tangles of the amyloid beta (Aβ) peptide that no longer prevent formation of aggregates (Desdouits et al., 1996) - all hallmarks of AD (Ladner et al., 1996, Ermak et al., 2001).

There is a strong genetic driving force behind mitochondria dysfunction, as it occurs early in fetal DS β-cells (Helguera et al., 2013). The DS patients β-cells have fragmented mitochondria and amyloid proteins are accumulated in insulin vesicles. This causes a significant decline in GSIS response and

increased pro-insulin exocytosis (Helguera et al., 2013), similar to islets of patients with T2D. Unlike age-matched insulin-dependent diabetics, insulin-dependent DS patients only require a lower insulin dose (Anwar et al., 1998), eluding to possible coping mechanisms such as increased insulin sensitivity in DS patients to compensate for β-cells defects.

Furthermore, DS abnormalities is highly complex and overexpression of RCAN1 is not the only contributing factor. Reverting RCAN1 to disomic levels in trisomy 16 mouse model of DS did not revert cardiac and craniofacial defects (Lange et al., 2005). Moreover, DS mouse models had trisomic RCAN1 locus and had hyperglycemia while those without this region were not hyperglycemic, indicating that a greater number of genes in this region is key to metabolism and glucose regulation (Peiris et al., 2016). Therefore, there are strong links between DS patients and T2D, even though this is not well understood. A study on the incidence of T2D in DS patients (Taggart et al., 2013) indicated higher fasting blood glucose and increased insulin resistance (Yahia et al., 2012, Real de Asua et al., 2014), however, these studies did not take into account obesity, a huge risk factor for T2D (Rohrer et al., 2010).

1.7.2 T2D and Obesity

Growing literature and work from the lab surround the role of RCAN1 in T2D and obesity, in a bid to better understand these severe metabolic conditions. Dysfunction of pancreatic β-cells and lowered insulin released upon glucose stimulation are not fully understood and other factors could be involved in the pathogenesis of T2D (Rahier et al., 2008). In T2D, dysfunction of β-cells led to decreased β-cells number and elevated RCAN1 expression. RCAN1 has a role as a regulator of vesicle exocytosis both in chromaffin cells (Keating et al., 2008) and best known to endogenously inhibit protein phosphatase, CN, essential for physiological and biologically functioning β-cells. RCAN1 is important for normal maintenance of plasma insulin levels through insulin secretion and loading in β-cells (Peiris et al., 2012). Several findings strongly implicate RCAN1 in T2D and is discussed in this thesis.

In β-cells, CN targets both NFAT and cAMP-responsive element-binding protein (CREB) transcriptional co-activator which is a transducer of regulated CREB activity-2 (TORC2) (Soleimanpour et al., 2010). *In vivo*, rise in intracellular Ca^{2+} in β-cells due an influx of glucose, activates CREB phosphorylation and downstream activity, modulating β-cell mass and function (Lipskaia and Lompre, 2004). The CN-NFAT signalling pathway is a regulator of pancreatic β-cell proliferation, mass and function. CN has major roles in the expression of β-cell factors including insulin and plays an essential role in activation of *insulin* transcription when Ca^{2+} signals are inducted. Transcription factors that regulate genes encoding *insulin* and *Glut2* includes *Pdx1*, *MafA* and *Beta2* that act via the CN-NFAT pathway where CN directly regulates insulin secretion (Heit et al., 2006a).

The CN-NFAT signalling pathway in β-cells regulate key factors necessary for normal endocrine pancreas development (Kim and Hebrok, 2001, Arron et al., 2006).

The CN/NFAT signalling controls cell cycle factors such as cyclin D1, cyclin D2, CDK4 in β-cells that are critical for the development and function of β-cells (Heit et al., 2006a). Additionally, knocking out *Cnb1* in mice β-cells (βCnb1KO), a regulatory subunit of CN, inhibited cyclin gene expression and significantly reduced β-cell proliferation and mass (Figure 1.19 A). This led to β-cell failure, decreased expression of insulin mRNA and proteins, perturbed insulin secretion and glucose intolerance -all hallmarks of T2D. Diabetes in these βCn1KO mice worsened with age (Figure 1.19 B). However, if NFAT1 is expressed in its activated form in β-cells, NFAT1 binds to the promotors, increasing expression of cyclin D1 (*Ccnd1*), cyclin D2 (*Ccnd2*) and *Cdk4*, thereby increasing β-cell proliferation in these mice (Heit et al., 2006a). In β-cells, CN inhibition is protective against apoptosis in the mitochondria caused by inflammatory cytokines and dexamethasone (Ranta et al., 2006, Grunnet et al., 2009).

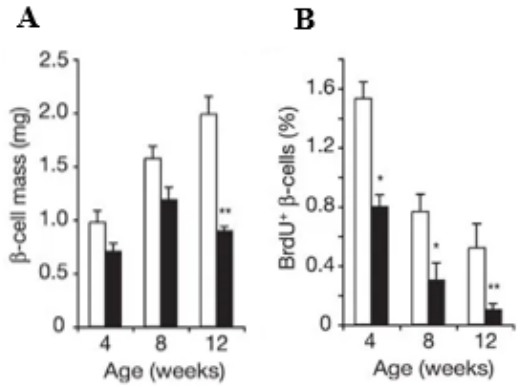

Figure 1.19 Effects of age in βCnb1KO mice on β-cell mass and β-cell mass number. **(A)** βCnb1KO mice had more severe diabetes with age indicated by the decrease in β-cell mass (black) compared to controls (white) **(B)** this induced diabetes worsened with increased age (Heit et al., 2006a).

Administration of synthetic CN inhibitors into rats caused reduced *insulin* transcription, hyperglycemia, decreased serum and pancreatic insulin output and glucose intolerance (Gillison et al., 1989). Patients treated with immunosuppressive drugs, CsA and FK506, had diabetes post-organ transplant and the CN/NFAT pathway could control islet coping mechanisms (Weir and Fink, 1999). Furthermore, the CN/NFAT signalling is also involved in regulating MODY genes (Heit, 2007). Therefore, there are implicating literature to support the study of CN/NFAT and role of RCAN1 in T2D and obesity.

1.7.2.1 RCAN1 regulate characteristics of T2D

Our laboratory identified a single gene, *RCAN1*, as a candidate gene linking hyperglycemia and functional changes in T2D β-cells. When *Rcan1* is over-expressed in mice, mice were observed to have characteristics of T2D (Peiris et al., 2016). Through the screening of regions of chromosome 21 linked to hyperglycemia in DS mice lines, 38 genes associated with hyperglycemic phenotype were identified. This technique of screening is possible as human DS β-cells have mitochondrial dysfunction and decreased GSIS similar to T2D β-cells. From human T2D islet data (Fadista et al., 2014), five key β-cells genes out of the original 38 genes identified in the DS mice lines were upregulated. These genes include *EVA1C*, *OLIG2*, *IFNAR1*, *RUNX1* and *RCAN1* (Figure 1.20A). Only RCAN1, when upregulated, had associations with mitochondrial function and exocytosis of insulin in mouse islets or mouse β-cell lines. Specifically, GSIS was reduced in T2D (Keating et al., 2008, Peiris et al., 2012, Peiris et al., 2016). Furthermore, RCAN1.1 and RCAN1.4 are expressed in both *db/db* mice islets (Figure 1.20B) and human islets (Figure 1.20C). Of the two isoforms of RCAN1, RCAN1.1 is expressed 10-fold more than RCAN1.4 in *db/db* islets (Figure 1.20B) which strengthens human T2D gene expression data implicating RCAN1 as a strong candidate for roles in T2D (Peiris et al., 2014).

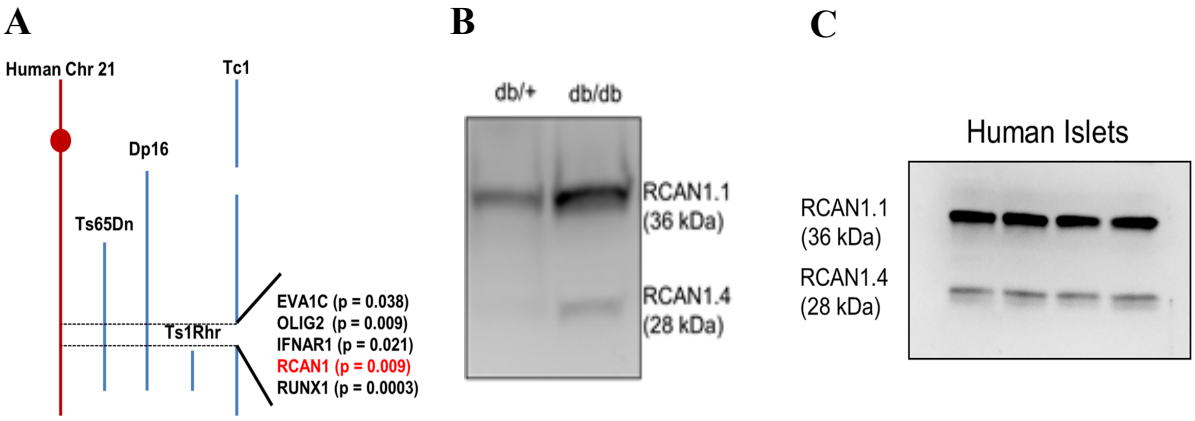

Figure 1.20 RCAN1 is linked to hyperglycemia. **(A)** Five genes linked to hyperglycemia in DS models trisomic regions, only RCAN1 increased in human islets with T2D **(B)** RCAN1.1 was expressed 10-fold more than RCAN1.4 in *db/db* mice **(C)** this is similar to increased RCAN1.1 expression compared to RCAN1.4 in human islets (Peiris et al., 2016).

Furthermore, *RCAN1* accounted for the top 13% most highly expressed gene in human islets (Fadista et al., 2014). There is a strong genetic basis for *RCAN1* gene as a candidate for T2D in β-cells. DNA methylation data from human islets is informative on how RCAN1 expression is increased in β-cells. At three different sites in the mouse islets, *RCAN1* methylation was reciprocal of RCAN1 expression

in human islets; increased RCAN1 expression at these same sites correlated with RCAN1 methylation status which was reduced in T2D islets (Dayeh et al., 2014). Our mouse model overexpressing RCAN1 is further validated by other independent studies also showing β-cell defects due to RCAN1 overexpression. Such studies include transient overexpression of RCAN1 decreasing GSIS in β-cell *in vitro* (Kim et al., 2011), β-cell number and islet size was significantly reduced in a RCAN1^{ox} line (Peiris et al., 2012). Additionally mice created independently of our study also exert β-cell changes (Gurda et al., 2015). RCAN1 expression is linked to hyperglycemia in DS mice, worsening metabolic proliferation in obese mice. The combination of data from both human and mouse studies therefore show that RCAN1 is implicated in the pathogenesis of T2D. In the next sub-section, our lab had shown that overexpression in RCAN1 is indeed a contributor to T2D.

1.7.2.2 RCAN1 is implicated in T2D

Overexpression of human RCAN1.1 isoform in mice causes diabetes, age-associated hyperglycemia (Figure 1.21A**),** reduced glucose tolerance, hypoinsulinemia, reduced islet size (Figure 1.21B), resulting from a reduction in total β-cell per islet (Figure 1.21C**),** not actual reduction of β-cell size itself (Figure 1.21D) and increased mitochondrial ROS production (Peiris et al., 2012). RCAN1 regulates β-cell proliferation; the reduced islet size of the RCAN1^{ox} can also be attributed to the reduction in β-cell proliferation (unpublished data from our lab, not shown).

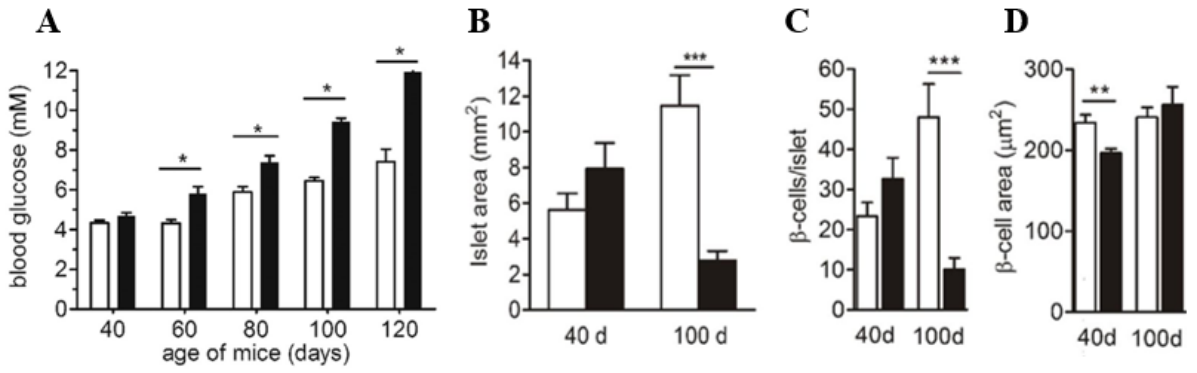

Figure 1.21 Diabetes worsen with age in RCAN1^{ox} mice. **(A)** RCAN1^{ox} mice had age-dependent diabetes. Pancreatic islets from WT and RCAN1^{ox} were stained for insulin and **(B)** islet size was significantly smaller for RCAN1^{ox} in aged mice at the 100th day time point compared to WT control, consistent with this **(C)** the number of β-cell islet was reduced and **(D)** there was no reduction in actual β-cell size at the 100th day time point for RCAN1^{ox} (Peiris et al., 2012). *White bars, WT; Black bars, mice overexpressing RCAN1.1 (RCAN1^{ox}).*

1.7.2.3 RCAN1 is implicated in β-cell mitochondrial dysfunction

In β-cells mitochondria function is key to GSIS and RCAN1 has a role in its regulation (Peiris et al., 2014) such as mitochondrial autophagy (Ermak et al., 2012), mitochondrial DNA content, number and size of mitochondria and mitochondrial enzymatic activities (Chang and Min, 2005). In RCAN1.1 overexpressed mice (RCAN1^{ox}), the mitochondrial electrochemical gradient is changed and there is a decline in insulin secretion both *in vivo* and *in vitro*. These mice have overt diabetes characterized by hypoinsulinemia, decreased β-cell number and mitochondria dysfunction. In islets of RCAN1^{ox} mice, mitochondrial respiration is reduced and is not attributed to changes in ETC proteins or decrease in mitochondrial mass. Furthermore, in RCAN1^{ox} mice there was a reduction in GSIS *in vivo* (Figure 1.22A) and *in vitro* (Figure 1.22B) and, reduced succinate-induced secretion (Figure 1.22C), reduced mitochondrial respiration and reduced ATP levels (Figure 1.22D) through downregulation of the ATP-ADP ratio. The decrease in mitochondrial respiration in RCAN1^{ox} islets is due to apparent mitochondrial dysfunction. The reduction of ATP causes reduction in depolarization-induced insulin exocytosis (Peiris et al., 2016). As ATP is necessary for vesicle transport in β-cells and membrane capacitance measurement of RCAN1^{ox}, using a series of depolarizing pulses increased membrane capacitance in both WT and RCAN1^{ox} β-cells due to insulin exocytosis, however, insulin secretion was not sustained in RCAN1^{ox} β-cells (Figure 1.22E). A lack of ATP decreases vesicle fusion.

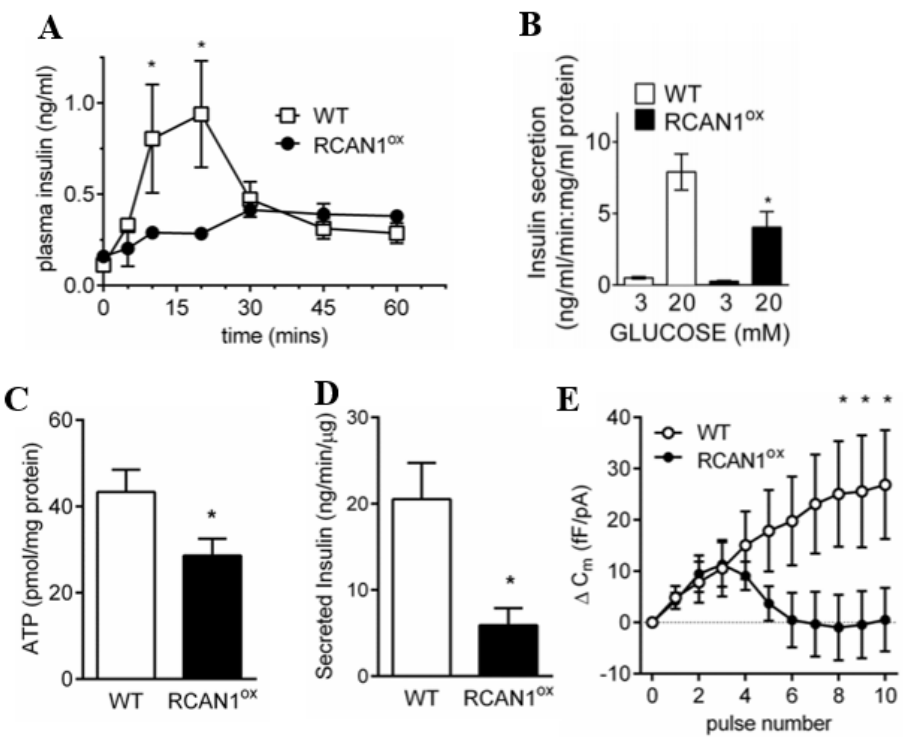

Figure 1.22 Overexpression of RCAN1 reduces GSIS in **(A)** cells and **(B)** in mice, **(C)** reduced succinate-induced insulin secretion, **(D)** ATP levels in islets of WT and RCAN1^{ox} mice **(E)** average capacitance change at each depolarizing pulse in islets of WT and RCAN1^{ox} mice (Peiris et al., 2016).

1.7.2.4 *Rcan1* regulates obesity, adipocyte function, metabolism and thermogenesis

Strong evidence exists for exploring the role of RCAN1 in the CN-dependent signalling in the adipose tissue to combat obesity and T2D. On a cellular level, CN has roles in adipocyte differentiation. Adipocyte differentiation in mature 3T3-L1 adipocytes is promoted through elevated PPARγ and the binding of NFAT4 binds to adipocyte protein 2 (AP-2) promoter (Ho et al., 1998). Knocking out *Nfat2* and *Nfat4* in mice resulted in a lean phenotype and resistance to diet-induced obesity. These mice also had reduced adiposity, heightened glucose and insulin sensitivity (Yang et al., 2006a). Additionally, NFAT has targets that are central to metabolism (Lawrence et al., 2002, Yang et al., 2006a, Soleimanpour et al., 2010). This demonstrates that NFAT signalling has a role in maintaining glucose and insulin homeostasis. Moreover, the promoter region of *G0S2*, a lipolysis gene, contains potential site for the transcription factor NFAT (Heckmann et al., 2013). Prostaglandin F2α (PGF2α), a potent biological inhibitor of adipocyte differentiation, is elevated in chronic obesity-induced inflammation (Liu and Clipstone, 2007) preventing adipocyte differentiation acting using its Gq-coupled FP prostanoid receptor which specifically binds CN (Liang et al., 2004) in the CN/NFAT pathway, thereby negatively regulating adipocyte differentiation (Neal and Clipstone, 2002).

The use of the CN inhibitor, CsA, elevated inhibition of differentiation of adipocytes and lipid accumulation in 3T3-L1 pre-adipocytes (Neal and Clipstone, 2002). This could contribute to the obesogenic effects such as weight gain and development of diabetes, well established in patients who use CN inhibitors for immunosuppression post-transplantation (Heisel et al., 2004). Polymorphisms in the NFATc4 locus is linked to increased risk for diabetes in post-transplant patients (Chen et al., 2012). Furthermore, CN can activate cAMP response element binding protein (CREB)-regulated transcription co-activator (CRTCs). CREB/CRTC cellular effects are essential to the metabolism of insulin-sensitive tissues such as the pancreas and adipose tissue (Altarejos and Montminy, 2011). CRTC3 isoforms are linked to adiposity (Song et al., 2010) and cholesterol levels (Ou et al., 2014).

Even though no GWAS studies in human has directly linked RCAN1 to metabolic disorders, SNPs at the locus had strong correlation to climate adaptation (Hancock et al., 2008) and QTL studies in cattle had strong links between RCAN1 and multiple adipose tissue traits (Dodson et al., 2010). Furthermore, the gene encoding the catalytic subunit of CN is linked to human BMI and insulin in serum (Ramos et al., 2014). The catalytic subunit of CnA encoded by the PPP3CA locus was found to be associated with both BMI and serum insulin levels in a human genome-wide association study (GWAS) (Harms and Seale, 2013, Ramos et al., 2014, Lee et al., 2014). Several obesity related genes are implicated in cancer and one of these genes is RCAN1 (Sebio et al., 2015). Taking these into account, CN has a role in metabolism and the study of RCAN1 could help garner understanding of the mechanisms underlying this. Therefore, CN-dependent signalling (e.g.CN/NFAT pathway) is implicated in metabolic regulation, however, underlying mechanisms are unknown. Our lab has published data implicating

RCAN1 in obesity, adipocyte metabolism and thermogenesis (Rotter et al., 2018) that could have therapeutic outcomes for obese patients and those with T2D.

1.7.2.5 *Rcan1*$^{-/-}$ mice are resistant to diet-induced obesity and inflammation and had increased metabolism

Rcan1 was shown to regulate fat mass; *Rcan1* knock out (KO; *Rcan1*$^{-/-}$) mice did not gain weight despite being on a high fat diet (Figure 1.23A), not due to reduced food intake, absorption of ingested fat or level of physical activity (Rotter et al., 2018). To further confirm this, MRI scans showed less fat in *Rcan1*$^{-/-}$ mice than controls after 8 weeks on a HFD (Figure 1.23B) and had less body fat volume (Figure 1.23C). Inflammation in WAT usually occurs prior to the onset of T2D and gene expression of inflammatory markers (*Tnfα*, *Tnfβ*, *Mcp-1* and *F480*) in gWAT of KO mice were normal regardless of diet, compared to WT which showed an increase in these inflammatory markers (Figure 1.23D). While WT mice on a HFD had increased leptin levels, KO did not (Figure 1.23E), consistent with the increase in body mass of WT mice on a HFD as leptin levels correlated with the amount of body fat. Additionally, these mice had improved peripheral insulin sensitivity as their glucose tolerance was not impaired (Rotter et al., 2018), therefore these KO mice were shown to be protected from age-dependent decline in glucose metabolism and handling. Metabolism for these mice were increased, shown by a higher resting energy expenditure (REE) when there was an increase in O_2 consumption (Figure 1.23F) and CO_2 production (Figure 1.23G) in *Rcan1*$^{-/-}$ mice not due to respiratory exchange ratio (Figure 1.23H) or reduced physical activity (Figure 1.23I), indicating that these mice are protected from obesity on a HFD compared to controls. Furthermore, expression of RCAN1 in adipose tissue of these mice correlated to body weight insulin and triglycerides from another data set (Figure 1.23J). Overall, the data is indicative of the benefits of targeting the adipose tissue.

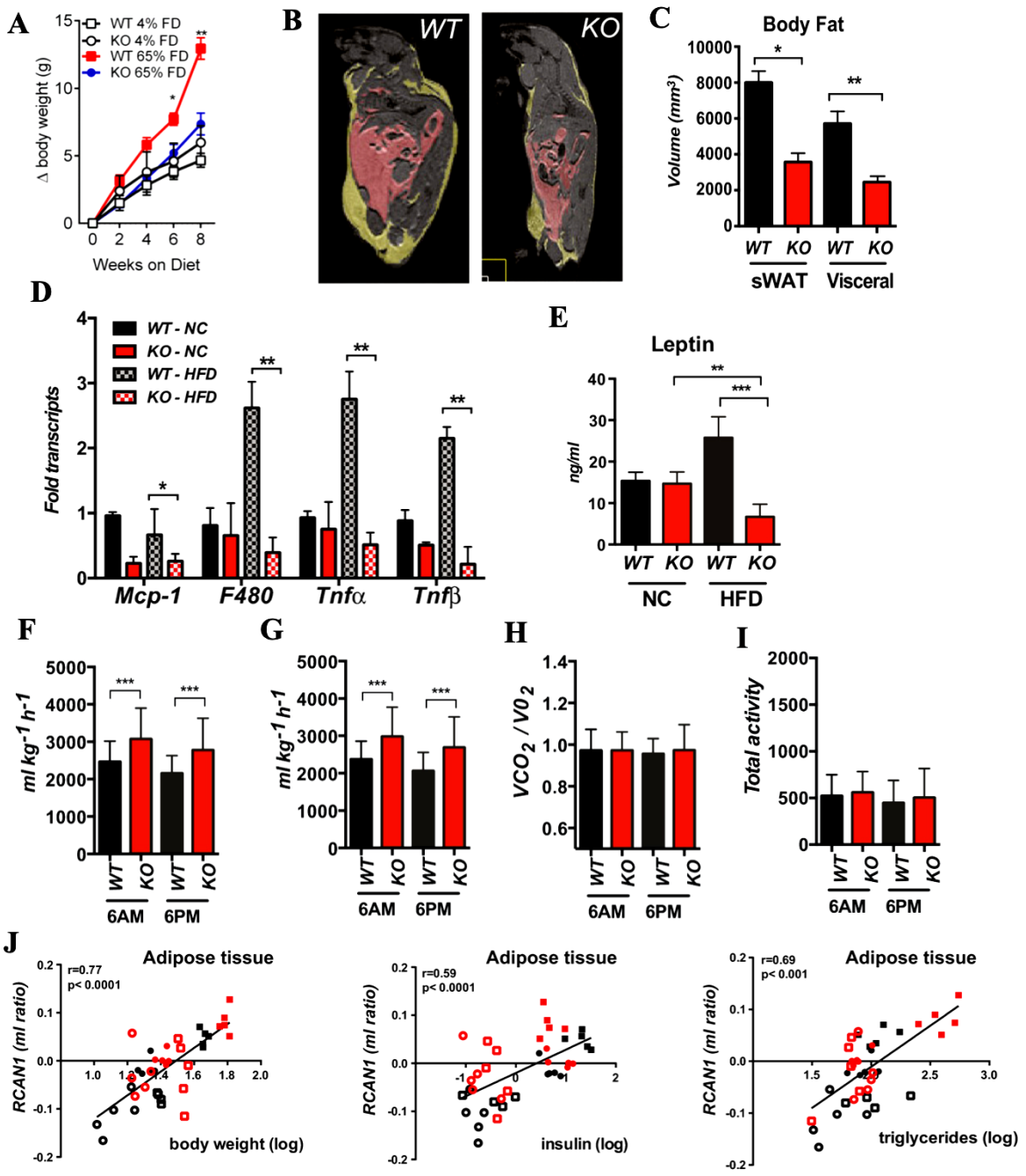

Figure 1.23 *Rcan1*$^{-/-}$ are resistant to diet induced obesity and had increased metabolism (Rotter et al., 2018). **(A)** *Rcan1* KO mice gain less weight on a HFD **(B)** illustrated in MRI scans and **(C)** KO mice had significantly reduced subcutaneous and visceral depots. **(D)** Expression of inflammatory markers in gWAT was absent in KO mice. **(E)** Serum leptin decreased in KO on a HFD. **(F)** Oxygen consumption **(G)** and carbon dioxide production were increased in *Rcan1* KO while **(H)** respiratory exchange ratio (RER) and **(I)** total physical activity were unchanged between KO and WT mice. **(J)** *RCAN1* was correlated to the expression in the adipose tissue with body weight, triglycerides and insulin in tissues from lean and obese mouse strains resistant or susceptible to diabetes from another data set (Keller et al., 2008).

1.7.2.6 RCAN1 has a cell autonomous role in adipocytes and regulates thermogenic processes

Metabolic homeostasis is vital for normal body weight, survival and heat generation such as thermogenesis (Bouret et al., 2015). Responsive thermogenic process involves an uprise in energy expenditure due to stimuli (e.g. cold) causes an activation of *UCP1* to generate heat in brown adipose tissue instead of ATP. Low levels of UCP1 is linked to genetic obesity (Nedergaard et al., 2001).

RCAN1 has adipose tissue autonomous role in the induction of white adipocytes transformed into brown adipocytes, via inhibition of adipocyte differentiation toward a brown phenotype. This can be seen in sWAT where cold-induced mice in KO mice had more browning in white adipose tissue compared to WT mice (Figure 1.24A). This is because *Rcan1*$^{-/-}$ mice had increase activation of adaptive thermogenesis in WAT in response to temperature or diet. RCAN1 has a role in inhibiting diet and cold induced thermogenesis in adipose tissue through the *Pgc1α/Ucp1* axis. *Pgc1α* is necessary for activation of cold-induced adaptive thermogenesis at the transcriptional level in BAT (Puigserver et al., 1998). After 1 day of cold exposure, transcript levels of *Pgc1α* and *UCP1* in WAT of female mice were increased in *Rcan1*$^{-/-}$ compared to WT (Figure 1.24 B, C). Diet-induced beiging of WAT in response to chronic HFD was increased in KO mice shown by the upregulation of *Pgc1α*, *Ucp1* and *Adrb3* transcripts (Figure 1.24 D).

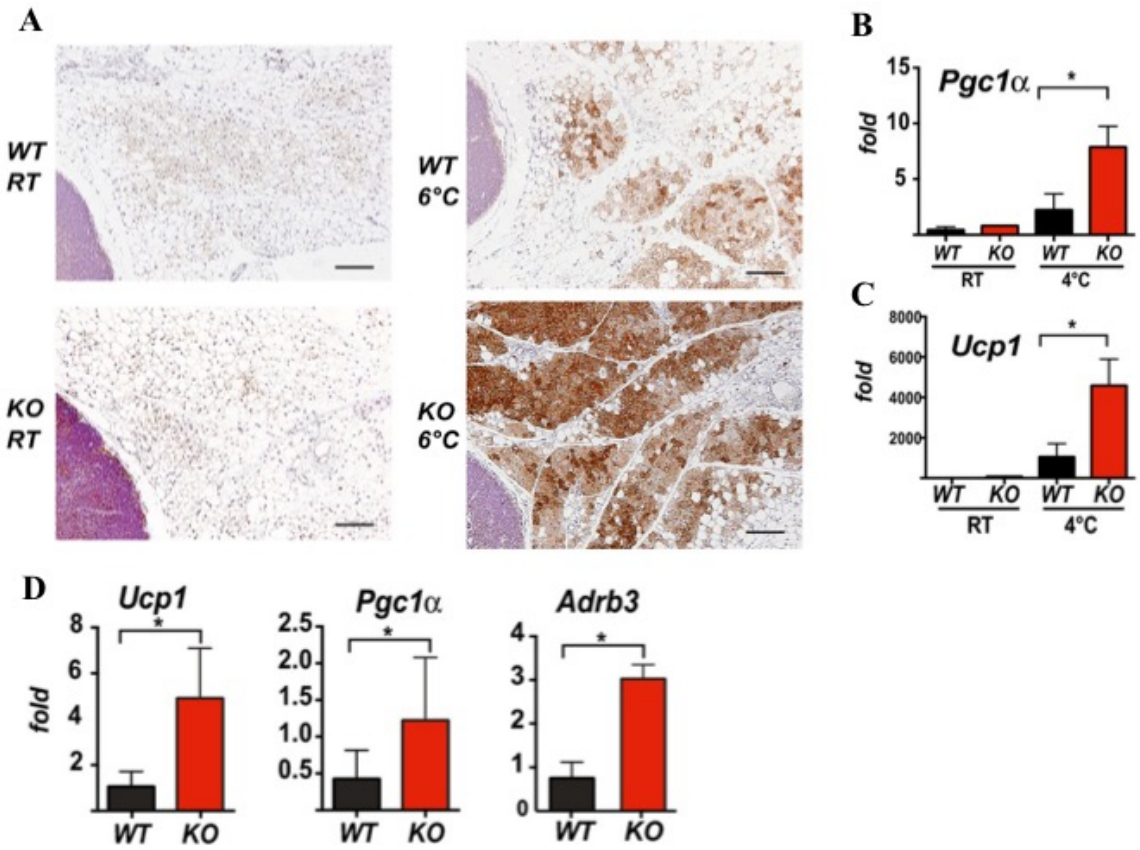

Figure 1.24 RCAN1 has a cell autonomous role in adipocytes, control and regulate thermogenic processes (Rotter et al., 2018). **(A)** H&E histological section of sWAT from KO and WT stained against *Ucp1* of KO and WT mice house at RT and 6 degrees for 5 days increased browning in KO at 6 degrees **(B)** Transcript levels of *Pgc1α* and **(C)** *Ucp1* in sWAT of female WT and *Rcan1*$^{-/-}$ mice after 1 day of RT or cold-induction (4 degrees) **(D)** Transcript level of *Ucp1*, *Pgc1a* and *Adrb3* were upregulated in sWAT of *Rcan1*$^{-/-}$ mice, compared to WT after 25 weeks on a HFD.

Moreover, *Rcan1*$^{-/-}$ mice had increased basal lipolysis and decreased activated lipolysis (Figure 1.25), which could explain their lean phenotype. Knocking down *Rcan1* in the 3T3-L1 adipocyte cell line reduced lipid content for both *Rcan1* isoforms. siRNA targeting *Rcan1.1* and *Rcan1.4* isoforms successfully knocked down RCAN1 transcripts (Figure 1.26A) prior to differentiation. Differentiation was not inhibited by the deletion of *Rcan1* as adiponectin release into media at a similar time. Oil Red-O staining quantified lipid droplets within cells, showing a significant decrease in *Rcan1.1* knocked down adipocytes compared to control (Figure 1.26B). These findings implicate RCAN1 which has a novel role in adipocyte biology (Rotter et al., 2018).

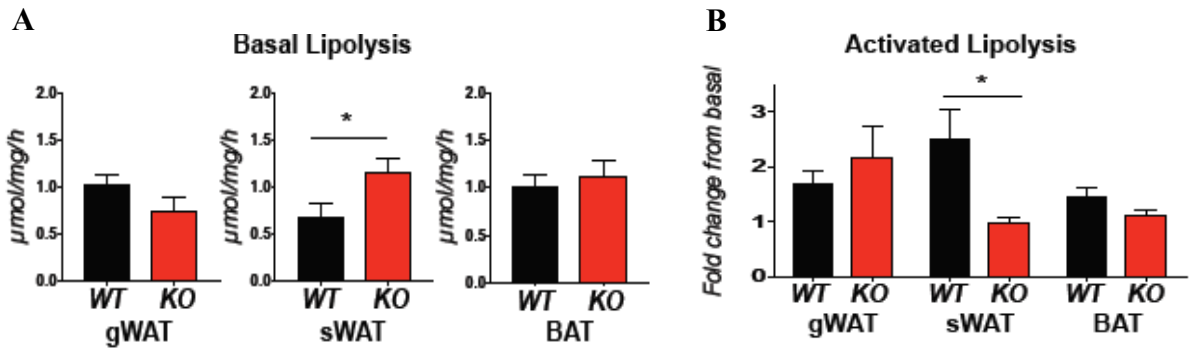

Figure 1.25 Basal and activated lipolysis showed significant changes between WT and KO in sWAT. **(A)** Basal rates of lipolysis in sWAT tissue explants from *Rcan1*$^{-/-}$ (KO) and *Rcan1*$^{+/+}$ (WT) mice **(B)** lipolysis fold change after administration of adrenergic stimulation (males, n=5, ± SEM) *P<0.05 (t-test in A; two-way ANOVA with multiple comparisons in B). gWAT: gonadal fat pads, sWAT: subcutaneous WAT, BAT: brown adipose tissue (Rotter et al., 2018).

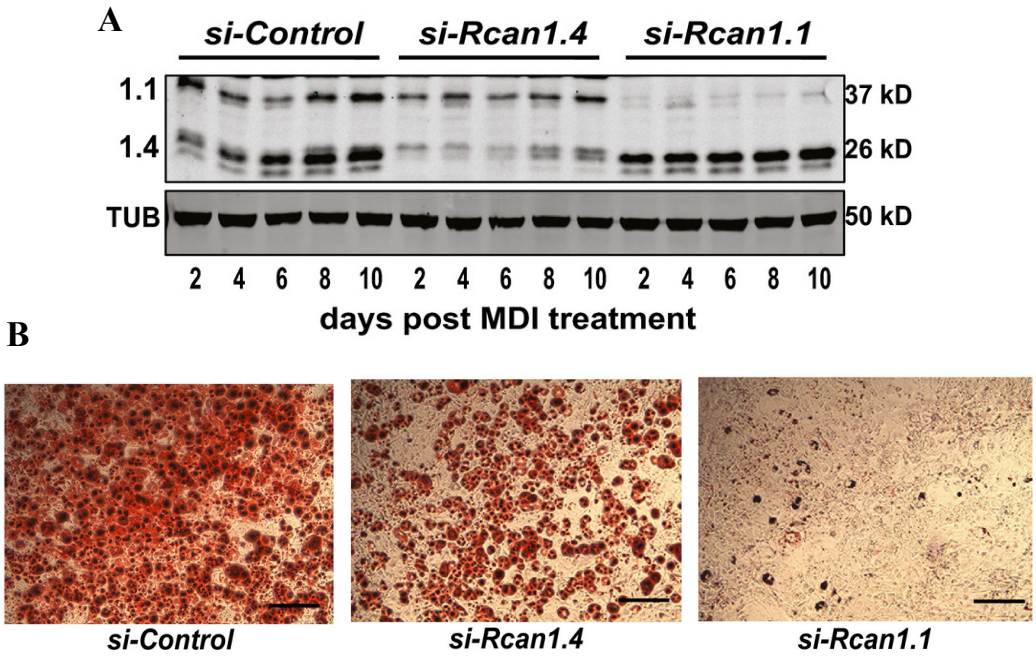

Figure 1.26 *Rcan1.1* decreased more lipids than *Rcan1.4*. **(A)**Western blot of *Rcan1* knockdown in 3T3-L1 adipocyte cell line showed the presence of both *Rcan1.1* and *Rcan1.4*. **(B)** 3T3-L1 cells were stained with Oil Red-O and the knock down of isoforms *Rcan1.1* and *Rcan1.4* reduced lipid storage compared to control.

These anti-obesity properties seen in *Rcan1*$^{-/-}$ mice might be beneficial for patients with DS who has increased adiposity and insulin resistance (Flore et al., 2008, Basil et al., 2016) and reduced resting energy expenditure (Hill et al., 2013). The overexpression of *Rcan1* in the pancreas led to β-cell mitochondrial dysfunction and *Rcan1* methylation is reduced at multiple sites in human T2D islets and correlated with RCAN1 expression in T2D islets. The absence of RCAN1 in mice protected it from diet-induced obesity, inflammation and had increased browning upon cold exposure indicative of thermogenic modulation. Metabolism of these mice were also increased. Therefore, knocking out *Rcan1* in metabolic tissues (e.g. pancreas and adipose tissue) could be therapeutic and inhibitors of RCAN1 that inhibits CN but not CN activity (Chan et al., 2005) could be beneficial for people with metabolic conditions such as T2D. This is discussed in the next section.

1.8 Therapeutics for T2D and Obesity: IRCA drugs inhibit RCAN1-Calcineurin interaction

To date, the mode of management of T2D focuses on reducing the effects of insulin resistance such as lifestyle and dietary transformation in addition to drug use to improve glycaemic control, reducing initial postprandial high blood glucose or improving insulin output. Pharmacological interventions like sulphonylureas or metformin, the most common drugs prescribed for diabetic patients, do not reverse loss of β-cells (Rao et al., 2012). Moreover, the mechanism underlying metformin therapeutic effects is still unclear. Lifestyle modifications and exercise are the prescribed treatment for obesity management, however, adherence to such methods are not always successful. While these treatments achieve partial effectiveness, many patients do not fully recover normal insulin levels. The advancement of therapeutic approaches using precision medicine is still a long way (Groop, 2016), therefore, despite the myriad of therapeutics available in the market there is still no cure for T2D. The evidence for the role RCAN1 in diabetes and obesity is on the rise. Inhibiting RCAN1 without disrupting CN activity could allow for better understanding of the pathology behind T2D so that T2D and associated risk factor, obesity, could be reduced.

A florescence-based binding assay in a high throughput screen of approximately 32,000 small molecules identified 5 lead compounds known as inhibitors of RCAN1-calcineurin association (IRCA) 1 to 5. These IRCA 1-5 drugs have the ability to dose-dependently interrupt the interaction between RCAN1 and CN at various potencies. These IRCA drugs were shown to rescue CN activity in the presence of exon 7 of RCAN1. IRCA4 fully restored CN activity at the lowest concentration tested (100nM) (Chan, 2007). Importantly, IRCA 1-5 inhibited the RCAN1-CN interaction but not CN activity (Figure 1.27). This is in contrast to immunosuppressive drugs cyclosporine A (CsA) and tacrolimus (FK506) that inhibits CN activity, inducing acute irreversible β-cell dysfunction and diabetes (Weir and Fink, 1999).

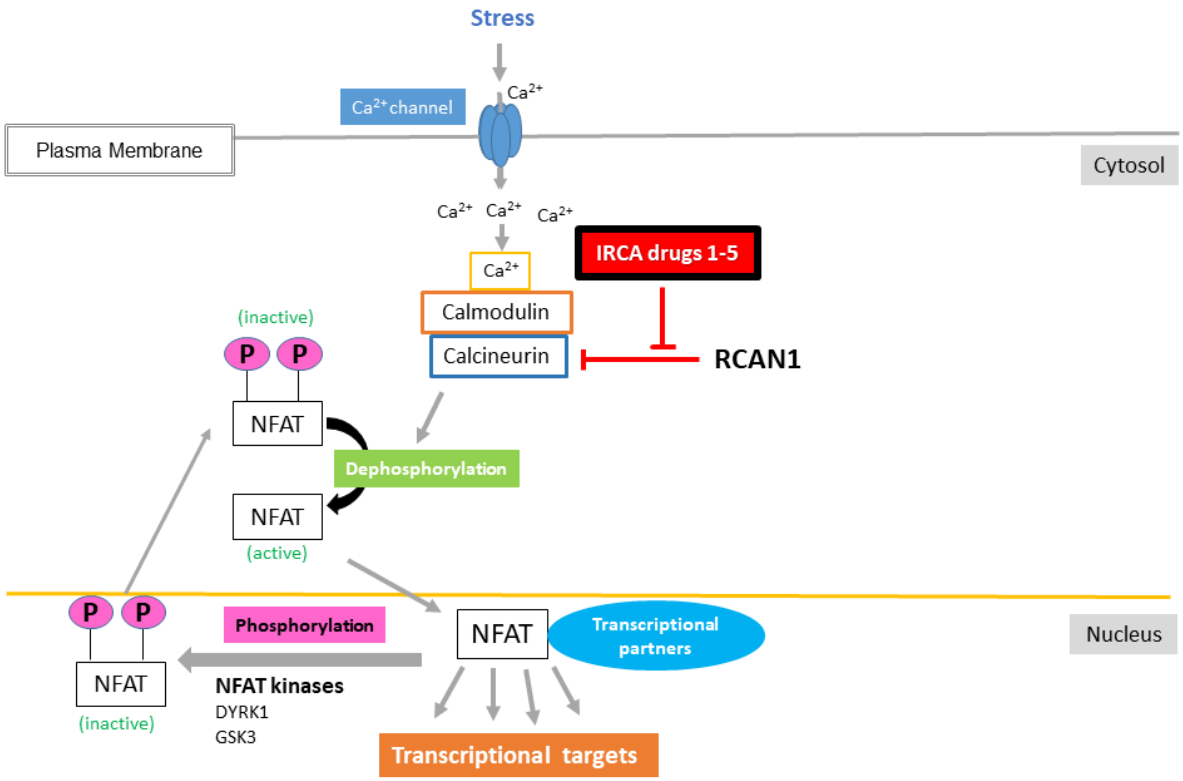

Figure 1.27 Inhibitors of RCAN1 (IRCA drugs 1-5) inhibiting RCAN1.

From the preliminary data in our lab (Figure 1.28), the inhibition of RCAN1 using these drugs could possibly reduce obesity and T2D β-cell dysfunction (Peiris et al., 2016, Rotter et al., 2018). The *Rcan1*$^{-/-}$ mice knocks out *Rcan1* throughout the whole mice and excludes tissue-specific effects of knocking out RCAN1. We hope to achieve similar results as those observed in the *Rcan1*$^{-/-}$ mice when using these IRCA drugs to inhibit RCAN1 in the adipose tissue and pancreatic β-cells. To our knowledge, no research has tested these drugs *in vivo*, inhibiting RCAN1 as a possible therapy for diabetes and obesity in humans through translational research surrounding the regulation of adipocyte biology, reversal of β-cell dysfunction and improvement of metabolic profiles of the obese mouse. Preliminary findings from our lab showed that these drugs can inhibit lipid accumulation in adipocyte cells (Figure 1.28). However, specific lipid pathways implicated is unknown and IRCA drug effects in pancreatic β-cells are unknown.

With the identification of RCAN1's role in reducing insulin secretion in mice with overexpressed *Rcan1* gene, IRCA drugs may be able to improve insulin secretion and serve as a novel therapeutic target for T2D. Furthermore, current drugs act to merely alleviate the symptoms of T2D rather than cure T2D. IRCA drugs maybe be able to reverse and even prevent T2D. Individuals with DS and AD might be able to use IRCA drugs to improve β-cell function, thereby, aiding symptoms associated with T2D.

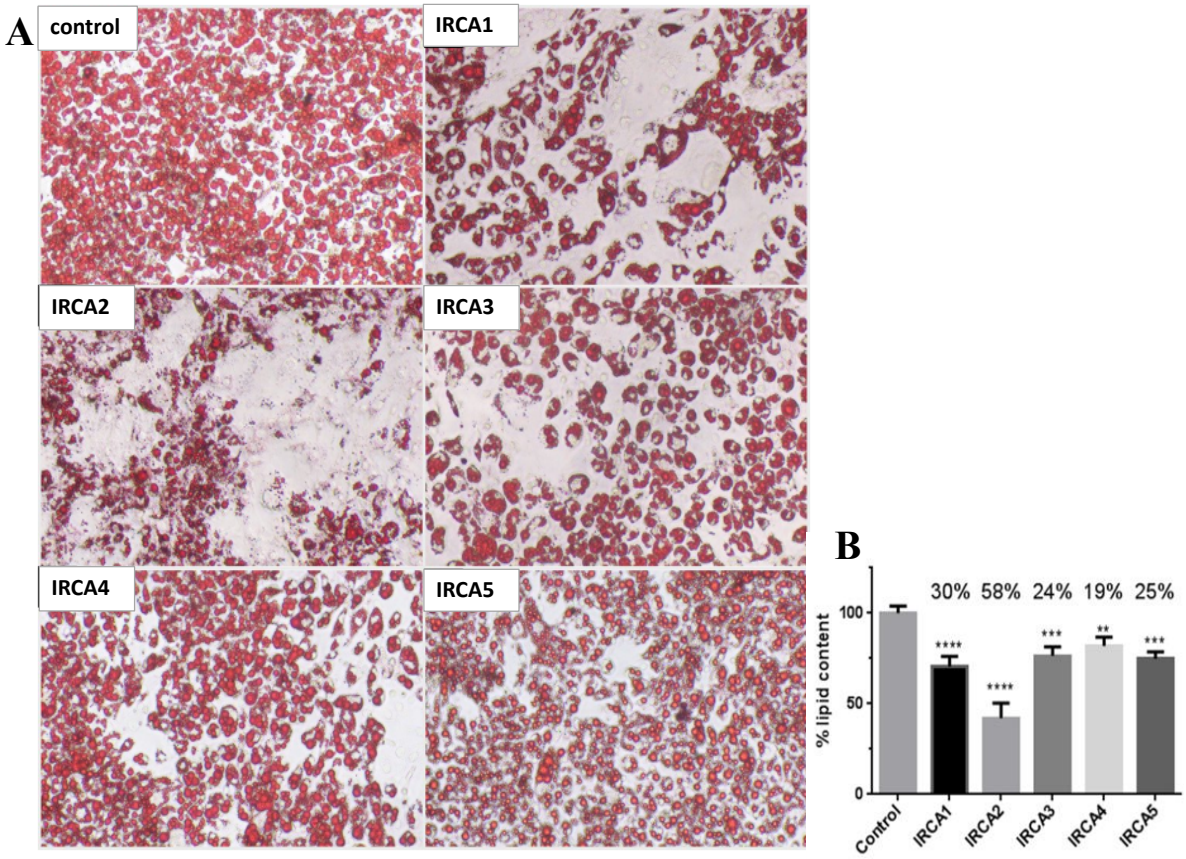

Figure 1.28 Preliminary data of 3T3-L1 cells treated with IRCA1-IRCA5 drugs stained with Oil Red-O (n=6). **(A)** IRCA1-5 drugs at 1x the K_i were applied on the fully differentiated 3T3-L1 cells for 6 days followed by staining with the Oil Red-O assay compared to control **(B)** Graphical representation of data in (A) showed a decrease in lipid content. IRCA1 showed 30%, IRCA2, 58%, IRCA3, 24%, IRCA4, 19% and IRCA5, 25% decrease in lipid content compared to control. The One-way ANOVA was used for the statistical determination of significance, $P<0.0001$ (Unpublished data).

Table 1.3 IRCA drugs inhibition potencies (Chan, 2007)

IRCA DRUGS	Inhibition potencies (K_i) of IRCAs (μM)
IRCA1	0.99±0.19
IRCA2	2.24±0.26
IRCA3	2.89±0.58
IRCA4	2.49±0.36
IRCA5	1.36±0.20

1.9 Project aims

This project will test the effect of these drugs on the function of β-cell and adipocyte cell lines. This will provide proof-of-principle data for the *in vivo* testing of these drugs in mice and in mouse models of T2D and obesity.

Overarching hypothesis: inhibition of calcineurin through RCAN1 causes the dysfunction of both β-cells and the adipose tissue in obesity and T2D.

Therefore, this Masters project aims to:

Aim 1: To determine the effective minimum concentration of IRCA drugs in reducing fat storage in the 3T3-L1 adipocyte cell line.

Aim 2: To determine the effective minimum concentration of IRCA drugs on proliferation and apoptosis of the β-TC6 cell line.

Aim 3: To determine the expression of lipolysis-, lipogenesis- and adipogenesis- related genes in epididymal white adipose tissue (eWAT) from *Rcan1*$^{-/-}$ mice and WT mice on a low-fat diet (LFD) and a high-fat diet (HFD).

Aim 4: To investigate factors that may regulate *Rcan1* expression in 3T3-L1 cells.

Chapter 2. GENERAL MATERIALS AND METHODS

2.1 IRCA drug preparation

Through a fluoresce based binding assay, a high throughput screening of approximately 32,000 small molecules were used to identify small molecules that inhibit the RCAN1- calcineurin interaction. Through this assay, a total of five lead compounds dose-dependently interfere with the RCAN1-calcineurin interaction (K_i values in Table 2.1) and are termed inhibitors of **R**CAN1-**c**alcineurin **a**ssociation (IRCA) (Chan, 2007). The IRCA drugs were prepared as a 100,000x stock concentration and dissolved in a volume of DMSO. Due to poor solubility of IRCA2 and IRCA5, these drugs were diluted down to 50,000xK_i and 10,000xK_i stock respectively. DMSO was use as a control for all experiments dealing with IRCA drug use. Serial dilutions were undertaken to achieve drug concentrations of 1,000xK_i, 100xK_i, 10xK_i and 1xK_i. All drug were aliquoted and stored at -20°C.

Table 2.1 IRCA drug concentrations

	Concentration (µM) x1000µM	Supplier
IRCA1	0.99	Sigma- Aldrich
IRCA2	2.24	Ambinter
IRCA3	2.89	USP reference standard
IRCA4	2.49	Ambinter
IRCA5	1.36	Ambinter

2.2 3T3-L1 cell line

2.2.1 Media preparation for 3T3-L1 cells

The maintenance media was prepared when required and supplemented accordingly (Table 2.2). The Fetal bovine serum that is mesenchymal stem cell-qualified (FBS-MSC) media, stored at -80°C, were aliquoted into 50mL aliquots, thawed at room temperature and heat-inactivated for half an hour at 56°C water bath. Prepared aliquots were stored at -20°C until required. Media preparation involved the supplementation of 50 mL of heat-inactivated FBS-MSC and 5 mL of *Penicillin* (10^5 Units/mL) /*Streptomycin* (10^5 µg/mL) to the DMEM (high glucose 4.5g/L) (500mL).

Table 2.2 Maintenance medium constituents

Components	Volume	Supplier
DMEM (high glucose 4.5g/L)	500mL	Gibco by Life technologies ThermoFisher Scientific, Australia
Fetal Bovine Serum, mesenchymal stem cell-qualified (FBS-MSC)	50 mL (10%)	ThermoFisher Scientific, USA
Penicillin, 10^5 Units/mL: Streptomycin, 10^5 µg/mL (100x Pen/Strep)	5 mL	ThermoFisher Scientific, USA

2.2.2 Seeding 3T3-L1 cells from liquid nitrogen storage

The 3T3-L1 cells (Passage 12) (ATCC) is a cell line derived through clonal isolation (Green and Kehinde, 1974, Zebisch et al., 2012) and obtained from Professor David James (Charles Perkins Centre, Sydney) and stored in liquid nitrogen. Using 1.8µL cryovials (Corning) that contained 1.5mL of cells (passage 12-15) was thawed on ice from the liquid nitrogen storage. All of the cells were transferred to a 15mL tube 1.5mL of pre-warmed maintenance media was added drop by drop over 5 minutes so as to not shock the cells. The cells were left to sit at room temperature for 5 minutes to calibrate and additional pre-warmed maintenance media topped up cells to the 10mL mark slowly. The cells were centrifuged at 400xg for 5 minutes and the supernatant was replaced with 1mL of fresh maintenance media. The tube was gently flicked to resuspend the cells in media and transferred into a T25 flask, incubated at 37°C and 5% CO_2 (SANYO CO_2 incubator). The media was changed every 3rd day by taking out ¾ of media from the flask and replacing it with fresh media of the same volume.

2.2.3 Subculturing, splitting and maintenance of the 3T3-L1 cell line

The cells were rinsed with PBS to remove all of the excess media. Trypsin 0.05%/ EDTA (Gibco, Thermofisher) 2mL was added and the flask was incubated for 2 minutes. Maintenance media (Table 2.2) was added to the cells to stop trypsin enzymatic action, all cells were transferred into a 15 mL tube, topped up to 10mL with media and centrifuged at 400 x g for 5 minutes. The supernatant was discarded and replaced with 10mL. The 3T3-L1 cells were subcultured in 1:4 in a 70% confluent flask of cells and split every three days.

2.2.4 Seeding cells, cell viability and cell count

A trypan blue cell viability test was performed along with a cell count prior to plating cells. The cells were washed in PBS once to remove medium that inhibits trypsin action. After which, 2mL of 0.25% trypsin (in EDTA) was added to the flask for 2 minutes. While lightly hitting the flask, cells were

removed from the inner flask surface observed under a light microscope. The cytoplasm in non-viable cells appear dark blue, stained with trypan blue.

The 3T3-L1 cells were seeded at 2000 cells/well in 100µl in a 96 well plate. Once seeded, cells were left to become confluent for 3 days before the media was replaced with differentiation media for another 3 days (Table 2.3).

Table 2.3 Differentiation media constituents

Components	In 50mL of media (µL)
Dexamethasone: 10,000x stock at 2.2mM	5
Biotin: 1000x Stock at 100µg/mL	50
Insulin: 100x stock (bovine, Calbiochem)	25
Isobutyl-methyl-xanthine (IBMX): 1000x stock at 500mM	50

After which, the differentiation media was replaced with post-differentiation media for 3 days (Table 2.4). After 3 days of post-differentiation media, the 3T3L1 cells are fully differentiated and they were treated with IRCA drug diluted in media, for 6 days, replaced daily.

Table 2.4 Post-differentiation media constituents

Components	Volume (µL)
DMEM (high glucose 4.5g/L) + 10% (FBS-MSC)	10000
Insulin: 100x stock (bovine, callbiochem)	5

2.3 MTT assay

The Vybrant® MTT (3-(4,5-Dimethylthiazol-2-yl)-2,5-Diphenyltetrazolium Bromide) cell proliferation assay kit (ThermoFisher Scientific) was used according to manufacturer's protocol and modified as required. A 12mM MTT stock solution was made by adding 1mL of sterile warm PBS to one vial containing 5mg of MTT. This vial was then mixed by vortexing till the MTT dissolved. The remainder of the unused solution was stored light protected in aluminium foil at 4°C.

2.3.1 Principles of the MTT assay for cell growth and viability

The microculture Vybrant® 3-(4,5-dimethylthiazol-2-yl)-2,5-diphenyltetrazolium bromide assay (MTT) (Thermofisher Scientific) is a colorimetric test used to determine cell growth and viability (Mosmann, 1983). The MTT assay converts water soluble MTT (yellow) into an insoluble purple formazan (Berridge and Tan, 1993, Vistica et al., 1991, Liu et al., 1997). The MTT reduction is enclosed in intracellular vesicles that result in needle-like MTT formazan at the cell surface that are either endosomes or lysosomes. The cells take up MTT via endocytosis, followed by gathering of formazan in the endosomal or lysosomal vesicles that translocates to the cell surface during exocytosis (Liu et al., 1997). The formazan products accumulate in lipid droplets (Stockert et al., 2012). The reduction occurs due to the oxidoreductase enzymes that depends on NADH or NADPH inside the cells. DMSO is applied to break the vesicles containing the purple formazan that is released into the media to be measured with the plate reader (Stockert et al., 2012). This is a widely used test for cell viability as the amount of formazan formed correlates to the number of cells alive.

2.3.2 Labelling and quantitating MTT-labelled cells

The maintenance medium containing phenol red was removed and replaced with 100µL per well of fresh phenol red-free warm medium. A volume of 10µL of the previously prepared 12mM MTT solution was added to each well including the negative control wells. The plate was then incubated at 37°C for 4 hours. After which, 85µL of media was removed from each well and replaced with 85 µL of DMSO and mixed thoroughly using a pipette. Using a light microscope (Olympus CKX41 microscope), cells were checked to ensure that all purple pigment were released from their membranes and further pipetting was performed to disrupt membranes. The formation of bubbles was removed by centrifuging the plate that was sealed and spun for 2 minutes at 13,000 rpm (Eppendorf 5810R). The absorbance was read at 520nM using the Beckman Coulter-DTX 880 Multimode Detector.

The β-TC6 cells used this same assay, however, after the incubation step, 85µL of media was removed from each well and replaced with 50 µL of DMSO and mixed thoroughly using a pipette. The formation of bubbles was removed by centrifuging the plate that was sealed and spun for 2 minutes at 13,000 rpm (Eppendorf 5810R).

2.4 β-TC6 cell line

Laurance et al (1998) defined a β-cell line as one that has capabilities in sustaining insulin secretion (Laurance et al., 1998). The Beta-TC6 (β-TC6) (passage 33-40) (ATCC ® CRL-11506™) insulinoma cell line, a widely used model of actual β-cells and a gift from Claudine Bonder (UniSA), was used in our experiments. This cell line originated from insulinoma of a transgenic *Mus musculus* with simian virus 40 (SV40) large T antigen. The mouse had a pseudogene component made up of the SV40 early region regulated by the promoter of the rat insulin II gene that caused multiple β-cell insulinomas.

Hybrids of the two genes were created to link the DNA 5' coding region of the rat insulin II gene with the structural large-T antigen (Hanahan, 1985).

2.4.1 Media preparation for β-TC6 cells

Media preparation involved the supplementation of 89 mL of heat-inactivated FBS-MSC (15%), 6 mL of *Penicillin* (10^5 Units/mL) /*Streptomycin* (10^5 µg/mL) and 6 mL of GlutaMAX was supplemented to the DMEM (high glucose 4.5g/L) (500mL) (Table 2.5). The maintenance media for the β-TC6 cells were replaced twice a week and split once every week.

Table 2.5 Maintenance medium constituents

Components	Volume	Supplier
DMEM (high glucose 4.5g/L, 4nM L-gultamine, 1 mM sodium pyruvate, and 1500 mg/L sodium bicarbonate)	500mL	ATCC, USA
Sterile Fetal Bovine Serum (FBS) (15%)	89 mL	Bovogen, France
Penicillin, 10^5 Units/mL: Streptomycin, 10^5 µg/mL (100x Pen/Strep)	6 mL	ThermoFisher Scientific, USA
GlutaMAX (100x)	6 mL	ThermoFisher Scientific, USA

2.5 Primer selection and design

Primers were selected from previous publications as primers used for experiments are specific for their target. Additionally, all primers used in this thesis have undergone analysis in the Primer-BLAST primer design tool (National library of Medicine; NCBI) (Ye et al., 2012). Primer-BLAST is a software able to generate candidate primer pairs and check the target specificity of the generated primer pairs by placing candidate primers on various unique template regions not similar to other targets. This ensures quality control of the primers used in this thesis. All primers in this thesis were ordered as custom-made Oligonucleotides, in desalted form, from ThermoFisher Scientific (Australia).

2.6 Animals

The *Rcan1*$^{-/-}$ lines were derived from two independent origins, one without exons 5 and 6 (Vega et al., 2003) and the other had absent coding regions of exons 6 and 7 (Porta et al., 2007b). The mice were from a mixed 129SvJ x C57BL/6 genetic background, homozygous for a wild-type allele of the nicotimamide nucleotide transhydrogenase locus (*Nnt*), a mutation that can impair glucose homeostasis and upregulate weight on a HFD (Parker et al., 2009, Nicholson et al., 2010). Metabolic phenotype of

both lines were indistinguishable. The littermates form (*Het* x *Het*) crosses were used when available. While sibling mice form (*Het* x *Het*) crosses set up the (*Het x KO*) and (*WT xWT*) crosses to obtain the KO and WT animals in this experiment. Periodically, new breeding pairs were obtained from offspring of (*Het* x *Het*) crosses. All animals used in experiments were age-matched, one generation away from the founding (*Het* x *Het*) cross. Animals were housed at 23ºC under standard vivarium conditions under a 12:12-h light:dark cycle. Animals were allowed free access to water and were fed *ad libitum* either a normal chow diet (NC) which was low-fat diet (LFD), in which 4% of the caloric content derived from fat (LabDiet 5001), a high-fat diet (HFD) in which 35% of the calories derived from fat produced by Specialty Feeds (WA, Australia). Food consumption and body weight were recorded weekly. All animal procedures were carried out with the oversight and approval of the University's Institutional Animal Care and Use Committee and conformed to the current Guide for the Care and Use of Laboratory Animals, published by the National Institutes of Health. Unless otherwise noted, tissues were harvested between 10 AM and 2 PM. The mouse tissues used in this thesis were already extracted and frozen down or dissected out from the live animal. Breeding and maintenance of animals were managed by animal facility staff and by Dr Alyce Martin.

2.7 Experiments involving quantitative Real Time PCR (RT-PCR)

The flow charts detail the steps involved in obtaining the RNA and performing the RT-PCR from cell lines (Figure 2.1A) and from adipose tissue depots (Figure 2.1B).

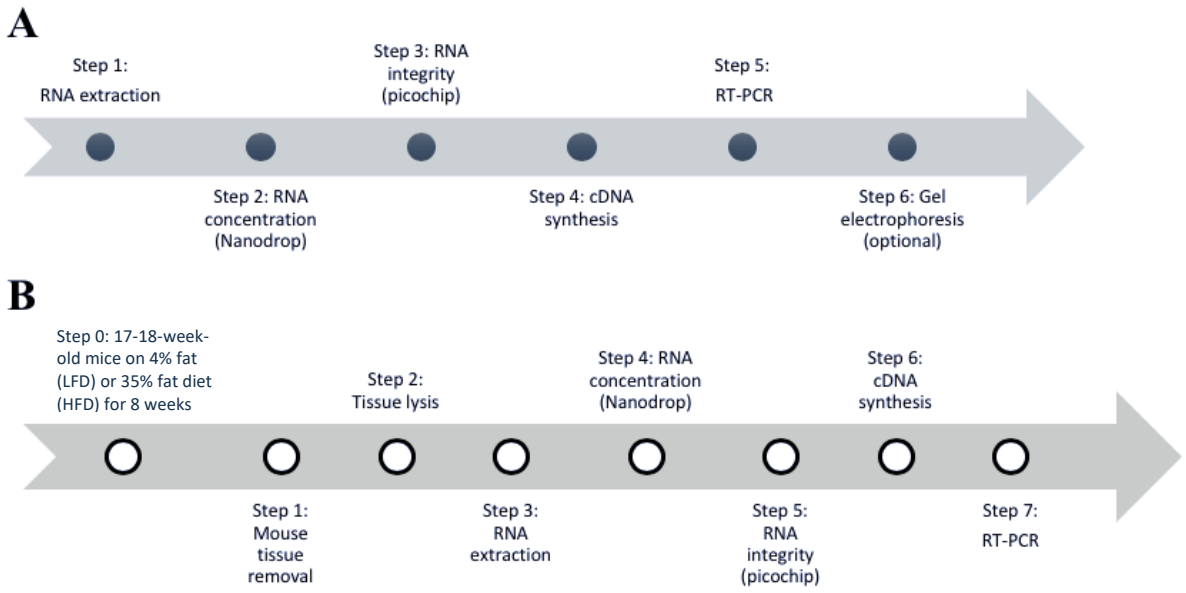

Figure 2.1 Summary of RT-PCR steps and RNA extraction from (A) cell lines and (B) adipose tissue depots.

2.7.1 Adipose tissue lysis and extraction of total RNA

Epididymal white adipose tissue (eWAT) which is the largest visceral adipose tissue linked to the epididymis and testis (de Jong et al., 2015) (Figure 1.4) was dissected from *Rcan1*$^{-/-}$ and WT mice of the different diets and immediately snap frozen in liquid nitrogen. Using RNeasy® Lipid Tissue Mini Kit (Qiagen, Australia) with optimisation of the manufacturer's instructions, adipose tissue was lysed from frozen samples previously acquired. The night before the procedure, 2.0mL safe-lock Eppendorf tubes were labelled and a steel bead was added, pre-chilled at 4°C. Approximately 100mg of frozen tissue samples were quickly placed into pre-chilled Eppendorf tubes containing steel bead and 1mL of QIAzol lysis buffer was added. Eppendorfs were placed on ice and this procedure was done in the 4°C cold room. This was done for all samples consecutively. All samples were homogenised using the tissue lyser (Qiagen, Australia) for 4 minutes at 30Hz. The samples were transported to a fume hood on ice and 200mL of chloroform was added. Each sample-containing tube was manually shaken by hand for 15 seconds and left to sit at room temperature for 1 minute before being put back on ice. This was done for all tubes consecutively. Tubes were transported to the 4°C cold room on ice and centrifuged at 12,000xg (or 12,753 RPM) for 20 minutes. All tubes were put on ice carefully to avoid disrupting phases. This includes 4 phases: Upper aqueous phase, Interphase (white), organic phase (pink) and lower phase (clear). In the fume hood, 500µL of the topmost layer (aqueous phase) containing RNA was extracted using a pipette fitted with barrier tips and place into a fresh pre-chilled Eppendorf tube and kept on ice.

2.7.2 Purification of extracted RNA

In tubes containing extracted RNA, 500µL 70% ethanol was added and vortexed for 10 seconds and placed back on ice. A volume of 500 µL was transferred to a pre-labelled RNeasy spin column attached to a collection tube and centrifuged (Eppendorf® mini-spin®) at maximum speed of 12,000 x g for 15 seconds and flow through was discarded. This was repeated again with the remaining 500µL of sample. The column was cleansed with 350µl of buffer RW1 and centrifuged at maximum speed for 15 seconds and flow through discarded. To a 10µl aliquot of DNase I (Qiagen), 70µL of buffer RDD was added and mixed gently and added to the membrane of the column, incubated at room temperature for 15 minutes. A volume of 350µl of buffer RW1 was added to the spin column and centrifuged, flow through discarded. Buffer RPE prepared with ethanol previously prepared, centrifuged for 15 seconds at maximum speed and flow through discarded. This step was repeated but spun for 2 minutes. Transferring columns to a fresh collection tube, tubes were dry-spun for 1 minute at maximum speed. Spin columns were transferred to a fresh pre-chilled and pre-labelled 1.5ml Eppendorf tube and 30µl of RNase-free water was added to the membrane of the column and left to incubate at room temperature for 5 minutes prior to being spun at maximum speed (12,000 x g) for 1 minute. The eluted RNA in the Eppendorf tubes were carefully transferred back into its spin column and spun again for another minute

to increase RNA yield. All tubes containing RNA was immediately place on ice. All RNA was stored at -80°C.

2.7.3 Determining concentration and quality of the RNA

Using the NanoDrop 2000^{TM} (Thermo Scientific, Australia), the concentration of RNA was determined. Using the Agilent RNA 6000 Pico kit (Agilent Technologies, Inc), a volume of sample was diluted to the pico chip range of 50-5000ng/µl, RNA quality was determined; RNA integrity (RIN) number 7 or more was deemed to be of an acceptable RNA integrity, measured on the Bioanalyzer instrument (Agilent) (Figure 2.2)

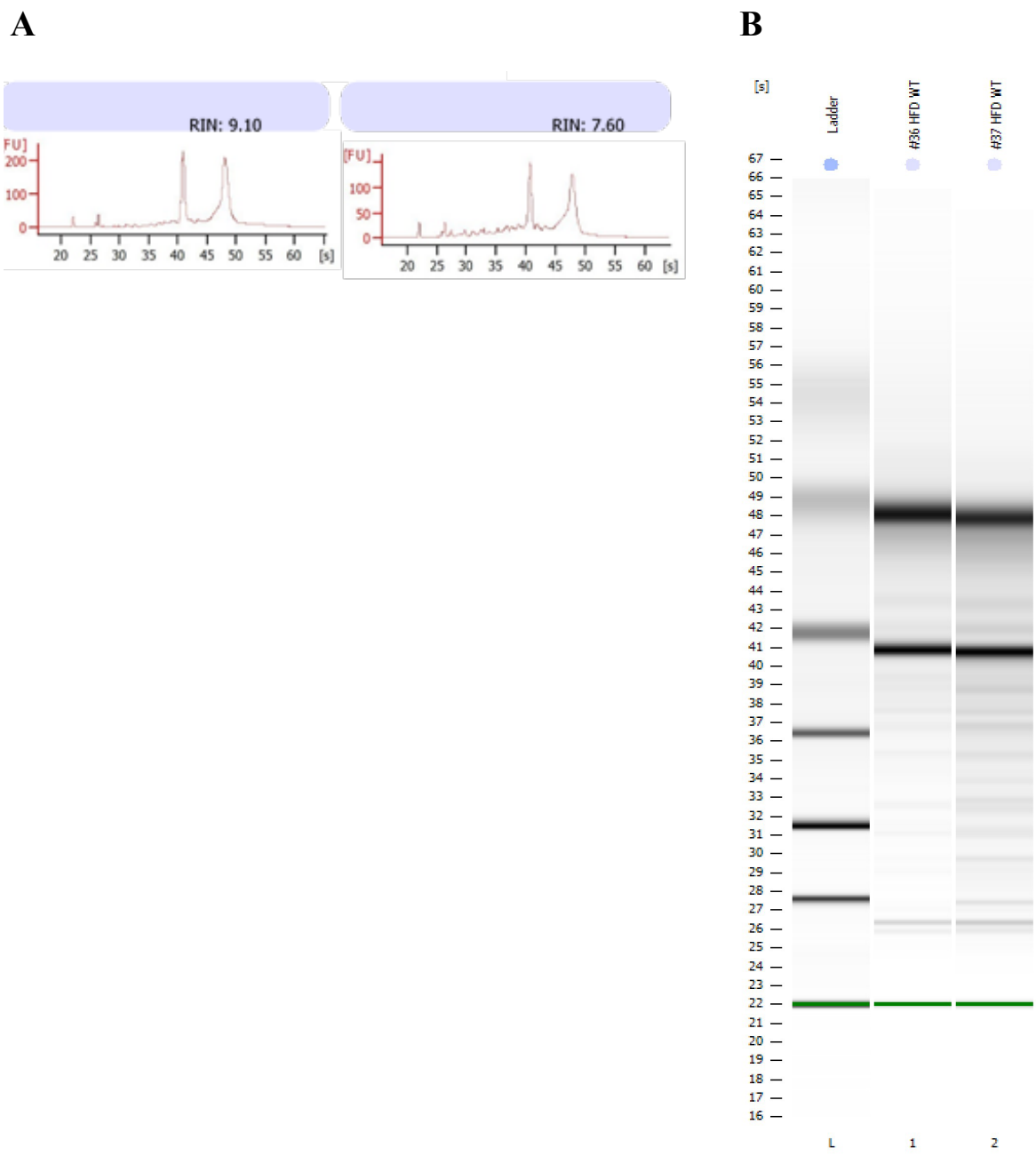

Figure 2.2 Example of measurements of RNA integrity. **(A)** A high Agilent RNA integrity with RIN number at 9.10 and 7.60 **(B)** RIN number was above 7 and associated gel image.

2.7.4 Reverse-transcription cDNA synthesis

Complementary DNA (cDNA) were synthesised using the Omniscript®RT Kit (Qiagen Australia) following manufacture's protocol. Depending on the RNA yield, 500ng, 1000ng, 1500ng or 2000ng of RNA was used to synthesise cDNA. The reaction mixture (Table 2.6) was prepared and added to each tube and incubated in a water bath at 37°C for an hour. Tubes were then immediately cooled on ice to stop reaction.

Table 2.6 Reverse transcription reaction reagents

Reagents	Volume per reaction (µl)
Template RNA	*x*
RNase-free water	(12-*x*)
10x Buffer RT	2
dNTP Mix (5mM each dNTP)	2
Oligo-dT primer (10µM) (Qiagen)	2
RNase inhibitor (Roche) (10 units/µl)	1
Ominiscript Reverse Transcriptase (Qiagen)	1
Total volume	20

2.7.5 SYBR® Green quantitative real-time PCR

Quantitect SYBR® Green PCR kit and the Rotor-Gene 3000 thermocycler (Corbett Research) were used (Table 2.7). *β-actin* gene was use as a housekeeper gene for normalisation as it is abundantly expressed. All target genes and their primer sequences were normalised to *β-actin* using the qgene software. The master mix (Table 2.7) for each quantitative PCR reaction was prepared fresh before each run. All samples were run in triplicate and each tube of the triplicate held 25µL sample and master mix volume in total. All targets had a negative control, termed 'no template control', in which 2µL of RNase-free water was added instead of cDNA.

Table 2.7 Quantitative real-time PCR reaction master mix constituents prior to addition of cDNA

Master mix constituents	Reaction volumes (µL)
SYBR Green qPCR master mix (2x)	12.5
Forward Primer (10 µM)	0.75
Reverse Primer (10 µM)	0.75
RNAse-free water	9
Total volume	**23**

The reaction cycling time (Table 2.8) was kept constant across all experiments in this thesis.

Table 2.8 Reaction cycling

PCR cycle	Settings	
Hold	95°C (15 minutes)	
Annealing	55°C (20 seconds)	45 cycles
Extension	72°C (25 seconds)	
Denaturation	94°C (15 seconds)	
Hold	72°C (4 minutes)	
Hold	60°C (1 minute)	
Melt	60°C to 99°C (with 0.5°C increments at each step)	

The use of Roter Gene software allowed for the melt curve (not shown) and comparative quantitation graph (Figure 2.3) and the take-off values can be used in the Qgene software to generate the mean normalised expression to be used in statistical analysis.

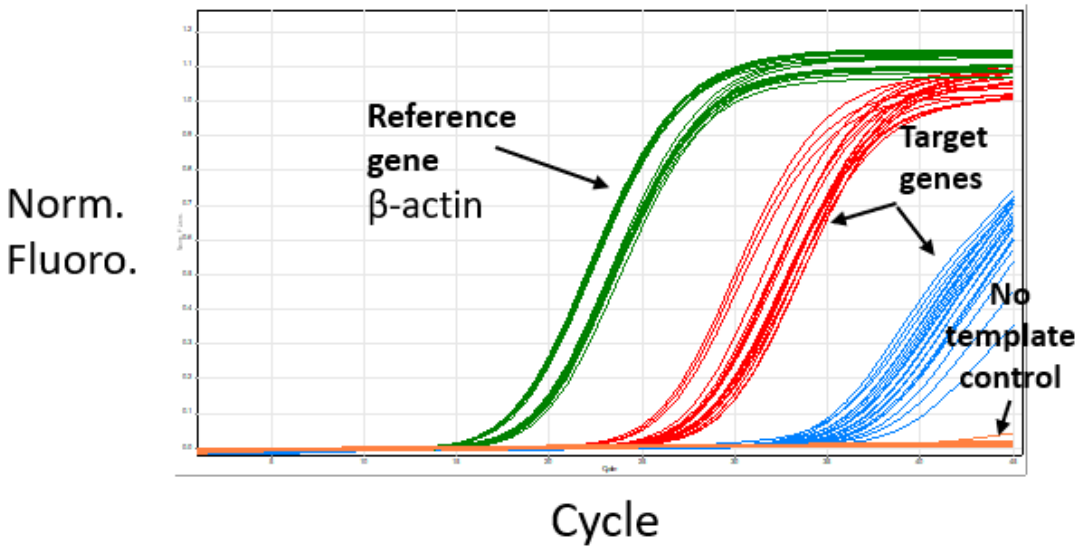

Figure 2.3 Generic example of a quantitation graph produced from the Rotor Gene software. *Green represents reference gene, β-actin; red represents target gene 1; blue represents target gene 2; orange represents the non-template control.*

2.7.6 Agarose gel electrophoresis

The agarose gel was used to test some initial primers to observe the specificity of the primers for its targets. An agarose gel (3%) was prepared with the use of 4.5 grams of multi-purpose agarose gel powder in 150mL of 1x TBE buffer. Once heated in a microwave for 2mins, the agarose gel solution was cooled to approximately 60°C and 7.5µL of Gel Red™ (Sigma) was added to detect amplified DNA. In the Bio-Rad gel electrophoresis set up, two combs were put in place and the gel solution was poured into the tray to solidify for 35 minutes at room temperature. The combs were removed and 1x TBE buffer was added to cover the gel. A quantity of 2µL Loading Dye (Sigma) was mixed with 10µL of each sample and loaded into its assigned well on the gel. The DNA ladder (1Kb Plus, Invitrogen) was prepared at a concentration of 200ng/µL. A quantity of 5µL of prepared ladder was mixed with 2µL of the 6x loading dye and loaded into its assigned well on the gel. Once the ladder and the samples were loaded onto the gel, the gel was run at 80V for 40 minutes. Using the Image Lab™ Software (Bio-Rad), the gel was imaged under ultra-violet light, exposed for 0.5 seconds, through the Gel Dox EZ Imager (Bio-Rad) software. The gels were run for some of the primers and it shows a single band, suggesting that the primers were specific for their target (Appendix C).

2.8 Statistical analysis

All data are normalised to β-actin housekeeper gene and presented as the mean normalised expression, generated using the Qgene software. The statistical analysis for each experiment will be discussed within each results chapter.

Chapter 3. THE MINIMUM EFFECTIVE CONCENTRATION OF INHIBITORS OF RCAN1-CALCINEURIN ON ADIPOCYTES

3.1 Introduction

Diabetes primarily involve tissues such as the pancreas and metabolically active tissue such as adipose tissue and skeletal muscles. While many therapeutic interventions employ multi-faceted therapeutic combinations to treat diabetes, no cure has been found. *RCAN1* is a gene located within the 21q22.12 region of human chromosome 21 and mouse chromosome 16 (Fuentes et al., 2000). RCAN1 has many roles but its best-known role is as an endogenous inhibitor of the Calcineurin (Fuentes et al., 2000, Rothermel et al., 2000, Ermak et al., 2002).

Interaction of RCAN1 and calcineurin inhibits the dephosphorylation of NFAT family of transcription factors in pancreatic β-cells, thereby allowing multiple downstream effects when NFAT is able to dephosphorylate and translocate into the nucleus (Peiris et al., 2012, Peiris et al., 2016). Metabolic effects of RCAN1 are not limited to pancreatic β-cells. RCAN1 is most highly expressed in adipocytes and skeletal muscle. The contribution to resting energy expenditure (REE) and obesity is associated with these metabolic tissues, with REE contribution of 5% from adipocytes and 20% from skeletal muscles (McClave and Snider, 2001). RCAN1 expression changes in metabolically important tissues, such as adipose tissue and correlates with impaired metabolic regulation (Parks et al., 2015). *RCAN1* overexpression in mice leads to an obesogenic phenotype. However, the lack of the *Rcan1* gene resulted in reduced weight gain in mice on a high-fat diet (HFD) compared to their WT controls ($RCAN1^{+/+}$ mice). This suggests that RCAN1 regulates obesity. This difference was not due to lesser food intake and the capacity to absorb nutritional fat is not altered (Rotter et al., 2018).

The inhibitors of RCAN1 were discovered from a high throughput method of a library of compounds that showed inhibition of the RCAN1-calcineurin interaction (Chan, 2007) and collectively termed ‘inhibitors of RCAN1-calcineurin association (IRCA)’ compounds. The screening of these drugs by Chan (2007) have been described in section 1.8 of this thesis. Unlike the immunosuppressant that targets calcineurin, cyclosporine A (CsA) and tacrolimus (FK506), that led to reversible β-cell dysfunction and post-transplant diabetes, these IRCA compounds inhibit RCAN1-calcineurin interaction but do not perturb calcineurin activity. Previously, our lab demonstrated that 3T3-L1 adipocyte cell line exposed to IRCA compounds decreased lipid content. IRCA2 was found to be the most effective drug being over two times as effective as the other drugs in reducing lipid content in the 3T3-L1 cell line (Figure 1.28).

These IRCA drugs may have therapeutic potential for diabetes and obesity with their capacity to specifically target RCAN1 without affecting calcineurin activity. These IRCA drugs have not been use in a physiological system. Therefore, my project is novel and aims to inhibit RCAN1-calcineurin interaction and possibly reduce lipid storage in adipocytes in a dose-dependent manner. This chapter

attempts to employ the MTT cell viability assay concurrently with an Oil Red-O assay to quantify lipid storage in adipocytes treated with IRCA drugs titrated up and down the original K_i.

3.2 Materials and methods

The 3T3-L1 cell line (passage 15-20) were maintained and differentiated as per methods described in Chapter 2. Cells were seeded at 60% confluence as the cell line is susceptible to spontaneous differentiation when it is 90-100% confluent. The image below shows an example of a 90% confluent flask (Figure 3.1). The cells were seeded onto the plate at the density of 2000 cells per well. The method for preparation of IRCA drugs, the culturing of 3T3L1 cells and the MTT cell viability assay, has been described in the previous in sections 2.1, 2.2 and 2.3, respectively.

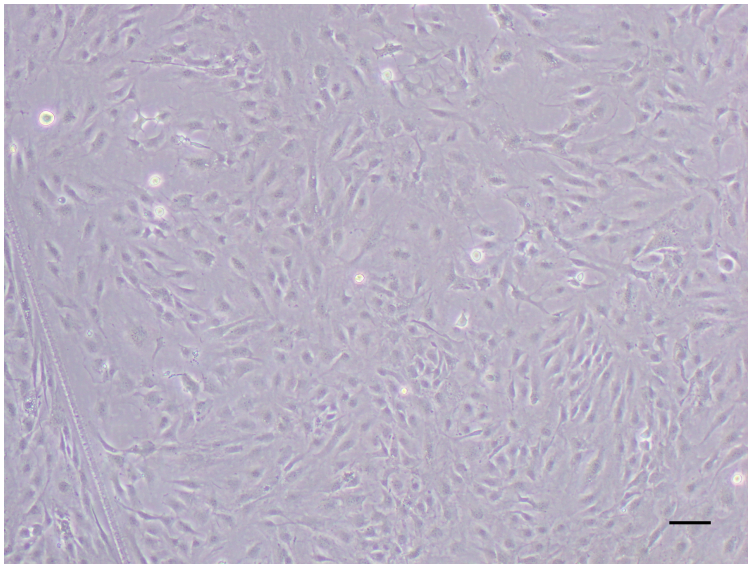

Figure 3.1 Sample image showing 3T3-L1 adipocytes at 90% confluence. Image taken using the 4x objective lens on the Olympus CXK43 Inverted microscope. Scale bar represents 100µm.

3.2.1 The MTT assay

The microculture Vybrant® 3-(4,5-dimethylthiazol-2-yl)-2,5-diphenyltetrazolium bromide assay (MTT) (Thermofisher Scientific) is a colorimetric test used to determine cell growth and viability (Mosmann, 1983) and was used in the experiments in this thesis. The principles of MTT and detailed methods are described in section 2.3 of this thesis.

3.2.2 Principles of the Oil Red-O assay

The Oil Red-O assay selectively stains and detects neutral lipids in cultured cells. The red stain is displaced from the isopropanol solution into the lipid droplets as there is greater solubility in the lipids than in the isoproterenol. The Oil Red-O assay has its limitations where the cells have to be fixed prior to staining in the presence of isopropanol (Majka et al., 2014). Due to its duration, cost-effectiveness and its ability to stain lipids, this assay is widely used (Kraus et al., 2016).

3.2.3 Oil Red-O staining for lipid droplets

3.2.3.1 Preparation of the Oil Red-O stain

The Oil Red-O is a specific lipid stain (Ramirez-Zacarias et al., 1992). The day before performing the Oil Red-O assay, three parts of the readily purchased Oil Red-O stain kept in 0.5% isopropanol (Sigma) was diluted in two parts of water to obtain a final concentration of 60% Oil Red-O. This solution was mixed thoroughly by inverting the tube several times and the tube was left to sit undisturbed on the bench for 10 minutes. In the fume hood, the diluted Oil Red-O mixture was filtered once using a glass funnel fitted with a 2.5µm filter paper (Filtech grade 1803) and the filtrate was collected in a new 50mL faclon tube. The tube was light-protected in aluminium foil and stored in the fridge at 4°C overnight. Before commencing the Oil Red-O assay, the 60% diluted Oil Red-O is filtered again with a glass funnel and filter paper in the fume hood.

3.2.3.2 Preparation of Oil Red-O standards

The Oil Red-O standards were prepared by serially diluting the Oil Red-O solution in the same amount of isopropanol. The table below shows how much Oil Red-O is in each dilution (Table 3.1).

Table 3.1 The table include the concentrations of 60% diluted Oil Red-O solution in 500mL of 100% isopropanol serially diluted.

Dilutions	60% diluted Oil Red-O working solution (µL)
Blank	0
1/128 dilution	8
1/64 dilution	16
1/32 dilution	31
1/16 dilution	63
1/8 dilution	125
¼ dilution	250
½ dilution	500

3.2.3.3 Oil Red-O staining procedure

Adipocytes were washed twice with phosphate-buffered saline (PBS) (Gibco) for 10 minutes each and removed. After which, the cells were fixed using 200 µL of PBS of 10% buffered formalin (home-made) that was added to each well and was left to incubate for 1 hour at room temperature. Following fixation, formalin was removed and cells were equilibrated by incubating for 10 minutes in 60% isopropanol before applying the Oil Red-O stain. A volume of 200µL of the twice-filtered 60% Oil Red-O was added to each well and incubated at room temperature for 20 minutes. The Oil Red-O stain is then removed and the cells undergo 5 washes in 200µL of distilled water. Before removing the last water wash, the cells were viewed under a light microscope (Olympus CKX41 microscope) to ensure that the Oil Red-O pigment stained all of the fat droplets. Upon removal of the last water wash, the Oil Red-O stain was eluted with 150µl of 100% isopropanol at room temperature for 10 minutes. To ensure all of the Oil Red-O dye has been eluted, the solution in each well was mixed several times by pipetting up and down with use of a multi-channel pipette. Using the multi-channel pipette, 100µL of eluted Oil Red-O was transferred into a fresh 96 well plate in the same sequence as the main 96 well plate. The 100µL of the previously prepared Oil Red-O standards and negative control (containing only 100% isoproterenol) were contained in individually labelled 1.5 mL Eppendorf tubes added to the 96 well plate. Using a plate reader (Beckman Coulter-DTX 880 Multimode Detector), the Oil Red-O absorbance was read at an excitation wavelength of 520nM.

3.2.4 Statistical analysis

All data are presented as mean ± standard error of mean (SEM). The drug-treated groups were relative to the control. Difference between drug concentrations were performed using a One-way ANOVA unpaired test with Dunnett *post-hoc* test to compare all drugs to its control. A two-tailed *P*-value <0.05 was considered statistically significant. Statistical analyses were performed using the Prism software (Prism 8.0).

3.3 Results

3.3.1 The 3T3-L1 adipocyte cell line transformed from fibroblast to mature adipocytes

To study the role of IRCA drugs in inhibition of the RCAN1-calcineurin interaction, we treated all cells with IRCA1 to IRCA5 for 6 days post-differentiation and post-adipogenesis. Successful transformation process of the 3T3-L1 adipocyte cell line is described below (Figure 3.2 A-D). After the 6 days of drug treatment, the cell viability was quantified using the MTT assay. Concurrently, the Oil red-O assay indicated lipid storage after 6 days of drug treatment. All cells in the IRCA drug-treated group were compared relative to control (Figure 3.3-3.7).

The 3T3-L1 fibroblast were cultured and differentiated according to standard procedure. Undifferentiated 3T3-L1 cells displayed a fibroblast-cell like structure (Figure 3.2A). These cells initiate adipogenesis by polarising their longitudinal structures into more localised, single globular structures with the influence of the adipocyte differentiation cocktail (Figure 3.2B). By Day 3, tiny lipid droplets are sparsely distributed within the cell and are more apparent (Figure 3.2C). Under the influence of the post-differentiation cocktail, the once-fibroblast cells are terminally differentiated, containing multiple lipid droplets and stained with Oil Red-O (Figure 3.2 D).

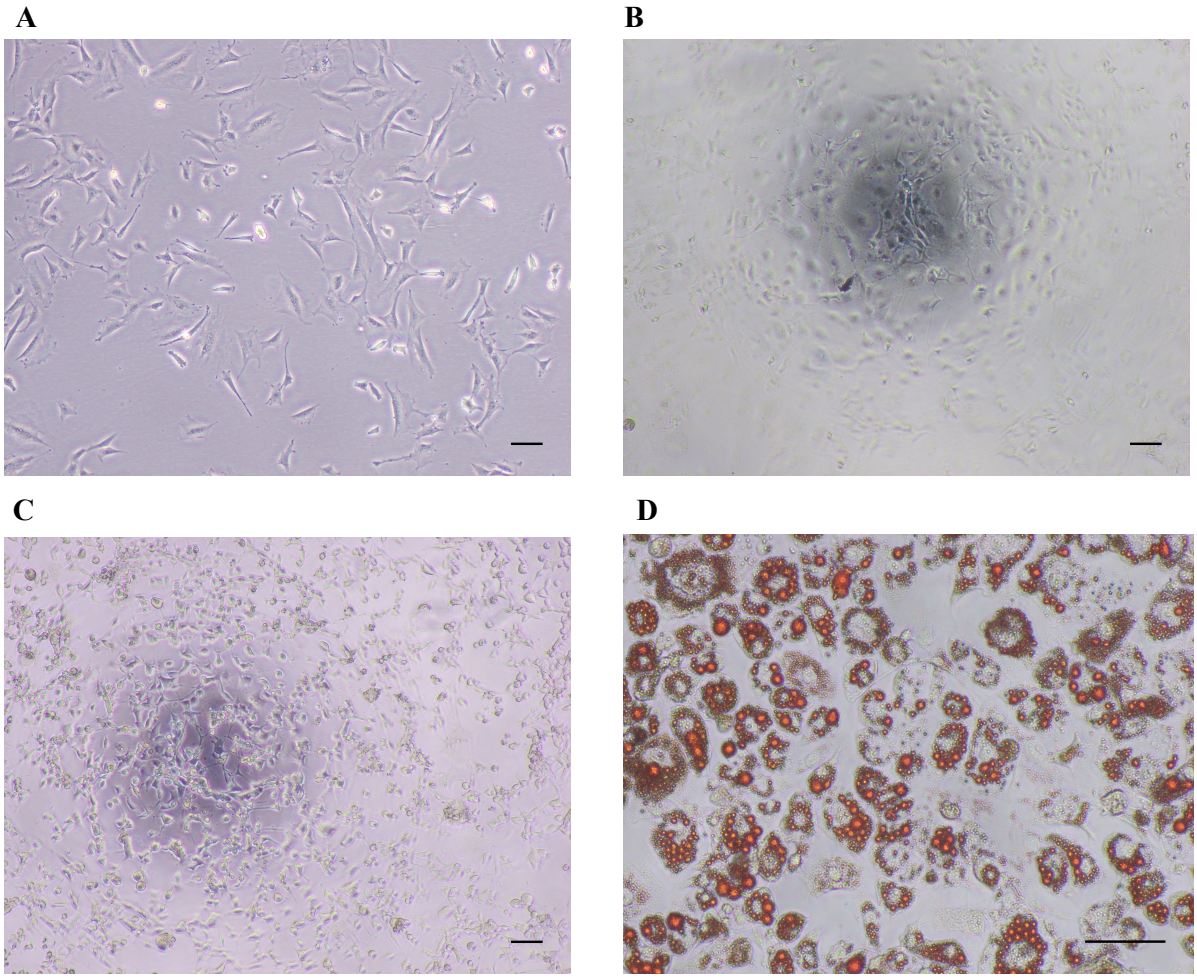

Figure 3.2 The 3T3-L1 cells from fibroblast differentiated to mature adipocytes. **(A)** Fibroblast 3T3L1 cells are transformed with **(B)** differentiation media on the 3rd day post-confluence into adipocytes. **(C)** Post-differentiation media is added after 3 days **(D)** and then the lipids in the adipocytes are stained with Oil Red-O. Image (A)-(C) are taken with a 4x objective lens on the Olympus CXK43 inverted microscope. Image (D) was taken with a 10x objective lens. Scale bar represents 100µm for images (A)-(D).

3.3.2 Increase lipid storage after drug treatment from 1xk_i and below

The 3T3-L1 cells were treated for 6 days using the IRCA1 drugs and were viable at all concentrations tested (Figure 3.3A). The 3T3-L1 cells showed an increase in lipid content at 1xK_i down to 0.001x K_i, relative to control using the Oil Red-O assay (Figure 3.3B). For IRCA2, 3T3-L1 cells were viable at all concentrations tested (Figure 3.4A) and showed an increase in lipid content at 0.001x K_i relative to control (Figure 3.4B).

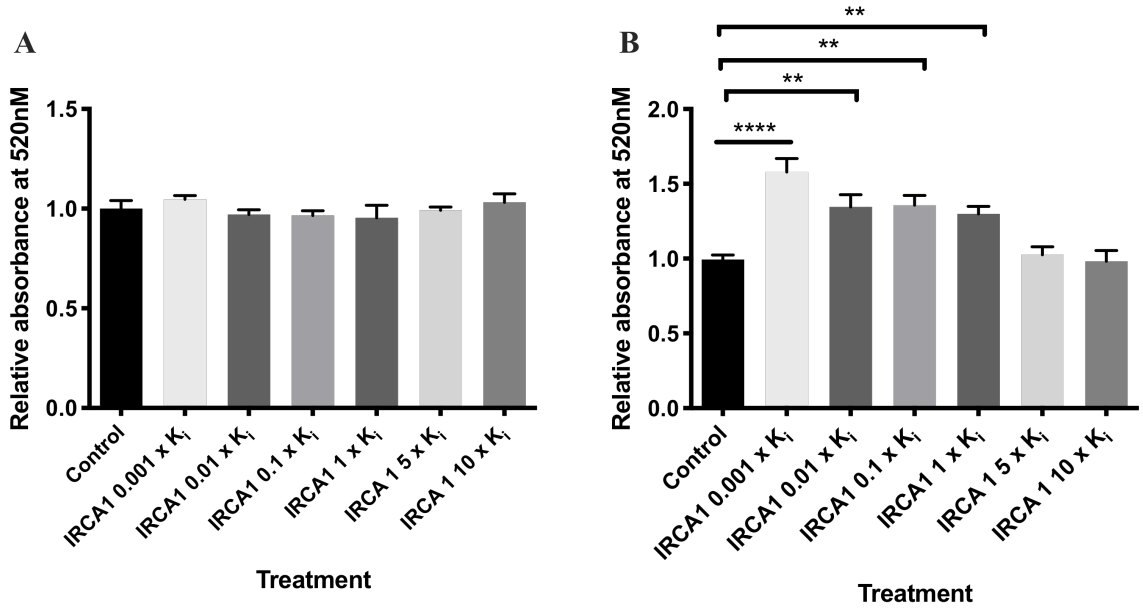

Figure 3.3 The 3T3-L1 mature adipocytes were treated with IRCA1 drugs for 6 days. **(A)** MTT cell viability assay (n=6) measured at 520nM. All 3T3-L1 cells were treated with IRCA drugs ranging from 10xK_i to 0.001xK_i. All results were normalised to control and **(B)** the Oil Red-O assay (n=15) measured at 520nM. All cells in the IRCA drug-treated groups were relative to DMSO control group across both assays. The n values in brackets indicate individual wells. Asterisks show where One-way ANOVA with Dunnett *post-hoc* test indicate difference (One-way ANOVA with Dunnett *post-hoc* analysis, *p<0.05, ** p<0.01, ****p<0.0001).

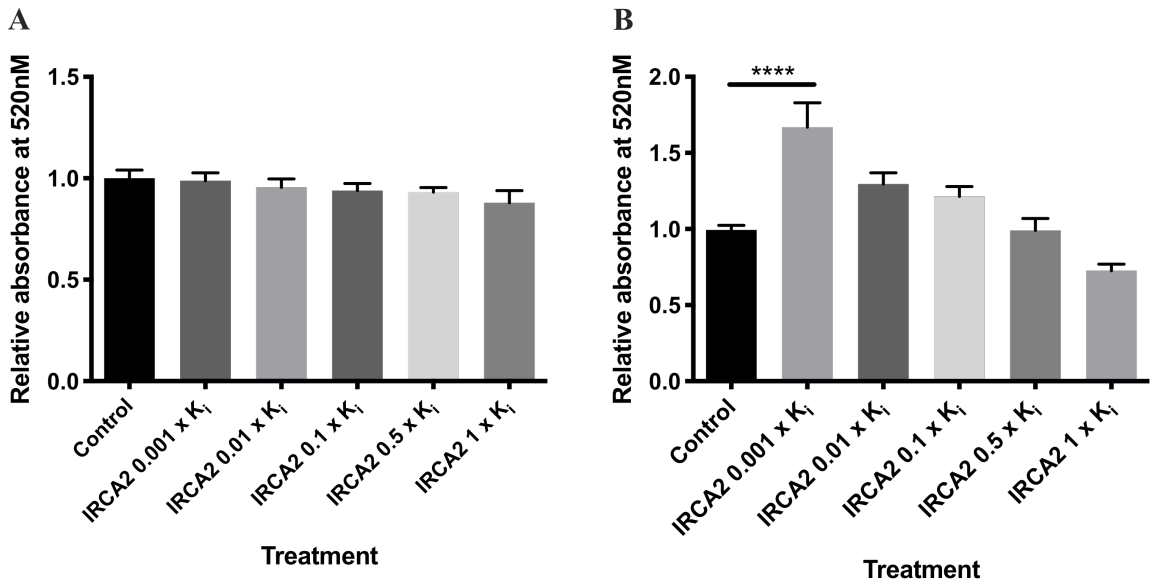

Figure 3.4 The 3T3-L1 mature adipocytes were treated with IRCA2 drugs for 6 days. **(A)** MTT cell viability assay (n=6) measured at 520nM. All 3T3-L1 cells were treated with IRCA drugs ranging from $1xK_i$ to $0.001xK_i$. All results were normalised to control and **(B)** Oil Red-O assay (n=15) was measured at 520nM. All cells in the IRCA drug-treated groups were relative to DMSO control across all both assays. The n values in brackets indicate individual wells. Asterisks show where One-way ANOVA with Dunnett *post-hoc* test indicate difference (One-way ANOVA with Dunnett *post-hoc* analysis, ****$p<0.0001$).

With the use of IRCA3, there was a reduction in lipid content following the use of 10x K_i concentration (Figure 3.5B), however, this was due to reduced cell viability and the loss of adipocytes (Figure 3.5A) rather than the reduction of lipid content within cells. There was an increase in lipid storage with the use of $0.01xK_i$ and $0.001xK_i$ concentrations (Figure 3.5B).

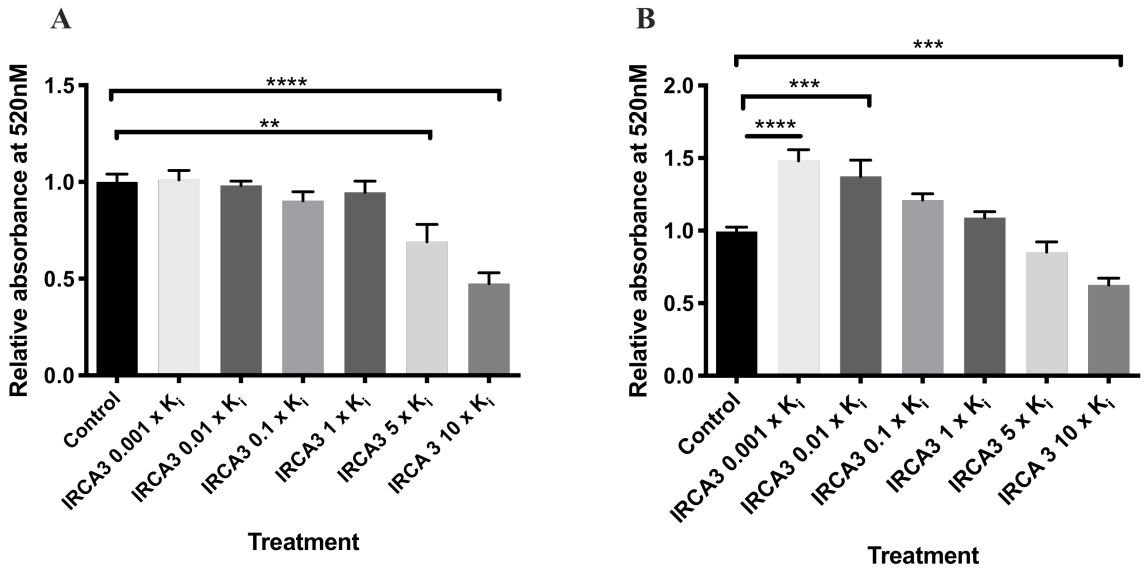

Figure 3.5 The 3T3-L1 mature adipocytes were treated with IRCA3 drugs ranging from 1xK_i to 0.001xK_i for 6 days. **(A)** All cells were viable using the MTT cell viability assay (n=6) measured at 520nM at 1xK_i down to 0.001x K_i. Reduced cell viability was quantified at 10x K_i and 5x K_i (One-way ANOVA with Dunnett *post-hoc* analysis, **<0.01 and *** p<0.001 respectively) **(B)** The 3T3-L1 cells showed an increase in lipid content at 0.01xK_i relative to control using the Oil Red-O assay (n=15) measured at 520nM. All cells in the IRCA drug-treated groups were relative to DMSO control across both assays. The n values in brackets indicate individual wells. Asterisks show where One-way ANOVA with Dunnett *post-hoc* test indicate difference (One-way ANOVA with Dunnett *post-hoc* analysis, *** p<0.001).

Similarly, there was an increase in lipid storage following 0.01x K_i and 0.001x K_i IRCA4 drug treatment (Figure 3.6B) and 0.001x K_i IRCA5 (Figure 3.7B) compared to their respective controls. Whilst there was an expected decrease in cell viability for 10x K_i, there was an unexpected increase in lipid storage at 10xK_i (Figure 3.6 A, B). This phenomenon also occurs for IRCA5 10x K_i (Figure 3.7A,B).

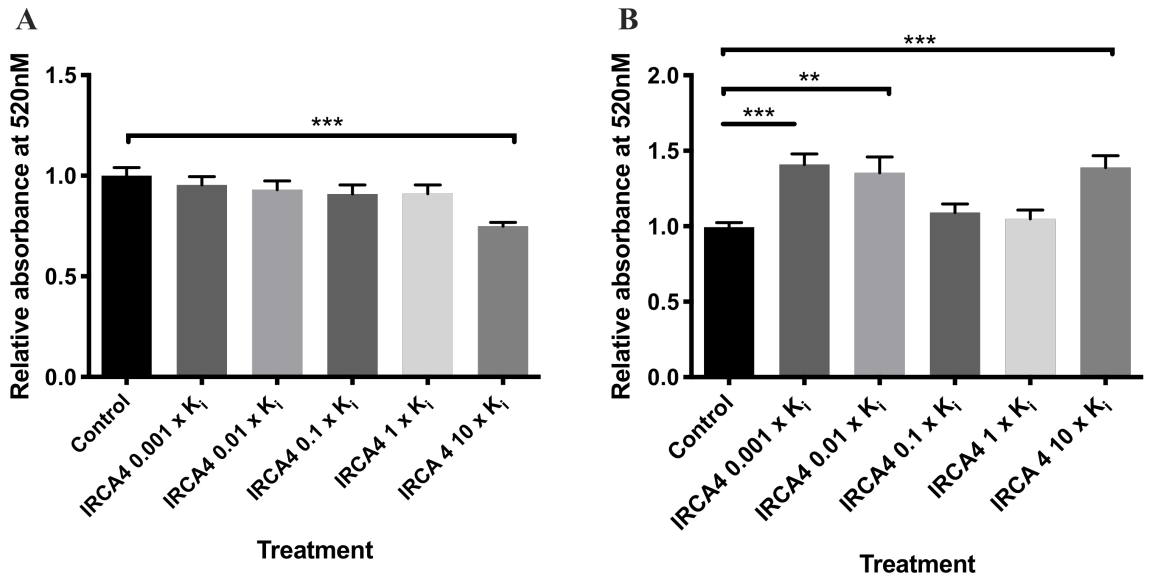

Figure 3.6 The 3T3-L1 mature adipocytes were treated with IRCA4 drugs ranging from 10xK_i to 0.001xK_i for 6 days. **(A)** All cells were viable using the MTT cell viability assay (n=6) measured at 520nM at 1x K_i down to 0.001x K_i. Reduced cell viability quantified at 10x K_i (One-way ANOVA with Dunnett *post-hoc* analysis, **<0.01) **(B)** The 3T3-L1 cells showed an increase in lipid content at 0.001x K_i, 0.01x K_i and 10x K_i relative to control using the Oil Red-O assay (n=15) measured at 520nM. All cells in the IRCA drug treated groups were relative to DMSO control across both assays. The n values in brackets indicate individual wells. Asterisks show where One-way ANOVA with Dunnett *post-hoc* test indicate difference (One-way ANOVA with Dunnett *post-hoc* analysis, **p<0.01, *** p<0.001).

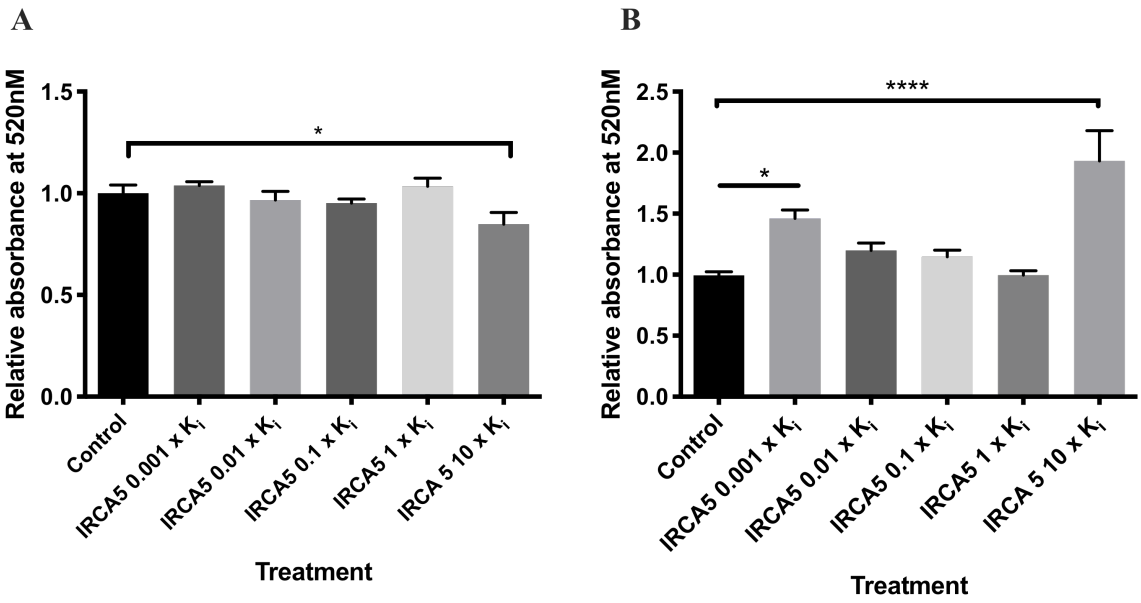

Figure 3.7 The 3T3-L1 mature adipocytes were treated with IRCA5 drugs ranging from 10x K_i to 0.001x K_i for 6 days. **(A)** using the MTT cell viability assay (n=6) measured at 520nM at 10xki down to 0.001x K_i. Reduced cell viability quantified at 10x K_i and 5x K_i (One-way ANOVA with Dunnett *post-hoc* analysis, * $P \leq 0.05$ and ****$p<0.0001$ respectively) **(B)** The 3T3-L1 cells showed an increase in lipid content at 0.001x K_i and 10x K_i relative to control using the Oil Red-O assay (n=15) measured at 520nM. All cells in the IRCA drug-treated groups were relative to DMSO control across both assays. The n values in brackets indicate individual wells. Asterisks show where One-way ANOVA with Dunnett *post-hoc* test indicate difference (One-way ANOVA with Dunnett *post-hoc* analysis, *$p<0.05$, **** $p<0.0001$).

3.4 Discussion

Diabetes and obesity are on the rise. The understanding of the Calcineurin-NFAT pathway in adipocytes are limited, while IRCA drugs targeting the RCAN1-calcineuin pathway, could have a therapeutic benefit of reducing lipid content in adipocytes. Based on the *Rcan1*$^{-/-}$ mice studies, similar to these results, we hypothesize that mice tissue, such as primary adipocytes treated with IRCA drugs would target the RCAN1-calcineurin interaction and reduce storage of lipids in adipocyte and induce proliferation in pancreatic β-cell (discussed in the next results chapter). To test the *in vitro* efficacy of these IRCA compounds on adipocyte function, we used the Oil Red-O assay on 3T3-L1 cells to undertake a full dose dependence test ranging from 1000-fold less to the highest dissolvable concentration, up to a 10-fold above (in 10-fold increments), starting with their K_i from the initial drug screen. This sets the platform for translation of cell culture work into whole animal experiments using these IRCA compounds i.e. once this minimum effective concentration is determined, the concentrations can be used on RCAN1^{ox} primary adipocytes to test the specificity of IRCAs for RCAN1 and their effects on adipocyte differentiation.

Chan et al. (2007) found that IRCA drugs inhibit RCAN1 directly without inhibiting calcineurin thereby blocking the interaction between RCAN1 and calcineurin. However, this was not tested in a physiological system. Using an isolated system of fully developed adipocytes that contain *Rcan1* gene expressed in these tissues, together with the treatment of drugs, we are able to reduce drug side-effects that may occur in a whole mice system. Currently, our knowledge of these drugs is limited. We only know their chemistry. In a whole organism system, the drug chemistry can change and therefore further studies will have to be conducted to optimise the effect of the drugs.

The transformation from fibroblast state to mature adipocytes in the 3T3-L1 cell line was confirmed with successful lipid formation in the adipocytes, stained with the Oil Red-O. Cell viability was tested using the MTT assay. All cells were viable at the maximum concentration used for IRCA1 and IRCA2. The absence of RCAN1 reduces lipid accumulation in mature differentiated 3T3-L1 adipocytes, however, surprisingly, there was an increase in lipid storage in drugs from 1xK_i titrated down; in the more diluted concentrations of the drugs used, there were more lipid storage compared to control. This indicates that with lesser inhibition of RCAN1-calcineurin interaction, lipid content increases. Decrease in lipid content at 1xK_i concentration for IRCA2 was not significant and all cells were still viable at that concentration. This suggests that other molecular pathways could be involved, causing lipid storage rather than reducing lipid storage. This a novel finding and these IRCA drugs could have off-target effects that are currently unknown and requires further investigation. It is possible that there is an upregulation of lipogenesis and a downregulation of lipolysis in these IRCA-drug treated cells, therefore increasing lipid storage. Also, there was a significant decrease in lipid content at 10x K_i and 5x K_i for IRCA3, however, cell viability using the MTT assay showed significantly reduced cell

viability, hence IRCA3 at 10xK_i was ineffective in reducing lipid content. At a lower concentration of IRCA3, there was an increase in lipid storage. The increase in lipid content at 10xK_i IRCA4 and IRCA5 was not expected as there was a significant decrease in cell viability at this concentration. Reasons for these results have to be further investigated.

Overall, my data was not similar to the previous data gathered which showed that all five IRCA drugs successfully decrease lipid content in mature adipocytes of the 3T3-L1 cell line (Figure 1.28). These results are overall contrary to pre-differentiation siRNA knockdowns of the two isoforms of the *Rcan1* gene in 3T3-L1 adipocytes with an observed reduction in lipid storage (Figure 1.26). In *Rcan1*$^{-/-}$ mice liver, lipid accumulation was lower compared to WT on either diets. This was assessed using the Oil Red-O assay. Furthermore, *Rcan1*$^{-/-}$ mice failed to gain weight on a HFD compared to those on a normal fat diet (Rotter et al., 2018), therefore the hypothesis that IRCA drugs inhibit the RCAN1-calcineurin interaction acts to decrease lipid content needs to be further investigated. The results presented in here showed an increase in lipid storage and this was only observed with the use more diluted IRCA 1-5 concentrations. This indicates that these IRCA drugs could potentially affect other pathways other than those associated with RCAN1 function. For example, RCAN1 may exert effects on calcineurin-independent signalling cascades such the MAPK/ERK signalling pathway and NFkB inflammatory pathway (Kim et al., 2006b, Hoeffer et al., 2007, Keating et al., 2008, Martin et al., 2012). Further investigation would be required to determine which pathways these drugs might affect.

There could be a number of reasons for the disparity in results. To ensure that this was not a difference due to a different person conducting these experiments, comparisons of the drugs used in this experiment and those used in the preliminary data were made (Appendix A-1). Shown in the Appendix of this thesis, both results, the drugs prepared by another member of the lab and drugs prepared by me, were similar for all of the drug concentrations. In this separate experiment, the Oil Red-O assay indicated a significant increase in lipid content at IRCA1 1xK_i using the drugs used in these experiments compared to DMSO control. This trend was consistent across five experiments and was observed in the drugs used for the preliminary experiment (Figure 1.28). There was a decrease in lipid content at IRCA2 1xK_i for both of our drugs and this is the only drug concentration that matches the preliminary data showing a decrease in lipid content using all five drugs at 1xK_i concentration. Therefore, the minimum effective dose that decrease lipid storage and does not cause reduced cell viability could not be determined. Further investigations have to be conducted to better understand the disparity in results between the preliminary data and those of the experiments conducted in this chapter. More essentially, other methods of testing these drugs could be employed. Oil Red-O is the most widely used assay used to quantify lipid content within adipocytes. However, recently, LipiD-QuantT live cell imaging was introduced and can also be used to quantify lipid droplets (Varinli et al., 2015). This is discussed in section 7.3 of this thesis.

Furthermore, other aspects of adipocyte functions, apart from lipid storage, could be tested. CsA, the calcineurin inhibitor, added to 3T3-L1 cells decreased basal and TNFα-induced lipolysis by half *in vitro* (Holowachuk, 2007). Isoproterenol activates PKA activity through cAMP stimulation (Anthonsen et al., 1998) and TNF-α induces lipolysis through the mitogen-activated protein kinases (MAPKs) (Ryden et al., 2004). Similarly, these IRCA drugs could be tested for its effects in lipolysis and lipid storage using gene expression studies involved in lipid metabolism other adipocyte associated pathways. Furthermore, the calcineurin inhibitor CsA and FK506 which prevents NFAT translocation, GSK3β inhibitors (Li+ or TZDZ-8) which increases NFAT translocation, can be use on 3T3-L1 cells to better understand the calcineurin downstream pathways in adipocytes (Holowachuk, 2007). This would add greater understanding of use of IRCA drugs to inhibit the RCAN1-calcineurin interaction without disrupting calcineurin and possibly alleviate post-transplant reversible diabetes when the calcineurin inhibitors are used. The limitations and future directions for this experiment will be discussed in greater detail in section 7.3.

Chapter 4. IRCA DRUGS INHIBITS RCAN1-CALCINERUIN INTERACTION IN β-TC6 CELL LINE

4.1 Introduction

Pancreatic β-cells are the primary source of endogenous insulin in the body and defects in β-cells result in dysregulation of glucose homeostasis and together with insulin resistance, result in diabetes. The molecular pathology of β-cell dysfunction during insulin resistance and hyperglycaemia is currently not known. One such gene is *RCAN1* and its best-known role is as an endogenous inhibitor of calcineurin (Fuentes et al., 2000, Kingsbury and Cunningham, 2000, Rothermel et al., 2000). In the recent publication, *Rcan1* was found in mouse islets and the cytosol of pancreatic β-cells, implicated in β-cell dysfunction evident by hyperglycaemia-induced RCAN1 expression in Down Syndrome mice and expression increase in islets of humans with type 2 diabetes (Peiris et al., 2016). The RCAN1 protein expression was increased in *db/db* mouse islets and in human and mouse islets under hyperglycaemic conditions. Mice overexpressing RCAN1 ($RCAN1^{ox}$) displayed a loss in *in vivo* glucose-stimulated insulin secretion and their β-cells had mitochondrial dysfunction (Peiris et al., 2016).

The molecular mechanisms in islets that maintain glucose homeostasis and the role they play in the β-cell dysfunction linked to the pathology of T2D, still remains elusive. β-cells have adaptive mechanisms such as hyperplasia, hypertrophy and increase insulin production to match the increase glucose load (Bonner-Weir et al., 1989). The mass of β-cells was determined by the β-cell growth (proliferation and differentiation) and β-cell death (apoptosis). Consequently, the mass of β-cells determine the amount of insulin produced (Bonner-Weir, 2000). Additionally, dysfunction in controlling β-cell proliferation or apoptosis, thereby the inability for β-cells to change its number or mass, leads to T2D (Heit et al., 2006b). Mice overexpressing *RCAN1* had a loss of β-cells and this could be due to reduced proliferation or increased apoptosis (Peiris et al., 2012). By investigating expression levels of markers of β-cell proliferation and apoptosis in cells treated with inhibitors of RCAN1 would allow us to understand the effects of inhibiting RCAN1-calcineurin interaction using these drugs and the impact on β-cell number and mass.

The gradual loss of insulin secreting β-cells resulted from the loss of mass due to apoptosis is characteristic of T2D (Jonas et al., 2009). Apoptosis is mediated through two converging pathways (Figure 1.12); the Bcl-2 family regulates the mitochondrial (intrinsic) pathway and caspase 8 mediates the extrinsic pathway. In the intrinsic pathway, BAX moves from the cytosol to the mitochondrial membrane and induces the release of mitochondrial cytochrome c into the cytosol that activates the caspase apoptotic cell death (Ness et al., 2006). Members of the Bcl-2 family members including Bcl-2–interacting mediator of cell death (BIM) and Bcl-2–associated X protein (BAX) are involved in programmed cell death activating caspase 9 and caspase 3 in neuronal cells (Niquet and Wasterlain, 2004) and modulating the integrity of the mitochondrial outer membrane (Ness et al., 2006). The extrinsic pathway involves caspase 8 and molecular processes are summarised in section 1.5.1.3.

Calcineurin inhibitor FK506 functions to immunosuppress the immune system via inhibition of calcineurin (Shirane and Nakayama, 2004). In leukemic cells, disruption of RCAN1 resulted in a decrease in Bcl-2 family proteins expression and increased anti-apoptotic Bcl-2 proteins expression (Nagao et al., 2012). Glucocorticoids (GCs), induce apoptosis in leukemic cells by modulating pro- and anti- apoptotic gene expression. The use of GCs led to an increase in RCAN1.1 but not RCAN1.4 in apoptotic leukemia cells. *BIM* expression was increase in response to GCs in healthy cells and tumour-affected cells (Saenz et al., 2015). In rat neurons, the upregulation of RCAN1.1 resulted in increased markers of apoptosis, caspase 9 and caspase 3, that resulted in apoptosis in neurons (Sun et al., 2011). The upregulation in expression of *caspase 3* and caspase *9* in the pancreas, together with the loss of β-cells were observed in islets overexpressing *Rcan1* (Peiris et al., 2012). This suggest that RCAN1 has a role in mediating apoptosis in β-cells. Furthermore, PUMA (p53-upregulated modulator of apoptosis) is a pro-apoptosis gene and part of the BH3-only protein that interacts with Bcl-2 family members induce the release of cytochrome c in mitochondrial apoptosis. PUMA is also able to activate BAX by inducing *Bax* expression in apoptosis (Liu et al., 2003). Therefore, we hypothesise that RCAN1-induced inhibition of calcineurin results in β-cell apoptosis and that inhibiting the RCAN1-calcuineurin interaction could reduce this apoptosis.

Post-transplant patients treated with calcineurin inhibitors for immunosuppression have an increased incidence of diabetes that is reversible upon cessation of immunosuppressant exposure (Heit et al., 2006a). The calcineurin-NFAT pathway is implicated in this and could regulate islet responses (Weir and Fink, 1999). In β-cells, the ablation of calcineurin b1 (Cnb1), a calcineurin phosphatase regulatory subunit decreases in specific regulators of β-cell proliferation such as cyclin D1 and cyclin D2 (Heit et al., 2006a). Markers such as cyclins D1 and D2 are vital for β-cell growth in mature mice (Georgia and Bhushan, 2004, Kushner et al., 2005). When NFATc1 was conditionally expressed and induced, these Cnb1-absent β-cells cause an anti-diabetic effect through increased expression of genes essential for normal β-cell physiology (Heit et al., 2006a). Therefore, with the use of the inhibitors of RCAN1-calicneurin association (IRCA) drugs (Chan, 2007) on β-cells, to assessed for proliferation and apoptosis activity, is essential in determining the effects of inhibiting the RCAN1-calcineurin interaction on the Calcineurin-NFAT pathway and impact on downstream apoptosis or proliferation effects that determines β-cell number and mass. Inhibiting calcineurin causes post-transplant diabetes using calcineurin inhibitors, however, inhibition of RCAN1-calcineurin interaction could be therapeutic as calcineurin itself is not disrupted, thereby allowing NFAT to be in its dephosphorylated state and translocated into the nucleus for downstream effects. Given that normal mature β-cells resulted in increased expression of important cell-cycle regulators that promoted β-cell proliferation and mass (Heit et al., 2006a), the translocation of NFAT into the nucleus could be therapeutic for diabetic patients.

Based on the current literature, I hypothesise that inhibiting RCAN1 would increase proliferation and decrease apoptosis in β-cells. This chapter aims to determine the effective minimum concentration of IRCA drugs on proliferation and apoptosis of the β-TC6 cell line. Once the optimal minimum effective concentration is determined with the use of a real-time proliferation assay, the xCELLigence assay, we aimed to test these optimal concentrations over an extended period to investigate the rate of proliferation in IRCA drug-treated cells. Concurrently, we aim to quantify expression of genes associated with proliferation and apoptosis in these drugs-treated cells.

4.2 Materials and methods

The preparation of the IRCA drug serial dilution has been described in section 2.1. The MTT cell-viability assay has also been previously described in section 2.3. This assay was used in this experiment to first determine the minimum effective concentration of IRCA drugs that could be use that does not cause reduced cell viability.

4.2.1 β-TC6 Cell line

The culturing and maintenance of the mouse-derived Beta-TC6 (β-TC6) cell line (ATCC ® CRL-11506™) is described in Chapter 2. The β-TC6 cells (Figure 4.1) derived from a transgenic mouse expressing large T-antigen of SV40 in pancreatic β-cells (passage number 36-40) were seeded at 12,000 cells per well in plates in the volume of 100µL and left overnight in the incubator to adhere to the surface at the bottom of the well for all experiments. Specifically, for the xCELLigence experiments, pancreatic β-cells (passage number 36-40) were seeded at 12,000 cells per well in plates in the volume of 150µL and left overnight in the incubator, at 37^{o}C and 5% CO_2 conditions, to adhere to the surface at the bottom of the well.

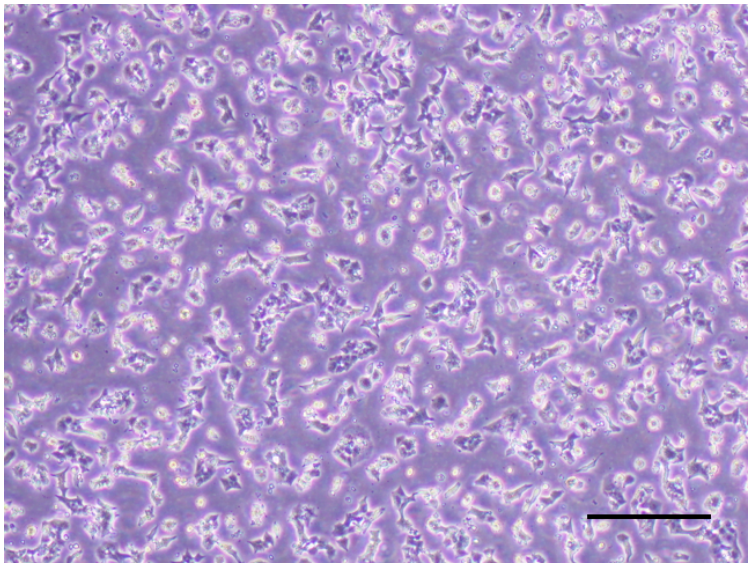

Figure 4.1 Sample image of β-TC6 cells at 60% confluence. Image taken with a 4x objective lens on the Olympus CXK43 inverted microscope. Scale bar represents 100μm.

4.2.2 Measuring real-time proliferation using the xCELLigence system

The xCELLigence system (Roche Applied Science and ACEA Biosciences) includes the real-time cell analysis (RTCA) analyser, RTCA dual purpose (DP) station, the computer with the integrated RTCA software (version 2.1.0, ACEA Biosciences, Inc.) and the disposable electronic microtiter plates (E-plate®16) (ACEA Biosciences, Inc.). The DP-type of the xcelligence system has a 3 individually-controlled measurement docks that cradles individual E-16 plates (each plate has 16 wells) (Moodley et al., 2011), within a regular tissue culture incubator (5% CO_2 at 37°C). The cell index (CI) is a unitless measure of relative change in electrical impedance reflective of cell viability. CI considers background impedance and therefore require a 'blanking' step as the first step correcting for impedance caused by medium alone. The xCELLigence system requires specific plates that have high-density gold electrode array and the use of adherent cells. When no cells are present, CI is zero and as more cells proliferate, cell index increases. Alternatively, when CI decreases this reflect decrease net adhesion. The diagram below summarises the principles of using electron impedance as a measure of cell proliferation (Figure 4.2).

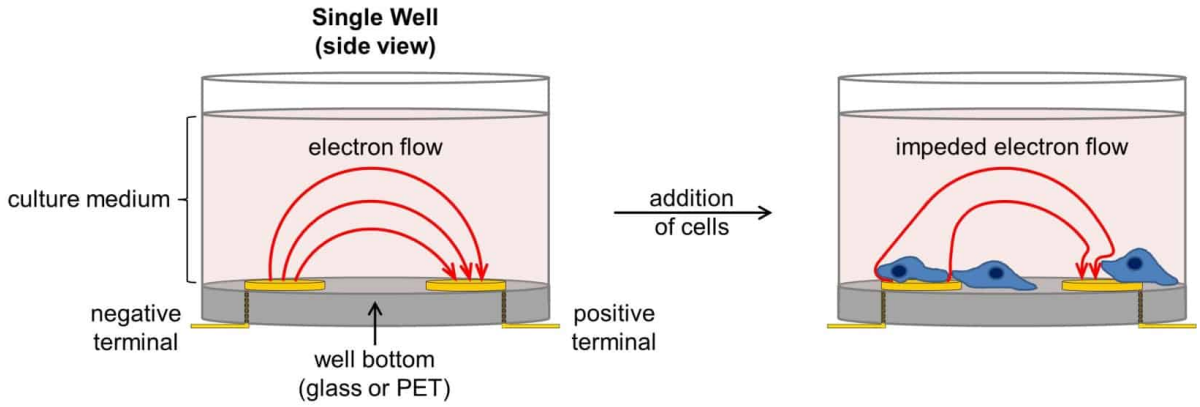

Figure 4.2 Diagram showing the electron flow and electrical impedance using adherent cells in the xCELLigence gold-plated electrode wells. When no cells are present, the electron flow is not impeded and flow is unaffected through culture medium, unlike in the well after the addition of cells (represented in blue in the diagram). As cells proliferate and adhere to the bottom of the well, there will be greater impedance which indicates greater electron flow as impedance is a sensitive measure for cell number (ACEA Biosciences Inc., 2019).

The xCELLigence software was used to measure the real-time effect of IRCA drugs on the β-TC6 using an amplitude detection method. A blanking step using 50µL of media is added to the wells using a multi-pipette in a reverse pipette fashion to eliminate the formation of bubbles. After which, 100µL of 12,000 cells were added to each well and left overnight in the incubator to adhere to the surface at the bottom of the well. The system was set to do its scan every hour. A volume of 0.7 µL of each IRCA drug diluted in 700µl media with the chosen concentrations was first prepared in an Eppendorf. Daily, 200µL of drugs were replaced at approximately the same hour using a reverse pipetting method. On the 19th day, the scans were stopped and data were exported and analysed. The xCELLigence system read amplitude readings every hour. Our data shows one time point in the 24 hours from when the first reading was taken.

4.2.3 Real-time PCR measured gene expression

The method for qPCR has been discussed in Chapter 2. The table below provides the forward and reverse sequences for the target apoptosis and proliferation genes used in this chapter (Table 4.1). The melt curves and quantitation graphs generated for each of these gene targets can be found in Appendix B.1.

Table 4.1 Genes targeted for apoptosis and proliferation in β-TC6 cell line

Marker for	Genes	Forward	Reverse	Length	Reference
Apoptosis	*Bim*[1]	GAGTTGTGACAAGTCAACACAAACC	GAAGATAAAGCGTAACAGTTGTAAGATAACC	256	(McKenzie et al., 2010)
Apoptosis	*Puma*[2]	ATGCCTGCCTCACCTTCATCT	AGCACAGGATTCACAGTCTGGA	61	(McKenzie et al., 2010)
Apoptosis	*Bax*[3]	TGAAGACAGGGGCCTTTTTG	AATTCGCCGGAGACACTCG	140	(Saksida et al., 2013)
Apoptosis	*Caspase 3*	TCTGACTGGAAAGCCGAAACT	AGGGACTGGATGAACCACGAC	207	(Saksida et al., 2013)
Apoptosis	*Caspase 8*	TCAACTTCCTAGACTGCAACCG	CTCAATTCCAACTCGCTCACTT	127	(Saksida et al., 2013)
Apoptosis	*Caspase 9*	TCCTGGTACATCGAGACCTTG	AAGTCCCTTTCGCAGAAACAG	109	(Saksida et al., 2013)
Proliferation	Cyclin D1 (*Ccnd1*)	CGTGGCCTCTAAGATGAAGG	CTGGCATTTTGGAGAGGAAG	185	(Cho et al., 2008)
Proliferation	Cyclin D2 (*Ccnd2*)	CACACCGTGAAACATTACAG	CAGTTGGTTTGGTTTTGTTT	326	(Rulifson et al., 2007)
		TCTCTCTCAAACTTCCCAAA	CACGTGGATGATATTCCTTT	307	(Rulifson et al., 2007)
Housekeeper	*β-actin*	GGGGCAAGAGAGGTATCCTGACC	CCCTGGATGCTACGTACATGGC	237	(Rotter et al., 2018)

[1] Bcl-2-interacting mediator of cell death (*Bim*)
[2] p53-upregulaed modulator of apoptosis (*Puma*)
[3] Bcl-2-associated X protein (*Bax*)

4.2.4 Statistical analysis

All data are presented as mean ± standard error of mean (SEM). The target genes were normalised to the house keeping gene *β-actin*. Difference between diet groups and mice groups were performed using a One-way ANOVA unpaired test with Dunnett's *post-hoc test*. For the data from the xCELLigence real-time proliferation experiment, a two-way ANOVA with Dunnett's *post-hoc test* was used to compare all 5 drugs at multiple time points to its control. A two-tailed *P*-value <0.05 was considered statistically significant. Statistical analyses were performed using the Prism software (Prism 8.0).

4.3 Results

4.3.1 Cell viability of IRCA drug-treated β-TC6 cells

The β-TC6 cell line was treated with IRCA1 to IRCA5 drugs for 3 days prior to conducting the MTT cell viability assay. This assay was used to determine the maximum concentration of the IRCA drugs that does not decrease cell viability. At 10 times the K_i, IRCA1 showed a significant decrease in cell viability, therefore this dose was considered lethal. For IRCA2, 1xK_i and half times the K_i were considered lethal to these cells and were considered non-viable at these concentrations. Similarly, 5 times K_i and 10 times the K_i for IRCA 3 was considered to cause reduced cell viability. Surprisingly, 20x K_i IRCA4 was not lethal, however, 1xki and 10x K_i was considered doses that significantly reduced cell viability. There were no significant reduction in cell viability caused for all concentrations tested for IRCA5 (Figure 4.3). The chosen minimum effective concentration for IRCA1 was 5x K_i, the next K_i down from 10x K_i which significantly reduced cell viability (Figure 4.3A), IRCA2 was 0.1x K_i (Figure 4.3B), IRCA3 was 1x K_i (Figure 4.3C), IRCA4 was 0.1x K_i (Figure 4.3 D) and IRCA5 was 10x K_i (Figure 4.3E). These optimal concentrations were considered to be the highest concentration that these β-cells were still viable.

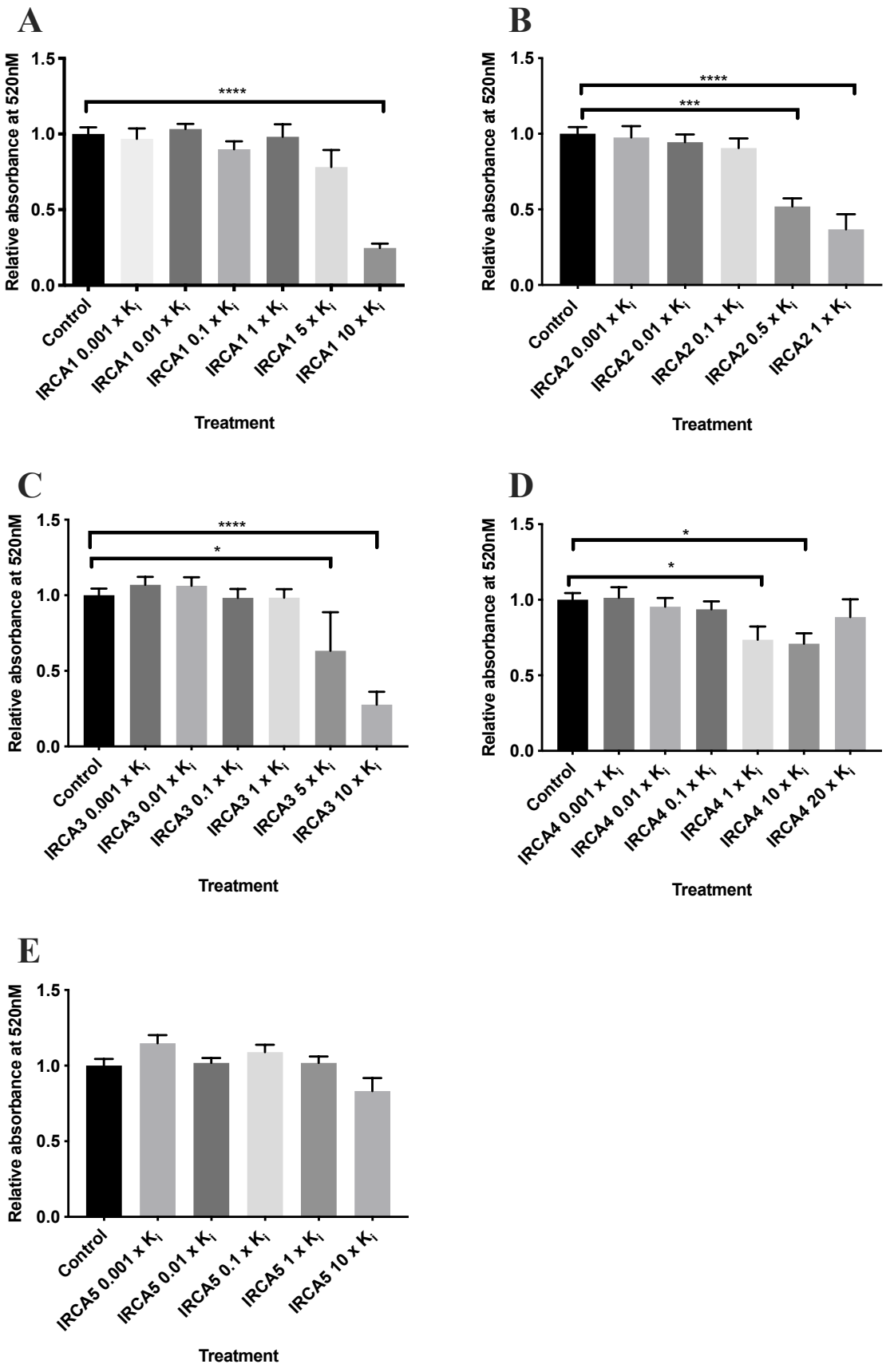
A
Relative absorbance at 520nM
1.5
1.0
0.5
0.0
****
Control
IRCA1 0.001 x Ki
IRCA1 0.01 x Ki
IRCA1 0.1 x Ki
IRCA1 1 x Ki
IRCA1 5 x Ki
IRCA1 10 x Ki
Treatment
B
Relative absorbance at 520nM
1.5
1.0
0.5
0.0
****
***
Control
IRCA2 0.001 x Ki
IRCA2 0.01 x Ki
IRCA2 0.1 x Ki
IRCA2 0.5 x Ki
IRCA2 1 x Ki
Treatment
C
Relative absorbance at 520nM
1.5
1.0
0.5
0.0
****
*
Control
IRCA3 0.001 x Ki
IRCA3 0.01 x Ki
IRCA3 0.1 x Ki
IRCA3 1 x Ki
IRCA3 5 x Ki
IRCA3 10 x Ki
Treatment
D
Relative absorbance at 520nM
1.5
1.0
0.5
0.0
*
*
Control
IRCA4 0.001 x Ki
IRCA4 0.01 x Ki
IRCA4 0.1 x Ki
IRCA4 1 x Ki
IRCA4 10 x Ki
IRCA4 20 x Ki
Treatment
E
Relative absorbance at 520nM
1.5
1.0
0.5
0.0
Control
IRCA5 0.001 x Ki
IRCA5 0.01 x Ki
IRCA5 0.1 x Ki
IRCA5 1 x Ki
IRCA5 10 x Ki
Treatment

Figure 4.3 The β-TC6 β-cells were treated with IRCA 1 to IRCA 5 drugs. Ranging from 10x K_i to 0.001x K_i for 3 days prior to MTT cell viability test measured at 520nM (n=6-12). The graphs show **(A)** IRCA 1, **(B)** IRCA2, **(C)** IRCA3, **(D)** IRCA4 and **(E)** IRCA5 -treated cells. All cells in the IRCA drug-treated groups were relative to DMSO control in both assays. Asterisks show where one-way ANOVA with Dunnett *post-hoc* test indicate difference (One-way ANOVA with Dunnett *post-hoc* analysis, *$p<0.05$, ***$p<0.001$, ****$p<0.0001$). All data shown are in SEM.

4.3.2 Inhibition of RCAN1-induced proliferation in β-TC6 cells

To further examine the effects of these IRCA drugs at a single concentration that does not reduce cell viability, we used the xCELLigence real-time cell proliferation assay. The β-TC6 cell line was treated with IRCA drugs for 18 days at the concentration discovered earlier and drugs-in-media were replaced daily to ensure consistency in daily dosage. There was a statistically significant increase in proliferation relative to control group for IRCA1 treated cells at 5x K_i compared to its DMSO control (Figure 4.4). This was not observed for the other IRCA drug groups.

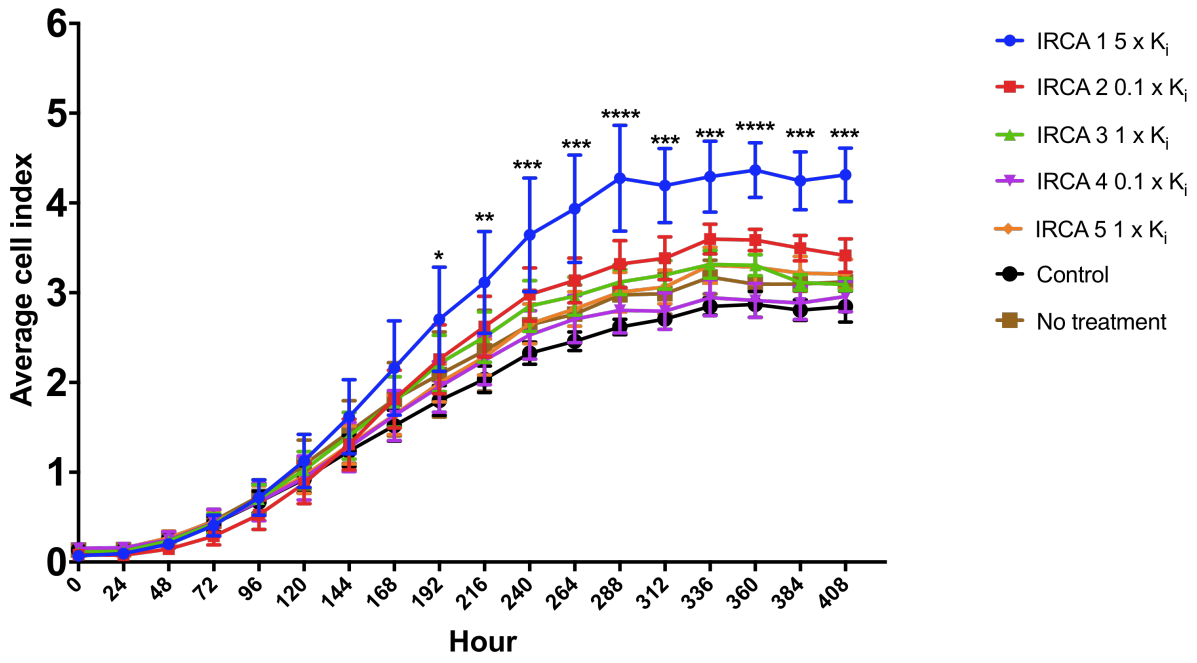

Figure 4.4 Using the xCELLigence system to measure real-time proliferation in the β-TC6 cell line treated with IRCA1- IRCA5 drugs at their minimum effective concentration that does not cause reduced cell viability. The average cell index (CI) from two experiments (n=3-4) involving BTC6 cell line treated over 18 days with the minimum effective concentration of IRCA1 to IRCA5 drug compared to a DMSO control. The no treatment group denotes just cells and media. Asterisks show where Two-way ANOVA with *post-hoc* test indicate difference (Two-way ANOVA with *post-hoc* analysis, * $p<0.05$, ** $p\leq0.01$, *** $p<0.001$, **** $p<0.0001$). All data shown are in SEM.

4.3.3 IRCA compounds had no effect on the RNA expression of genes associated with β-cell proliferation and apoptosis

The expression of genes associated with β-cell proliferation and apoptosis was investigated in the β-cell line treated with IRCA drugs for 3 days. Primers specific for the proliferation genes Cyclin D1 (*Ccnd1*) and Cyclin D2 (*Ccnd2*) and apoptosis genes, *Bax*, *Puma*, *Bim* and *Caspase 3*, *Caspase 8* and *Caspase 9* of Mus musculus were used on these β-cells template cDNA from real-time PCR reactions. These primer sequences were previously used in our lab (Table 4.1). There were no significant expression changes in apoptosis and proliferation genes between control groups and their various IRCA drug treatment groups (Figure 4.5).

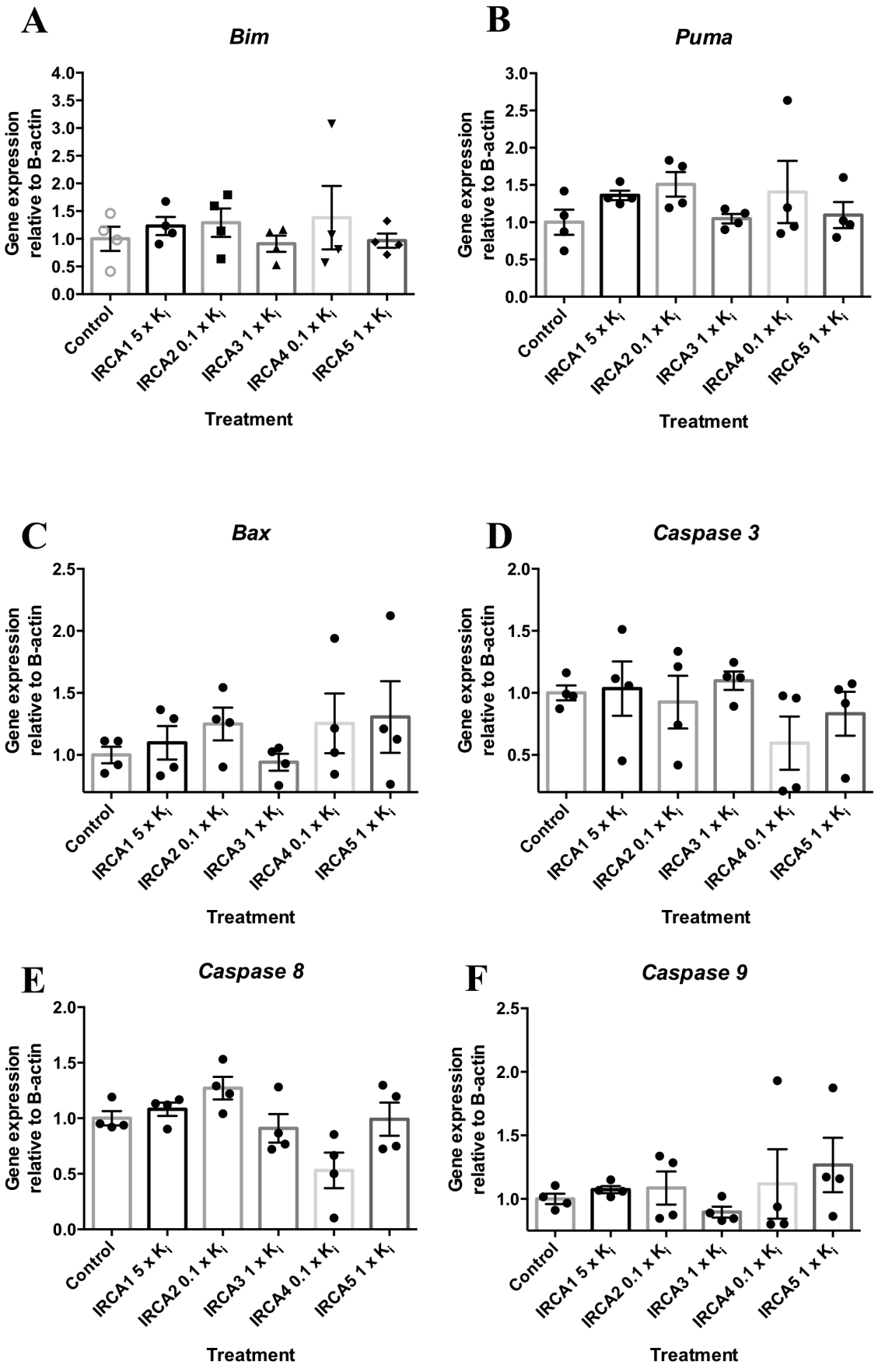
A
Bim
Gene expression relative to B-actin
4.0
3.5
3.0
2.5
2.0
1.5
1.0
0.5
0.0
Control
IRCA1 5 x Ki
IRCA2 0.1 x Ki
IRCA3 1 x Ki
IRCA4 0.1 x Ki
IRCA5 1 x Ki
Treatment
B
Puma
Gene expression relative to B-actin
3.0
2.5
2.0
1.5
1.0
0.5
0.0
Control
IRCA1 5 x Ki
IRCA2 0.1 x Ki
IRCA3 1 x Ki
IRCA4 0.1 x Ki
IRCA5 1 x Ki
Treatment
C
Bax
Gene expression relative to B-actin
2.5
2.0
1.5
1.0
Control
IRCA1 5 x Ki
IRCA2 0.1 x Ki
IRCA3 1 x Ki
IRCA4 0.1 x Ki
IRCA5 1 x Ki
Treatment
D
Caspase 3
Gene expression relative to B-actin
2.0
1.5
1.0
0.5
Control
IRCA1 5 x Ki
IRCA2 0.1 x Ki
IRCA3 1 x Ki
IRCA4 0.1 x Ki
IRCA5 1 x Ki
Treatment
E
Caspase 8
Gene expression relative to B-actin
2.0
1.5
1.0
0.5
0.0
Control
IRCA1 5 x Ki
IRCA2 0.1 x Ki
IRCA3 1 x Ki
IRCA4 0.1 x Ki
IRCA5 1 x Ki
Treatment
F
Caspase 9
Gene expression relative to B-actin
2.5
2.0
1.5
1.0
Control
IRCA1 5 x Ki
IRCA2 0.1 x Ki
IRCA3 1 x Ki
IRCA4 0.1 x Ki
IRCA5 1 x Ki
Treatment

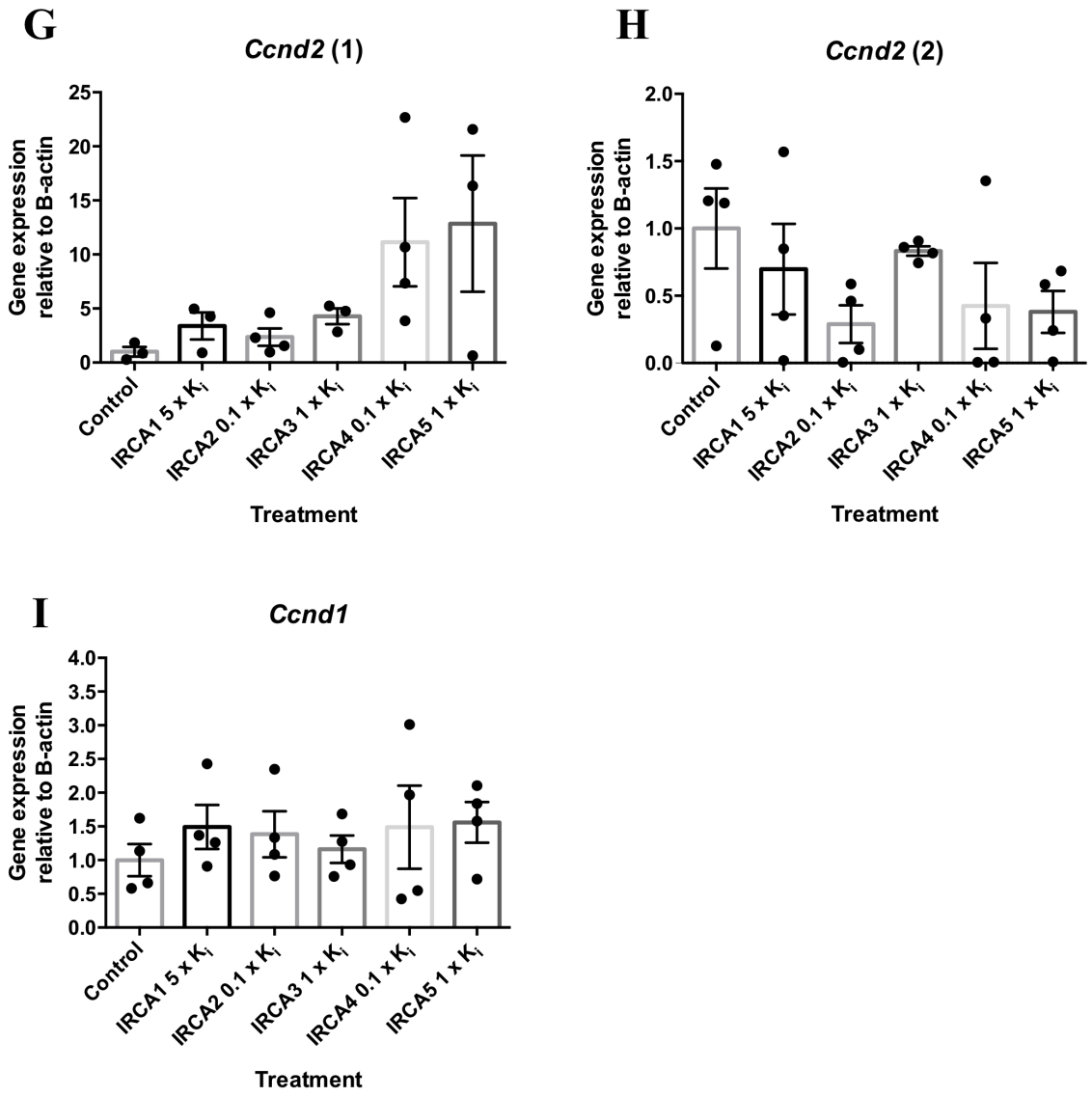

Figure 4.5 The expression of proliferation and apoptosis genes in β-TC6 β-cells were treated with IRCA drug at their minimum effective concentration for 3 days (n=3-4). The graphs **(A)** – **(F)** shows the apoptosis-associated genes and **(G)- (I)** shows the proliferation-associated genes. All data shown is in SEM and all genes were normalised to β-actin. Statistical significance was determined by comparing control group with treatment group using the One-way ANOVA with Dunnett's *post-hoc* test.

Taken together, the data indicates that inhibiting RCAN1-calcineurin interaction has a positive effect of inducing proliferation in the β-cell line. This suggests that IRCA drugs could be of therapeutic value in the treatment of diabetes. At gene level, IRCA drugs did not have an effect on the profile of pro-survival or apoptosis-associated genes after 3 days of drug treatment. This may reflective that changes could be happening earlier or after this point that was examined. Further investigation is necessary.

4.4 Discussion

In this study we attempted to understand the effects of inhibition of RCAN1-calcineurin interaction, using IRCA compounds, on β-cell apoptosis and proliferation and on the expression of markers of apoptosis and proliferation in the β-TC6 β-cell line. The optimal drug concentrations that had minimal effects on cell viability were initially determined as shown in Figure 4.3. These concentrations were then used for the rest of the experiments as optional drug concentrations to examine the effects on proliferation via real-time or measuring gene expression. Using the xCELLigence software to monitor the real-time proliferation effects of IRCA drugs on these β-cells over 18 days, IRCA1 at 5x K_i was shown to induce proliferation. There were no gene expression changes in the markers of apoptosis and proliferation in these β-cells treated with IRCA drugs for 3 days. The timeframe of 3 days was selected, mirroring the duration that the minimum effective concentration of drugs were tested for. The effects on gene and protein expression changes likely preceded the downstream effects of proliferation seen in the xcelligence experiment, however, this might have occurred before or after the time point of 3 days of IRCA drug treatment. These time points were not tested in this current chapter.

Glucose homeostasis requires normal β-cell function and insulin secretion as β-cells are the only source of endogenous insulin in the body. RCAN1, an inhibitor of calcineurin, has been implicated in the pathogenesis of T2D, where the expression of RCAN1 is upregulated in hyperglycaemic conditions (Peiris et al., 2012, Peiris et al., 2016). Additionally, $RCAN1^{ox}$ mice had smaller islets, increased ROS production, reduced GSIS, therefore RCAN1 could affect the balance between proliferation and apoptosis. There is strong evidence that *Rcan1* is a key gene in metabolism and upregulation of *RCAN1* is linked to the pathology of T2D.

The MTT assay, a metabolic assay, was vital in this experiment as it indicates cell viability which is especially important when testing drugs of various concentrations. In my results, the MTT assay was successful in obtaining the minimum effective concentration of each drug as follows: IRCA1 at 5x K_i, IRCA2 and IRCA4 at 0.1x K_i, IRCA3 and IRCA5 at 1x K_i were the chosen drug potencies selected for the experiments in this chapter, based on the results from the MTT assay. The cells being viable at 20x K_i for IRCA4 is surprising as we see that the previous two concentrations IRCA4 at 1xK_i and 10xK_i had significantly reduced absorbance readings compared to control and therefore, we would expect that at 20xK_i, this downward trend would follow. Reasons for this is unclear.

In β-cells, proliferation is important for normal insulin exocytosis and regulation of glucose homeostasis (Georgia and Bhushan, 2004). Particularly in the onset of management of chronic hyperglycaemia, β-cells proliferate to release more insulin as a coping mechanism for the influx of glucose (Heit et al., 2006a). The label-free xCELLigence biosensor technology has wide applications in cellular drug activity, viability and drug profiling. With the use of the xCELLigence real-time cell proliferation assay,

the minimum effective concentration was used for 18 days. The reason for conducting the experiment for 18 days is so that we can see a full plateau of the growth curve where the cells in the well are extremely confluent and proliferation can no longer be detected. These drugs were replaced daily in media for the duration of 18 days, as the half-life of these drugs are currently unknown. There was a significant increase in β-cell proliferation with the use of IRCA1 at 5x K_i from the 8th day of drug treatment compared to the control (DMSO) group. The β-cells treated with IRCAs 2-5 showed no significant changes to the rates of proliferation compared to control. This is helpful in indicating that IRCA1 at 5x K_i is the most effective drug for inducing the highest rate of proliferation compared to its control. Further experiments regarding potency and half-life of the drug can be conducted. The inhibitory effect of the IRCA drugs on RCAN1-calcineurin interaction could also target other molecular pathways. The limitations of the xCELLigence is that, cell index measurements which is reflective of the proliferation of β-cells does not distinguish between more cells, larger cell size or change in cell shape (Kho et al., 2015). Therefore, the effects of IRCA drug use on these β-cells needs to be further quantified through immunohistological means or the use of FACS sorting to determine proliferation and cell histology.

The inhibition of RCAN1-calcineurin with use of IRCA drugs resulted in no significant changes at transcriptional level for the genes associated with apoptosis and proliferation. Western blot can be used to confirm if protein expression changes occur. This suggest that apoptosis and proliferation rates could cancel each other out therefore manifesting as no change in expression rates in the short term of 3 days. This is supported by the data obtained for the xCELLigence experiment where only on the 8th day proliferation rate is significantly increased compared to control. Therefore, drug treatment over longer than 3 days in culture might enable us to observe expression changes in apoptosis and proliferation genes. Ideally, a time-dependent analysis of gene expression changes from 1 day, 3 days, 6 days, 9 days, 12 days, 18 days could be conducted to better understand the apoptosis and proliferation gene expression changes in IRCA drug β-cells in the short-term and long-term.

The D-type cyclins are important in the mitogenic signalling pathway, functioning to progress the cell cycle. Therefore, they are important in the proliferation of β-cells (He et al., 2009). In *Cnb1*$^{-/-}$ mice islets, *Ccnd1* mRNA levels had no change. However, upon selective NFAT activation, there was a significant increase in *Ccnd1* gene expression (Heit et al., 2006a). Therefore, our results using IRCA drugs to disrupt the RCAN1-calcineurin interaction resulting in no expression changes in *Ccnd1* expression is similar to that of *Cnb1*$^{-/-}$ mice, suggesting that the IRCA drugs could have other off-target effects that might perturb NFAT translocation in to the nucleus in the calcineurin-NFAT pathway. It would be necessary to induce selective NFAT activity in these cells to investigate this hypothesis. Cyclin D2 is required for mature β-cell proliferation. There was no change in *Ccnd2* mRNA levels, despite significant acute increase in Cyclin D2 protein after a small part of the pancreas was dissected

out from mice (He et al., 2009). This could also be the case with the data presented in this chapter, where *Ccnd2* showed no change at mRNA level and could potentially have post-transcriptional modifications at protein level.

Mitochondrial dysfunction is characteristic to T2D. The mitochondria are sensitive to overt levels of oxidative stress which results in apoptosis. This is evident in islets overexpressing RCAN1, in low and high glucose conditions (Peiris et al., 2016). The RCAN1^{ox} islets had a greater mitochondrial ROS production in the high glucose condition compared to low glucose and WT in the same conditions reflected by relative fluorescence using the MitoSox fluorescence assay (Peiris et al., 2012). RCAN1 is a stress-inducible protein that is involved in mitochondrial function in neuronal cells and more recently, the pancreatic β-cells (Peiris et al., 2012). In high glucose conditions, both RCAN1.1 and RCAN1.4 protein expression is increased in mouse pancreatic islets compared to low glucose conditions. There was a reduction in ATP availability in RCAN1^{ox} islets and reduced GSIS (Peiris et al., 2016).The expression of apoptosis markers can be correlated to the glucose-induced oxidative stress that increases ROS production, resulting in mitochondrial dysfunction and an induced increase in apoptotic genes. Therefore, future experiments can involve exposure of IRCA drug-treated cells to oxidative stress. To better understand mitochondrial dysfunction, mitophagy, a type of autophagy occurring specifically in the mitochondria can be measured in cells treated with IRCA drugs.

Additionally, to further the drug study, changes in expression of transcription factors that regulate genes important to β-cell function such as *Pdx1, Beta2*, *Hnf4α*, *Hnf1α*, *Hnf1β,* as a well as, β-cell cycle regulators including cyclin-dependent kinase 4 (*Cdk4*) and *c-myc* (Heit et al., 2006a) can be analysed in IRCA drug-treated cells. This is important for our understanding of the functionality of these β-cells to secrete insulin post-drug treatment. Also, an ELISA can be used by extracting lysates from drug-treated β-cells to investigate insulin content in these cells and therefore test for the β-cell's ability to secrete insulin (Peiris et al., 2012). This can be helpful in understanding the effects of IRCA drugs on the β-cell's functional capacity to secrete insulin following the increase in proliferation rate with the use of the IRCA1 drug at 5x K_i. Limitations in this study include the lack of direct measurement of β-cell number, β-apoptosis and calcineurin activity post-drug use. Such experiments would clarify the effect of using IRCA drugs to inhibit the RCAN1-claicnuerin interaction, discussed in section 7.4.

The recent publications from our lab used mice that had a global *RCAN1* overexpression (Peiris et al., 2012). Consideration needs to be made when comparing results from RCAN1^{ox}, *Rcan1*$^{-/-}$ mice islets or β-cells with that of IRCA drug-treated islets or β-cells as RCAN1 was globally expressed or knocked out in the whole animal. This is a limitation to such studies as other pathways could be implicated. Furthermore, the use of islets explant from RCAN1^{ox} mice were kept in culture for a few days prior to experiments conducted in these publications. Therefore, *in vivo* effects could be loss through this process. However, the use of primary islets and β-cells obtained from wild-type mice treated with IRCA

drugs might provide a better understanding of true effect of these inhibitors upon the RCAN1-calcineurin interaction and the downstream NFAT translocation and effects. Apart from Calcineurin inhibitor CsA, which prevents NFAT translocation, the GSK3β inhibitors (Li+ or TZDZ-8) which increases NFAT translocation can be use on β-TC6 cells to better understand the RCAN1-calcineurin pathway (Holowachuk, 2007). These results can be compared with the effects of using IRCA drugs on β-TC6 where RCAN1-Calcineurin interaction would be inhibited and calcineurin, essential to NFAT translocation, should continue.

The first study investigated the optimal drug concentrations that does not affect cell viability, with treatment of cells for 3 days, was helpful in determining the minimum effective drug concentrations that does not reduce cell viability. Even though differences in proliferation rates were only observed from day 8 in the xCELLgience experiment that occurred over 18 days, the viability of cells can be determined in a shortest amount of time and the study investigating the minimum effective concentration of drug that does not cause reduced cell viability was merely a gauge for cell viability at a single concentration. Overall, the significance of this study is the therapeutic gain of being able to induce proliferation by targeting the RCAN1-calcineurin interaction in β-cells. The capacity of inducing the proliferation of β-cells for the treatment of diabetes could have an immense change to the way diabetes is being treated. Although more work is still required, this is a promising finding that could be further developed to combat diabetes.

Chapter 5. ANALYSIS OF ADIPOSE TISSUE METABOLIC GENES IN WT AND *Rcan1*$^{-/-}$ MURINE eWAT ON HIGH- AND LOW-FAT DIETS

5.1 Introduction

The *RCAN1* gene, found on chromosome 21, has been associated with pancreatic β-cell mitochondrial dysfunction, T2D (Peiris et al., 2012, Peiris et al., 2016) and supresses non-shivering thermogenesis (NST) through inhibition of the induction of uncoupling protein 1 (UCP1) expression in white adipose tissue and through sarcolipin in skeletal muscles (Rotter et al., 2018). Apart from functional mechanisms such as NST, the adipose tissue undergoes several other metabolic processes such as lipolysis, lipogenesis and adipogenesis. We are interested in extending our understanding of the role of RCAN1 in other metabolic pathways within the adipose tissue. The regulation of lipolysis and lipogenesis are essential in determining energy distribution and maintenance of the fat depot size within the organism (Kersten, 2001). Downregulated lipolytic activity could contribute to increased TG storage in the adipose tissue, resulting in obesity. While lipodystrophy, due to abnormally high rates of lipolysis, could result in lipotoxicity that contributes to insulin resistance (Jaworski et al., 2007, Morigny et al., 2016). In an obese individual, excess fatty acids could be released in excess, insulin resistance, endothelial and pancreatic β-cell dysfunction (Cerf, 2013, Ormazabal et al., 2018) might eventually result in T2D. The regulation of lipolysis is complex, involving metabolic hormones, neuronal input and metabolites that changes in response in nutritional states (Lass et al., 2011, Nielsen et al., 2014). In a recent publication, RCAN1 KO (*Rcan1*$^{-/-}$) mice fed a high fat diet (HFD) did not gain weight compared to WT and displayed a lean phenotype confirmed with nuclear magnetic resonance spectroscopy (Figure 1.23B). *Rcan1*$^{-/-}$ and WT mice on a HFD displayed no differences in faeces cholesterol and triglyceride content (Rotter et al., 2018) suggesting that nutritional uptake in the intestines was not disrupted and the lack of weight gain in these *Rcan1*$^{-/-}$ mice on a HFD was not due to defects in dietary absorption or NST. Additionally, the data showed a reduction in adipocyte size in fat pads between *Rcan1*$^{-/-}$ and WT mice on either diets, indicative of lesser fat storage in adipocytes. Therefore, other metabolic mechanisms could contribute to the lean phenotype observe in *Rcan1*$^{-/-}$ mice on a HFD. In this chapter, we explore gene expression changes associated with lipolysis, lipogenesis and adipogenesis in epididymal white adipose tissue (eWAT) of *Rcan1*$^{-/-}$ and WT mouse on high- and low- fat diets. The eWAT fat depot was used in this experiment as it is the largest visceral fat depot in the body of the mouse and description of its location is described in chapter 1 (Figure 1.4).

Lipolysis is the breakdown of triacylglycerol (TG) to produce non-esterified fatty acids (NEFA) and glycerol under fasting and cold-induced adrenergic conditions and during elevated energy demands. The expression of key genes known to be associated with lipolysis such as perilipin 1 (*Plin1*), comparative gene identification 58 (*Cgi-58*), adipose triglyceride lipase (*Atgl*), G0/G1 switch gene 2 (*G0s2*) and hormone sensitive lipase (*Hsl*) were measured using quantitative real-time PCR in this study (Table 5.1). The function of these enzymes and their role in the lipolytic pathway have been described in detail in Chapter 1 (Figure 1.7). Based on a recent publication, basal lipolysis was increased in the

Rcan1$^{-/-}$ mice compared to its WT in subcutaneous white adipose tissue (sWAT). In the activated lipolysis state, activated lipolysis is decreased in the *Rcan1*$^{-/-}$ mice compared to WT in sWAT (Rotter et al., 2018) (Figure 1.25). Therefore, this chapter aims to investigate lipolysis-associated gene expression and discuss possible functional changes due to expression changes.

Both lipogenesis and adipogenesis have not been directly measured in *Rcan1*$^{-/-}$ mice and studying these processes will expand our understanding of the role of RCAN1 in adipocyte biology and function. Lipogenesis is the process of fatty acid synthesis and subsequent triglyceride synthesis occurring in both liver and adipose tissue (Kersten, 2001). The lipogenic pathway has been described in detail in Chapter 1 (Figure 1.6) and the lipogenesis-associated genes such as ATP-citrate lyase (*Acl*), Acetyl CoA carboxylase alpha (*Acc1*), ACC-beta (*Acc2*), fatty acid synthase (*Fas*), sterol regulatory element binding transcription factor 1 (*Srebp1*), *Srebp -1a*, *-1c*, carbohydrates response element binding protein (*Chrepb*), *Chrebp-α* and *-β* are investigated in this chapter (Table 5.1). In lipolysis, the breakdown of triacylglycerol to fatty acids and glycerol, involves the sequential actions of three important lipases, namely, ATGL, HSL and MGL (Lass et al., 2011). It is important to first consider the function of these proteins, when trying to understand how gene expression changes could affect function and the overall significance of these findings. SREBP1 and ChREBP are key transcription factors that regulate genes in the *de novo* lipogenesis (DNL) and glycolysis pathways (Brown and Goldstein, 1997, Ruiz et al., 2014). SREBP-1c is involved in insulin-mediated effects on lipogeneic gene expression in adipocytes (Kim et al., 1998, Foretz et al., 1999). Furthermore, SREBP-1c activate genes for fatty acid biosynthesis but not cholesterol synthesis while SREBP-1a activates genes for both cholesterol and fatty acid biosynthesis (Amemiya-Kudo et al., 2002, Horton et al., 2002, Iizuka et al., 2004). *Srebp1*$^{-/-}$ mice has decreased synthesis of fatty acids, given the reduced expression of genes for fatty acid synthesis enzymes in the liver (Ruiz et al., 2014). *Srebp1c* mRNA expression is elevated in islets (3.4 times higher than lean control), liver (2.4 times higher than lean control) (Kakuma et al., 2000) and the SREBP-1c protein levels are increased in the kidney of HFD-induced diabetic animal models (Saravanan and Pari, 2016). In pathogenic states, SREBP-1c is upregulated in the liver in insulin-resistant animals and is involved in the pathogenesis of T2D (Shimano et al., 1996, Tobe et al., 2001), insulin resistance in skeletal muscle (Bi et al., 2014) and β-cell dysfunction (Wang et al., 2003).

ChREBP is a glucose-responsive transcription factor, involved in DNL, and regulate genes of enzymes involved in fatty acid synthesis and glycolysis (Uyeda et al., 2002, Iizuka et al., 2004). ChREBP has two isoforms, ChREBP-α and ChREBP-β, alternative splice variants of the same *Mlxipl* gene (Herman et al., 2012). GLUT 4-mediated glucose uptake induces ChREBP which activates adipose tissue DNL (Herman et al., 2012). ChREBP-α is constitutively expressed in metabolic tissues such as the adipose tissue (Iizuka et al., 2004). ChREBP-α in combination with max-like protein X is bound to the carbohydrate response elements in promoters of target genes involved in lipogenesis and ChREBP-β.

Once activated, ChREBP-β also activates target genes that synthesises fatty acids (Song et al., 2018) (Figure 1.6). Overall, dysregulation of DNL can result in adverse metabolic effects (Ameer et al., 2014). Therefore, we were interested in investigating the expression of lipogenic enzyme gene expression the expression of their transcriptional regulators.

Obesity can involve both hypertrophy (increase size of adipocyte) or hyperplasia (formation of new adipocytes by adipogenesis, therefore, the study of adipogenesis is important for the understanding of obesity (Ghaben and Scherer, 2019). Adipogenesis is defined as the differentiation of adipocytes from pre-adipocytes into mature fat cells (Kersten, 2001) (Figure 1.4). Both CCAAT/enhancer-binding protein alpha (C/EBP-α) and leptin are involved in adipogenesis and we investigated the expression of these genes within eWAT of these mice (Table 5.1). The differentiation cocktail used to transform fibroblast cells to adipocyte cells has been discussed in section 2.2.1 of this thesis. Expression of C/EBPα is necessary for pre-adipocyte differentiation. In the absence of C/EBPα, adipose-specific genes were not expressed and triacylglycerol accumulation was not detected (Freytag et al., 1994, Shao and Lazar, 1997). Leptin is a cytokine produced mainly by WAT and is highly linked to weight and food intake (Gallardo et al., 2007); dysregulation of leptin results in metabolic conditions and obesity. In the recent publication, leptin serum levels were decreased in *Rcan1*$^{-/-}$ mice on a HFD compared to WT on a HFD and compared to *Rcan1*$^{-/-}$ on normal chow, which is expected as *Rcan1*$^{-/-}$ had anti-obesogenic effects (Rotter et al., 2018) (Figure 1.23E). Moreover, leptin has multiple roles and is involved in the regulation of fatty acid homeostasis where it restricts lipid storage in adipocytes, and limits lipid accumulation in non-adipocytes, functioning to protect against lipotoxicity (Unger et al., 1999, Unger, 2002) and prevents the overexpression of SREBP-1c. Furthermore, peroxisome proliferator-activated gamma (PPAR γ), key in gluconeogenesis as well as adipogenesis (Tontonoz and Spiegelman, 2008), showed a significant downregulation of PPARγ in *Rcan1*$^{-/-}$ compared to WT on a HFD (Figure 5.1), indicative of reduction in adipogenesis in *Rcan1*$^{-/-}$ mice on a HFD compared to WT. Therefore, these two genes in the present study, involved in adipogenesis, are essential to our investigation of phenotypic effects observed in *Rcan1*$^{-/-}$ compared to WT and with diets of different fat levels. In this study, it is hypothesized that there will be decrease in lipogenic- and adipogenesis-related genes in *Rcan1*$^{-/-}$ compared to WT on a HFD. To investigate this hypothesis, RT-PCR was used to examine genes associated with lipogenesis, adipogenesis and lipolysis.

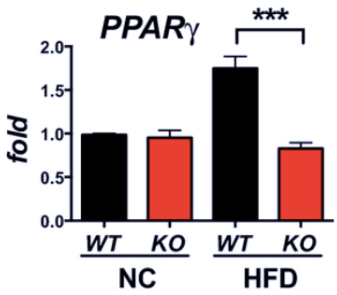

Figure 5.1 Transcript level of peroxisome proliferator-activated gamma (*Pparg*) involved in adipogenesis in liver of WT and KO mice on normal chow (NC) and high fat diet (HFD) (Rotter et al., 2018).

Overall, obesity can result from expansion of individual adipocyte size or increase in abundance of adipocytes due to increased differentiation (Spiegelman and Flier, 1996) and understanding of adipogenic genes is important. Lipolysis and lipogenesis determine the amount of fat accumulated (Kersten, 2001). Therefore, our study aims to understand the effects of diet on *Rcan1*$^{-/-}$ and WT gene expression in the processes related to lipolysis, lipogenesis and adipogenesis in eWAT. This will also further our understanding of the role of RCAN1 in adipose tissue function. I hypothesise that RCAN1 decrease lipolysis, increase lipogenesis and adipogenesis in mice on a HFD compared to LFD through its role as an inhibitor of calcineurin.

5.2 Materials and methods

5.2.1 Animals

Rcan1$^{-/-}$ mice (Flinders University) or wild-type (WT) were generated and fed a high (35%) fat diet (HFD) produced by Speciality Feeds (WA, Australia) or and a low (4%) fat diet (LFD; Normal chow) (LabDiet 5001) for 8 weeks by Dr Alyce Martin (Keating lab) and were humanely euthanised at 17-18 weeks old. Details of mice breeding can be found in section 2.6. The epididymal white adipose tissue (eWAT) was dissected and snap frozen for later use. Total RNA was extracted from mice eWAT using the RNeasy® Lipid Tissue Mini Kit (Qiagen, Australia) following manufacturer's instructions and described in detail in section 2.7 of this thesis.

5.2.2 Adipose tissue Gene Expression Profile

The list of gene targets for lipolysis, lipogenesis and adipogenesis can be found in the table below (Table 5.1) and the general quantitative PCR method has been described previously in Chapter 2. The melt curves and quantitation graphs generated for each of these gene targets can be found in Appendix B.2.

Table 5.1 Primer forward and reverse sequences and size and source

Lipolysis				
Gene target	**Forward**	**Reverse**	**Length**	**Reference**
Perilipin 1 (*Plin1*)	GGGACCTGTGAGT GCTTCC	GTATTGAAGAGC CGGGATCTTTT	228	(Cai et al., 2012)
Adipose triglyceride lipase (*Atgl*)	ATTTATCCCGGTGT ACTGTG	GGGACACTGTGA TGGTATTC	119	(Lee et al., 2009)
Comparative gene identification 58 (*Cgi-58*)	GGTTAAGTCTAG TGCAGC	AAGCTGTCTCAC CACTTG	126	(Zierler et al., 2013)
Hormone Sensitive lipase (*Hsl*)	GCTGGGCTGTCA AGCACTGT	GTAACTGGGTAG GCTGCCAT	160	(Taschler et al., 2011)
G0/G1 switch gene 2 (*G0s2*)	AGTGCTGCCTCTCT TCCCAC	TTTCCATCTGAGC TCTGGGC	65	(Zandbergen et al., 2005)
Lipogenesis				
Gene target	**Forward**	**Reverse**	**Length**	**Reference**
Sterol regulatory element-binding transcription factor 1 (*Srebp1- total*)	GCTCCAGCTCATC AACAACCA	CAGGAAGGCTTC CAGAGAGGA	160	(Le Lay et al., 2002)
Srebp1c	ATCGGCGCG GAAGCTGTC GGGGTAGCGTC	ACTGTCTTGGTT GTTGATGAGCTG GAGCAT	116	(Rinella et al., 2008)
Srebp1a	CATAGGGGGCGTC AAACAG	GATGTGCGAACT GGACACAG	104	(Green et al., 2007)
Carbohydrate-responsive element-binding protein (*Chrebp- total*)	CACTCAGGGAATA CACGCCTAC	ATCTTGGTCTTAG GGTCTTCAGG	110	(Herman et al., 2012)
Carbohydrate-responsive element-binding protein - alpha (*Chrebp-α)*	CGACACTCACCCA CCTCTTC	TTGTTCAGCCGG ATCTTGTC	121	(Herman et al., 2012)
Carbohydrate-responsive element-binding protein-beta (*Chrebp-β)*	TCTGCAGATCGCG TGGAG	CTTGTCCCGGCAT AGCAAC	87	(Savage et al., 2006, Jois et al., 2016)

Acetyl-CoA carboxylase alpha (*Acc1*)	ATTGTGGCTCAAA CTGCAGGT	GCCAATCCACTC GAAGACCA	67	(Savage et al., 2006)
Acetyl-CoA carboxylase beta (*Acc2*)	GGGCTCCCTGGAT GACAAC	GCTCTTCCGGGA GGAGTTCT	73	(Im et al., 2009)
ATP-citrate lyase (*Acl*)	ACCCTCTTCAGCC GACATACC	CTGCTTGTGATCC CCAGTGA	147	(Schirra et al., 2006)
Fatty acid synthase (*Fas*)	CCAAGCAGGCACA CACAA	CACTCACACCCA CCCAGA	132	(Hessel et al., 2007)
Adipogenesis				
Gene target	**Forward**	**Reverse**	**Length**	**Reference**
CCAAT/enhancer-binding protein alpha (*Cebp-a*)	TGGACAAGAACAG CAACGAGTAC	GCAGTTGCCCAT GGCCTTGAC	239	(Sandhir and Berman, 2010)
Leptin	TCTATCAACAGGT CCTCACC	ACTGTTGAAGAA TGTCCTGC	240	(Lee et al., 2009)
Housekeeper				
Gene target	**Forward**	**Reverse**	**Length**	**Reference**
β-actin	GGGGCAAGAGAG GTATCCTGACC	CCCTGGATGCTA CGTACATGGC	237	(Rotter et al., 2018)

5.2.3 Statistical analysis

Data are presented as mean ± standard error of mean (SEM). The results for each RT-PCR run was inserted into the Qgene spreadsheet that automates delta-delta CT readings and generates the calculated mean normalised expression. The mean normalised expression for the target genes were normalised to the house keeping gene *β-actin*. Difference between diet groups and mice groups were performed using a One-way ANOVA unpaired test with Tukey *post-hoc* test. A two-tailed *P*-value <0.05 was considered statistically significant. Statistical analyses were performed using the Prism software (Prism 8.0).

5.3 Results

5.3.1 Lipolysis associated gene expression changes in *Rcan1*$^{-/-}$ mice

Lipolysis gene expression in epididymal white adipose tissue (eWAT) in the absence or presence of RCAN1 on mice fed a normal chow (4% fat), denoted as low-fat diet (LFD) and a 35% high fat diet for 8 weeks. There was significant decrease in *Plin1* and *Hsl* expression in *Rcan1*$^{-/-}$ on a LFD compared to WT. This was roughly 0.5-fold decrease for both genes. (Figure 5.2 A, E). No significant changes were observed in transcript levels of *Cgi-58* and *G0s2* (Figure 5.2 B, D). On a HFD, there was an 2- fold increase in transcript levels in *Rcan1*$^{-/-}$ compared to WT and LFD groups (Figure 5.2 C). Taken together, RCAN1 may have a role in the lipolytic pathway at a transcriptional level, as it highly affects the rate-limiting enzyme ATGL, evident by the significant increase in *Atgl* in *Rcan1*$^{-/-}$on a HFD compared to WT and all diet groups. The increase in *Atgl* mRNA in KO mice on a HFD suggest that basal lipolysis is increased in these mice compared to WT and all diet groups. Additionally, consumption of LFD showed a significant decrease in *Plin1* and *Hsl* expression compared to WT on the same diet further suggesting that RCAN1 plays a role in the lipolytic process. Overall, this supports the data showing RCAN1 decreases lipolysis in WT mice (Rotter et al., 2018) (Figure 1.25).

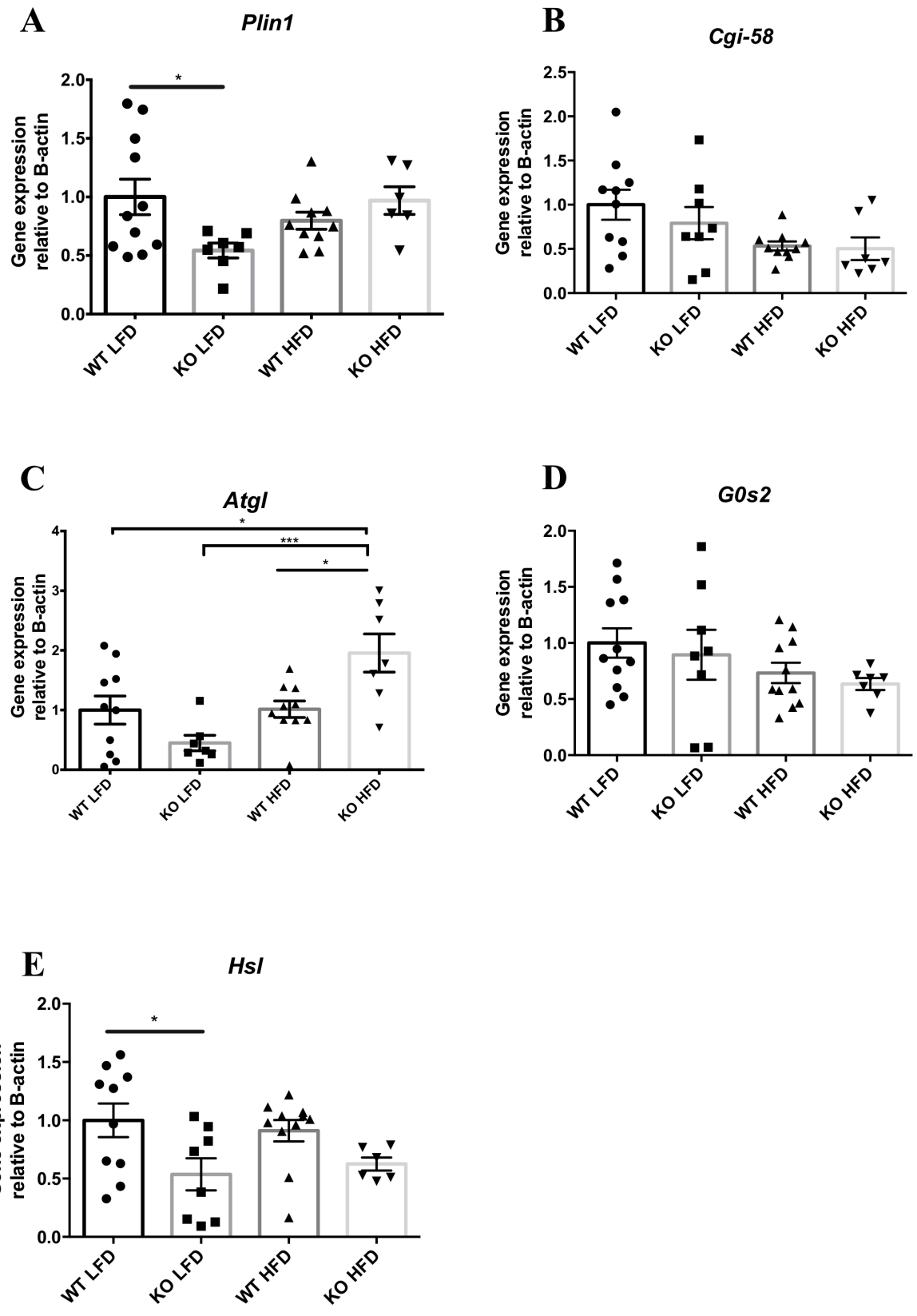
A
Plin1
Gene expression relative to B-actin
2.0
1.5
1.0
0.5
0.0
*
WT LFD
KO LFD
WT HFD
KO HFD
B
Cgi-58
Gene expression relative to B-actin
2.5
2.0
1.5
1.0
0.5
0.0
WT LFD
KO LFD
WT HFD
KO HFD
C
Atgl
Gene expression relative to B-actin
4
3
2
1
0
*
***
*
WT LFD
KO LFD
WT HFD
KO HFD
D
G0s2
Gene expression relative to B-actin
2.0
1.5
1.0
0.5
0.0
WT LFD
KO LFD
WT HFD
KO HFD
E
Hsl
Gene expression relative to B-actin
2.0
1.5
1.0
0.5
0.0
*
WT LFD
KO LFD
WT HFD
KO HFD

Figure 5.2 Expression of lipolysis-associated genes were analysed from murine eWAT tissue of WT LFD, *Rcan1*$^{-/-}$ LFD, WT HFD and *Rcan1*$^{-/-}$ HFD groups. **(A)** Perilipin 1 (*Plin1*) (n=6 -11) **(B)** Comparative gene identification 58 (*Cgi-58*) (n=7-10) **(C)** adipose triglyceride lipase (*Atgl*) (n=7-10) **(D)** G0/G1 switch gene 2 (*G0s2*) (n=7-11) and **(E)** hormone sensitive lipase (*Hsl*) (n=6-11). Asterisks show where one-way ANOVA with Tukey *post-hoc* test indicate difference (One-way ANOVA with Tukey *post-hoc* analysis, *$p<0.05$, *** $p<0.001$).

5.3.2 Lipogenic gene expression was altered in *Rcan1*$^{-/-}$ mice

In our study, we compared directly the expression level of genes in the lipogenic pathway in adipose tissue of WT and *Rcan1*$^{-/-}$mice. To determine whether diet causes a difference between *Rcan1*$^{-/-}$ mice and WT, the eWAT of mice fed on these diets were isolated. SREBP-1 and ChREBP are key transcription factors involved in the regulation of enzymes involved in lipogenesis such as ACC1 and ACC2, ACL and FAS. There was a significant decrease in *Srebp1c* transcript levels in *Rcan1*$^{-/-}$ mice on a LFD and WT on a LFD (2.6-fold) (Figure 5.3C). Overall expression changes were not observed in *Srebp1*-total and *Srebp1a* (Figure 5.3 A and B). The transcript levels of *Chrebp*-total were significantly increased (2.3-fold) in *Rcan1*$^{-/-}$ on a HFD compared to WT on a HFD (Figure 5.3 D). No expression changes observed in *Chrebp-α* and *Chrebp-β* (Figure 5.3 E).

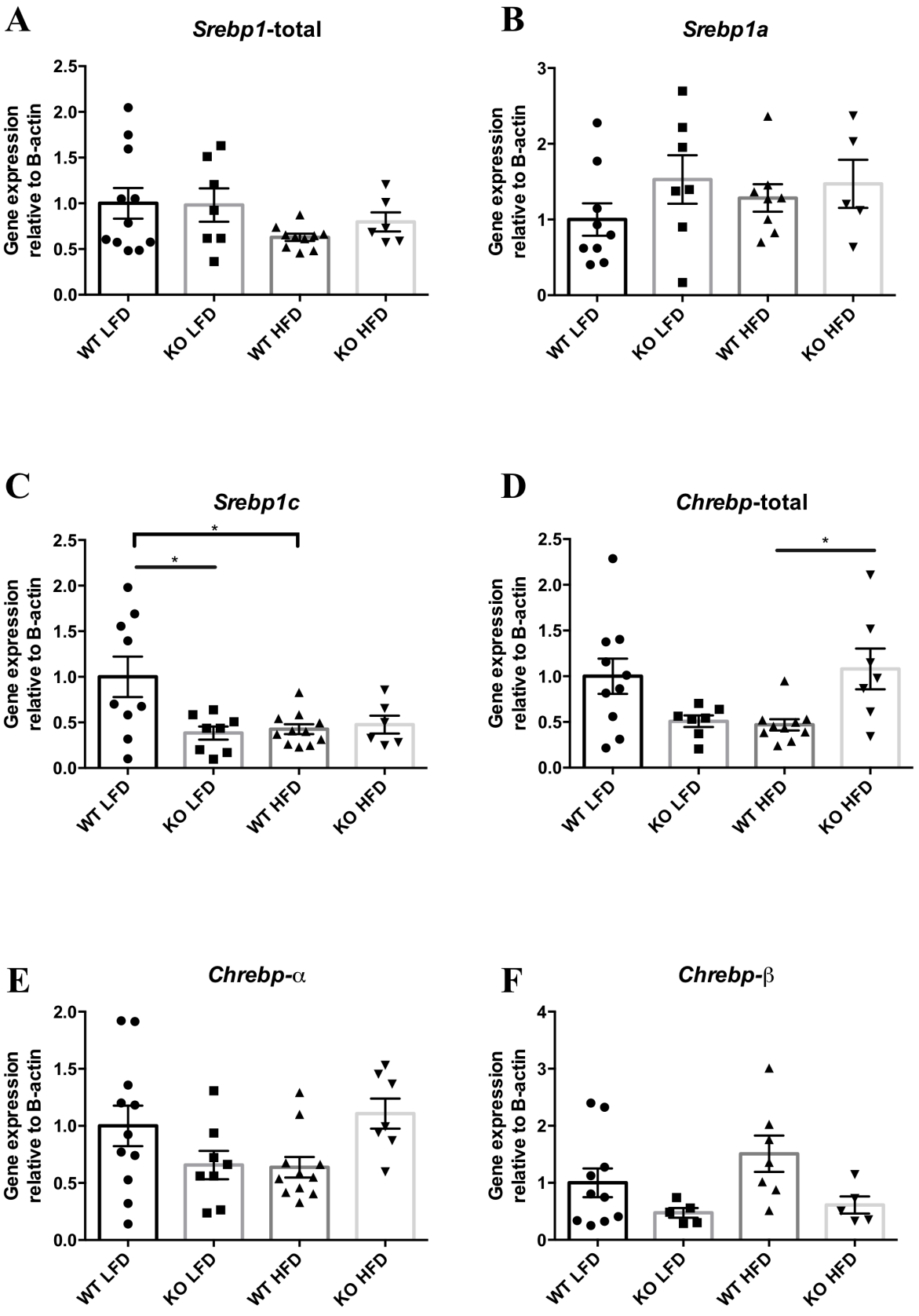
A
Srebp1-total
Gene expression relative to B-actin
2.5
2.0
1.5
1.0
0.5
0.0
WT LFD
KO LFD
WT HFD
KO HFD
B
Srebp1a
Gene expression relative to B-actin
3
2
1
0
WT LFD
KO LFD
WT HFD
KO HFD
C
Srebp1c
Gene expression relative to B-actin
*
*
2.5
2.0
1.5
1.0
0.5
0.0
WT LFD
KO LFD
WT HFD
KO HFD
D
Chrebp-total
Gene expression relative to B-actin
*
2.5
2.0
1.5
1.0
0.5
0.0
WT LFD
KO LFD
WT HFD
KO HFD
E
Chrebp-α
Gene expression relative to B-actin
2.0
1.5
1.0
0.5
0.0
WT LFD
KO LFD
WT HFD
KO HFD
F
Chrebp-β
Gene expression relative to B-actin
4
3
2
1
0
WT LFD
KO LFD
WT HFD
KO HFD

Figure 5.3 Expression of transcription factors involved in lipogenesis in murine eWAT tissue. **(A)** Sterol regulatory element-binding transcription factor 1 (*Srebp-1*) (n=6-11) **(B)** Sterol-regulatory element binding protein -1 alpha (*Srebp1a*) (n=5-9) **(C)** sterol regulatory element binding protein-1c (*Srebp1c*) (n=6-11) **(D)** Carbohydrate-responsive element binding protein (*Chrebp*-total) (n=7-10) **(E)** Carbohydrate-responsive element binding protein-alpha (*Chrebp-α*) (n=7-11) and **(F)** Carbohydrate-responsive element binding protein-beta (*Chrebp-β*) (n=5-10). Asterisks show where One-way ANOVA with Tukey *post-hoc* test indicate difference (One-way ANOVA with Tukey *post-hoc* analysis, *p<0.05, *** p<0.001).

FAS is a key lipogenic enzyme. While there were no changes in the *Fas* and *Acc2* transcript levels (Figure 5.4 B,D), *Acl* was significantly increased in *Rcan1*$^{-/-}$ on a HFD compared to WT HFD (8.7-fold increase) and LFD groups (Figure 5.4A). The *Acc1* transcript levels decreased significantly in *Rcan1*$^{-/-}$ on a LFD compared to WT on a LFD (3.5-fold decrease). Comparing WT in LFD to HFD groups, there was a significant 5.6-fold decrease in *Acc1* gene expression (Figure 5.4C).

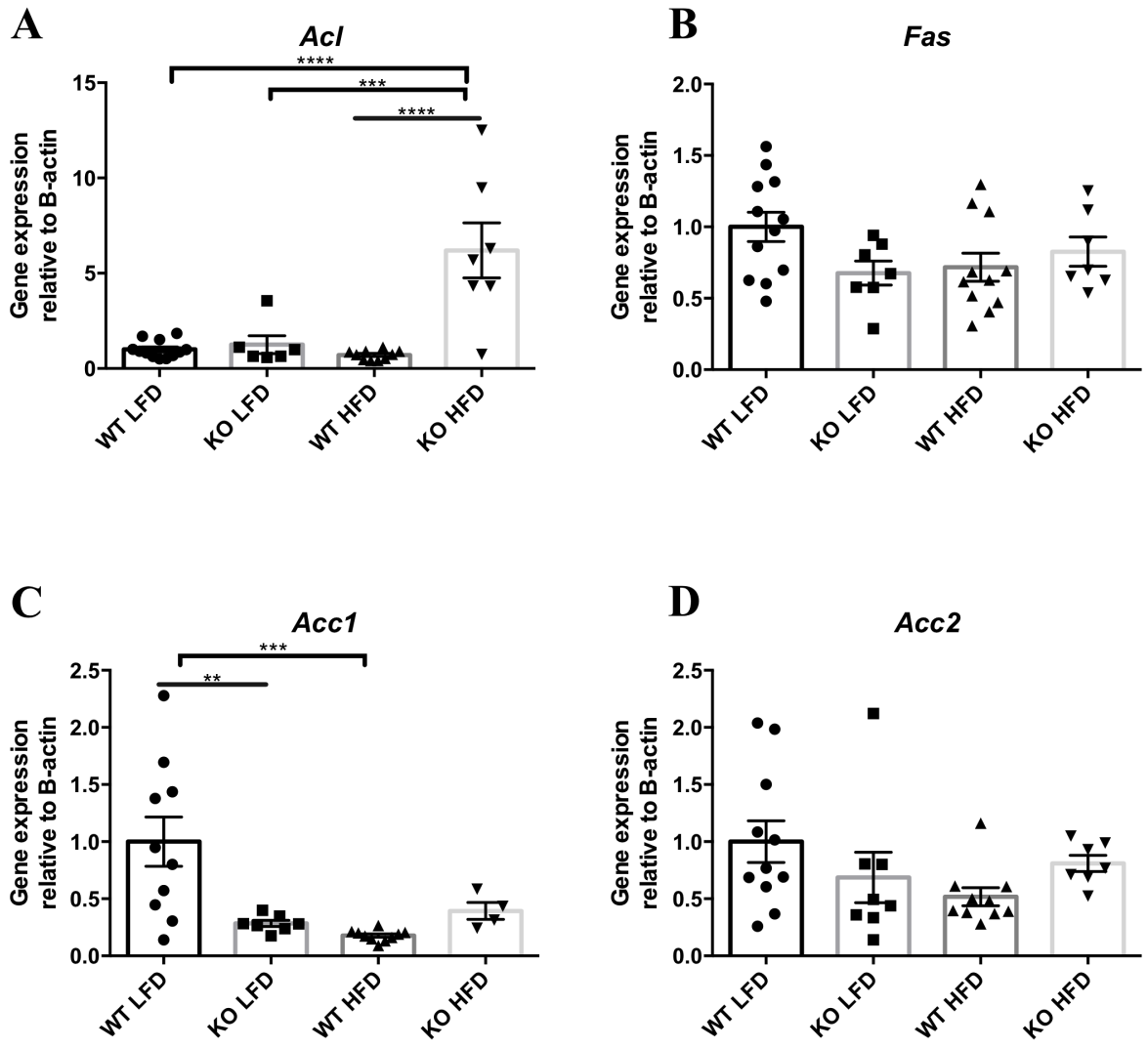

Figure 5.4 Expression of genes of lipogenic enzymes in murine eWAT tissue. **(A)** ATP-citrate lyase (ACL) (n=6-12) **(B)** fatty acid synthase (*Fas*) (n=7-12) **(C)** acetyl-CoA carboxylase alpha (*Acc1*) (n=4-10) **(D)** Acetyl-CoA carboxylase beta (*Acc2*) (n=7-11). Asterisks show where one-way ANOVA with Tukey *post-hoc* test indicate difference (One-way ANOVA with Tukey *post-hoc* analysis, *p<0.05, *** p<0.001).

5.3.3 Adipogenesis gene expression change with diet type in *Rcan1*$^{-/-}$ mice

In the recently published work, *Pparg*, part of the adipogenic process, showed a decreased in mRNA expression in *Rcan1*$^{-/-}$ on a HFD compared to WT. This was similar for leptin serum levels, where *Rcan1*$^{-/-}$ mice had decreased leptin levels compared to WT on a HFD (Rotter et al., 2018). CCAAT/enhancer-binding protein alpha (*Cebp-a*) and *Leptin* were the two genes we looked at for adipogenesis. There was a significant 2.4-fold increase in leptin gene expression in *Rcan1*$^{-/-}$ mice on a HFD compared to WT on a HFD, a 9.1- fold increase in *leptin* gene expression in *Rcan1*$^{-/-}$ HFD compared to *Rcan1*$^{-/-}$ LFD and a 3.9-fold increase in *leptin* gene expression in WT HFD compared to WT LFD (Figure 5.5).

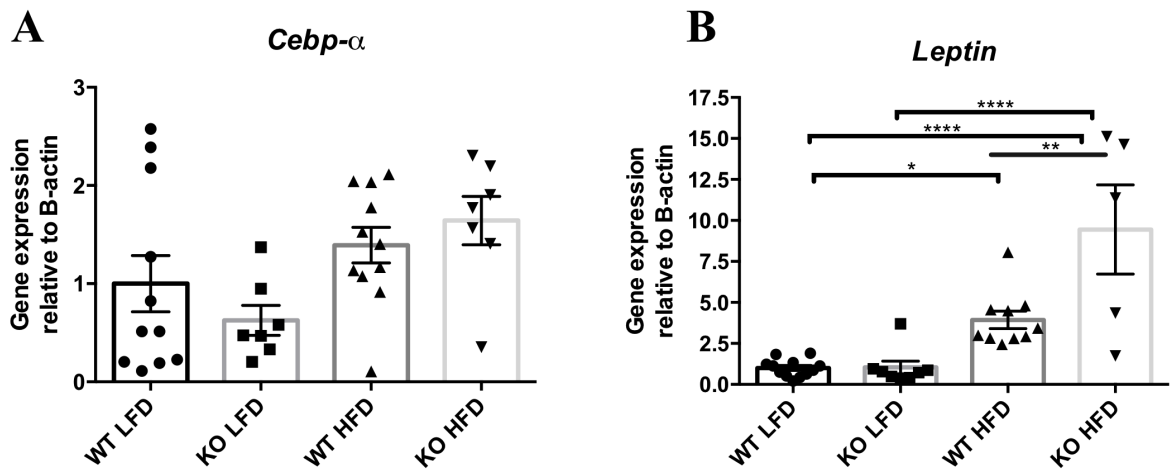

Figure 5.5 The expression of adipogenesis-associated gene in murine eWAT tissue. **(A)** CCAAT/enhancer-binding protein alpha (*Cebp-a*) (n=7-11) and **(B)** *Leptin* (n=5-12). Asterisks show where one-way ANOVA with Tukey *post-hoc* test indicate difference (One-way ANOVA with Tukey *post-hoc* analysis, *p<0.05, *** p<0.001).

Taken together, these data demonstrate that diet-specific changes affected *leptin* at the transcriptional level and not *Cebp-a* expression in *Rcan1*$^{-/-}$ mice and WT mice eWAT. Furthermore, leptin is important in the expansion of fat and the adipogenic process. Overall, RCAN1 has a regulatory role in lipid metabolism.

5.4 Discussion

Obesity is linked to increased risk for T2D, cancer and cardiovascular disease (Fruh, 2017). The ablation of *Rcan1*, an endogenous inhibitor of calcineurin, has been recently linked to an anti-obesogenic phenotype in mice (Rotter et al., 2018) and the overexpression of *RCAN1* was linked to diabetes in mice (Peiris et al., 2012, Peiris et al., 2016). There is need for greater understanding of the role of RCAN1 in the adipose tissue given that metabolic effects of RCAN1 is not limited to β-cells (Peiris et al., 2012, Peiris et al., 2016). Furthermore, synthetic inhibitors of calcineurin used for immunosuppression in organ transplant patients have increased risk for weight gain and post-transplant diabetes (Heisel et al., 2004, Chakkera et al., 2017), presenting a link between calcineurin, a target of RCAN1 inhibitory effect, and diabetes. The results of this chapter have highlighted the diverse range of effects of knocking-out *Rcan1* and the differences in diets have on adipogenic, lipolytic and lipogenic gene expression. This study is novel and understanding of gene expression changes in the adipose tissue of *Rcan1*$^{-/-}$ mice could inform us of the role of RCAN1 in adipose tissue function discussed below.

5.4.1 *Plin1* and *Hsl* gene expression decreased in *Rcan1*$^{-/-}$ mice on a LFD

Functionally, PLIN1 proteins have dual roles, functioning as a barrier to lipid droplet breakdown (Ueno et al., 2013) and has a role in regulating lipolysis rate as it functions as a barrier to lipases, such as HSL, thus maintaining low basal lipolysis (Brasaemle et al., 2000b, Miyoshi et al., 2006, Jaworski et al., 2007). This is important as obese patients and animals have elevated basal lipolysis (Reynisdottir et al., 1995) and stimulated lipolysis is reduced (Large et al., 1999), reviewed by (Morigny et al., 2016). Insulin resistance in obese patients can dysregulate adipocyte metabolic activities and increase basal lipolysis (Morigny et al., 2016). PLIN1 also acts to increase activated lipolysis by regulating the hydrolytic action of HSL, through both phosphorylation independent and dependent mechanisms (Miyoshi et al., 2006). My results show a decrease in *Plin1* gene expression in *Rcan1*$^{-/-}$ mice compared to WT, which is indicative of reduced barrier protection against lipases, inherently increasingly basal lipolysis as evident in the recent publication where *Rcan1*$^{-/-}$ mice had increased basal lipolysis compared to WT (Rotter et al., 2018). Basal lipolysis in *Plin1*$^{-/-}$ adipocytes was increased compared to WT (Tansey et al., 2001) where *Plin1*$^{-/-}$ mice had a lean body mass, upregulated metabolic rate but increased glucose intolerance and peripheral insulin resistance. This is most evident when these mice were fed a HFD, resulting in an increased in ectopic fat which contributed to the development of insulin resistance (Martinez-Botas et al., 2000, Tansey et al., 2001) and the promotion of inflammatory responses (Sohn et al., 2018). Therefore, decreased expression of lipid-droplet protein PLIN1 is linked to insulin resistance - the lack of PLIN1 in *Plin1*$^{-/-}$ mice results in induction of inflammatory responses and lipolysis was promoted (Sohn et al., 2018). Furthermore, adipose-specific *Plin1* overexpression and mice on a HFD, resulted in resistance to obesity, improved insulin sensitivity and increased WAT browning (Miyoshi et al., 2010), indicating that PLIN1 is important for the proper regulation of

lipolysis. These studies help us understand the importance of PLIN1 in obese and diabetic states. However, in contrast to these *Plin1*$^{-/-}$ mice, the *Rcan1*$^{-/-}$ mice did not develop insulin resistance as they had normal blood glucose, maintained normal lipid and insulin sensitivity after a HFD (Rotter et al., 2018). The current literature has no studies on the relationship between PLIN1, calcineurin or RCAN1 therefore, more research needs to be conducted to investigate the role of RCAN1 in the adipose tissue.

Lipolysis is complex and a relationship exist between PLIN1 and HSL. In basal lipolysis, HSL is associated with the lipid droplet (LD) and is not phosphorylated (Miyoshi et al., 2006). With stimulation, PLIN1 is phosphorylated by PKA at serine residue Ser-517, which controls PKA-stimulated activated lipolysis in adipocytes (Miyoshi et al., 2007). When HSL is phosphorylated, HSL moves from the cytosol to the LD surface as PLIN1 undergoes conformational changes to bring LD-associated HSL in close proximity with stored neutral lipids, increasing hydrolysis of TG through PKA-stimulated lipolysis (Moore et al., 2005, Miyoshi et al., 2006, Jaworski et al., 2007). Here, my results show a decreased in *Hsl* gene expression in *Rcan1*$^{-/-}$ compared to WT on a LFD. This is a similar decrease observed in activated lipolysis in sWAT in *Rcan1*$^{-/-}$ mice compared to WT. The decrease in activated lipolysis could be specific to sWAT (subcutaneous) (Figure 1.25) and eWAT (visceral), reflected as gene expression decrease in eWAT, in contrast to no change in activated lipolysis observed in gWAT and BAT (Figure 1.25). Caesar et al. (2010) proposes that variations could exist, dependent on depot-specific location, affecting gene expression changes (Caesar et al., 2010). Furthermore, HSL and PLIN1 are differentially expressed between omental and subcutaneous adipose tissue and could cause depot differences in lipolysis (Ray et al., 2009, Lee et al., 2013), therefore, depot differences in gene expression and proteins can influence obesogenic fat accumulation that is linked to diabetes with visceral accumulation being more susceptible than subcutaneous fat depots (Arner, 1998). In the literature, NFAT proteins have roles in the control of gene transcription in mature adipocyte metabolism and lipolysis (Holowachuk, 2007) and HSL can be dephosphorylated by calcineurin *in vitro* (Olsson and Belfrage, 1987). Lipolysis was reduced by 50% with CsA treatment, specific calcineurin inhibitor, that resulted in reduced expression of lipolytic genes *Hsl*, *aP2*, *Pparg* and *Acs* (Holowachuk, 2007). This is consistent with the present results where *Hsl* was decreased in *Rcan1*$^{-/-}$ mice compared to WT, indicative of reduced activated lipolysis. However, in another study, the calcineurin inhibitors CsA, tacrolimus and rapamycin (mTOR) significantly elevated isoproterenol-stimulated phosphorylation of HSL on Ser552 (Pereira et al., 2013) thereby regulating HSL hydrolytic activity (Anthonsen et al., 1998). In studies involving the ablation of *Hsl*, mice were resistant to obesity caused by a HFD (Osuga et al., 2000, Harada et al., 2003) or when bred with *ob/ob* mice (Sekiya et al., 2004). Therefore, the downregulation of *Hsl* could contribute to the anti-obesity phenotype in *Rcan1*$^{-/-}$ mice. Further work needs to determine post-translational changes to HSL levels and also investigate HSL activity in these *Rcan1*$^{-/-}$ mice to understand the differences in *Hsl* expression decrease in *Rcan1*$^{-/-}$ compared to WT.

5.4.2 *Atgl* gene expression increased in *Rcan1*$^{-/-}$ mice on a HFD

Given that *Rcan1*$^{-/-}$ may be contributing to changes in lipolysis when on a HFD, we then chose to examine other molecules involved in the lipolytic pathway. Stimulation of PKA led to the activation of the lipolytic pathway activating the thermogenic pathway in BAT and activation of UCP1 (Caron et al., 2019). Adipose Triglyceride lipase (ATGL) is the rate-limiting enzyme in lipolysis (Lu et al., 2010) and is highly expressed at transcriptional level in adipose tissue in mice (Zimmermann et al., 2004). When overexpressed in adipocytes, there was an increased in diacylglycerol. Similarly, fatty acid released increased after isoproterenol stimulated lipolysis. This is in contrast to decreased basal lipolysis when *Atgl* gene was silenced. Therefore, ATGL has ability to modulate both basal and stimulated lipolysis (Zimmermann et al., 2004). Both the phosphorylation of ATGL's coactivator CGI-58 and phosphorylation of Perilipin, facilitates access of ATGL to lipid droplets to promote triglyceride hydrolysis (Greenberg et al., 2011).

Both lipolytic lipase proteins, ATGL and HSL (Pereira et al., 2013), are direct targets of AMPK (Kim et al., 2016) and both had gene expression changes opposite to each other in this present study. Both ATGL and HSL work sequentially to generate monoglyceride. It has been proposed that HSL is mainly responsible for stimulated lipolysis while ATGL is the main lipase for basal lipolysis (Ducharme and Bickel, 2008). The gene expression of *Atgl* in *Rcan1*$^{-/-}$ was increased compared to WT on a HFD. Basal lipolysis is primarily due to actions of ATGL (Haemmerle et al., 2006, Miyoshi et al., 2008) and these results could explain the increase in basal lipolysis in *Rcan1*$^{-/-}$ mice (Rotter et al., 2018). The results are consistent with adipose-specific overexpression of *Atgl* in mice, resulting in an increased lipolysis, was unchanged in serum free fatty acid levels but these animals had reduced body fat which allowed resistance to diet-induced obesity and insulin resistance, elevated adipose mitochondrial biogenesis and whole-body oxygen consumption (Ahmadian et al., 2009). In a study by Wueest et al. (2008), basal lipolysis was two times higher in larger adipocytes than smaller adipocytes and mRNA expression of *Atgl* and *Hsl* was higher in larger adipocytes derived from eWAT in mice (Wueest et al., 2009). It is known that larger adipocytes could produce higher pro-inflammatory cytokines (Skurk et al., 2007). The increase in *Atgl* gene expression could also indicate that other metabolic processes could be involved as ATGL has been shown to elevate activity of nuclear receptor PPARα which is a PGC-1α binding partner to promote fatty acid oxidation (Haemmerle et al., 2011, Ong et al., 2011, Obrowsky et al., 2013, Khan et al., 2015) that breaks down fatty acids into acetyl-CoA and enters the Krebs cycle to generate ATP.

Also in *Atgl*$^{-/-}$ mice, thermoregulation was affected due to impaired TG hydrolysis, reduced lipolysis by 85% in BAT and 82% in WAT of these animals. Consistent with this, *Atgl*$^{-/-}$ mice had 80% decreased PGC1α and 53% UCP1 expression (Haemmerle et al., 2006). The lack of ATGL resulted in the build-up of triglycerides in multiple tissues (Haemmerle et al., 2006, Schweiger et al., 2009) and delayed

cholesterol absorption in the intestines (Ahmadian et al., 2010). Moreover, the reduction in lipolysis resulted in fatty acid oxidation shifts to glucose oxidation and protects mice against HFD-induced insulin resistance (Haemmerle et al., 2006, Hoy et al., 2011). As lipolysis is decreased, fatty acid oxidation and UCP1 induction for thermogenesis decreased (Ahmadian et al., 2011). Consistent with literature, adipose-specific *Atgl* ablation study where there was a reduction of BAT UCP1 expression, O_2 consumption and mitochondrial biogenesis (Ahmadian et al., 2011). In *Rcan1*$^{-/-}$ mice, particularly in the female mice, *Pgc1α* and *Ucp1* both increased gene expression (Rotter et al., 2018), indicative of increased thermogenesis. Moreover, the decreased *Atgl* gene expression in WT on a HFD and possibly reduced lipolysis was due to the presence of high nutrient availability (Obrowsky et al., 2013). These results are expected as lipolysis is upregulated during energy shortage or in times of starvation. Furthermore, mice fed a HFD increased ATGL and CGI-58 expression, while HSL and PLIN1 protein was reduced (Gaidhu et al., 2010). Therefore, diet changes greatly affected the expression of these proteins involved in lipolysis and could provide explanation for the increase in gene expression of *Atgl* in eWAT from *Rcan1*$^{-/-}$ on a HFD. These mice displayed a lean phenotype, did not gain weight, had no change in serum fatty acid levels and increased whole-body oxygen consumption rate (Rotter et al., 2018). PLIN1 binds strongly to CGI-58, a co-activator of ATGL, and contributes to the decrease in basal lipolysis (Granneman et al., 2009). In contrast to the present data, which suggest increase lipolysis occurring in the *Rcan1*$^{-/-}$ HFD group paralleled with the increase in *Atgl* gene expression, *Tnfα* gene expression was decreased in the same mice on the same diet in gWAT (Rotter et al., 2018). It is known that *Tnfα* is able to stimulate lipolysis locally in adipocytes (Jaworski et al., 2007). Further investigation is required to explain this.

Furthermore, G0S2, present in abundance in adipose tissue, can selectively and directly inhibit ATGL (Yang et al., 2010), binding to ATGL regardless of its activity status or the presence of CGI-58 (Lu et al., 2010, Yang et al., 2010, Schweiger et al., 2012). Both ATGL and G0S2 are can affect each other's localisation to lipid droplets (Russell and Forsdyke, 1991). There were no significant changes in transcript levels of *Cgi-58* (co-activator of ATGL (Lass et al., 2006)) and *G0s2* (co-inhibitor of ATGL) despite an increase in *Atgl Rcan1*$^{-/-}$ HFD group compared to WT and these enzymes are important in the lipolytic process. In the present study, *Atgl* is significantly upregulated in *Rcan1*$^{-/-}$ mice on a HFD and as expected, there is a trend showing decrease in *G0s2*. The increase in ATGL protein and decrease G0S2 protein is similarly observed in fasting in humans (Nielsen et al., 2011). Moreover, overexpression of *G0s2* deceases both basal and stimulated lipolysis in both adipocytes and adipose tissue explants. While the ablation of *G0s2* increased lipolysis in mature adipocytes (Yang et al., 2010, Schweiger et al., 2012). TNF-α is a known potent simulator of basal lipolysis in adipocytes that could cause insulin resistance in obesity (Uysal et al., 1997, Cawthorn and Sethi, 2008, Chen et al., 2009). TNF-α treatment results in suppression of G0S2 expression and vice versa, ectopic expression of G0S2 reduced TNF-α stimulated lipolysis by inhibiting ATGL (Yang et al., 2011). In *Rcan1*$^{-/-}$ mice compared

to WT, basal lipolysis was increased, while *Tnfα* gene expression was decreased in *Rcan1*$^{-/-}$ compared to WT on a HFD in gWAT (Rotter et al., 2018), therefore we would expect that *G0s2* gene expression would also decrease in *Rcan1*$^{-/-}$ on a HFD. On a HFD, G0S2 protein decreased in perigonadal fat depots but was elevated in mesenteric fat depot compared to mice on a normal chow diet (Wueest et al., 2012) suggesting that there could be fat depot differences as well. Additionally, G0S2, which has potential NFAT binding sites (Ma et al., 2006), was reversibly inhibited by CsA, therefore, via the NFAT pathway, G0S2 may be involved in the post-transplant patient diabetes (Cristillo et al., 1997). Furthermore, in T2D patients, G0S2 in subcutaneous fat had reduced expression of G0S2 transcripts and proteins (Nielsen et al., 2012, Schweiger et al., 2012). The increase in lipolysis by ATGL, concurrently the decrease in G0S2, results in insulin resistance (Schweiger et al., 2012). These were similar to my results where *Rcan1*$^{-/-}$ mice on a HFD had a reduced expression of *G0s2* in the same group and diet in Figure 5.2 and the difference is that *Rcan1*$^{-/-}$ mice were not insulin resistant but were protected against obesity (Rotter et al., 2018), likely a phenotypic effect of knocking out *Rcan1* in these mice. Moreover, the ablation of *Cgi-58* in adipocytes resulted in the blockage of insulin-stimulated suppression of lipolysis (Stockli et al., 2019), therefore lipolysis was unrestrained in these mice. When G0S2 is overexpressed in adipocytes specifically, there is a reduction in lipolysis and an increase in fat mass in mice but improved glucose and insulin tolerance (Heckmann et al., 2014). In WAT of humans, G0S2 protein is reduced by fasting (Nielsen et al., 2011) and in T2D that is not managed (Nielsen et al., 2012). The ablation of G0S2 protein resulted in a lean mouse, resistant to HFD-induced obesity and insulin resistance, increased stimulated lipolysis and increased thermogenesis (El-Assaad et al., 2015).

5.4.3 Expression of *Srebp1c* changed in WT mice with diet and in *Rcan1*$^{-/-}$ mice

Lipogenesis is mainly regulated at a transcriptional level by SREBP proteins (Strable and Ntambi, 2010, Plantier et al., 2012). We hypothesise that RCAN1 increases lipogenesis in mice on HFD compared to LFD through its role as an inhibitor of calcineurin as *Rcan1*$^{-/-}$ mice remain lean on a HFD (Rotter et al., 2018). SREBPs are involved in elevating the expression of lipogenic enzymes such as ACC, FAS, SCD, GPAT and ACL (Shimomura et al., 1998, Horton et al., 2002). It is known that the overexpression of *nSrebp1a* in adipose tissue controlled by the aP2 promoter activated both cholesterol and fatty acid synthesis genes causing higher lipid accumulation in adipocytes causing hypertrophy, higher rates of lipogenesis and increase fatty acid secretion from adipocytes into the medium used (Horton et al., 2003). The aP2 promoter is found not only in adipocytes but also macrophages (Makowski et al., 2001) that play a role in adipocyte metabolism (Biswas and Mantovani, 2012) therefore there is compounding results with the use of aP2 promoter. When mice overexpressing *Srebp1a* were bred with the *ob/ob* mice, their offspring had weight reduction. However, compared to original *ob/ob* mice, these mice had worst insulin resistance (Ohno et al., 2018). We would expect that *Rcan1*$^{-/-}$ would have an opposite effect to mice overexpressing *Srebp1a*, as they had lesser lipid accumulation, apparent in their lean mass. The present data shows no gene expression changes in *Srebp1a* for both diet groups and between

Rcan1$^{-/-}$ or WT. Both SREBP-1c and -1a, alternative splice variants that encodes the *Srebf1* gene, are controlled independently and have distinct roles in lipid synthesis (Horton et al., 2003); SREBP-1c is mainly involved in FA synthesis upon insulin stimulation while SREBP-1a is implicated in both FA synthesis and cholesterol synthesis (Eberle et al., 2004). Even though SREBP-1a is more potent of the two isoforms, SREBP-1c is more highly expressed than SREBP-1a in the adipose tissue (Shimomura et al., 1997, Shimomura et al., 1998). In contrast to *Srebp1a*, *Srebp1c* gene expression changes were observed in the present study, discussed in the next paragraph. More investigation is required to understand gene expression changes of *Srebp1a*.

In general, a HFD reduces the expression of all DNL enzymes in the adipose tissue (Nadler et al., 2000, Caesar et al., 2010) correlating to insulin resistance (Ranganathan et al., 2006, Hoffstedt et al., 2007, Roberts et al., 2009, Kursawe et al., 2010). Similarly, obese mice and humans have reduced expression of lipogenic enzymes in the adipose tissue causing a downregulation of the DNL flux (Diraison et al., 2002, Eissing et al., 2013, Duarte et al., 2014). However, differences between *Srebp1c* and *Chrebp* gene expression could exist; HFD reduced ChREBP but not SREBP-1c expression in WAT (Caesar et al., 2010). However, in the present study, there was a decrease in *Srebp1c* gene expression in WT mice on a HFD compared to WT mice on LFD. The literature is mixed. A similar decrease in *Srebp-1c* gene expression was found in isolated adipocytes from sWAT obtained from obese T2D patients, where T2D patients had insulin-resistance and *Srebp1c* gene expression negatively correlated with BMI, suggesting that SREBP-1c is affected by HFD-induced obesity (Sewter et al., 2002). Furthermore, the decrease in SREBP-1c, over time, could potentially result in lipotoxcity contributing to insulin resistance as *Srebp1c* gene is downregulated, affecting lipogenesis in adipocytes (Sewter et al., 2002). From the recent publication, it is known that WT mice on a HFD became obese and sWAT from these mice possess a larger cross-sectional area of adipocytes with a higher insulin serum level (Rotter et al., 2018), therefore the present results are consistent with previous findings.

In the liver, *Pparg* mRNA expression in *Rcan1*$^{-/-}$ mice was significantly reduced compared to WT on a HFD (Rotter et al., 2018) which is involved in gluconeogenesis and shares a common role with SREBP-1 in being a major transcription factor that is involved in lipogenesis (Strable and Ntambi, 2010). The increased PPAR-γ and SREBP-1c expression in the liver of obese patients is strongly linked to fatty liver disease (Pettinelli and Videla, 2011). Therefore, we expect that *Srebp1c* expression in the adipose tissue would mirror that of *Pparg* expression, however, in the present study, a decrease in *Srebp1c* gene expression in *Rcan1*$^{-/-}$ mice compared to WT was found in mice fed a LFD. This is a novel finding that RCAN1 impacts lipogenic *Srebp1c* expression at transcription level, however, specific mechanisms should be investigated to understand the implications of knocking out *Rcan1* affecting lipogenesis in the adipose tissue. Mentioned earlier in the introduction of this chapter, SREBP-1c is a transcriptional factor involved in controlling gene expression of various lipogenic enzymes. Interestingly, there is a

similar decrease found between *Rcan1*$^{-/-}$ and WT on LFD *Acc1* gene expression that converts acetyl-CoA to malonyl-CoA in the lipogenesis pathway. There could be novel links between ACC1 and SREBP-1c in the adipose tissue metabolism in *Rcan1*$^{-/-}$ mice which needs to be further investigated.

5.4.4 Expression of *Chrebp* increased in *Rcan1*$^{-/-}$ mice on a HFD

ChREBP is a glucose-responsive transcription factor that acts to upregulate genes involved in *de novo* lipogenesis in the adipose tissue (fatty acid synthesis) and glycolysis (Iizuka et al., 2004). A list of lipogenesis-associated genes that ChREBP regulates include *Fas*, *Accl* and *Scd1* (Figure 1.6). ChREBP is also involved in gluconeogenesis and glycolysis pathways as well (Iizuka, 2013). ChREBP is regulated by GLUT4 in the adipose tissue and is necessary for improved glucose homeostasis via increased GLUT4 expression (Herman et al., 2012). GLUT4 overexpressed in mice fed a HFD had normal glucose tolerance owing to ChREBP-induced lipogenesis in WAT. GLUT4^{ox} mice crossed with ChREBP-KO mice resulted in a loss of glucose tolerance (Herman et al., 2012). CHREBP is found in significant amounts in tissues involved in metabolism such as the pancreatic islets, adipocytes and liver. ChREBP-β is the shorter ChREBP isoform compared to ChREBP-α (Richards et al., 2017). In this study, ChREBP gene expression showed a trend to decreased in WT on a HFD compared to LFD. This is expected as literature supports WT mice on a HFD diminishes ChREBP expression in WAT, downregulating DNL enzymes ACL and FAS in mWAT and sWAT (Caesar et al., 2010, Herman et al., 2012). However, in the study by Caesar et al., *Chrebp*, *Acl* and *Fas* showed no significant differences in gene expression (Caesar et al., 2010). Similarly, ChREBP expression is decreased in adipose tissue of obese adults compared to lean subjects (Hurtado del Pozo et al., 2011). There were no expression changes in the isoforms of *Chrebp* gene, however, *Chrebp* gene expression was increased in *Rcan1*$^{-/-}$ mice compared to WT on a HFD, suggesting that there could be an increase in lipogenesis in the absence of *Rcan1*. This is contrary to our hypothesis where we postulated that the presence of *Rcan1* would increase lipogenesis, giving rise to HFD-induced obesity in WT mice. We have to measure lipogenesis directly to ascertain the changes in gene expression in the present study and this can be done by direct labelled carbon incorporation into lipids. Similar to the study by Eissing et al., ChREBP-β mRNA in subcutaneous fat depot was too lowly expressed for RT-PCR (Eissing et al., 2013) and in our study, the melt curve shows multiple peaks and the quantification curve showed rise in *Chrebp-β* expression in eWAT coming up later, meaning that it is very lowly expressed (Appendix B.2). In the study by Lextexier et al., ChREBP mRNA in rat or human adipose tissue was not affected by HFD (Letexier et al., 2003). The expression of GLUT4, FAS and ACC in visceral adipose tissue were significantly reduced in obese and obese-diabetic patients (Eissing et al., 2013). ChREBP is associated with GLUT4 being activated by glucose and *ChREBP-β* gene expression was significantly decreased in obese and obese-diabetic compared to non-obese controls, while SREBP1 showed no changes in gene expression between groups (Eissing et al., 2013).

In particular, it is important to measure lipogenesis in the adipose tissue, as liver DNL and adipose tissue DNL differs; obese subjects had increased ChREBP expression in the liver but decreased expression in the adipose tissue (Letexier et al., 2003, Eissing et al., 2013, Kursawe et al., 2013). It has been suggested that in the adipose tissue, ChREBP-β expression, but not ChREBP-α, is linked with insulin sensitivity and is decreased in the adipose tissue but heighted in the liver (Herman et al., 2012). There is inter-tissue communication between the adipose tissue and liver, where deletion of hepatic ChREBP changed gene expression in adipose tissue, where there was an upregulation of lipogenic genes in WAT in the fasting state in mice with liver-ChREBP KO (Jois et al., 2017). In the adipose tissue of liver-specific ChREBP KO mice, expression of lipogenesis genes *Acc1* (2.7-fold) and *Scd1* (2-fold) were increased in fasted animals (Jois et al., 2017). The adipose-specific ChREBP knockout had reduced rates of lipogenesis in the adipose tissue, are insulin resistant with dysfunctional insulin action in the liver, muscle and white adipose tissue in both chow-fed and HFD (Vijayakumar et al., 2017). In the adipose tissue, ChREBP partners with lipolytic HSL enzyme (Morigny et al., 2019). The interaction between HSL and ChREBP disrupted the nuclear translocation of ChREBP-α which usually activates ChREBP-β (Morigny et al., 2019). The two isoforms ChREBP-α and -β acts to target FAS and ACC1 (Herman et al., 2012) in the lipolysis pathway. Mice on a HFD had decreased protein expression of lipogenic enzymes, ACL and FAS, in the white adipose tissue (Jiang et al., 2009). Similar to the present study, the expression of *Acc1* decreased in WT mice on a HFD compared to WT on a LFD and this trend was seen in *Fas* expression of WT mice fed a HFD where there was a decrease in *Fas* expression compared to WT on LFD. Moreover, the global *Acc1* knockout was embryonically lethal (Abu-Elheiga et al., 2005) while adipose-specific *Acc1* knockout was prone to HFD-induced obesity (Mao et al., 2009). Therefore, the reduced *Acc1* expression is expected in WT mice and results in obesity.

5.4.5 Lipogenic enzyme expression were affected by diet and *Rcan1*$^{-/-}$ mice.

Decrease in *Acl* gene expression in WT mice on either diet was unexpected. ACL is involved in converting citrate that exits the glycolytic pathway into acetyl-CoA in the lipogenic pathway (Figure 1.6). Following the lipolysis pathway, WT mice on LFD decrease in *Acl* gene expression indicating a reduction of the amount of citrate converted to acetyl-CoA cycled downstream of the lipogenic pathway. Despite the availability of *Acc* and *Fas* in WT mice on a LFD, having insufficient citrate converted to acetyl-CoA upstream of the lipogenic pathway fatty acids cannot be cycled downstream, eventually resulting in decreased lipogenesis in the WT mice.

In *Srebp1* null mice adipose tissue mass was not affected and FAS and ACC expression remined the same (Shimano et al., 1997), therefore, changes observed in SREBP1 may not be reflected on the enzymes they control as observed in Figure 5.4. In humans, expression of *FAS*, *ACC1*, *SREBP-1c* genes and SREBP-1c protein were not modified by consumption of a HFD (Letexier et al., 2003). However, interpretation of data in this work is difficult as the use of HFDs in various experiments to induce

obesity had varying influence on lipogenesis (Strable and Ntambi, 2010). Moreover, under caloric restriction, in the adipose tissue, SREBP-1c deficiency inhibits the upregulation of lipogenic genes associated with caloric restriction (Fujii et al., 2017). Therefore, SREBP-1c expression changes may not directly correlate with changes in lipogenic enzymes. Even though SREBP-1c is required to promote lipogenic enzyme expression in the adipocytes *in vitro* (Kim and Spiegelman, 1996). SREBP-1c deficiency and effects on DNL could be compensated by SREBP-2 as Shimano et al. suggest (Shimano et al., 1997). In the present study, no changes were observed in the expression of *Acc2* between WT and *Rcan1*$^{-/-}$ across both diet groups. However, it is known that global *Acc2* knockout mice are protected against obesity and diabetes induced by a HFD (Abu-Elheiga et al., 2003). In the recent publication, the *Rcan1*$^{-/-}$ mice were lean, healthy and were protected against obesity-induced diabetes (Rotter et al., 2018) this phenotypic effect is similar to that of *Acc2* global knockout. Mechanisms controlling these genes and the resulting phenotypes require further investigation to better understand phenotypic changes with relation to the ablation of these genes.

Taken together, the upregulation of *Srebp1c*, the upregulation of *Acc1* and the trend for increase in *Chrebp*-total in WT LFD group compared to *Rcan1*$^{-/-}$, this trend is further mirrored in the expression of *Fas* and *Acc2* genes, suggesting that an increase in overall lipogenesis occurred in adipocytes of WT mice on a LFD. Caution needs to be taken when considering overall lipogenesis in these mice as the liver is also a major contributor to overall lipogenesis and there are differences in lipogenesis where the liver and adipose tissue are measured in obesity (Diraison et al., 2002).

5.4.6 Leptin expression increased in WT mice on a HFD

Leptin has many roles in the body and is a marker of adipogenesis. Leptin send signals to the hypothalamus to increase sympathetic tone supressing adipocyte proliferation and therefore modulates the size of WAT depots to keep adipocyte homeostasis. Leptin acts to suppress lipogenesis and fatty acid oxidation and induces lipolysis (Siegrist-Kaiser et al., 1997, Jiang et al., 2009). The phenotype of *Rcan1*$^{-/-}$ on a HFD is lean, indicating that other pathways could be involved. For example, an increase in resting energy expenditure in skeletal muscles (Rotter et al., 2018) could have a larger overall effect on the *Rcan1*$^{-/-}$ mice to cause this lean phenotype, however more investigation is needed. In the present study, the aim was to investigate other possible pathways that could be affected. It is more likely that adipogenesis in *Rcan1*$^{-/-}$ mice is reduced as the histological sections of gWAT from *Rcan1*$^{-/-}$ on a HFD were smaller than WT (Rotter et al., 2018). In WT mice, leptin expression is increased when on a HFD (Frederich et al., 1995), therefore our data showing the significant increase in *leptin* mRNA in WT mice on a HFD diet is consistent with literature. This is because obesity is associated with increased circulating levels of leptin (Considine et al., 1996, Ahren and Scheurink, 1998). The overproduction of leptin in obesity, could result in leptin resistance due to the overproduction of leptin from adipocytes (Koch et al., 2014). In a leptin-deficient insulin-sensitive mice model (*Lep*$^{ob/ob}$), mice fed a HFD could

induce leptin resistance (Koch et al., 2014). Therefore, it is important to investigate leptin gene expression and production. Conversely, the lack of an obesogenic phenotype in *Rcan1*$^{-/-}$ resulted in a decrease in plasma leptin levels in *Rcan1*$^{-/-}$ on a HFD compared to *Rcan1*$^{-/-}$ on normal chow (Rotter et al., 2018). A similar decrease in leptin was found in *Nfatc2*$^{-/-}$ and *Nfatc4*$^{-/-}$ mice on either LFD or HFD compared to WT (Yang et al., 2006a). Mechanisms for the decrease in *Leptin* levels need to be further investigated. Leptin levels should correlate to proportion of fat cells in proportion to body fat stores (Hwang et al., 1997). However, serum leptin levels were lower in *Rcan1*$^{-/-}$ compared to WT mice on a HFD (Rotter et al., 2018), the increase in *leptin* gene expression in the current results may be a compensatory response in adipocytes to the low leptin production. It is essential to perform functional studies to understand the underlying mechanisms for the results shown.

Even though no *Cebp-α* gene expression changes were observed across all diet groups and between *Rcan1*$^{-/-}$ and WT mice, the family of C/EBP are key transcriptional regulators for induction of the adipogenic genes during differentiation (Lin and Lane, 1994). In particular, C/EBPα and PPARγ2 are essential in the regulation of expression of adipocyte genes required for function and maturation of adipocytes (Freytag et al., 1994, Shao and Lazar, 1997). C/EBPβ and δ induces and activates C/EBPα and PPARγ2 and there are C/EBPβ binding sites on the PPARγ2 promoter that later induces downstream expression of adipogenic genes. C/EBPβ and δ binds both the C/EBPα and PPARγ2 promoter regions during the post-differentiation period (Salma et al., 2006). The ectopic expression of C/EBPα can activate differentiation of fibroblast cells into mature adipocytes (Freytag et al., 1994) therefore it is a good marker of adipogenesis. The results for *Cebp-α* are inconsistent with the increase in *Pparg* in WT compared to *Rcan1*$^{-/-}$ on a HFD (Rotter et al., 2018). The binding of C/EBP proteins happens quickly after the activation of C/EBP protein levels (Salma et al., 2006), however, the expression of adipogenic genes may not correlate with C/EBP protein activity during adipogenesis.

PPARγ, C/EBPα and SREBP-1c are transcriptional activators that upregulate adiponectin gene expression during adipogenesis (Kim et al., 2006a). The *Srebp1c* data was not similar to expression of *Cebp-α* or *Pparg* (Figure 5.1). This suggest that NFAT has other downstream effects in the adipogenesis pathway and *Cebp-α*, *Srebp1c* and *Pparg* should increase in WT mice on a HFD and *Pparg* showed an increase in the recent publication (Rotter et al., 2018). The present data could suggest that the storage of fat was of higher priority than adipogenesis and diet changes played a role in these animals. Furthermore, NF-kB and C/EBP trigger genes associated with early inflammation (Yang et al., 2006b). However, unlike the inflammatory gene markers *Mcp1*, *F480*, *Tnfα* and *Tnfβ* that showed significant increase in expression in WT on a HFD compared to *Rcan1*$^{-/-}$ on a HFD (Rotter et al., 2018), *Cebp-α* gene expression in *Rcan1*$^{-/-}$ on a HFD showed a trend to increase compared to WT on the same diet.

Overall, these findings suggest that *Rcan1*$^{-/-}$ enhances lipolysis, inhibit lipid storage and expression of lipogenic genes in adipose tissue, which may contribute to the development of dyslipidemia and insulin

resistance associated with diet changes. Furthermore, other factors could be involved in causing the lean phenotype in *Rcan1*$^{-/-}$ on a HFD. The limitations and future directions for this study are discussed further in sections 7.3 and 7.4 of this thesis.

Chapter 6. FACTORS THAT MAY IMPACT RCAN1 EXPRESSION IN THE ADIPOCYTE CELL LINE

6.1 Introduction

The *Regulator of Calcineurin 1* (*RCAN1*), a gene located on human chromosome 21, is present as two splice variants, RCAN1.1 and RCAN1.4, in mammalian tissue such as the brain, pancreas, heart and skeletal muscle (Fuentes et al., 1997). In non-pathological states, protein expression of RCAN1.1 is higher than RCAN1.4 protein in these tissues (Crawford et al., 1997). RCAN1 is an endogenous inhibitor of calcineurin and both isoforms have a putative calcineurin-binding motif on exon 7 (Rothermel et al., 2000) enough to bind to calcineurin alone and inhibit calcineurin (Chan et al., 2005). Calcineurin itself controls transcription of *RCAN1.4* but not *RCAN1.1* owing to the NFAT initiation sites upstream of exon 4 (Yang et al., 2000). The expression of RCAN1 at transcriptional and translational level can be induced by multiple stress-related stimuli (Crawford et al., 1997) and is associated with pathology. The chronic overexpression of RCAN1 (weeks to years) appears with evident pathology in chronic conditions such as DS and AD (Fuentes et al., 2000, Ermak et al., 2001, Harris et al., 2007, Peiris and Keating, 2017). RCAN1^{ox} mice had β-cell dysfunction linked to T2D where high glucose, increase in oxidative stress (Prentki et al., 2013), increased expression of *RCAN1.1* transcripts in pancreatic β-cells (Lin et al., 2003, Peiris et al., 2012) were linked to mitochondrial dysfunction and hypoinsulemia in T2D in patients (Peiris et al., 2016). Increased RCAN1.1 expression is also linked to dysfunction in neuronal mitochondrial function (Chang and Min, 2005), dysfunction in adrenal chromaffin cell's ability to secrete catecholamines (Keating et al., 2008), negatively affects cardiac cell proliferation (Rothermel et al., 2001) and tumour growth (Baek et al., 2009). While, the short-term (acute) induction of RCAN1.1 (hours to days) caused by stress stimuli such as calcium and oxidative stress, can be protective against additional cellular damage such as calcineurin-dependent apoptosis depending on cell type (Ermak et al., 2001, Ermak et al., 2002, Wu and Song, 2013). This is essential as pro-survival genes in multiple cell types are affected via the Calcineurin/NFAT pathway (Peiris and Keating, 2017).

Stress-induced expression of RCAN1 can occur at varying degrees, depending on type of cell. For example, RCAN1 expression is induced by calcium where calcium ionophore causes a strong upregulation of RCAN1 RNA (Leahy et al., 1999), while the intracellular calcium chelator, acetomethyl bis(aminophenoxy)ethane N, N'-tetraacetic acid (BAPTA-AM) inhibited oxidative stress-induced *Rcan1* RNA expression in fibroblast derived from hamster ovary cells (Crawford et al., 1997). To widen our scope in factors that might induce *Rcan1* expression in adipocytes, these studies can be replicated in adipocytes, therefore, calcium ionomycin was incubated with 3T3-L1 cells in the present study. Previously mentioned in section 1.5.1.4, oxidative stress can result from the downregulation of antioxidants and the increased exposure to oxidants such as ROS and ER stress (Riemer et al., 2009). Similar to a mice model of T2D, RCAN1^{ox} β-cells had small mitochondrial size and ROS production was greater in hyperglycaemic conditions (Peiris et al., 2012). Moreover, H_2O_2 was used to induce

oxidative stress through the upregulation of ROS in RCAN1^{ox} neurons decreasing cell viability with increasing concentration of H_2O_2 (Peiris et al., 2014). Therefore, to extend our understanding of whether H_2O_2 would also upregulate *Rcan1* expression in adipocytes, we incubated the 3T3-L1 cells with H_2O_2.

Forskolin, a pharmacological compound, causes an increase in cyclic adenosine monophosphate (cAMP) levels through activation of adenylate cyclase (AC) (Alasbahi and Melzig, 2012) (Figure 6.1), increasing RCAN1 expression via the increase in cyclic adenosine 3′ ,5′ -monophosphate (cAMP) and protein kinase A (PKA) in PC12 cell models (Kim et al., 2012). cAMP activates PKA that binds to cAMP response element binding protein (CREB) which interacts with RCAN1 and has a functional cAMP response binding element (CRE) (Lee et al., 2015). PKA has the ability to induce RCAN1 expression (Kim et al., 2012). Additionally, inhibition of calcineurin by RCAN1 is enhanced in the presence of forskolin (Seo et al., 2009). cAMP/PKA signalling positively modulates lipolysis in WAT as PKA phosphorylates PLIN1(Miyoshi et al., 2007), HSL (Krintel et al., 2008) and ATGL (Pagnon et al., 2012). cAMP/PKA also inhibits leptin expression and secretion (Szkudelski et al., 2005, Maeda and Horiuchi, 2009). Adiponectin expression is upregulated by activation of PKA (Otani et al., 2015) and CREB signalling in adipocytes (Kim et al., 2010). In the brains of DS patients, the overexpression of RCAN1 resulted in an upregulated phosphorylation of CREB gene and protein expression, a transcription factor in the cAMP/PKA pathway that depended on the inhibition of calcineurin activity (Kim and Seo, 2011). The increase in RCAN1, increased CREB activity that protected against H_2O_2 toxicity (Kim et al., 2013). Similarly, CREB phosphorylation is upregulated in response to the calcineurin inhibitors, FK506 and cyclosporine A (Kim and Seo, 2011). Conversely, the absence of RCAN1 resulted in inhibition of CREB phosphorylation despite exposure to forskolin (Kim and Seo, 2011). Moreover, a HFD-induced obesity upregulated the phosphorylation of CREB (Altarejos and Montminy, 2011). As the adipose tissue is implicated in obesity, therefore, to extend our knowledge on factors that could upregulate *Rcan1*, in the present study, we incubated 3T3-L1 cells with forskolin.

Conversely, an inhibitor of adenyl cyclase (AC) was used. There are two distinct pools of adenylyl cyclases (Zippin et al., 2003) that produces cAMP, namely G-protein -regulated transmembrane adenylyl cylcases (tmACs) and bicarbonate-and calcium-regulated soluble adenylyl cyclase (sAC), both widely expressed in mammalian cells (Kamenetsky et al., 2006, Chen et al., 2013). In the present study, we use KH7 (2-(1H-benzimidazol-2-ylthio)-2-[(5-bromo-2 hydroxyphenyl)methylene]hydrazide,propanoic acid), a selective inhibitor of sAC, an enzyme that reduces cAMP activity (Hess et al., 2005, Bitterman et al., 2013) (Figure 6.1). The actions of KH7 usually results in inhibition of ATP production in the mitochondria and inhibit cAMP production (Jakobsen et al., 2018). KH7, is an inhibitor of the form of AC that lacks a transmembrane (i.e. sAC), exhibits inhibitory concentration (IC_{50}) values of 3-10μM towards sAC, is key in physiological processes such as insulin release and energy metabolism (Zippin et al., 2013, Jakobsen et al., 2018) and

is not responsive to forskolin or to G-proteins (Forte et al., 1983). To our knowledge no published literature surrounds the effect of the KH7 and the expression of RCAN1, therefore in the present study, we hypothesise that the inhibition of sAC by KH7 will downregulate cAMP and impact *Rcan1* expression.

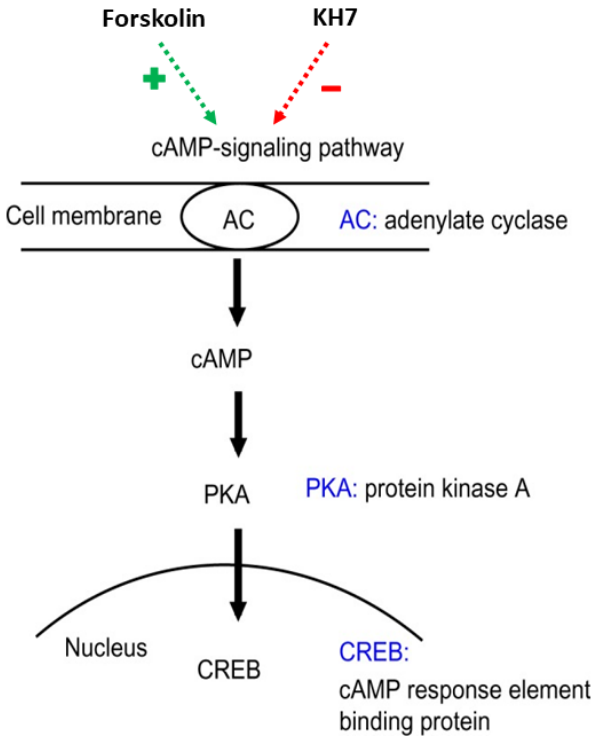

Figure 6.1 cAMP/PKA signalling pathway. Figure modified from (Ikuta et al., 2013). When adenylate cyclase (AC), an enzyme in the cell membrane, is activated this results in cAMP formation. cAMP exerts multiple actions by binding to the regulatory subunits of PKA, resulting in the release of catalytic subunits that move into the nucleus. In the nucleus, PKA phosphorylates CREB that binds to transcription factors causing gene transcription. In this pathway, forskolin, is an activator of AC and KH7 is an example of an inhibitor of AC (Sassone-Corsi, 2012).

Recently WAT is found to have an important role in modulating whole-body metabolism through release of leptin and adiponectin previously mentioned in section 1.4.3. Adipokines are signalling molecules that affects insulin sensitivity and appetite regulation (Yadav et al., 2013). Leptin, produced in adipocytes, is a 16kDa protein encoded by the *ob* gene mutation that results in the obese phenotype in mice (Zhang et al., 1994). Leptin sends energy-storage signals from the adipose tissue to the central nervous system in a range of physiological functions such as to reduce food-intake, satiety, energy expenditure, blood pressure and impacts glucose and lipid metabolism (Makki et al., 2013). The janus kinase 2-signal transducer and activator of transcription 3 (JAK2-STAT3) pathway causes and increase

in energy expenditure, satiety and reduction in body weight (Fruhbeck et al., 2001). Leptin expression is impacted by the amount of stored fat, as there is more *ob* mRNA and serum leptin in obese humans and animals. Therefore, the size of adipocyte impacts leptin synthesis dependent on fat stores. In humans, leptin levels correlate positively with insulin levels. Additionally, leptin is increased in adipocytes treated with glucocorticoids. Cytokines such as TNF-α can stimulate leptin synthesis (Ahima and Flier, 2000). Recently, WT mice on a HFD significantly increased circulating leptin levels, compared to *Rcan1*$^{-/-}$, consistent with their increased body fat mass (Rotter et al., 2018). In the islets of the leptin receptor deficient T2D mouse model, *db/db*, a significant increase RCAN1.1 and RCAN1.4 protein was observed (Peiris et al., 2016), indicating that hyperglycaemia causes an increase in RCAN1 expression. Adiponectin, a 30KDa plasma protein, is an anti-inflammatory protein secreted by the adipocyte (Yadav et al., 2013). Mice overexpressing adiponectin are not glucose intolerant or have dyslipidaemia despite being on a HFD. WAT specific secretion of adiponectin is found to rescue the diabetic leptin-deficient *ob/ob* mouse (Ouchi et al., 2011). In this present study, we hypothesise that 3T3-L1 adipocytes exposed to leptin and adiponectin would result in an upregulation of *Rcan1* expression.

Serotonin (5-hydroxytryptamine, 5-HT), a bioamine originating from tryptophan, is synthesized by neurons in the brain and enterochromaffin cells in the gut. The blood brain barrier separates these two pools. The rate-limiting enzymes tryptophan hydroxylase 1 (Tph1) in the periphery and tryptophan hydroxylase 2 (Tph2) in the brain controls the biosynthesis of serotonin. 5-HT has many roles (Wyler et al., 2017) such as the decrease thermogenesis in BAT thereby promoting obesity, regulating whole body metabolism and weight gain (Crane et al., 2015), promoting gluconeogenesis in the liver, contributing to increased hepatic glucose production (Sumara et al., 2012), acting to increase insulin secretion in pancreatic β-cells (Kim et al., 2015). In adipocytes, gut-derived serotonin signals through the HTR2B receptor to induce lipolysis by upregulating phosphorylation and action of HSL (Sumara et al., 2012). Therefore, we seek to investigate the effects of 5-HT on the expression of RCAN1 in adipocytes. Moreover, isoproterenol was used as a positive control in culture studies of *Htr2b* adipocyte-specific knockout and induced the release of FFAs and glycerol in both WT and *Htr2b* adipose tissue-specific knockouts (Sumara et al., 2012). Isoproterenol is a pan beta adrenergic receptor agonist that induces lipolysis. In the recent publication, isoproterenol induced stimulated lipolysis in the sWAT, gWAT and BAT of *Rcan1*$^{-/-}$ and WT. Stimulated lipolysis was significantly decreased in *Rcan1*$^{-/-}$ mice sWAT compared to WT (Rotter et al., 2018). Recent studies show that isoproterenol induces thermogenesis in mature 3T3-L1 adipocytes (Miller et al., 2015), reduces leptin expression in adipose tissue of obese humans (Ricci and Fried, 1999) and rats (Ricci et al., 2005). In the present study, we hypothesise that isoproterenol will upregulate *Rcan1* expression in 3T3-L1 adipocytes.

Obesity and T2D are characterized by chronic, low-grade inflammation (Donath and Shoelson, 2011, Gregor and Hotamisligil, 2011) marked by increased circulating cytokines (TNFα and IL-6). TNF-α induces lipolysis in adipocytes could lead to hyperlipidemia and peripheral insulin resistance in obesity (Uysal et al., 1997, Cawthorn and Sethi, 2008, Chen et al., 2009). The incubation of 3T3-L1 cells with these cytokines would likely upregulate *Rcan1* expression as WT mice on a HFD increased the expression of these cytokines (Rotter et al., 2018). Therefore, the aim of this study is to identify whether any of these pathways discussed above, including stress-stimuli and pharmacological activators and inhibitors of cAMP, induces the expression of *Rcan1* in adipocytes. The adipose tissue has been greatly studied in obesity and T2D, however, limited study has been conducted on RCAN1's role in adipocytes. We hypothesized that an increase in RCAN1 expression of either isoforms will result from acute exposure to these factors. This could be protective for adipocyte cells as suggested by Wu and Song (Wu and Song, 2013).

6.2 Materials and methods

As a pilot study, the 3T3-L1 cell line was incubated for 24 hours with compounds that may increase *Rcan1* expression. Hydrogen peroxide was made at the concentrations of 10µM and 50µM (Peiris et al., 2014). All other concentrations were derived from physiological range in human plasma (Table 6.1). The methods for RT-PCR can be found in Chapter 2. The melt curves and quantitation graphs generated for each of these gene targets can be found in Appendix B.3.

Table 6.1 Compounds used for incubating the 3T3-L1 cell line

Compounds	Supplier	Solvent	Final Concentration	References
Calcium ionomycin	Thermofisher	DMSO	2 µM	(Neal and Clipstone, 2002, Pramme-Steinwachs et al., 2017)
Hydrogen peroxide	Sigma-Aldrich	Water	10µM and 50 µM	(Peiris et al., 2014)
Leptin	Sigma-Aldrich	20mM Tris/HCl	20ng/ml	(Ostlund et al., 1996, Askari et al., 2010)
Adiponectin	Sigma-Aldrich	PBS with 0.1% BSA	10 µg/ml	(Ahl et al., 2015, Jiang et al., 2016)
Serotonin	Sigma-Aldrich	Ethanol	10 µM	(Li et al., 2013, Tsubai et al., 2017)
Interleukin 6 (IL-6)	Sigma-Aldrich	Water	20ng/ml	(Rotter et al., 2003, Hahn et al., 2014)
TNF-alpha (TNF-α)	Sigma-Aldrich	Water	20ng/ml	(Rotter et al., 2003, Jang et al., 2011, Wang et al., 2013)
Isoproterenol	Sigma-Aldrich	Ethanol	10 µM	(Brasaemle et al., 2000a)
Forskolin	Sigma-Aldrich	DMSO	10 µM	(Cliff and Frizzell, 1990, Zhou et al., 2011)
Adenylyl cyclase inhibitor (KH7)	Sigma-Aldrich	DMSO	100 µM	(Bitterman et al., 2013)

Differences in RCAN1 isoform expression exist in response to stress. For example, the expression of RCAN1.4 protein was induced with exposure to oxidative stress in primary mouse neuronal cell while RCAN1.1 expression was not changed (Crawford et al., 1997). Therefore, in this present study, we investigate the effects of exposing adipocytes to various factors and quantify the expression increase or decrease of both RCAN1 isoforms. The primer sequence used are sequences used in our lab previously and also in recent lab publications (Table 6.2). In the Appendix, melt curves and quantitation graphs are shown to demonstrate the quality of the data obtained in this thesis using these primer sequences (Appendix B.3).

Table 6.2 Gene sequence for RT-PCR

Gene	Forward sequence	Reverse sequence	Length	Reference
Rcan1.1	ATGGAGGAGGTGGATCTGC	TTTATCCGGACACGTTTGAAG	170	(Peiris et al., 2016)
Rcan1.4	CTGATTGCTTGTGTGGCAAA	GCAGATAAGGGGTTGCTGAA	155	(Peiris et al., 2016)
β-actin	GGGGCAAGAGAGGTATCCTGACC	CCCTGGATGCTACGTACATGGC	237	(Rotter et al., 2018)

6.2.1 Statistical analysis

Results are given as mean ± SEM. All data were normalised to the *β-actin* housekeeper. The mean normalised expression was obtained from the raw take-off values entered into the Qgene software. Statistical significance was assessed by unpaired, parametric and two-tailed T-test using the Prism Graph pad software (Prism 8).

6.3 Results

6.3.1 *Rcan1.1* expression was decreased by IL-6 and increased by KH7 and Serotonin

The 3T3-L1 cells were incubated with compounds that could increase RCAN1 expression for 24 hours. The *Rcan1.1* and *Rcan1.4* gene expression were measured using quantitative real-time PCR (qPCR). There were significant increases in *Rcan1.1* expression in response to KH7 and serotonin. A significant decrease was observed in *Rcan1.1* in cells treated with IL-6 ($P<0.05$) (Figure 6.2).

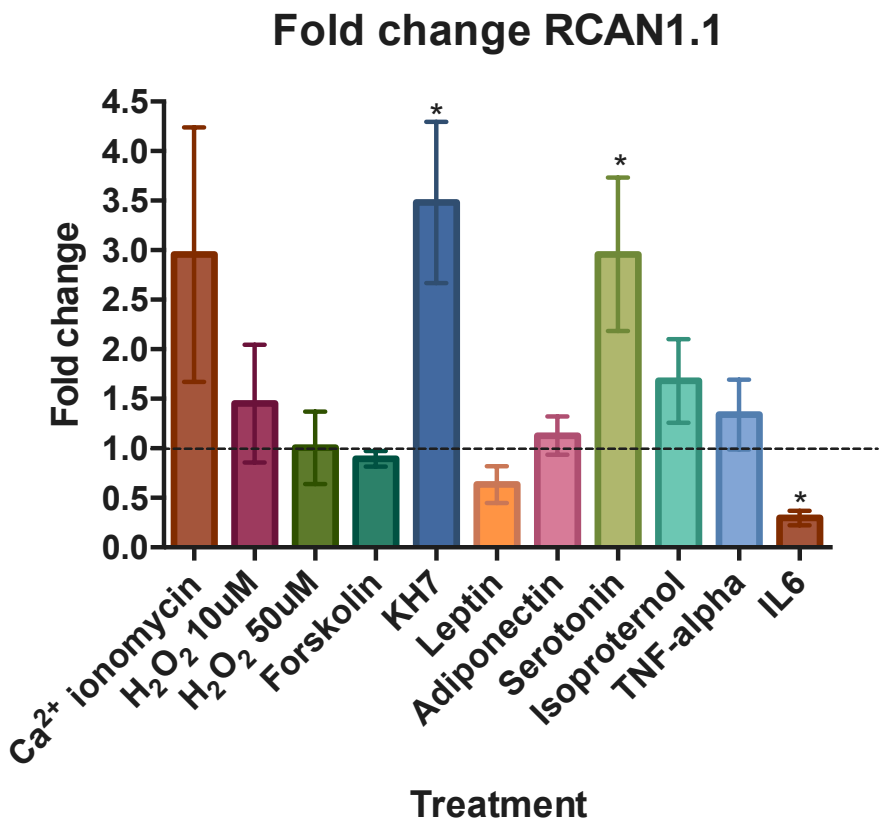

Figure 6.2 Transcript levels for *Rcan1.1* after 3T3-L1 cells were incubated for 24 hours with various treatments normalised to *β-actin* housekeeper (n=4-8). Unpaired T-test, two-tailed and parametric. Asterisks (*) indicate significance $P<0.05$. Graph showing fold change ±SEM. The dotted line indicates control.

6.3.2 Increase in *Rcan1.4* expression in adipocytes incubated with Forskolin

The 3T3-L1 cells treated with forskolin increased *Rcan1.4* expression significantly after 24 hours. Forskolin significantly increased *Rcan1.4* gene expression (P≤0.0001**)**. While Ca^{2+} ionomycin (p=0.05), KH7 (p=0.05) and TNF-α (p=0.05) were also increased (Figure 6.3).

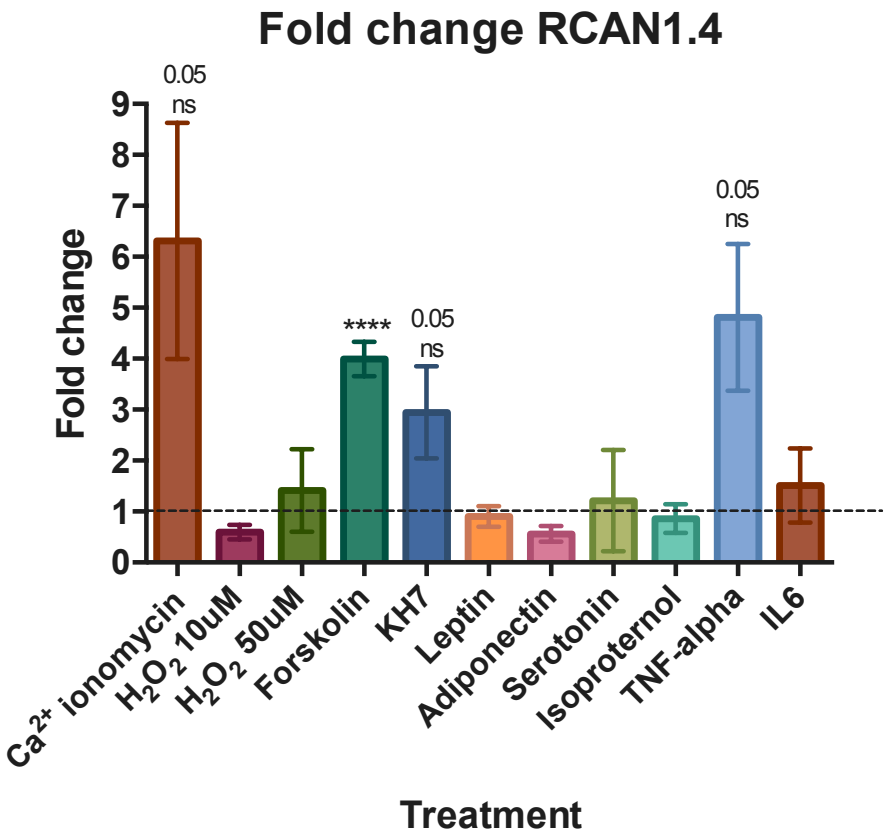

Figure 6.3 Transcript levels for *Rcan1.4* after 3T3-L1 incubation incubated for 24 hours with various treatments normalised to β-actin housekeeper (n=4-8). Unpaired T-test, two-tailed and parametric. Asterisks (****) indicate significance P≤0.0001. Graph showing fold change ± SEM. Dotted line indicates control.

6.4 Discussion

In the present study, the aim was to investigate factors that could increase or decrease *Rcan1* gene expression in 3T3-L1 cells. In particular, isoforms of RCAN1, namely *Rcan1.1* and *Rcan1.4* gene expression were quantified after the 3T3-L1 cells were acutely (24 hours) incubated with factors listed in the Table 6.1 that were previously linked to an increase in RCAN1 expression in other tissues or is involved in metabolism. In chronic metabolic conditions such as T2D, RCAN1 expression was chronically upregulated in β-cells of T2D patients and mice (Peiris et al., 2016). However, in neurons, acute induction of RCAN1 by stress-stimuli such as Ca^{2+} and oxidative stress protected against cellular damage (Ermak et al., 2001, Ermak et al., 2002) due to the stress-inducible factors having a role in mediating apoptosis in a calcineurin-dependent manner (See and Loeffler, 2001, Shou et al., 2004). Currently, no study has been undertaken to stimulate the upregulation of *Rcan1* genes in an acute setting in adipocytes. Therefore, in this chapter we aim to investigate such factors involved in upregulating or downregulating *Rcan1* expression and hypothesise that *Rcan1.1* and *Rcan1.4* would increase gene expression after 24 hours of incubation with these factors.

6.4.1 Serotonin upregulates *Rcan1.1* expression in adipocytes

The current study showed that an increase in gene expression of *Rcan1.1* in cells treated with serotonin (5-hydroxytryptamine, 5-HT) compared to control. This is not unexpected as adipocytes have serotonin receptors expressed and functions to modulate serotonin availability through synthesis and reuptake (Stunes et al., 2011). In obese humans, increased serotonin is produced and released (Young et al., 2018). Additionally, 5-HT is required for adipocyte differentiation and 5-HT2A or C receptor antagonists blocks adipogenesis (Kinoshita et al., 2010). Moreover, in diabetic patients, the use of HTR2A antagonists resulted in increased in serum adiponectin (Nomura et al., 2005). The perturbation of *Tph1* gene in 3T3-L1 preadipocytes decreased adipogenesis (Kinoshita et al., 2010) and 5-HT upregulated lipid storage in human and mouse adipocytes (Gres et al., 2013). Amongst the 14 known 5-HT receptors, the HTR2B is the most highly expressed, especially during fasting, in mouse adipocytes (Berger et al., 2009). Sumara et al.(2012) showed that treatment of epididymal and subcutaneous fat pad and isolated adipocytes from epigonadal region with serotonin dose-dependently increased glycerol and FFAs by activating HSL and inducing lipolysis by increasing cAMP or phosphorylating perilipin (Sumara et al., 2012). Furthermore, gut-derived serotonin induced lipolysis through the HTR2B in fat-specific *Htr2b* KO mice (Sumara et al., 2012). In 3T3-L1 adipocytes that hypertrophied in white adipose tissue from *db/db* mice had increased expression of HTR2A. The increase in HTR2A expression also resulted in a decrease in adiponectin expression in adipocytes (Uchida-Kitajima et al., 2008). In mature 3T3-L1 cells, the use of HTR2A agonist resulted in increased levels of lipogenesis-associated genes, thereby increasing lipid accumulation. Conversely, HTR2A antagonist (Ketanserin) had the opposite effect, decreasing lipid accumulation (Oh et al., 2015). From the evidence, serotonin has a role in

adipocyte functions; increase lipogenesis via the HTR2A receptor and increases lipolysis via the HTR2B receptor in the white adipose tissue. Moreover, pyridine, a molecule that activates myocyte hypertrophy, functions as a selective serotonin receptor agonist known as 5-$HT_{2A/2B}$, acting to cause hypertrophy in cardiac myocytes by increasing RCAN1 expression through calcineurin signalling pathway (Bush et al., 2004). Therefore, there are links between RCAN1 and serotonin where increase in serotonin, increased RCAN1 expression. Our current results further links RCAN1 expression to serotonin. Therefore, RCAN1 can activate the serotonin receptor and plays a role in the adipocyte. Further investigation of the increase in RCAN1.1 post-serotonin incubation is required to understand the impact of upregulating serotonin in adipocytes, the downstream implications on RCAN1's enhanced inhibition of calcineurin and the possible decrease in subsequent NFAT translocation. Follow up experiments can include incubation of serotonin with WAT explants from $RCAN1^{ox}$ and *Rcan1*$^{-/-}$ mice, to understand the interaction of RCAN1 and impact of serotonin on the adipose tissue.

6.4.2 IL-6 treated cells decreased *Rcan1.1* mRNA expression in adipocytes

IL-6 is a major pro-inflammatory cytokine produced by the adipose tissue. Circulating levels of IL-6 is increased in obesity and T2D (Mohamed-Ali et al., 1997, Kado et al., 1999, Sindhu et al., 2015) and the release of IL-6 in the plasma is linked to insulin resistance (Burhans et al., 2018). This suggests importance of understanding if cytokines such as IL-6 could induce *Rcan1* expression in adipocytes. Majority of the studies involving IL-6 measured cytokine gene expression rather than exogenous introduction of cytokine. There are links between RCAN1 and inflammation as RCAN1 is involved in determining CD36 expression that is implicated in aortic vessels during atherosclerosis inflammatory disease. *Rcan1*$^{-/-}$ mice had reduced CD36 expression in aortic arches while in *CD36*$^{-/-}$ mice, cAMP was increased, basal lipolysis and insulin sensitivity were elevated and mice had HFD-induced obesity (Vroegrijk et al., 2013). Therefore, inflammatory cytokines and RCAN1 could also impact adipocyte function. RCAN1.4 is primarily transcribed when stress stimuli activate the calcineurin-NFAT pathway (Crawford et al., 1997), however, it is unknown if increased levels of cytokines directly or indirectly impact calcineurin activation. The 3T3-L1 adipocytes incubated with IL-6 had disrupted insulin signalling as insulin receptor 1 (IRS-1) gene and protein expression were reduced (Rotter et al., 2003), therefore suggesting that IL-6 has a role in glucose metabolism. Interestingly, differentiated human adipocytes exposed to 10nmol/L of IL-6 for 24 hours caused a reduction in glycerol-3-phosphate dehydrogenase (GPDH) activity (a marker of adipocyte differentiation) and increased both basal and stimulated lipolysis (Path et al., 2001). Similarly, IL-6 induced downregulation of lipoprotein lipase activity in mouse explants and 3T3-L1 adipocytes (Greenberg et al., 1992, Berg et al., 1994). We expect that adipocytes incubated with IL-6 would increase *Rcan1.1* expression in adipocytes *in vitro*, however, our current results showed a decrease in *Rcan1.1* expression, suggesting that exposure to exogenous IL-6 significantly downregulated *Rcan1.1* in adipocytes and NFAT-dependent interactions could be implicated downstream due to reduced inhibitory effects of RCAN1 on calcineurin. The current

experiment is novel and more investigation needs to be conducted to explain the mechanisms behind the downregulation *Rcan1.1* with IL-6 exposure in adipocytes and the role of RCAN1 in inflammation in adipocytes.

6.4.3 KH7 upregulates *Rcan1.1* and *Rcan1.4* expression in adipocytes

KH7 is an inhibitor of soluble adenylate cyclase (sAC), an enzyme that converts ATP to cAMP, therefore acting to inhibit cAMP production (Jakobsen et al., 2018). sAC is distributed in subcellular compartments of the cell such as mitochondria and nuclei where cAMP is present (Zippin et al., 2003). By using an inhibitor of PKA, we are able to investigate the effects of the presence and absence of sAC in adipocytes. The increase in RCAN1 expression after induction of the CREB pathway resulted in the glucocorticoid-induced apoptosis in leukemic lymphoid cells. Calcineurin has anti-apoptotic effects of glucocorticoids, therefore, the upregulation of RCAN1 could prevent calcineurin action via the cAMP/PKA/CREB pathway (Nagao et al., 2012). Calcineurin also has roles in lipid homeostasis via the cAMP/PKA signalling pathway. The *CnAβ*$^{-/-}$ mice are hyperlipidemic partly due to increase lipolysis in adipose tissue mediated by β-adrenergic G-protein-coupled receptor (GPCR) signalling pathways and has age-dependent insulin resistance (Suk et al., 2013). To determine the indirect regulation of calcineurin on PKA activation in *CnAβ*$^{-/-}$ mice, mouse embryonic fibroblast (MEFs) isolated from *CnAβ*$^{+/+}$ mice were treated with CsA to inhibit calcineurin and mimic *CnAβ*$^{-/-}$ MEFs. The presence of IBMX, that inhibits cAMP, had similar phosphorylation PKA substrate levels compared to control and CsA-treated MEFs. This was a similar potentiation of phosphorylation of PKA substrates found in 3T3-L1 mature adipocytes upon CsA treatment. Therefore, the inhibition of calcineurin by CsA, similar to *CnAβ*$^{-/-}$, resulted in an adipose-specific sustained and elevated cAMP/PKA activation, as well as, cAMP accumulation, resulting in hyperlipidemia (Suk et al., 2013). KH7 is highly effective in inhibiting sAC. The use of KH7 should downregulate cAMP production as the reduction in cAMP, decrease PKA and decrease expression *Rcan1.1* (Kim et al., 2012). The present results show an increase in *Rcan1.1* gene expression and *Rcan1.4* mRNA expression ($p=0.05$) with the use of KH7 which suggest a likely decrease in calcineurin activity, increased lipolysis, increase in cAMP production and increase CREB binding to RCAN1, despite the inhibition of sAC in the cAMP/PKA pathway. Therefore, inhibition of the sAC by KH7 upregulated *Rcan1.1* and *Rcan1.4* expression in adipocytes. It is highly unlikely that KH7 was ineffective in inhibiting sAC as other studies were successful in using KH7 as an inhibitor (Tresguerres et al., 2011, Kikuchi et al., 2017, Schirmer et al., 2018, Parker et al., 2019). Other factors could be involved to inducing the cAMP and PKA signalling pathway. As the sAC is activated by Ca^{2+} and manganese ions (Mn^{2+}) (Braun and Dods, 1975, Litvin et al., 2003) and is responsive to intracellular bicarbonate and ATP levels (Rahman et al., 2013, Zippin et al., 2013). ATP levels in the current experiment could be measured using an ATP quantitation kit (Sigma Aldrich) following manufacturer's instructions to measure ATP levels normalised against total protein content (Peiris et al., 2016). If ATP content increases, it is may be indicative of decreased cAMP/PKA/CREB activity. It is possible that

cAMP was produced by the other pool of adenyl cyclase, tmAC, that was not inhibited in this experiment. tmAC are regulated by G-proteins and hormonal stimulation (e.g. isoproterenol) in the study of increased lipolysis in adipose tissue (Suk et al., 2013). Ideally, blocking both tmAC and sAC using inhibitors would have fully inhibited AC and indirectly inhibit cAMP production reducing cAMP/PKA/CREB signalling. Several other inhibitors of cAMP can be tested on 3T3-L1 cell lines (Ho et al., 2012) to validate our data. Furthermore, transcription factors CREB and HSL, substrates of PKA, could be tested in the current experiment for phosphorylation status using phospho-specific antibodies (Suk et al., 2013) in adipocyte explants to determine PKA phosphorylation status. A chromatin immunoprecipitation (ChIP) assay, a technique used to probe protein-DNA interactions within the chromatin of the cell, can be performed to confirm if the increased expression of *Rcan1* mRNA in response to activation of sAC correlated with the physical binding of CREB to the RCAN1 promoter in *in vivo* experiments (Lee et al., 2015) to identify if RCAN1 expression was increased by the cAMP/PKA pathway. To understand the underlying cellular mechanism, protein expression of CREB can be analysed using a Western blot. Overall, the functional implications of indirectly inhibiting cAMP on RCAN1 expression in adipocytes needs to be further explored.

6.4.4 Forskolin increased *Rcan1.4* expression in adipocytes

Increased RCAN1 protein is linked to pathology such as DS, AD and T2D. Current literature found that RCAN1, overexpressed in DS brains, activated the cAMP pathway, increasing the phosphorylation of CREB and cAMP response element-mediated gene transcription. The upregulated phosphorylation of CREB and CREB gene expression via the cAMP pathway depended on the inhibition of calcineurin activity (Kim and Seo, 2011). CREB phosphorylation is upregulated in response to the calcineurin inhibitors FK506 and cyclosporine A (Kim and Seo, 2011), suggesting that inhibition of calcineurin led to increased CREB phosphorylation. In PC12 cells stably overexpressing either an empty vector or HA-tagged RCAN1 neuronal cells were treated with forskolin and cell extracts were immunoblotted with anti-phospho-CREB and anti-CREB antibodies. Forskolin is a pharmacological compound that causes an increase in cyclic adenosine monophosphate (cAMP) levels through activation of adenylate cyclase (AC) (Alasbahi and Melzig, 2012). The expression of CnA resulted in reversed CREB activation in cells overexpressing RCAN1. The phosphorylation of CREB in these cells overexpressing RCAN1, regardless of the presence of forskolin were suppressed by the presence of CnA. The forskolin-induced CRE-reporter activity was analysed showing that co-expression of CnA with RCAN1 caused a suppression of RCAN1 and upregulated CRE-luciferase activity in response to forskolin. Kim and Seo concluded that this was due to the inhibition of RCAN1 on calcineurin contribute to increased phosphorylation of CREB. Furthermore, siRNA knockdown of calcineurin showed that RCAN1 was unable to increase phosphorylation of CREB using forskolin (Kim and Seo, 2011). In a study using PC12 cells, inhibition of PKA and siRNA knock down of PKA catalytic subunit decreased RCAN1 expression (Kim et al., 2012). Therefore, PKA is important to the regulation of RCAN1 function and

phosphorylation status *in vitro* and *in vivo* where increased PKA phosphorylation of RCAN1 increased RCAN1 inhibitory action towards calcineurin (Kim et al., 2012). Furthermore, increase in RCAN1 led to the increase in CREB activity and protected against H_2O_2 toxicity (Kim et al., 2013). Calcineurin also has an influence on downstream transcription activity in cells related to metabolism by activating CREB-regulated transcription co-activators (CRTCs) (Altarejos and Montminy, 2011), important to metabolic responses in different tissues and their polymorphisms (Choong et al., 2013, Quteineh et al., 2017) and variants (Song et al., 2010, Ou et al., 2014) are linked with the adipose tissue and metabolism. Therefore, downstream CREB targets influence metabolism and adipocyte biology which could be activated with cAMP using forskolin. In the present experiment, the increase in *Rcan1.4* by forskolin is expected. This suggest that cAMP/CREB production was increased through RCAN1 inhibition of calcineurin that is enhanced in the presence of forskolin (Seo et al., 2009, Kim and Seo, 2011). This is similar to adipocytes in the hamster where forskolin can stimulate cAMP activity and lipolysis (Schimmel, 1984). In rats, high concentrations of forskolin increases cAMP in adipocytes via the activation of adenylate cyclase and induce lipolysis (Litosch et al., 1982). An increase in lipolysis could indicate reduced lipid storage (lipogenesis), therefore there could be a reduction in lipids within these adipocytes. The Oil Red-O assay can be used to determine lipid storage of these cells post-forskolin treatment. The effects of increased *Rcan1.4* on adipocyte functionality needs to be further investigated to understand the functional mechanisms and implications of upregulated *Rcan1.4* in the adipocytes through this pathway and its possible link to obesity and T2D.

6.4.5 Ca^{2+} ionomycin and TNF-α treated adipocytes resulted in increased *Rcan1.4* gene expression

The Ca^{2+} ionomycin ($p=0.05$) and TNF-α ($p=0.05$) treated adipocytes upregulated *Rcan1.4* gene expression. Calcium ionophores are stress agents (Crawford et al., 1997, Leahy and Crawford, 2000) that act to mobilize Ca^{2+} in cells. Ca^{2+} activates CnA dephosphorylating NFAT and upregulating RCAN1.4 expression in a feedback loop (Hogan et al., 2003). Moreover, Ca^{2+} ionophore reduced adipogenesis in fibroblast 3T3-L1 cells. In the presence of Cyclosporin A and FK506, inhibitors specific for calcineurin, resulted in greater adipogenesis of 3T3-L1 cells into mature adipocytes (Neal and Clipstone, 2002). This suggests that calcineurin plays a role in adipogenesis and the increase in *Rcan1.4* expression would result in reduced adipogenesis in immature adipocytes through the calcineurin-NFAT pathway. Furthermore, Rotter et al. showed that siRNA knockdown of both isoforms of RCAN1 resulted in reduced lipid storage (Rotter et al., 2018) (Figure 1.26), suggesting that calcium could activate calcineurin and drive NFAT-dependent increase in *Rcan1.4* expression observed in this experiment. The elevated Ca^{2+} entry and increased ROS resulted in the induction of RCAN1 in β-cells that caused dysfunction in mitochondria decreasing respiratory rates and ATP levels (Peiris et al., 2016). Therefore, there is support for the increased expression of *Rcan1.4* with the use of exogenous Ca^{2+} entering the adipocytes causing this intracellular Ca^{2+} effects at transcriptional level.

There is evidence for an increase in *Rcan1.4* after TNF-α exposure, similar to our data. The upregulation of *Rcan1.4* expression post-TNF-α incubation in adipocytes were induced during inflammation (Crabtree and Olson, 2002). Furthermore, TNF-α upregulation can induce expression of *Rcan1.4* in neuronal cells in stroke models (Cho et al., 2008). Mouse mesangial cells were stimulated with TNF-α that were causatively associated with diabetic nephropathy. In this experiment, TNF-α significantly increased *Rcan1.4* mRNA by 3-fold over control (Jang et al., 2011). RCAN1 expression was induced in endothelial cells in the calcineurin-NFAT pathway when treated with TNF-α and Ca^{2+} chelator (Yao and Duh, 2004). The upregulation of *Rcan1.4* mRNA expression after TNF-α exogenous treatment, could be indicative of possible inflammation occurring as in the case of obesity. However, cells treated with IL-6 resulted in no change in *Rcan1.4* mRNA expression. A Western blot analysis of RCAN1.4 expression is required to confirm this. As RCAN1.4 is an endogenous inhibitor of CaN, it is also important to test if these factors affect the Calcineurin-NFAT pathway, an upregulation of RCAN1.4 protein would cause a downregulation of NFAT translocation into the nucleus thereby downregulating downstream effects of NFAT within the nucleus.

It is important to first understand factors that could upregulate or downregulate RCAN1 expression in the short-term (hours) in adipocytes as this would extend our understanding of factors which can induce RCAN1 expression that might play a role in adipocyte biology. This can be further followed up with investigation of these factors in the longer-term (days) that might cause an upregulation of RCAN1 for prolong periods, such as those observed in T2D (Peiris et al., 2016), allowing us to understand the impact of upregulating RCAN1 in adipose tissue. Overall, there were significant increases in gene expression of *Rcan1.1* after treatment with KH7 and serotonin. *Rcan1.1* expression decreased with IL-6 treatment. Forskolin significantly increased *Rcan1.4* expression in adipocytes. This indicate a true understanding of physiological implications of these proteins within the adipocytes. Other factors such as VEGF (Abe and Sato, 2001) and transforming growth factor-β1 (TGF-β1) (Mann et al., 2004) are known to upregulate expression of RCAN1 and can be tested on adipocytes. Moreover, other time points by hours and by days could be tested to observe both acute and chronic gene expression changes of *Rcan1.1* and *Rcan1.4*, validated with protein analysis of RCAN1 isoform expression. The limitations and future directions for this study are discussed in further sections 7.3 and 7.4 of this thesis.

Chapter 7. GENERAL DISCUSSION AND CONCLUSION

7.1 Summary of results

The main aims of this project were to determine the effective minimum concentration of IRCA drugs in reducing fat storage in the 3T3-L1 adipocyte cell line and on proliferation and apoptosis of the β-TC6 cell line. This project also aimed to determine the expression of lipolysis-, lipogenesis- and adipogenesis- related genes in epididymal white adipose tissue (eWAT) from *Rcan1*$^{-/-}$ mice and WT mice on a low-fat diet (LFD) and a high fat diet (HFD). Additionally, this project investigated factors that may regulate *Rcan1* gene expression in 3T3-L1 cells. Further investigation is required to investigate the overarching hypothesis that the inhibition of calcineurin through RCAN1, causes the dysfunction of both β-cells and the adipose tissue in obesity and T2D.

The aim of determining the effective minimum concentration of IRCA drugs in reducing fat storage in the 3T3-L1 adipocyte cell line was partially met. There was an increase in lipid storage instead of a reduction and this could indicate that the IRCA drugs could have off-target effects not specific to RCAN1-calcineruin interaction. Molecular pathways and mechanisms of off-target effects are yet to be elucidated. Furthermore, we were successful in determining the effective minimum concentration of IRCA drugs on proliferation and apoptosis of the β-TC6 cell line. There were no changes at transcriptional level of genes associated with apoptosis and proliferation, however, protein analysis is required to determine post-translational expression changes that could affect function, upregulating or downregulating apoptosis and proliferation in β-cells. The significant increase in proliferation of IRCA1-treated β-cells is a positive finding for future experiments.

We were successful in determining the expression of lipolysis-, lipogenesis- and adipogenesis- related genes in eWAT from *Rcan1*$^{-/-}$ mice and WT mice on a LFD and a HFD. Lipolysis-related gene, *Plin1* and *Hsl* were decreased in *Rcan1*$^{-/-}$ mice compared to WT on a LFD. The *Atgl* gene expression increased in *Rcan1*$^{-/-}$ mice compared to WT on a HFD. Additionally, the master regulator of lipogenesis, *Srebp1c*, decreased gene expression in *Rcan1*$^{-/-}$ mice compared to WT mice on a LFD. Similarly, another major regulator of lipogenesis, *Chrebp*, showed decreased gene expression in WT mice compared to *Rcan1*$^{-/-}$ on HFD. No gene expression changes were observed in the alpha and beta isoforms of *Chrebp*. Downstream of the lipogenic pathway, *Acc1* had decreased gene expression in *Rcan1*$^{-/-}$ compared to WT. With reference to the lipogenesis pathway (Figure 1.6), despite the availability of *Fas*, *Acc1* and *Acc2* genes present upstream of the lipogenic pathway there was a significant decrease in *Acl* gene expression in WT mice. Should protein expression be similar to the gene expression, this suggests reduced ACL could result in reduced citrate converted to acetyl-CoA cycled downstream in the lipogenic pathway. Increase in *Acl* expression in *Rcan1*$^{-/-}$ mice on a HFD was observed compared to WT and groups on a LFD and further experiments are required to validate protein expression. For adipogenesis related gene, *leptin* gene expression was increased in *Rcan1*$^{-/-}$ mice on a HFD compared to WT and *Rcan1*$^{-/-}$ on a LFD. This could point to compensatory mechanisms as serum leptin levels

were decreased in *Rcan1*$^{-/-}$ mice (Rotter et al., 2018). These novel pieces of data add to our understanding of the anti-obesogenic phenotype seen in our *Rcan1*$^{-/-}$ mice in the lab's most recent publication (Rotter et al., 2018).

In our final experiment, we met our aim of investigating factors that may upregulate *Rcan1* expression in 3T3-L1 cells. I found that serotonin and KH7 and serotonin increased *Rcan1.1* ($p<0.05$) gene expression while IL-6 decreased *Rcan1.1* ($p<0.05$) gene expression in adipocytes. Forskolin increased *Rcan1.4* ($p<0.0001$) gene expression. It was also found that Ca^{2+} ionomycin ($p=0.05$) and TNF-α ($p=0.05$) increased *Rcan1.4* expression. This provides a broad overview of factors that could upregulate *Rcan1.1* and *Rcan1.4* gene expression changes in adipocytes.

7.2 Implications of this study

The results of this study are novel and extend our understanding of the role of RCAN1 in regulating adipocyte biology as well as the effects of the novel suite of drugs used to inhibit RCAN1-calcineurin interaction in the adipose tissue and pancreatic β-cells. Type 2 diabetes (T2D) linked to obesity, is a major problem in Australia and the world (Diabetes Australia, 2015). Obesity is defined as the expansion of adipocyte mass and functionally dysregulated in persons who have obesity-induced diabetes (Bouret et al., 2015). Currently no cure is found to effectively cure T2D. The commonly used treatment interventions for management of T2D do not directly target the improvement in β-cell function. The inhibition of RCAN1 could be therapeutic and enable greater proliferation in β-cells. To enable normal β-cell function, the balance between apoptosis and proliferation is necessary. My findings in the use of IRCA drugs presents an exciting opportunity for use of this drug as a therapeutic intervention. In this thesis, I found that IRCA1 at optimal concentrations can cause significant proliferation in β-cells. This has implications for the use of drugs in T1D patients who undergo islet transplant and faces immune disruption of existing pools of pancreatic β-cells. With regards to T2D, the ability to proliferate functional β-cells could outnumber dysfunctional pools of β-cells and provide sufficient insulin production to combat diabetes.

RCAN1, recently linked to T2D, plays a role in non-shivering thermogenesis. It was a particularly interesting finding that *Rcan1*$^{-/-}$ mice on a HFD did not gain weight (Rotter et al., 2018) and this provided the basis for exciting new research to try to understand mechanisms in the adipose tissue biology and function that could be affected by diet changes and *Rcan1*$^{-/-}$ changes. My findings of expression changes in genes associated with lipolysis, lipogenesis and adipogenesis helps us better appreciate the complexity of the role of RCAN1 in adipose tissue function. Furthermore, the study involving factors that could induce expression of either RCAN1 isoforms in adipocytes is important in furthering our understanding and scope of various pathways that these factors are implicated in.

7.3 Limitations of this study

In Chapter 3, the limitations to this study include the fact that *in vitro* culture of adipocytes may not mimic the biological processes in adipocytes *in vivo* as it does not consider neuroendocrine effects (Sjostrand and Eriksson, 2009) such as sympathetic and parasympathetic (Kreier et al., 2002) regulation of lipid metabolism in the adipose tissue. Therefore *in vitro* data must be followed up with *in vivo* experiments and possibly compare IRCA drug effects with those seen in *Rcan1*$^{-/-}$ mice. The experiments with IRCA drugs performed, highlights its novelty, as these drugs have not been tested in a physiology system and the experiments carried out in this thesis pioneers the use of these compounds on cells. This presents a limitation as there is no data available to make comparisons to for the effective dose range used for *in vivo* or *in vitro* experiments. Furthermore, the images of the adipocyte-containing lipid droplets stained with Oil Red-O were not of a quality high enough to further quantify lipid droplet size by measuring lipid droplet number and diameter by hand. This presents a limitation in the experiment analysis. With quality images, systems such as LipiD-QuantT could be applied to measure size and distribution of lipid droplets (Varinli et al., 2015). LipiD-QuantT is automated for image analysis and can quantify lipid droplet accumulation in live cells on a per cell basis, using phase contrast microscopy. This is an automated, non-invasive live cell imaging tool that does not require fixation would enable further use of these cells instead of an end point Oil Red-O assay (Varinli et al., 2015). The use of this tool could also account for possible loss of lipids that detach during the Oil Red-O washing procedures. Even though the same protocol was used, small variations exist between experiments and there is reliance on statistical analysis to account for such variations. Alternatively, lipid storage can be measured using ^{14}C incorporation of glucose (measures lipogenesis) and palmitate into lipids combined with a scintillation counting to quantify lipid content (Pereira et al., 2013).

In Chapter 5, genes associated with one pathway in adipocyte metabolism could be implicate in other pathways. For example, SREBP-1c is known as a major transcriptional regulator of lipogenesis, however, it is also implicated in adipogenesis (Letexier et al., 2003). ChREBP-*a* transcription factor associated with DNL, also modulates the PPARγ adipogenic master regulator, therefore ChREBP expression can affect PPARγ activity and downstream adipogenic-gene expression during adipogenesis (Witte et al., 2015). Overall, the genes studied in this thesis, could be implicated in more than one pathway, giving rise to complexity in the interpretation of gene or protein expression in relation to function. Measurement of actual enzyme activity is necessary to test the enzymatic activity of these targets, similar to the study by Letexier et al. (Letexier et al., 2003), with the aims of investigating the different metabolic pathways more thoroughly. Furthermore, the level of lipases present does not always parallel lipase activity due to posttranslational regulation of ATGL and HSL (Zechner et al., 2012). The products generated by the various enzymes should be measured, indicative of enzyme activity and allows for a better understanding of true effects of these enzymes in impacting *de novo* lipogenesis. For example, hepatocytes that had ACC1 suppressed, had a 50% decrease in malonyl-CoA

content in tissues (Savage et al., 2006). Once we gain a better understanding of metabolic processes in the adipose tissue, we can determine the overall effect of these adipocyte metabolic processes. For example, if overall lipolysis is increased and lipid storage decreased, this could explain increased circulating FFAs and VLDL involved in contributing to insulin resistance in WT mice on a HFD.

Furthermore, the eWAT used in Chapter 5 is derived from mice where RCAN1 is completely ablated in cells that normally expresses RCAN1. Therefore, it is important to note that interpretation of this work cannot be restricted to the effects of RCAN1 directly on adipose tissue even though tissue explants from the globally knocked out RCAN1 mice has been used in experiments in this thesis. Indirect effects may have occurred that were not specific to adipose tissue but due to changes in the body can exist *in vivo* in the adipose tissue of *Rcan1*$^{-/-}$ mice. Therefore, interpretation of gene expression, even though restricted to adipose tissue explants, needs to be taken into consideration as *Rcan1* is knocked out completely from these mice. It would be ideal to have adipose-specific tissue knock-down of RCAN1 to ensure a more targeted approach.

Additionally, gene expression changes may not always correlate with protein expression due to translational efficacy (Maier et al., 2009, Vogel and Marcotte, 2012, Koussounadis et al., 2015, Edfors et al., 2016). Therefore, protein expression using Western blots or proteomics analysis needs to be undertaken to validate the gene expression changes observed in proliferation and apoptosis genes of β-TC6 drug-treated cells, the lipolysis, lipogenesis and adipogenesis-related gene expression changes, the expression changes in the study involving 3T3-L1 and expression changes of *Rcan1.1* or *Rcan1.4* inducted by certain factors. Initially, an 18S housekeeper gene was used, however, the particular sequence of 18S used presented technical difficulties. The use of the β-actin housekeeper gene was chosen for all experiments in this thesis. In future experiments, other sequences of the 18S housekeeper gene can be used in addition to the β-actin housekeeping gene to ensure double validation of results.

All primer sequences were checked for primer specificity using the primer-BLAST software that indicated that the primers used in this thesis were specific for their target. According to the melt curves in the Appendix, *Ccnd2*(1) gene (Appendix B.1) and *Chrebp-β* (Appendix B.2), in Chapter 4 and Chapter 5 respectively, were extremely lowly expressed resulting in large variations in the melt curves and quantitation graphs. The *Rcan1.1* (Appendix B.3) primers used in Chapter 6 had two peaks in the melt curve. The melt curves should only have a single peak as this would indicate a single distinct species. When multiple peaks are present, this indicates the presence of contamination or off-target amplification products (Varga and James, 2006). It is more likely that there are off-target amplification products present as the no template control did not indicate contamination. Therefore, caution needs to be taken when analysing and interpreting the results from the use of these primers. The products from the current *Rcan1.1* primers can be tested on a agarose gel to identify the presence of a single band. The RT-PCR products can also be sequenced. Alternatively, new primer sequences can be used in a repeat

experiment in the future. Additionally, primer amplification efficiency needs to be calculated for all genes analysed in this thesis using serial dilutions. The primer is deemed to be efficient at 90-100% and is specific for its target (Thornton and Basu, 2011). Low primer efficiency could be indicative of poor primer design, non-optimal reagents or reaction conditions. This could affect complete strand separation, reduce amplification efficiency, therefore, affecting experiment results (Bustin and Huggett, 2017). Reaction conditions and primer concentrations can be adjusted to improve its efficacy for future experiments and interpretation of expression changes needs to be validated with protein analysis.

7.4 Future directions

In Chapter 3, the nuclear localisation of NFAT in adipocytes under the influence of IRCA drugs can be measured to better understand the calcineurin-NFAT pathway. Quantifying the amount of NFAT in the nucleus would provide a better indication of the effects of these drugs in causing NFAT translation in this pathway. Also, these drugs could be tested on an alternative cell line such as the myoblast cells. In a recent publication, the activity of the *Sln-Luc* construct using the Luciferase assay measured *Sln-Luc* activity alone or as a combination of *Sln-Luc*, active CnA and RCAN1 in myoblast cells. The myoblast cells showed a significant additive effect on the activity of *Sln-Luc* reporter when active CnA was present (Rotter et al., 2018). With the use of IRCA drugs we would expect that the RCAN1 transfected group would increase back to the same level as the activated CnA and *Sln-Luc* group. This would indicate that the IRCA drugs share inhibitory effects similar to those of the calcineurin inhibitors CsA and FK506, without affecting calcineurin activity itself, therefore this would be proof of concept that the IRCA drugs target the RCAN1-calcineurin interaction that affects pathways downstream of calcineurin. Alternatively, we could measure calcineurin activity using commercially avaliable assays such as those from abcam and enzolifesicence (Jin et al., 2017) in IRCA-drug treated β-cells derived from RCAN1^{ox} mice. We hypothesize that the drugs should increase calcineurin activity and return to normal levels, given that calcineurin activity is reduced in RCAN1^{ox} cells (Peiris et al., 2012). Furthermore, the potency and half-life of the IRCA drugs used in Chapter 3 and Chapter 4 can be further investigated. This is especially important if further experiments are to progress to whole animal level as it would enable understanding of the frequency and dosage of drugs required in animal studies.

It has been well established that RCAN1 is an endogenous inhibitor of calcineurin and acts to inhibit the calcineurin-RCAN1 interaction. The role of calcineurin in RCAN1-dependent changes in β-cell function could be analysed. The current experiment where the use of IRCA1 increased proliferation of β-cells, is limited as it only provides an estimate for the increased rate of proliferation by estimating increase in electrical impedance in the xCELLigence system as β-cell number increases. The increased rate of proliferation has not been validated for β-cell function. Functional tests are required to understand if these fast growing β-cells are functionally able to produce insulin. This is important as β-

cells are the main source of endogenous insulin in the body that enables glucose homeostasis to be maintained. Furthermore, flow cytometry analysis of the effects of IRCA1 treatment on β-TC6 can be undertaken by staining these β-cells with Ki67 proliferation marker to quantify proliferation of these cells. Immunofluorescent imaging analysis can indicate cell morphology, size and number of these β-cells. Moreover, insulin co-labelled cells could also be analysed to determine β-cells that secrete insulin. Functional test could include the Seahorse XF24 Flux analyser that measures mitochondrial respiration, an assay that measures mitochondrial activity, measurement of total ATP content using a luciferase assay and measurements of the mitochondrial membrane potential using the TMRM staining can be used to better understand the effect of IRCA drugs on β-TC6 cells. Furthermore, glucose- and succinate-induced insulin secretion can be measured using an ELISA to understand the ability of these fast proliferating IRCA1-treated β-TC6 to secrete insulin. These assays have been previously used in this lab and work involving these techniques have been published in recent years (Peiris et al., 2012, Peiris et al., 2016).

To follow up, results from β-cell line experiments can be verified using islets from RCAN1^{ox} and *Rcan1*$^{-/-}$ mice. In the presence of low or high glucose, islets derived from WT and *Rcan1*$^{-/-}$ mice can be stained with Ki67 and insulin to indicate proliferation in these islets. To understand the effects of IRCA drugs on the RCAN1-calcineurin pathway, NFAT localisation can be analysed in either *Rcan1*$^{-/-}$ islets or in β-TC6 cell line, incubated in high glucose in the absence or presence of IRCA compounds. NFAT localization can be quantified using immunohistochemistry (Heit et al., 2006a). As these experiments are done at cell level or isolated islet explants, to further investigate the effectiveness of the drug and for the development of these drugs for therapeutic use, these drugs need to be tested at whole organism level and functional studies done in whole animal level will be important. Recently, the overexpression of RCAN1 in β-cells resulted in multiple changes to β-cell function (Peiris et al., 2012, Peiris et al., 2016), likewise, studies can be expanded to adipocyte function and biology, involving the use of RCAN1$^{-/-}$ mice in future experiments, thereby allow for the broadening of our understanding of the significance of RCAN1 expression on adipocyte function.

In the study relating to the gene expression of lipolytic-, lipogenic- and adipogenic- related genes in eWAT of *Rcan1*$^{-/-}$and WT mice on a LFD and HFD, a few further considerations can be made. Other mechanisms could be involved, driving the lean phenotype observed in the *Rcan1*$^{-/-}$mice on HFD. For example, aldosterone could be reduced in these mice. The ablation of *Cgi-58* in adipocytes resulted in the blockage of insulin-stimulated suppression of lipolysis (Stockli et al., 2019). The inhibition of the aldosterone synthase mRNA (CYP11B2) in 3T3-L1 cells reduced the expression of essential transcriptional factors associated with adipogenesis (Briones et al., 2012). In the study by Briones et al. (2012), calcineurin and NFAT inhibitors inhibited Ang II-induced aldosterone secretion by adipocytes, calcineurin inhibitors rescued Ang II reduction of NFATc4 phosphorylation and Ang II type I receptor

antagonist (candesartan) inhibited Ang II stimulated NFAT nuclear translocation (Briones et al., 2012). This suggests that aldosterone production has effects on adipocyte differentiation and could affect the calcineurin-NFAT pathway as calcineurin controls Ang II-mediated aldosterone synthase that enables adipocytes to synthesize aldosterone (Briones et al., 2012). Future experiments can investigate this to help us understand possible mechanisms occurring when RCAN1 is knocked out in mice and investigate therapeutic benefits of reducing RCAN1 pharmacologically in humans in the treatment of obesity.

The results from this project have extended our knowledge of the role of RCAN1 in adipocytes. Mentioned in the previous section regarding limitations of experiments, protein expression, enzyme activity and functional test are required in future experiments to provide understanding of possible mechanisms underlying the lean phenotype seen in *Rcan1*$^{-/-}$ mice. Method of measuring HSL enzyme activity can also be measured on fat-free infranatant with the use of diolein analogues as described previously (Ray et al., 2009). Additionally, we could measure monoglyceride lipase (MGL) mRNA and protein expression as this enzyme is involved in the final step of lipolysis, converting monoglyceride to fatty acids and glycerol (Fredrikson et al., 1986) which was not measured in the present study. Furthermore, it might be worthwhile measuring lipolysis rates in eWAT directly as there seems to be differences in rates of lipolysis depending on WAT depot seen in *Rcan1*$^{-/-}$ mice (Rotter et al., 2018). Fatty acid accumulation had regional variations in eWAT where proximal eWAT had 70% less *de novo* lipogenesis than distal eWAT (Caesar et al., 2010). This highlights the complexity of studying gene expression changes within a single fat depot. In our current experiment, we used the whole eWAT fat explant for qPCR analysis. Taking the study by Caesar et al. into account (Caesar et al., 2010), we could potentially select a specific region on the fat depot of interest and conduct future investigation on gene expression changes. Additionally, there is value in classifying adipocytes according to size and relating it to mRNA expression of lipolysis gene expression. Higher *Hsl* and *Atgl* gene expression were linked to larger adipocyte size and increased basal lipolysis (Wueest et al., 2009). With data specific to gene and protein expression changes linked to adipocyte morphology and function, we are able to better understand the phenotypic changes of *Rcan1*$^{-/-}$mice and the anti-HFD-induced obesity phenotype observed in the recent publication (Rotter et al., 2018).

A further study into the mechanisms by which serotonin and KH7 upregulates *Rcan1.1* gene expression in adipocytes and mechanisms by which IL-6 downregulates *Rcan1.1* gene expression could be investigated. The factors that increased *Rcan1.1* and *Rcan1.4* expression in the 3T3-L1 cell line can be tested on the β-TC6 cell line to understand expression changes in pancreatic β-cells as well as other metabolic organs such as skeletal muscles and the liver. *Rcan1.1* can be upregulated by glucocorticoids and vascular endothelial growth factor (VEGF) (Hirakawa et al., 2009) and downregulated by the Notch signaling pathway, therefore, in future experiments these factors can used to investigate expression changes in *Rcan1* in both adipocytes and β-cells. The use of KH7 specifically inhibited soluble adenylyl

cyclase, therefore, the use of the inhibitor specific of transmembrane adenylyl cyclase, such as 2′ ,5′ -dideoxyadenosine, could be used in future experiments to understand the impact of inhibiting the two main types of adenylyl cyclase that produces cAMP (Bitterman et al., 2013). The quantity of cAMP can also be measured which builds up in the cell when phosphodiesterase inhibitors are used, thereby reflecting the amount of cAMP converted by the adenylyl cyclase from ATP (Bitterman et al., 2013).

The mitochondria are the primary source of reactive oxygen species (ROS), driver of ATP production, regulates intracellular Ca^{2+} homeostasis and apoptosis in cells (Youle and van der Bliek, 2012). Measures of mitochondria dysfunction in WAT should be quantified as WAT is an important metabolic organ and not many studies have investigated this, as explained in section 1.5.1.5, which could play a role in insulin resistance, obesity and T2D. Mitophagy, a type of autophagic disposal of selected damaged mitochondria, could be measured in both adipocytes and β-cells (Klionsky et al., 2016). In mammalian cells, Parkin, an E3 ubiquitin ligase, causes selective degradation of dysfunctional mitochondria via autophagy, specifically via mitophagy (Narendra et al., 2008). Cells could be treated with the mitochondrial uncoupler carbonyl cynide m-chrlorophenylhydrazone (CCCP) for an hour to induce mitochondrial fragmentation to investigate whether mitochondrial depolarization causes Parkin accumulation in the mitochondria. The control group could include cells treated with media containing DMSO. These cells can be stained for Parkin and the mitochondria can be stained for cytochrome c using immunohistochemistry (Narendra et al., 2008). Mitophagy requires targeted labelling of the mitochondria and recruitment into individual membranes. In yeast, autophagy related 32 protein (Atg32) binds to the isolated membrane, while in the brain, damaged mitochondria result in an increased PTEN-induced putative kinase protein 1 (PINK1) and parkin that ubiquitylates the mitochondrial proteins causing signalling engulfment by isolated membranes that undergoes lysosomal degradation (Youle and Narendra, 2011). Other autophagy receptor proteins involved in mitophagy has been reviewed by (Pickles et al., 2018). Recently, it was shown that mitophagy is involved in Parkin-dependent beiging of adipocytes (Lu et al., 2018, Taylor and Gottlieb, 2017). Another study investigated that β-cells and adipocyte mitochondria health were maintained independent of parkin in diet-related obesity (Corsa et al., 2019), however, another study showed that pancreatic β-cells had parkin-mediated mitophagy (Hoshino and Matoba, 2018). In a human study, an upregulation of mitophagy slowed T2D progression by prolonging health of functioning β-cells (Bhansali et al., 2017). A study by Li et al. (2020) involves the overexpression of islet-specific RCAN1 mice fed a high-fat diet that induced a pre-diabetic phenotype in these mice. These mice had RCAN1 islet-specific overexpression and were GFP-tagged. The colocalization of LC3-GFP was quantified using a lysosome-specific LysoTracker which provided an indication that overexpressing RCAN1 resulted in the impairment of autophagosome-lysosome fusion. Therefore, there are links associated with overexpression of RCAN1 and β-cell mitophagy implicated is in T2D (Li et al., 2020).The limitation of measuring mitophagy is that it is not

a static process (Klionsky et al., 2016) and finding methods that best measure mitophagy in cells would further our understand of the role of RCAN1 in both β-cell and adipocyte function.

7.5 Concluding remarks

The results of this study indicate that RCAN1 has a role in adipocyte biology and highlight other possible roles of RCAN1 in the adipose tissue-specific functional changes. The previous links made between RCAN1 and diabetes and the link between RCAN1 and thermogenesis can now be extended to the study of RCAN1 in the adipose tissue as well as other metabolic organs. Mice that have a deficiency in RCAN1 compared to WT on both high and low-fat diets had a multitude of effects on lipolysis, lipogenesis and adipogenesis gene expression changes. These changes highlight the role of RCAN1 in adipocyte function and in response to dietary changes. Mechanisms of the effects of RCAN1 on these pathways require further investigation through functional tests. The current lack of pharmacological agents targeting improved β-cell number in the treatment of both Type 1 and Type 2 diabetes render urgent need to find a cure for diabetes. The increased proliferation rate with the use IRCA1 drug on β-cell presents a unique opportunity for the potential use this drug to combat T2D. The results in this thesis presents a novel pharmaceutical therapeutic, IRCA drugs, that target RCAN1 implicated in the regulation of adipocyte metabolism and β-cell growth, where both tissues are of vital importance to the regulation of obesity and T2D.

REFERENCES

ABBASI, S., LEE, J. D., SU, B., CHEN, X., ALCON, J. L., YANG, J., KELLEMS, R. E. & XIA, Y. 2006. Protein kinase-mediated regulation of calcineurin through the phosphorylation of modulatory calcineurin-interacting protein 1. *J Biol Chem,* 281**,** 7717-26.

ABE, M. & SATO, Y. 2001. cDNA microarray analysis of the gene expression profile of VEGF-activated human umbilical vein endothelial cells. *Angiogenesis,* 4**,** 289-98.

ABU-ELHEIGA, L., MATZUK, M. M., KORDARI, P., OH, W., SHAIKENOV, T., GU, Z. & WAKIL, S. J. 2005. Mutant mice lacking acetyl-CoA carboxylase 1 are embryonically lethal. *Proc Natl Acad Sci U S A,* 102**,** 12011-6.

ABU-ELHEIGA, L., OH, W., KORDARI, P. & WAKIL, S. J. 2003. Acetyl-CoA carboxylase 2 mutant mice are protected against obesity and diabetes induced by high-fat/high-carbohydrate diets. *Proc Natl Acad Sci U S A,* 100**,** 10207-12.

ACEA BIOSCIENCES INC. 2019, *Technological Overview: Cellular Impedance Explained,* San Diego, viewed on 30 August 2019, <https://www.aceabio.com/products/rtca-dp/>.

AHIMA, R. S. & FLIER, J. S. 2000. Leptin. 62**,** 413-437.

AHL, S., GUENTHER, M., ZHAO, S., JAMES, R., MARKS, J., SZABO, A. & KIDAMBI, S. 2015. Adiponectin Levels Differentiate Metabolically Healthy vs Unhealthy Among Obese and Nonobese White Individuals. *J Clin Endocrinol Metab,* 100**,** 4172-80.

AHMADIAN, M., ABBOTT, M. J., TANG, T., HUDAK, C. S., KIM, Y., BRUSS, M., HELLERSTEIN, M. K., LEE, H. Y., SAMUEL, V. T., SHULMAN, G. I., WANG, Y., DUNCAN, R. E., KANG, C. & SUL, H. S. 2011. Desnutrin/ATGL is regulated by AMPK and is required for a brown adipose phenotype. *Cell Metab,* 13**,** 739-48.

AHMADIAN, M., DUNCAN, R. E., VARADY, K. A., FRASSON, D., HELLERSTEIN, M. K., BIRKENFELD, A. L., SAMUEL, V. T., SHULMAN, G. I., WANG, Y., KANG, C. & SUL, H. S. 2009. Adipose overexpression of desnutrin promotes fatty acid use and attenuates diet-induced obesity. *Diabetes,* 58**,** 855-66.

AHMADIAN, M., WANG, Y. & SUL, H. S. 2010. Lipolysis in adipocytes. *Int J Biochem Cell Biol,* 42**,** 555-9.

AHREN, B. & SCHEURINK, A. J. 1998. Marked hyperleptinemia after high-fat diet associated with severe glucose intolerance in mice. *Eur J Endocrinol,* 139**,** 461-7.

AILHAUD, G., DANI, C., AMRI, E. Z., DJIAN, P., VANNIER, C., DOGLIO, A., FOREST, C., GAILLARD, D., NEGREL, R. & GRIMALDI, P. 1989. Coupling growth arrest and adipocyte differentiation. *Environ Health Perspect,* 80**,** 17-23.

ALASBAHI, R. H. & MELZIG, M. F. 2012. Forskolin and derivatives as tools for studying the role of cAMP. *Pharmazie,* 67**,** 5-13.

ALTAREJOS, J. Y. & MONTMINY, M. 2011. CREB and the CRTC co-activators: sensors for hormonal and metabolic signals. *Nat Rev Mol Cell Biol,* 12**,** 141-51.

AMEER, F., SCANDIUZZI, L., HASNAIN, S., KALBACHER, H. & ZAIDI, N. 2014. De novo lipogenesis in health and disease. *Metabolism,* 63**,** 895-902.

AMEMIYA-KUDO, M., SHIMANO, H., HASTY, A. H., YAHAGI, N., YOSHIKAWA, T., MATSUZAKA, T., OKAZAKI, H., TAMURA, Y., IIZUKA, Y., OHASHI, K., OSUGA, J., HARADA, K., GOTODA, T., SATO, R., KIMURA, S., ISHIBASHI, S. & YAMADA, N. 2002. Transcriptional activities of nuclear SREBP-1a, -1c, and -2 to different target promoters of lipogenic and cholesterogenic genes. *J Lipid Res,* 43**,** 1220-35.

AMERICAN DIABETES, A. 2010. Diagnosis and classification of diabetes mellitus. *Diabetes Care,* 33 Suppl 1**,** S62-9.

AMERICAN DIABETES, A. 2019. 2. Classification and Diagnosis of Diabetes: Standards of Medical Care in Diabetes-2019. *Diabetes Care,* 42**,** S13-S28.

ANELLO, M., LUPI, R., SPAMPINATO, D., PIRO, S., MASINI, M., BOGGI, U., DEL PRATO, S., RABUAZZO, A. M., PURRELLO, F. & MARCHETTI, P. 2005. Functional and morphological alterations of mitochondria in pancreatic beta cells from type 2 diabetic patients. *Diabetologia,* 48**,** 282-9.

ANTHONSEN, M. W., RONNSTRAND, L., WERNSTEDT, C., DEGERMAN, E. & HOLM, C. 1998. Identification of novel phosphorylation sites in hormone-sensitive lipase that are phosphorylated in response to isoproterenol and govern activation properties in vitro. *J Biol Chem,* 273**,** 215-21.

ANWAR, A. J., WALKER, J. D. & FRIER, B. M. 1998. Type 1 diabetes mellitus and Down's syndrome: prevalence, management and diabetic complications. *Diabet Med,* 15**,** 160-3.

ARNER, P. 1998. Not all fat is alike. *Lancet,* 351**,** 1301-2.

ARRON, J. R., WINSLOW, M. M., POLLERI, A., CHANG, C. P., WU, H., GAO, X., NEILSON, J. R., CHEN, L., HEIT, J. J., KIM, S. K., YAMASAKI, N., MIYAKAWA, T., FRANCKE, U., GRAEF, I. A. & CRABTREE, G. R. 2006. NFAT dysregulation by increased dosage of DSCR1 and DYRK1A on chromosome 21. *Nature,* 441**,** 595-600.

ASAI, A., QIU, J., NARITA, Y., CHI, S., SAITO, N., SHINOURA, N., HAMADA, H., KUCHINO, Y. & KIRINO, T. 1999. High level calcineurin activity predisposes neuronal cells to apoptosis. *J Biol Chem,* 274**,** 34450-8.

ASKARI, H., TYKODI, G., LIU, J. & DAGOGO-JACK, S. 2010. Fasting plasma leptin level is a surrogate measure of insulin sensitivity. *J Clin Endocrinol Metab,* 95**,** 3836-43.

BAEK, K. H., ZASLAVSKY, A., LYNCH, R. C., BRITT, C., OKADA, Y., SIAREY, R. J., LENSCH, M. W., PARK, I. H., YOON, S. S., MINAMI, T., KORENBERG, J. R., FOLKMAN, J., DALEY, G. Q., AIRD, W. C., GALDZICKI, Z. & RYEOM, S. 2009. Down's syndrome suppression of tumour growth and the role of the calcineurin inhibitor DSCR1. *Nature,* 459**,** 1126-30.

BAGDADE, J. D., BIERMAN, E. L. & PORTE, D., JR. 1967. The significance of basal insulin levels in the evaluation of the insulin response to glucose in diabetic and nondiabetic subjects. *J Clin Invest,* 46**,** 1549-57.

BANKS, W. A., JASPAN, J. B., HUANG, W. & KASTIN, A. J. 1997. Transport of insulin across the blood-brain barrier: saturability at euglycemic doses of insulin. *Peptides,* 18**,** 1423-9.

BARBATELLI, G., MURANO, I., MADSEN, L., HAO, Q., JIMENEZ, M., KRISTIANSEN, K., GIACOBINO, J. P., DE MATTEIS, R. & CINTI, S. 2010. The emergence of cold-induced brown adipocytes in mouse white fat depots is determined predominantly by white to brown adipocyte transdifferentiation. *Am J Physiol Endocrinol Metab,* 298**,** E1244-53.

BARTELT, A., BRUNS, O. T., REIMER, R., HOHENBERG, H., ITTRICH, H., PELDSCHUS, K., KAUL, M. G., TROMSDORF, U. I., WELLER, H., WAURISCH, C., EYCHMULLER, A., GORDTS, P. L., RINNINGER, F., BRUEGELMANN, K., FREUND, B., NIELSEN, P., MERKEL, M. & HEEREN, J. 2011. Brown adipose tissue activity controls triglyceride clearance. *Nat Med,* 17**,** 200-5.

BASIL, J. S., SANTORO, S. L., MARTIN, L. J., HEALY, K. W., CHINI, B. A. & SAAL, H. M. 2016. Retrospective Study of Obesity in Children with Down Syndrome. *J Pediatr,* 173**,** 143-8.

BEALS, C. R., CLIPSTONE, N. A., HO, S. N. & CRABTREE, G. R. 1997. Nuclear localization of NF-ATc by a calcineurin-dependent, cyclosporin-sensitive intramolecular interaction. *Genes Dev,* 11**,** 824-34.

BELL, C. G., WALLEY, A. J. & FROGUEL, P. 2005. The genetics of human obesity. *Nat Rev Genet,* 6**,** 221-34.

BELTOWSKI, J., WOJCICKA, G., GORNY, D. & MARCINIAK, A. 2000. The effect of dietary-induced obesity on lipid peroxidation, antioxidant enzymes and total plasma antioxidant capacity. *J Physiol Pharmacol,* 51**,** 883-96.

BERG, M., FRAKER, D. L. & ALEXANDER, H. R. 1994. Characterization of differentiation factor/leukaemia inhibitory factor effect on lipoprotein lipase activity and mRNA in 3T3-L1 adipocytes. *Cytokine,* 6**,** 425-32.

BERGER, M., GRAY, J. A. & ROTH, B. L. 2009. The expanded biology of serotonin. *Annu Rev Med,* 60**,** 355-66.

BERGMAN, R. N. & ADER, M. 2000. Free fatty acids and pathogenesis of type 2 diabetes mellitus. *Trends Endocrinol Metab,* 11**,** 351-6.

BERRIDGE, M. V. & TAN, A. S. 1993. Characterization of the cellular reduction of 3-(4,5-dimethylthiazol-2-yl)-2,5-diphenyltetrazolium bromide (MTT): subcellular localization, substrate dependence, and involvement of mitochondrial electron transport in MTT reduction. *Arch Biochem Biophys,* 303**,** 474-82.

BHANSALI, S., BHANSALI, A., WALIA, R., SAIKIA, U. N. & DHAWAN, V. 2017. Alterations in Mitochondrial Oxidative Stress and Mitophagy in Subjects with Prediabetes and Type 2 Diabetes Mellitus. *Front Endocrinol (Lausanne),* 8**,** 347.

BI, Y., WU, W., SHI, J., LIANG, H., YIN, W., CHEN, Y., TANG, S., CAO, S., CAI, M., SHEN, S., GAO, Q., WENG, J. & ZHU, D. 2014. Role for sterol regulatory element binding protein-1c activation in mediating skeletal muscle insulin resistance via repression of rat insulin receptor substrate-1 transcription. *Diabetologia,* 57**,** 592-602.

BISWAS, S. K. & MANTOVANI, A. 2012. Orchestration of metabolism by macrophages. *Cell Metab,* 15**,** 432-7.

BITTERMAN, J. L., RAMOS-ESPIRITU, L., DIAZ, A., LEVIN, L. R. & BUCK, J. 2013. Pharmacological distinction between soluble and transmembrane adenylyl cyclases. *J Pharmacol Exp Ther,* 347**,** 589-98.

BONNER-WEIR, S. 2000. Islet growth and development in the adult. *J Mol Endocrinol,* 24**,** 297-302.

BONNER-WEIR, S., DEERY, D., LEAHY, J. L. & WEIR, G. C. 1989. Compensatory growth of pancreatic beta-cells in adult rats after short-term glucose infusion. *Diabetes,* 38**,** 49-53.

BOONE, C., MOUROT, J., GREGOIRE, F. & REMACLE, C. 2000. The adipose conversion process: regulation by extracellular and intracellular factors. *Reprod Nutr Dev,* 40**,** 325-58.

BOURET, S., LEVIN, B. E. & OZANNE, S. E. 2015. Gene-environment interactions controlling energy and glucose homeostasis and the developmental origins of obesity. *Physiol Rev,* 95**,** 47-82.

BRASAEMLE, D. L. 2007. Thematic review series: adipocyte biology. The perilipin family of structural lipid droplet proteins: stabilization of lipid droplets and control of lipolysis. *J Lipid Res,* 48**,** 2547-59.

BRASAEMLE, D. L., LEVIN, D. M., ADLER-WAILES, D. C. & LONDOS, C. 2000a. The lipolytic stimulation of 3T3-L1 adipocytes promotes the translocation of hormone-sensitive lipase to the surfaces of lipid storage droplets. *Biochim Biophys Acta,* 1483**,** 251-62.

BRASAEMLE, D. L., RUBIN, B., HARTEN, I. A., GRUIA-GRAY, J., KIMMEL, A. R. & LONDOS, C. 2000b. Perilipin A increases triacylglycerol storage by decreasing the rate of triacylglycerol hydrolysis. *J Biol Chem,* 275**,** 38486-93.

BRAUN, T. & DODS, R. F. 1975. Development of a Mn-2+-sensitive, "soluble" adenylate cyclase in rat testis. *Proc Natl Acad Sci U S A,* 72**,** 1097-101.

BRIONES, A. M., NGUYEN DINH CAT, A., CALLERA, G. E., YOGI, A., BURGER, D., HE, Y., CORREA, J. W., GAGNON, A. M., GOMEZ-SANCHEZ, C. E., GOMEZ-SANCHEZ, E. P., SORISKY, A., OOI, T. C., RUZICKA, M., BURNS, K. D. & TOUYZ, R. M. 2012. Adipocytes produce aldosterone through calcineurin-dependent signaling pathways: implications in diabetes mellitus-associated obesity and vascular dysfunction. *Hypertension,* 59**,** 1069-78.

BROWN, M. S. & GOLDSTEIN, J. L. 1997. The SREBP pathway: regulation of cholesterol metabolism by proteolysis of a membrane-bound transcription factor. *Cell,* 89**,** 331-40.

BURHANS, M. S., HAGMAN, D. K., KUZMA, J. N., SCHMIDT, K. A. & KRATZ, M. 2018. Contribution of Adipose Tissue Inflammation to the Development of Type 2 Diabetes Mellitus. *Compr Physiol,* 9**,** 1-58.

BUSH, E., FIELITZ, J., MELVIN, L., MARTINEZ-ARNOLD, M., MCKINSEY, T. A., PLICHTA, R. & OLSON, E. N. 2004. A small molecular activator of cardiac hypertrophy uncovered in a chemical screen for modifiers of the calcineurin signaling pathway. *Proc Natl Acad Sci U S A,* 101**,** 2870-5.

BUSTIN, S. & HUGGETT, J. 2017. qPCR primer design revisited. *Biomol Detect Quantif,* 14**,** 19-28.

BUTLER, A. E., JANSON, J., BONNER-WEIR, S., RITZEL, R., RIZZA, R. A. & BUTLER, P. C. 2003. Beta-cell deficit and increased beta-cell apoptosis in humans with type 2 diabetes. *Diabetes,* 52**,** 102-10.

CAESAR, R., MANIERI, M., KELDER, T., BOEKSCHOTEN, M., EVELO, C., MULLER, M., KOOISTRA, T., CINTI, S., KLEEMANN, R. & DREVON, C. A. 2010. A combined transcriptomics and lipidomics analysis of subcutaneous, epididymal and mesenteric adipose tissue reveals marked functional differences. *PLoS One,* 5**,** e11525.

CAI, D., LI, H., ZHOU, B., HAN, L., ZHANG, X., YANG, G. & YANG, G. 2012. Conjugated linoleic acid supplementation caused reduction of perilipin1 and aberrant lipolysis in epididymal adipose tissue. *Biochem Biophys Res Commun,* 422**,** 621-6.

CANNON, B. & NEDERGAARD, J. 2004. Brown adipose tissue: function and physiological significance. *Physiol Rev,* 84**,** 277-359.

CAO, Z., UMEK, R. M. & MCKNIGHT, S. L. 1991. Regulated expression of three C/EBP isoforms during adipose conversion of 3T3-L1 cells. *Genes Dev,* 5**,** 1538-52.

CARMEN, G. Y. & VICTOR, S. M. 2006. Signalling mechanisms regulating lipolysis. *Cell Signal,* 18**,** 401-8.

CARNAGARIN, R., DHARMARAJAN, A. M. & DASS, C. R. 2015. Molecular aspects of glucose homeostasis in skeletal muscle--A focus on the molecular mechanisms of insulin resistance. *Mol Cell Endocrinol,* 417**,** 52-62.

CARON, A., REYNOLDS, R. P., CASTORENA, C. M., MICHAEL, N. J., LEE, C. E., LEE, S., BERDEAUX, R., SCHERER, P. E. & ELMQUIST, J. K. 2019. Adipocyte Gs but not Gi signaling regulates whole-body glucose homeostasis. *Mol Metab*.

CASAS, C., MARTINEZ, S., PRITCHARD, M. A., FUENTES, J. J., NADAL, M., GUIMERA, J., ARBONES, M., FLOREZ, J., SORIANO, E., ESTIVILL, X. & ALCANTARA, S. 2001. Dscr1, a novel endogenous inhibitor of calcineurin signaling, is expressed in the primitive ventricle of the heart and during neurogenesis. *Mech Dev,* 101**,** 289-92.

CATERSON, I. D. & GILL, T. P. 2002. Obesity: epidemiology and possible prevention. *Best Pract Res Clin Endocrinol Metab,* 16**,** 595-610.

CAWTHORN, W. P. & SETHI, J. K. 2008. TNF-alpha and adipocyte biology. *FEBS Lett,* 582**,** 117-31.

CERF, M. E. 2013. Beta cell dysfunction and insulin resistance. *Front Endocrinol (Lausanne),* 4**,** 37.

CERK, I. K., SALZBURGER, B., BOESZOERMENYI, A., HEIER, C., PILLIP, C., ROMAUCH, M., SCHWEIGER, M., CORNACIU, I., LASS, A., ZIMMERMANN, R., ZECHNER, R. & OBERER, M. 2014. A peptide derived from G0/G1 switch gene 2 acts as noncompetitive inhibitor of adipose triglyceride lipase. *J Biol Chem,* 289**,** 32559-70.

CHAKKERA, H. A., KUDVA, Y. & KAPLAN, B. 2017. Calcineurin Inhibitors: Pharmacologic Mechanisms Impacting Both Insulin Resistance and Insulin Secretion Leading to Glucose Dysregulation and Diabetes Mellitus. *Clin Pharmacol Ther,* 101**,** 114-120.

CHAN, B. 2007. *Functional Studies of the Calcineurin-DSCR1 Complex.* Doctor of Philosophy Harvard University

CHAN, B., GREENAN, G., MCKEON, F. & ELLENBERGER, T. 2005. Identification of a peptide fragment of DSCR1 that competitively inhibits calcineurin activity in vitro and in vivo. *Proc Natl Acad Sci U S A,* 102**,** 13075-80.

CHANG, K. T. & MIN, K. T. 2005. Drosophila melanogaster homolog of Down syndrome critical region 1 is critical for mitochondrial function. *Nat Neurosci,* 8**,** 1577-85.

CHANG, K. T. & MIN, K. T. 2009. Upregulation of three Drosophila homologs of human chromosome 21 genes alters synaptic function: implications for Down syndrome. *Proc Natl Acad Sci U S A,* 106**,** 17117-22.

CHATTOPADHYAY, M., KHEMKA, V. K., CHATTERJEE, G., GANGULY, A., MUKHOPADHYAY, S. & CHAKRABARTI, S. 2015. Enhanced ROS production and oxidative damage in subcutaneous white adipose tissue mitochondria in obese and type 2 diabetes subjects. *Mol Cell Biochem,* 399**,** 95-103.

CHEN, J., MARTINEZ, J., MILNER, T. A., BUCK, J. & LEVIN, L. R. 2013. Neuronal expression of soluble adenylyl cyclase in the mammalian brain. *Brain Res,* 1518**,** 1-8.

CHEN, X., XUN, K., CHEN, L. & WANG, Y. 2009. TNF-alpha, a potent lipid metabolism regulator. *Cell Biochem Funct,* 27**,** 407-16.

CHEN, Y., SAMPAIO, M. S., YANG, J. W., MIN, D. & HUTCHINSON, I. V. 2012. Genetic polymorphisms of the transcription factor NFATc4 and development of new-onset diabetes after transplantation in Hispanic kidney transplant recipients. *Transplantation,* 93**,** 325-30.

CHEUNG, W. Y., LYNCH, T. J., WALLACE, R. W. & TALLANT, E. A. 1981. cAMP renders Ca2+-dependent phosphodiesterase refractory to inhibition by a calmodulin-binding protein (calcineurin). *J Biol Chem,* 256**,** 4439-43.

CHO, K. O., KIM, Y. S., CHO, Y. J. & KIM, S. Y. 2008. Upregulation of DSCR1 (RCAN1 or Adapt78) in the peri-infarct cortex after experimental stroke. *Exp Neurol,* 212**,** 85-92.

CHOO, H. J., KIM, J. H., KWON, O. B., LEE, C. S., MUN, J. Y., HAN, S. S., YOON, Y. S., YOON, G., CHOI, K. M. & KO, Y. G. 2006. Mitochondria are impaired in the adipocytes of type 2 diabetic mice. *Diabetologia,* 49**,** 784-91.

CHOONG, E., QUTEINEH, L., CARDINAUX, J. R., GHOLAM-REZAEE, M., VANDENBERGHE, F., DOBRINAS, M., BONDOLFI, G., ETTER, M., HOLZER, L., MAGISTRETTI, P., VON GUNTEN, A., PREISIG, M., VOLLENWEIDER, P., BECKMANN, J. S., PRALONG, F. P., WAEBER, G., KUTALIK, Z., CONUS, P., BOCHUD, M., EAP, C. B. & TEAM, O. 2013. Influence of CRTC1 polymorphisms on body mass index and fat mass in psychiatric patients and the general adult population. *JAMA Psychiatry,* 70**,** 1011-9.

CHOUCHANI, E. T. & KAJIMURA, S. 2019. Metabolic adaptation and maladaptation in adipose tissue. *Nature Metabolism,* 1**,** 189-200.

CLIFF, W. H. & FRIZZELL, R. A. 1990. Separate Cl- conductances activated by cAMP and Ca2+ in Cl(-)-secreting epithelial cells. *Proc Natl Acad Sci U S A,* 87**,** 4956-60.

CLIPSTONE, N. A. & CRABTREE, G. R. 1992. Identification of calcineurin as a key signalling enzyme in T-lymphocyte activation. *Nature,* 357**,** 695-7.

COELHO, M., OLIVEIRA, T. & FERNANDES, R. 2013. Biochemistry of adipose tissue: an endocrine organ. *Arch Med Sci,* 9**,** 191-200.

COGHLAN, V. M., PERRINO, B. A., HOWARD, M., LANGEBERG, L. K., HICKS, J. B., GALLATIN, W. M. & SCOTT, J. D. 1995. Association of protein kinase A and protein phosphatase 2B with a common anchoring protein. *Science,* 267**,** 108-11.

COLBERG, S. R., SIGAL, R. J., FERNHALL, B., REGENSTEINER, J. G., BLISSMER, B. J., RUBIN, R. R., CHASAN-TABER, L., ALBRIGHT, A. L., BRAUN, B., AMERICAN COLLEGE OF SPORTS, M. & AMERICAN DIABETES, A. 2010. Exercise and type 2 diabetes: the American College of Sports Medicine and the American Diabetes Association: joint position statement. *Diabetes Care,* 33**,** e147-67.

CONSIDINE, R. V., SINHA, M. K., HEIMAN, M. L., KRIAUCIUNAS, A., STEPHENS, T. W., NYCE, M. R., OHANNESIAN, J. P., MARCO, C. C., MCKEE, L. J., BAUER, T. L. & ET AL. 1996. Serum immunoreactive-leptin concentrations in normal-weight and obese humans. *N Engl J Med,* 334**,** 292-5.

CORSA, C. A. S., PEARSON, G. L., RENBERG, A., ASKAR, M. M., VOZHEIKO, T., MACDOUGALD, O. A. & SOLEIMANPOUR, S. A. 2019. The E3 ubiquitin ligase parkin is dispensable for metabolic homeostasis in murine pancreatic beta cells and adipocytes. *J Biol Chem,* 294**,** 7296-7307.

COWHERD, R. M., LYLE, R. E. & MCGEHEE, R. E., JR. 1999. Molecular regulation of adipocyte differentiation. *Semin Cell Dev Biol,* 10**,** 3-10.

CRABTREE, G. R. 1999. Generic signals and specific outcomes: signaling through Ca2+, calcineurin, and NF-AT. *Cell,* 96**,** 611-4.

CRABTREE, G. R. & OLSON, E. N. 2002. NFAT signaling: choreographing the social lives of cells. *Cell,* 109 Suppl**,** S67-79.

CRANE, J. D., PALANIVEL, R., MOTTILLO, E. P., BUJAK, A. L., WANG, H., FORD, R. J., COLLINS, A., BLUMER, R. M., FULLERTON, M. D., YABUT, J. M., KIM, J. J., GHIA, J. E., HAMZA, S. M., MORRISON, K. M., SCHERTZER, J. D., DYCK, J. R., KHAN, W. I. & STEINBERG, G. R. 2015. Inhibiting peripheral serotonin synthesis reduces obesity and metabolic dysfunction by promoting brown adipose tissue thermogenesis. *Nat Med,* 21**,** 166-72.

CRAWFORD, D. R., LEAHY, K. P., ABRAMOVA, N., LAN, L., WANG, Y. & DAVIES, K. J. 1997. Hamster adapt78 mRNA is a Down syndrome critical region homologue that is inducible by oxidative stress. *Arch Biochem Biophys,* 342**,** 6-12.

CRISTILLO, A. D., HEXIMER, S. P., RUSSELL, L. & FORSDYKE, D. R. 1997. Cyclosporin A inhibits early mRNA expression of G0/G1 switch gene 2 (G0S2) in cultured human blood mononuclear cells. *DNA Cell Biol,* 16**,** 1449-58.

CURTIS, J. M., GRIMSRUD, P. A., WRIGHT, W. S., XU, X., FONCEA, R. E., GRAHAM, D. W., BRESTOFF, J. R., WICZER, B. M., ILKAYEVA, O., CIANFLONE, K., MUOIO, D. E., ARRIAGA, E. A. & BERNLOHR, D. A. 2010. Downregulation of adipose glutathione S-transferase A4 leads to increased protein carbonylation, oxidative stress, and mitochondrial dysfunction. *Diabetes,* 59**,** 1132-42.

CZECH, M. P. 2017. Insulin action and resistance in obesity and type 2 diabetes. *Nat Med,* 23**,** 804-814.

DAHLMAN, I. & ARNER, P. 2007. Obesity and polymorphisms in genes regulating human adipose tissue. *Int J Obes (Lond),* 31**,** 1629-41.

DANFORTH, E., JR. 2000. Failure of adipocyte differentiation causes type II diabetes mellitus? *Nat Genet,* 26**,** 13.

DAVAL, M., FOUFELLE, F. & FERRE, P. 2006. Functions of AMP-activated protein kinase in adipose tissue. *J Physiol,* 574**,** 55-62.

DAVIES, K. J. 1999. The broad spectrum of responses to oxidants in proliferating cells: a new paradigm for oxidative stress. *IUBMB Life,* 48**,** 41-7.

DAVIES, K. J., ERMAK, G., ROTHERMEL, B. A., PRITCHARD, M., HEITMAN, J., AHNN, J., HENRIQUE-SILVA, F., CRAWFORD, D., CANAIDER, S., STRIPPOLI, P., CARINCI, P., MIN, K. T., FOX, D. S., CUNNINGHAM, K. W., BASSEL-DUBY, R., OLSON, E. N., ZHANG, Z., WILLIAMS, R. S., GERBER, H. P., PEREZ-RIBA, M., SEO, H., CAO, X., KLEE, C. B., REDONDO, J. M., MALTAIS, L. J., BRUFORD, E. A., POVEY, S., MOLKENTIN, J. D., MCKEON, F. D., DUH,

E. J., CRABTREE, G. R., CYERT, M. S., DE LA LUNA, S. & ESTIVILL, X. 2007. Renaming the DSCR1/Adapt78 gene family as RCAN: regulators of calcineurin. *FASEB J,* 21**,** 3023-8.

DAVIES, K. J., HARRIS, C. D. & ERMAK, G. 2001. The essential role of calcium in induction of the DSCR1 (ADAPT78) gene. *Biofactors,* 15**,** 91-3.

DAYEH, T., VOLKOV, P., SALO, S., HALL, E., NILSSON, E., OLSSON, A. H., KIRKPATRICK, C. L., WOLLHEIM, C. B., ELIASSON, L., RONN, T., BACOS, K. & LING, C. 2014. Genome-wide DNA methylation analysis of human pancreatic islets from type 2 diabetic and non-diabetic donors identifies candidate genes that influence insulin secretion. *PLoS Genet,* 10**,** e1004160.

DE JONG, J. M., LARSSON, O., CANNON, B. & NEDERGAARD, J. 2015. A stringent validation of mouse adipose tissue identity markers. *Am J Physiol Endocrinol Metab,* 308**,** E1085-105.

DE MEYTS, P. 2004. Insulin and its receptor: structure, function and evolution. *Bioessays,* 26**,** 1351-62.

DEAN, L. M., J. 2004. The Genetic Landscape of Diabetes. US: Bethesda (MD) National Center for Biochenology Information

DEMOZAY, D., MAS, J. C., ROCCHI, S. & VAN OBBERGHEN, E. 2008. FALDH reverses the deleterious action of oxidative stress induced by lipid peroxidation product 4-hydroxynonenal on insulin signaling in 3T3-L1 adipocytes. *Diabetes,* 57**,** 1216-26.

DESDOUITS, F., BUXBAUM, J. D., DESDOUITS-MAGNEN, J., NAIRN, A. C. & GREENGARD, P. 1996. Amyloid beta peptide formation in cell-free preparations. Regulation by protein kinase C, calmodulin, and calcineurin. *J Biol Chem,* 271**,** 24670-4.

DESPRES, J. P. 1993. Abdominal obesity as important component of insulin-resistance syndrome. *Nutrition,* 9**,** 452-9.

DEURENBERG, P., WESTSTRATE, J. A. & SEIDELL, J. C. 1991. Body mass index as a measure of body fatness: age- and sex-specific prediction formulas. *Br J Nutr,* 65**,** 105-14.

DIABETES AUSTRALIA 2015, *Managing type 2,* Canberra, viewed on 29 November 2017, <https://www.diabetesaustralia.com.au/managing-type-2>.

DIRAISON, F., DUSSERRE, E., VIDAL, H., SOTHIER, M. & BEYLOT, M. 2002. Increased hepatic lipogenesis but decreased expression of lipogenic gene in adipose tissue in human obesity. *Am J Physiol Endocrinol Metab,* 282**,** E46-51.

DO, O. H., GUNTON, J. E., GAISANO, H. Y. & THORN, P. 2016. Changes in beta cell function occur in prediabetes and early disease in the Lepr (db) mouse model of diabetes. *Diabetologia,* 59**,** 1222-30.

DODSON, M. V., HAUSMAN, G. J., GUAN, L., DU, M., RASMUSSEN, T. P., POULOS, S. P., MIR, P., BERGEN, W. G., FERNYHOUGH, M. E., MCFARLAND, D. C., RHOADS, R. P., SORET, B., REECY, J. M., VELLEMAN, S. G. & JIANG, Z. 2010. Lipid metabolism, adipocyte depot physiology and utilization of meat animals as experimental models for metabolic research. *Int J Biol Sci,* 6**,** 691-9.

DONATH, M. Y. & HALBAN, P. A. 2004. Decreased beta-cell mass in diabetes: significance, mechanisms and therapeutic implications. *Diabetologia,* 47**,** 581-589.

DONATH, M. Y. & SHOELSON, S. E. 2011. Type 2 diabetes as an inflammatory disease. *Nat Rev Immunol,* 11**,** 98-107.

DOTTA, F., FONDELLI, C. & DI MARIO, U. 2005. Type 1 diabetes mellitus as a polygenic multifactorial disease: immunopathogenic mechanisms of beta-cell destruction. *Acta Biomed,* 76 Suppl 3**,** 14-8.

DOYLE, M. E. & EGAN, J. M. 2003. Pharmacological agents that directly modulate insulin secretion. *Pharmacol Rev,* 55**,** 105-31.

DUARTE, J. A., CARVALHO, F., PEARSON, M., HORTON, J. D., BROWNING, J. D., JONES, J. G. & BURGESS, S. C. 2014. A high-fat diet suppresses de novo lipogenesis and desaturation but not elongation and triglyceride synthesis in mice. *J Lipid Res,* 55**,** 2541-53.

DUCHARME, N. A. & BICKEL, P. E. 2008. Lipid droplets in lipogenesis and lipolysis. *Endocrinology,* 149**,** 942-9.

DUNCAN, R. E., AHMADIAN, M., JAWORSKI, K., SARKADI-NAGY, E. & SUL, H. S. 2007. Regulation of lipolysis in adipocytes. *Annu Rev Nutr,* 27**,** 79-101.

EBERLE, D., HEGARTY, B., BOSSARD, P., FERRE, P. & FOUFELLE, F. 2004. SREBP transcription factors: master regulators of lipid homeostasis. *Biochimie,* 86**,** 839-48.

EDFORS, F., DANIELSSON, F., HALLSTROM, B. M., KALL, L., LUNDBERG, E., PONTEN, F., FORSSTROM, B. & UHLEN, M. 2016. Gene-specific correlation of RNA and protein levels in human cells and tissues. *Mol Syst Biol,* 12**,** 883.

EDWARDS, P. A., TABOR, D., KAST, H. R. & VENKATESWARAN, A. 2000. Regulation of gene expression by SREBP and SCAP. *Biochim Biophys Acta,* 1529**,** 103-13.

EISSING, L., SCHERER, T., TODTER, K., KNIPPSCHILD, U., GREVE, J. W., BUURMAN, W. A., PINNSCHMIDT, H. O., RENSEN, S. S., WOLF, A. M., BARTELT, A., HEEREN, J., BUETTNER, C. & SCHEJA, L. 2013. De novo lipogenesis in human fat and liver is linked to ChREBP-beta and metabolic health. *Nat Commun,* 4**,** 1528.

EL-ASSAAD, W., EL-KOUHEN, K., MOHAMMAD, A. H., YANG, J., MORITA, M., GAMACHE, I., MAMER, O., AVIZONIS, D., HERMANCE, N., KERSTEN, S., TREMBLAY, M. L., KELLIHER, M. A. & TEODORO, J. G. 2015. Deletion of the gene encoding G0/G 1 switch protein 2 (G0s2) alleviates high-fat-diet-induced weight gain and insulin resistance, and promotes browning of white adipose tissue in mice. *Diabetologia,* 58**,** 149-57.

ERMAK, G., HARRIS, C. D., BATTOCCHIO, D. & DAVIES, K. J. 2006. RCAN1 (DSCR1 or Adapt78) stimulates expression of GSK-3beta. *FEBS J,* 273**,** 2100-9.

ERMAK, G., HARRIS, C. D. & DAVIES, K. J. 2002. The DSCR1 (Adapt78) isoform 1 protein calcipressin 1 inhibits calcineurin and protects against acute calcium-mediated stress damage, including transient oxidative stress. *FASEB J,* 16**,** 814-24.

ERMAK, G., MORGAN, T. E. & DAVIES, K. J. 2001. Chronic overexpression of the calcineurin inhibitory gene DSCR1 (Adapt78) is associated with Alzheimer's disease. *J Biol Chem,* 276**,** 38787-94.

ERMAK, G., SOJITRA, S., YIN, F., CADENAS, E., CUERVO, A. M. & DAVIES, K. J. 2012. Chronic expression of RCAN1-1L protein induces mitochondrial autophagy and metabolic shift from oxidative phosphorylation to glycolysis in neuronal cells. *J Biol Chem,* 287**,** 14088-98.

FADISTA, J., VIKMAN, P., LAAKSO, E. O., MOLLET, I. G., ESGUERRA, J. L., TANEERA, J., STORM, P., OSMARK, P., LADENVALL, C., PRASAD, R. B., HANSSON, K. B., FINOTELLO, F., UVEBRANT, K., OFORI, J. K., DI CAMILLO, B., KRUS, U., CILIO, C. M., HANSSON, O.,

ELIASSON, L., ROSENGREN, A. H., RENSTROM, E., WOLLHEIM, C. B. & GROOP, L. 2014. Global genomic and transcriptomic analysis of human pancreatic islets reveals novel genes influencing glucose metabolism. *Proc Natl Acad Sci U S A,* 111**,** 13924-9.

FAJAS, L., SCHOONJANS, K., GELMAN, L., KIM, J. B., NAJIB, J., MARTIN, G., FRUCHART, J. C., BRIGGS, M., SPIEGELMAN, B. M. & AUWERX, J. 1999. Regulation of peroxisome proliferator-activated receptor gamma expression by adipocyte differentiation and determination factor 1/sterol regulatory element binding protein 1: implications for adipocyte differentiation and metabolism. *Mol Cell Biol,* 19**,** 5495-503.

FANG, H. & JUDD, R. L. 2018. Adiponectin Regulation and Function. *Compr Physiol,* 8**,** 1031-1063.

FANTUZZI, G. & MAZZONE, T. 2014. *Adipose tissue and adipokines in health and disease,* New York, Humana Press.

FARISS, M. W., CHAN, C. B., PATEL, M., VAN HOUTEN, B. & ORRENIUS, S. 2005. Role of mitochondria in toxic oxidative stress. *Mol Interv,* 5**,** 94-111.

FARMER, S. R. 2006. Transcriptional control of adipocyte formation. *Cell Metab,* 4**,** 263-73.

FEDERICI, M., HRIBAL, M., PEREGO, L., RANALLI, M., CARADONNA, Z., PEREGO, C., USELLINI, L., NANO, R., BONINI, P., BERTUZZI, F., MARLIER, L. N., DAVALLI, A. M., CARANDENTE, O., PONTIROLI, A. E., MELINO, G., MARCHETTI, P., LAURO, R., SESTI, G. & FOLLI, F. 2001. High glucose causes apoptosis in cultured human pancreatic islets of Langerhans: a potential role for regulation of specific Bcl family genes toward an apoptotic cell death program. *Diabetes,* 50**,** 1290-301.

FERNANDEZ-SANCHEZ, A., MADRIGAL-SANTILLAN, E., BAUTISTA, M., ESQUIVEL-SOTO, J., MORALES-GONZALEZ, A., ESQUIVEL-CHIRINO, C., DURANTE-MONTIEL, I., SANCHEZ-RIVERA, G., VALADEZ-VEGA, C. & MORALES-GONZALEZ, J. A. 2011. Inflammation, oxidative stress, and obesity. *Int J Mol Sci,* 12**,** 3117-32.

FESKE, S., OKAMURA, H., HOGAN, P. G. & RAO, A. 2003. Ca2+/calcineurin signalling in cells of the immune system. *Biochem Biophys Res Commun,* 311**,** 1117-32.

FLANAGAN, W. M., CORTHESY, B., BRAM, R. J. & CRABTREE, G. R. 1991. Nuclear association of a T-cell transcription factor blocked by FK-506 and cyclosporin A. *Nature,* 352**,** 803-7.

FLORE, P., BRICOUT, V. A., VAN BIESEN, D., GUINOT, M., LAPORTE, F., PEPIN, J. L., EBERHARD, Y., FAVRE-JUVIN, A., WUYAM, B., VAN DE VLIET, P. & FAURE, P. 2008. Oxidative stress and metabolism at rest and during exercise in persons with Down syndrome. *Eur J Cardiovasc Prev Rehabil,* 15**,** 35-42.

FORETZ, M., GUICHARD, C., FERRE, P. & FOUFELLE, F. 1999. Sterol regulatory element binding protein-1c is a major mediator of insulin action on the hepatic expression of glucokinase and lipogenesis-related genes. *Proc Natl Acad Sci U S A,* 96**,** 12737-42.

FORTE, L. R., BYLUND, D. B. & ZAHLER, W. L. 1983. Forskolin does not activate sperm adenylate cyclase. *Mol Pharmacol,* 24**,** 42-7.

FREDERICH, R. C., HAMANN, A., ANDERSON, S., LOLLMANN, B., LOWELL, B. B. & FLIER, J. S. 1995. Leptin levels reflect body lipid content in mice: evidence for diet-induced resistance to leptin action. *Nat Med,* 1**,** 1311-4.

FREDRIKSON, G., TORNQVIST, H. & BELFRAGE, P. 1986. Hormone-sensitive lipase and monoacylglycerol lipase are both required for complete degradation of adipocyte triacylglycerol. *Biochim Biophys Acta,* 876**,** 288-93.

FREYTAG, S. O., PAIELLI, D. L. & GILBERT, J. D. 1994. Ectopic expression of the CCAAT/enhancer-binding protein alpha promotes the adipogenic program in a variety of mouse fibroblastic cells. *Genes Dev,* 8**,** 1654-63.

FRUH, S. M. 2017. Obesity: Risk factors, complications, and strategies for sustainable long-term weight management. *J Am Assoc Nurse Pract,* 29**,** S3-S14.

FRUHBECK, G., GOMEZ-AMBROSI, J., MURUZABAL, F. J. & BURRELL, M. A. 2001. The adipocyte: a model for integration of endocrine and metabolic signaling in energy metabolism regulation. *Am J Physiol Endocrinol Metab,* 280**,** E827-47.

FUENTES, J. J., GENESCA, L., KINGSBURY, T. J., CUNNINGHAM, K. W., PEREZ-RIBA, M., ESTIVILL, X. & DE LA LUNA, S. 2000. DSCR1, overexpressed in Down syndrome, is an inhibitor of calcineurin-mediated signaling pathways. *Hum Mol Genet,* 9**,** 1681-90.

FUENTES, J. J., PRITCHARD, M. A. & ESTIVILL, X. 1997. Genomic organization, alternative splicing, and expression patterns of the DSCR1 (Down syndrome candidate region 1) gene. *Genomics,* 44**,** 358-61.

FUENTES, J. J., PRITCHARD, M. A., PLANAS, A. M., BOSCH, A., FERRER, I. & ESTIVILL, X. 1995. A new human gene from the Down syndrome critical region encodes a proline-rich protein highly expressed in fetal brain and heart. *Hum Mol Genet,* 4**,** 1935-44.

FUJII, N., NARITA, T., OKITA, N., KOBAYASHI, M., FURUTA, Y., CHUJO, Y., SAKAI, M., YAMADA, A., TAKEDA, K., KONISHI, T., SUDO, Y., SHIMOKAWA, I. & HIGAMI, Y. 2017. Sterol regulatory element-binding protein-1c orchestrates metabolic remodeling of white adipose tissue by caloric restriction. *Aging Cell,* 16**,** 508-517.

FUJIMOTO, T. & PARTON, R. G. 2011. Not just fat: the structure and function of the lipid droplet. *Cold Spring Harb Perspect Biol,* 3.

FURUKAWA, S., FUJITA, T., SHIMABUKURO, M., IWAKI, M., YAMADA, Y., NAKAJIMA, Y., NAKAYAMA, O., MAKISHIMA, M., MATSUDA, M. & SHIMOMURA, I. 2004. Increased oxidative stress in obesity and its impact on metabolic syndrome. *J Clin Invest,* 114**,** 1752-61.

GAIDHU, M. P., ANTHONY, N. M., PATEL, P., HAWKE, T. J. & CEDDIA, R. B. 2010. Dysregulation of lipolysis and lipid metabolism in visceral and subcutaneous adipocytes by high-fat diet: role of ATGL, HSL, and AMPK. *Am J Physiol Cell Physiol,* 298**,** C961-71.

GALLARDO, N., BONZON-KULICHENKO, E., FERNANDEZ-AGULLO, T., MOLTO, E., GOMEZ-ALONSO, S., BLANCO, P., CARRASCOSA, J. M., ROS, M. & ANDRES, A. 2007. Tissue-specific effects of central leptin on the expression of genes involved in lipid metabolism in liver and white adipose tissue. *Endocrinology,* 148**,** 5604-10.

GARVER, T. D., KINCAID, R. L., CONN, R. A. & BILLINGSLEY, M. L. 1999. Reduction of calcineurin activity in brain by antisense oligonucleotides leads to persistent phosphorylation of tau protein at Thr181 and Thr231. *Mol Pharmacol,* 55**,** 632-41.

GENESCA, L., AUBAREDA, A., FUENTES, J. J., ESTIVILL, X., DE LA LUNA, S. & PEREZ-RIBA, M. 2003. Phosphorylation of calcipressin 1 increases its ability to inhibit calcineurin and decreases calcipressin half-life. *Biochem J,* 374**,** 567-75.

GEORGIA, S. & BHUSHAN, A. 2004. Beta cell replication is the primary mechanism for maintaining postnatal beta cell mass. *J Clin Invest,* 114**,** 963-8.

GESTA, S., TSENG, Y. H. & KAHN, C. R. 2007. Developmental origin of fat: tracking obesity to its source. *Cell,* 131**,** 242-56.

GEVA, M., SHLOMAI, G., BERKOVICH, A., MAOR, E., LEIBOWITZ, A., TENENBAUM, A. & GROSSMAN, E. 2019. The association between fasting plasma glucose and glycated hemoglobin in the prediabetes range and future development of hypertension. *Cardiovasc Diabetol,* 18**,** 53.

GHABEN, A. L. & SCHERER, P. E. 2019. Adipogenesis and metabolic health. *Nat Rev Mol Cell Biol*.

GHADGE, A. A., KHAIRE, A. A. & KUVALEKAR, A. A. 2018. Adiponectin: A potential therapeutic target for metabolic syndrome. *Cytokine Growth Factor Rev,* 39**,** 151-158.

GILLESPIE, K. M. 2006. Type 1 diabetes: pathogenesis and prevention. *CMAJ,* 175**,** 165-70.

GILLISON, S. L., BARTLETT, S. T. & CURRY, D. L. 1989. Synthesis-secretion coupling of insulin. Effect of cyclosporin. *Diabetes,* 38**,** 465-70.

GRANNEMAN, J. G., MOORE, H. P., KRISHNAMOORTHY, R. & RATHOD, M. 2009. Perilipin controls lipolysis by regulating the interactions of AB-hydrolase containing 5 (Abhd5) and adipose triglyceride lipase (Atgl). *J Biol Chem,* 284**,** 34538-44.

GREEN, C. B., DOURIS, N., KOJIMA, S., STRAYER, C. A., FOGERTY, J., LOURIM, D., KELLER, S. R. & BESHARSE, J. C. 2007. Loss of Nocturnin, a circadian deadenylase, confers resistance to hepatic steatosis and diet-induced obesity. *Proc Natl Acad Sci U S A,* 104**,** 9888-93.

GREEN, H. & KEHINDE, O. 1974. Sublines of mouse 3T3 cells that accumulate lipid. *Cell,* 1**,** 113-116.

GREEN, H. & KEHINDE, O. 1976. Spontaneous Heritable Changes Leading to Increased Adipose Conversion in 3t3-Cells. *Cell,* 7**,** 105-113.

GREEN, H. & MEUTH, M. 1974. An Established Pre-Adipose Cell Line and Its Differentiation in Culture. *Cell,* 3**,** 127-133.

GREENBERG, A. S., COLEMAN, R. A., KRAEMER, F. B., MCMANAMAN, J. L., OBIN, M. S., PURI, V., YAN, Q. W., MIYOSHI, H. & MASHEK, D. G. 2011. The role of lipid droplets in metabolic disease in rodents and humans. *J Clin Invest,* 121**,** 2102-10.

GREENBERG, A. S., NORDAN, R. P., MCINTOSH, J., CALVO, J. C., SCOW, R. O. & JABLONS, D. 1992. Interleukin 6 reduces lipoprotein lipase activity in adipose tissue of mice in vivo and in 3T3-L1 adipocytes: a possible role for interleukin 6 in cancer cachexia. *Cancer Res,* 52**,** 4113-6.

GREGOR, M. F. & HOTAMISLIGIL, G. S. 2011. Inflammatory mechanisms in obesity. *Annu Rev Immunol,* 29**,** 415-45.

GRES, S., CANTEIRO, S., MERCADER, J. & CARPENE, C. 2013. Oxidation of high doses of serotonin favors lipid accumulation in mouse and human fat cells. *Mol Nutr Food Res,* 57**,** 1089-99.

GROOP, L. 2016. New approaches beyond genetics: towards precision medicine in diabetes. *Diabetologia,* 59**,** 2495-2496.

GRUNDY, S. M., BREWER, H. B., JR., CLEEMAN, J. I., SMITH, S. C., JR., LENFANT, C., AMERICAN HEART, A., NATIONAL HEART, L. & BLOOD, I. 2004. Definition of metabolic

syndrome: Report of the National Heart, Lung, and Blood Institute/American Heart Association conference on scientific issues related to definition. *Circulation,* 109**,** 433-8.

GRUNNET, L. G., AIKIN, R., TONNESEN, M. F., PARASKEVAS, S., BLAABJERG, L., STORLING, J., ROSENBERG, L., BILLESTRUP, N., MAYSINGER, D. & MANDRUP-POULSEN, T. 2009. Proinflammatory cytokines activate the intrinsic apoptotic pathway in beta-cells. *Diabetes,* 58**,** 1807-15.

GURDA, G., BARAS, A., WILLIAMS, J. & CORNISH, T. 2015. Alteration of murine Regulator of Calcineurin 1 (Rcan1) results in dysmorphogenesis of pancreatic islets. 29**,** 765.1.

HAEMMERLE, G., LASS, A., ZIMMERMANN, R., GORKIEWICZ, G., MEYER, C., ROZMAN, J., HELDMAIER, G., MAIER, R., THEUSSL, C., EDER, S., KRATKY, D., WAGNER, E. F., KLINGENSPOR, M., HOEFLER, G. & ZECHNER, R. 2006. Defective lipolysis and altered energy metabolism in mice lacking adipose triglyceride lipase. *Science,* 312**,** 734-7.

HAEMMERLE, G., MOUSTAFA, T., WOELKART, G., BUTTNER, S., SCHMIDT, A., VAN DE WEIJER, T., HESSELINK, M., JAEGER, D., KIENESBERGER, P. C., ZIERLER, K., SCHREIBER, R., EICHMANN, T., KOLB, D., KOTZBECK, P., SCHWEIGER, M., KUMARI, M., EDER, S., SCHOISWOHL, G., WONGSIRIROJ, N., POLLAK, N. M., RADNER, F. P., PREISS-LANDL, K., KOLBE, T., RULICKE, T., PIESKE, B., TRAUNER, M., LASS, A., ZIMMERMANN, R., HOEFLER, G., CINTI, S., KERSHAW, E. E., SCHRAUWEN, P., MADEO, F., MAYER, B. & ZECHNER, R. 2011. ATGL-mediated fat catabolism regulates cardiac mitochondrial function via PPAR-alpha and PGC-1. *Nat Med,* 17**,** 1076-85.

HAHN, W. S., KUZMICIC, J., BURRILL, J. S., DONOGHUE, M. A., FONCEA, R., JENSEN, M. D., LAVANDERO, S., ARRIAGA, E. A. & BERNLOHR, D. A. 2014. Proinflammatory cytokines differentially regulate adipocyte mitochondrial metabolism, oxidative stress, and dynamics. *Am J Physiol Endocrinol Metab,* 306**,** E1033-45.

HALBAN, P. A. 1991. Structural domains and molecular lifestyles of insulin and its precursors in the pancreatic beta cell. *Diabetologia,* 34**,** 767-78.

HANAHAN, D. 1985. Heritable formation of pancreatic beta-cell tumours in transgenic mice expressing recombinant insulin/simian virus 40 oncogenes. *Nature,* 315**,** 115-22.

HANCOCK, A. M., WITONSKY, D. B., GORDON, A. S., ESHEL, G., PRITCHARD, J. K., COOP, G. & DI RIENZO, A. 2008. Adaptations to climate in candidate genes for common metabolic disorders. *PLoS Genet,* 4**,** e32.

HANSEN, J. S., DE MARE, S., JONES, H. A., GORANSSON, O. & LINDKVIST-PETERSSON, K. 2017. Visualization of lipid directed dynamics of perilipin 1 in human primary adipocytes. *Sci Rep,* 7**,** 15011.

HARADA, K., SHEN, W. J., PATEL, S., NATU, V., WANG, J., OSUGA, J., ISHIBASHI, S. & KRAEMER, F. B. 2003. Resistance to high-fat diet-induced obesity and altered expression of adipose-specific genes in HSL-deficient mice. *Am J Physiol Endocrinol Metab,* 285**,** E1182-95.

HARMS, M. & SEALE, P. 2013. Brown and beige fat: development, function and therapeutic potential. *Nat Med,* 19**,** 1252-63.

HARRIS, C. D., ERMAK, G. & DAVIES, K. J. 2005. Multiple roles of the DSCR1 (Adapt78 or RCAN1) gene and its protein product calcipressin 1 (or RCAN1) in disease. *Cell Mol Life Sci,* 62**,** 2477-86.

HARRIS, C. D., ERMAK, G. & DAVIES, K. J. 2007. RCAN1-1L is overexpressed in neurons of Alzheimer's disease patients. *FEBS J,* 274**,** 1715-24.

HASHIMOTO, N. & TANAKA, T. 2017. Role of miRNAs in the pathogenesis and susceptibility of diabetes mellitus. *J Hum Genet,* 62**,** 141-150.

HE, L. M., SARTORI, D. J., TETA, M., OPARE-ADDO, L. M., RANKIN, M. M., LONG, S. Y., DIEHL, J. A. & KUSHNER, J. A. 2009. Cyclin D2 protein stability is regulated in pancreatic beta-cells. *Mol Endocrinol,* 23**,** 1865-75.

HECKMANN, B. L., ZHANG, X., XIE, X. & LIU, J. 2013. The G0/G1 switch gene 2 (G0S2): regulating metabolism and beyond. *Biochim Biophys Acta,* 1831**,** 276-81.

HECKMANN, B. L., ZHANG, X., XIE, X., SAARINEN, A., LU, X., YANG, X. & LIU, J. 2014. Defective adipose lipolysis and altered global energy metabolism in mice with adipose overexpression of the lipolytic inhibitor G0/G1 switch gene 2 (G0S2). *J Biol Chem,* 289**,** 1905-16.

HECTOR, J., SCHWARZLOH, B., GOEHRING, J., STRATE, T. G., HESS, U. F., DEURETZBACHER, G., HANSEN-ALGENSTAEDT, N., BEIL, F. U. & ALGENSTAEDT, P. 2007. TNF-alpha alters visfatin and adiponectin levels in human fat. *Horm Metab Res,* 39**,** 250-5.

HEINONEN, S., BUZKOVA, J., MUNIANDY, M., KAKSONEN, R., OLLIKAINEN, M., ISMAIL, K., HAKKARAINEN, A., LUNDBOM, J., LUNDBOM, N., VUOLTEENAHO, K., MOILANEN, E., KAPRIO, J., RISSANEN, A., SUOMALAINEN, A. & PIETILAINEN, K. H. 2015. Impaired Mitochondrial Biogenesis in Adipose Tissue in Acquired Obesity. *Diabetes,* 64**,** 3135-45.

HEISEL, O., HEISEL, R., BALSHAW, R. & KEOWN, P. 2004. New onset diabetes mellitus in patients receiving calcineurin inhibitors: a systematic review and meta-analysis. *Am J Transplant,* 4**,** 583-95.

HEIT, J. J. 2007. Calcineurin/NFAT signaling in the beta-cell: From diabetes to new therapeutics. *Bioessays,* 29**,** 1011-21.

HEIT, J. J., APELQVIST, A. A., GU, X., WINSLOW, M. M., NEILSON, J. R., CRABTREE, G. R. & KIM, S. K. 2006a. Calcineurin/NFAT signalling regulates pancreatic beta-cell growth and function. *Nature,* 443**,** 345-9.

HEIT, J. J., KARNIK, S. K. & KIM, S. K. 2006b. Intrinsic regulators of pancreatic beta-cell proliferation. *Annu Rev Cell Dev Biol,* 22**,** 311-38.

HELGUERA, P., SEIGLIE, J., RODRIGUEZ, J., HANNA, M., HELGUERA, G. & BUSCIGLIO, J. 2013. Adaptive downregulation of mitochondrial function in down syndrome. *Cell Metab,* 17**,** 132-40.

HERMAN, M. A. & KAHN, B. B. 2006. Glucose transport and sensing in the maintenance of glucose homeostasis and metabolic harmony. *J Clin Invest,* 116**,** 1767-75.

HERMAN, M. A., PERONI, O. D., VILLORIA, J., SCHON, M. R., ABUMRAD, N. A., BLUHER, M., KLEIN, S. & KAHN, B. B. 2012. A novel ChREBP isoform in adipose tissue regulates systemic glucose metabolism. *Nature,* 484**,** 333-8.

HESS, K. C., JONES, B. H., MARQUEZ, B., CHEN, Y., ORD, T. S., KAMENETSKY, M., MIYAMOTO, C., ZIPPIN, J. H., KOPF, G. S., SUAREZ, S. S., LEVIN, L. R., WILLIAMS, C. J., BUCK, J. & MOSS, S. B. 2005. The "soluble" adenylyl cyclase in sperm mediates multiple signaling events required for fertilization. *Dev Cell,* 9**,** 249-59.

HESSEL, S., EICHINGER, A., ISKEN, A., AMENGUAL, J., HUNZELMANN, S., HOELLER, U., ELSTE, V., HUNZIKER, W., GORALCZYK, R., OBERHAUSER, V., VON LINTIG, J. & WYSS, A. 2007. CMO1 deficiency abolishes vitamin A production from beta-carotene and alters lipid metabolism in mice. *J Biol Chem,* 282**,** 33553-61.

HILIOTI, Z. & CUNNINGHAM, K. W. 2003. The RCN family of calcineurin regulators. *Biochem Biophys Res Commun,* 311**,** 1089-93.

HILIOTI, Z., GALLAGHER, D. A., LOW-NAM, S. T., RAMASWAMY, P., GAJER, P., KINGSBURY, T. J., BIRCHWOOD, C. J., LEVCHENKO, A. & CUNNINGHAM, K. W. 2004. GSK-3 kinases enhance calcineurin signaling by phosphorylation of RCNs. *Genes Dev,* 18**,** 35-47.

HILL, D. L., PARKS, E. P., ZEMEL, B. S., SHULTS, J., STALLINGS, V. A. & STETTLER, N. 2013. Resting energy expenditure and adiposity accretion among children with Down syndrome: a 3-year prospective study. *Eur J Clin Nutr,* 67**,** 1087-91.

HIRAKAWA, Y., NARY, L. J. & MEDH, R. D. 2009. Glucocorticoid evoked upregulation of RCAN1-1 in human leukemic CEM cells susceptible to apoptosis. *J Mol Signal,* 4**,** 6.

HO, D., UMEMURA, M., BRAVO, C. & IWATSUBO, K. 2012. Recent Advance in Isoform-Specific Regulation of Adenylyl Cyclase. *Current Enzyme Inhibition,* 8**,** 170-182.

HO, I. C., KIM, J. H., ROONEY, J. W., SPIEGELMAN, B. M. & GLIMCHER, L. H. 1998. A potential role for the nuclear factor of activated T cells family of transcriptional regulatory proteins in adipogenesis. *Proc Natl Acad Sci U S A,* 95**,** 15537-41.

HOEFFER, C. A., DEY, A., SACHAN, N., WONG, H., PATTERSON, R. J., SHELTON, J. M., RICHARDSON, J. A., KLANN, E. & ROTHERMEL, B. A. 2007. The Down syndrome critical region protein RCAN1 regulates long-term potentiation and memory via inhibition of phosphatase signaling. *J Neurosci,* 27**,** 13161-72.

HOFFSTEDT, J., FORSTER, D. & LOFGREN, P. 2007. Impaired subcutaneous adipocyte lipogenesis is associated with systemic insulin resistance and increased apolipoprotein B/AI ratio in men and women. *J Intern Med,* 262**,** 131-9.

HOGAN, P. G., CHEN, L., NARDONE, J. & RAO, A. 2003. Transcriptional regulation by calcium, calcineurin, and NFAT. *Genes Dev,* 17**,** 2205-32.

HOLMAN, R. R. 1998. Assessing the potential for alpha-glucosidase inhibitors in prediabetic states. *Diabetes Res Clin Pract,* 40 Suppl**,** S21-5.

HOLOWACHUK, E. W. 2007. Nuclear factor of activated T cell (NFAT) transcription proteins regulate genes involved in adipocyte metabolism and lipolysis. *Biochem Biophys Res Commun,* 361**,** 427-32.

HORTON, J. D., GOLDSTEIN, J. L. & BROWN, M. S. 2002. SREBPs: activators of the complete program of cholesterol and fatty acid synthesis in the liver. *J Clin Invest,* 109**,** 1125-31.

HORTON, J. D., SHIMOMURA, I., IKEMOTO, S., BASHMAKOV, Y. & HAMMER, R. E. 2003. Overexpression of sterol regulatory element-binding protein-1a in mouse adipose tissue produces adipocyte hypertrophy, increased fatty acid secretion, and fatty liver. *J Biol Chem,* 278**,** 36652-60.

HOSHINO, A. & MATOBA, S. 2018. Observation of Parkin-Mediated Mitophagy in Pancreatic beta-Cells. *Methods Mol Biol,* 1759**,** 41-46.

HOTAMISLIGIL, G. S., ARNER, P., CARO, J. F., ATKINSON, R. L. & SPIEGELMAN, B. M. 1995. Increased adipose tissue expression of tumor necrosis factor-alpha in human obesity and insulin resistance. *J Clin Invest,* 95**,** 2409-15.

HOU, J. C., MIN, L. & PESSIN, J. E. 2009. Insulin granule biogenesis, trafficking and exocytosis. *Vitam Horm,* 80**,** 473-506.

HOY, A. J., BRUCE, C. R., TURPIN, S. M., MORRIS, A. J., FEBBRAIO, M. A. & WATT, M. J. 2011. Adipose triglyceride lipase-null mice are resistant to high-fat diet-induced insulin resistance despite reduced energy expenditure and ectopic lipid accumulation. *Endocrinology,* 152**,** 48-58.

HURTADO DEL POZO, C., VESPERINAS-GARCIA, G., RUBIO, M. A., CORRIPIO-SANCHEZ, R., TORRES-GARCIA, A. J., OBREGON, M. J. & CALVO, R. M. 2011. ChREBP expression in the liver, adipose tissue and differentiated preadipocytes in human obesity. *Biochim Biophys Acta,* 1811**,** 1194-200.

HUSAIN, S. & THROWER, E. 2009. Molecular and cellular regulation of pancreatic acinar cell function. *Curr Opin Gastroenterol,* 25**,** 466-71.

HWANG, C. S., LOFTUS, T. M., MANDRUP, S. & LANE, M. D. 1997. Adipocyte differentiation and leptin expression. *Annu Rev Cell Dev Biol,* 13**,** 231-59.

IIZUKA, K. 2013. Recent progress on the role of ChREBP in glucose and lipid metabolism. *Endocr J,* 60**,** 543-55.

IIZUKA, K., BRUICK, R. K., LIANG, G., HORTON, J. D. & UYEDA, K. 2004. Deficiency of carbohydrate response element-binding protein (ChREBP) reduces lipogenesis as well as glycolysis. *Proc Natl Acad Sci U S A,* 101**,** 7281-6.

IKUTA, T., KUROYANAGI, Y., ODO, N. & LIU, S. 2013. A common signaling pathway is activated in erythroid cells expressing high levels of fetal hemoglobin: a potential role for cAMP-elevating agents in beta-globin disorders. *J Blood Med,* 4**,** 149-59.

IM, S. S., HAMMOND, L. E., YOUSEF, L., NUGAS-SELBY, C., SHIN, D. J., SEO, Y. K., FONG, L. G., YOUNG, S. G. & OSBORNE, T. F. 2009. Sterol regulatory element binding protein 1a regulates hepatic fatty acid partitioning by activating acetyl coenzyme A carboxylase 2. *Mol Cell Biol,* 29**,** 4864-72.

IMAI, T., TAKAKUWA, R., MARCHAND, S., DENTZ, E., BORNERT, J. M., MESSADDEQ, N., WENDLING, O., MARK, M., DESVERGNE, B., WAHLI, W., CHAMBON, P. & METZGER, D. 2004. Peroxisome proliferator-activated receptor gamma is required in mature white and brown adipocytes for their survival in the mouse. *Proc Natl Acad Sci U S A,* 101**,** 4543-7.

IRMLER, M., THOME, M., HAHNE, M., SCHNEIDER, P., HOFMANN, K., STEINER, V., BODMER, J. L., SCHROTER, M., BURNS, K., MATTMANN, C., RIMOLDI, D., FRENCH, L. E. & TSCHOPP, J. 1997. Inhibition of death receptor signals by cellular FLIP. *Nature,* 388**,** 190-5.

JAKOBSEN, E., LANGE, S. C., ANDERSEN, J. V., DESLER, C., KIHL, H. F., HOHNHOLT, M. C., STRIDH, M. H., RASMUSSEN, L. J., WAAGEPETERSEN, H. S. & BAK, L. K. 2018. The inhibitors of soluble adenylate cyclase 2-OHE, KH7, and bithionol compromise mitochondrial ATP production by distinct mechanisms. *Biochem Pharmacol,* 155**,** 92-101.

JANG, C., LIM, J. H., PARK, C. W. & CHO, Y. J. 2011. Regulator of Calcineurin 1 Isoform 4 (RCAN1.4) Is Overexpressed in the Glomeruli of Diabetic Mice. *Korean J Physiol Pharmacol,* 15**,** 299-305.

JAWORSKI, K., SARKADI-NAGY, E., DUNCAN, R. E., AHMADIAN, M. & SUL, H. S. 2007. Regulation of triglyceride metabolism. IV. Hormonal regulation of lipolysis in adipose tissue. *Am J Physiol Gastrointest Liver Physiol,* 293**,** G1-4.

JENSEN, M. D. 1997. Lipolysis: contribution from regional fat. *Annu Rev Nutr,* 17**,** 127-39.

JIANG, L., WANG, Q., YU, Y., ZHAO, F., HUANG, P., ZENG, R., QI, R. Z., LI, W. & LIU, Y. 2009. Leptin contributes to the adaptive responses of mice to high-fat diet intake through suppressing the lipogenic pathway. *PLoS One,* 4**,** e6884.

JIANG, Y., OWEI, I., WAN, J., EBENIBO, S. & DAGOGO-JACK, S. 2016. Adiponectin levels predict prediabetes risk: the Pathobiology of Prediabetes in A Biracial Cohort (POP-ABC) study. *BMJ Open Diabetes Res Care,* 4**,** e000194.

JIN, H., WANG, C., JIN, G., RUAN, H., GU, D., WEI, L., WANG, H., WANG, N., ARUNACHALAM, E., ZHANG, Y., DENG, X., YANG, C., XIONG, Y., FENG, H., YAO, M., FANG, J., GU, J., CONG, W. & QIN, W. 2017. Regulator of Calcineurin 1 Gene Isoform 4, Down-regulated in Hepatocellular Carcinoma, Prevents Proliferation, Migration, and Invasive Activity of Cancer Cells and Metastasis of Orthotopic Tumors by Inhibiting Nuclear Translocation of NFAT1. *Gastroenterology,* 153**,** 799-811 e33.

JOIS, T., CHEN, W., HOWARD, V., HARVEY, R., YOUNGS, K., THALMANN, C., SAHA, P., CHAN, L., COWLEY, M. A. & SLEEMAN, M. W. 2017. Deletion of hepatic carbohydrate response element binding protein (ChREBP) impairs glucose homeostasis and hepatic insulin sensitivity in mice. *Mol Metab,* 6**,** 1381-1394.

JOIS, T., HOWARD, V., YOUNGS, K., COWLEY, M. A. & SLEEMAN, M. W. 2016. Dietary Macronutrient Composition Directs ChREBP Isoform Expression and Glucose Metabolism in Mice. *PLoS One,* 11**,** e0168797.

JONAS, J. C., BENSELLAM, M., DUPREZ, J., ELOUIL, H., GUIOT, Y. & PASCAL, S. M. 2009. Glucose regulation of islet stress responses and beta-cell failure in type 2 diabetes. *Diabetes Obes Metab,* 11 Suppl 4**,** 65-81.

JONES, J. R., BARRICK, C., KIM, K. A., LINDNER, J., BLONDEAU, B., FUJIMOTO, Y., SHIOTA, M., KESTERSON, R. A., KAHN, B. B. & MAGNUSON, M. A. 2005. Deletion of PPARgamma in adipose tissues of mice protects against high fat diet-induced obesity and insulin resistance. *Proc Natl Acad Sci U S A,* 102**,** 6207-12.

JOUVET, N. & ESTALL, J. L. 2017. The pancreas: Bandmaster of glucose homeostasis. *Exp Cell Res*.

JUNG, M. S., PARK, J. H., RYU, Y. S., CHOI, S. H., YOON, S. H., KWEN, M. Y., OH, J. Y., SONG, W. J. & CHUNG, S. H. 2011. Regulation of RCAN1 protein activity by Dyrk1A protein-mediated phosphorylation. *J Biol Chem,* 286**,** 40401-12.

KADO, S., NAGASE, T. & NAGATA, N. 1999. Circulating levels of interleukin-6, its soluble receptor and interleukin-6/interleukin-6 receptor complexes in patients with type 2 diabetes mellitus. *Acta Diabetol,* 36**,** 67-72.

KAHN, S. E. & HALBAN, P. A. 1997. Release of incompletely processed proinsulin is the cause of the disproportionate proinsulinemia of NIDDM. *Diabetes,* 46**,** 1725-32.

KAHN, S. E., PRIGEON, R. L., MCCULLOCH, D. K., BOYKO, E. J., BERGMAN, R. N., SCHWARTZ, M. W., NEIFING, J. L., WARD, W. K., BEARD, J. C., PALMER, J. P. & ET AL. 1993.

Quantification of the relationship between insulin sensitivity and beta-cell function in human subjects. Evidence for a hyperbolic function. *Diabetes,* 42**,** 1663-72.

KAISER, N., CORCOS, A. P., SAREL, I. & CERASI, E. 1991. Monolayer culture of adult rat pancreatic islets on extracellular matrix: modulation of B-cell function by chronic exposure to high glucose. *Endocrinology,* 129**,** 2067-76.

KAKIUCHI, S. 1983. Calmodulin-binding proteins in brain. *Neurochem Int,* 5**,** 159-69.

KAKUMA, T., LEE, Y., HIGA, M., WANG, Z., PAN, W., SHIMOMURA, I. & UNGER, R. H. 2000. Leptin, troglitazone, and the expression of sterol regulatory element binding proteins in liver and pancreatic islets. *Proc Natl Acad Sci U S A,* 97**,** 8536-41.

KAMENETSKY, M., MIDDELHAUFE, S., BANK, E. M., LEVIN, L. R., BUCK, J. & STEEGBORN, C. 2006. Molecular details of cAMP generation in mammalian cells: a tale of two systems. *J Mol Biol,* 362**,** 623-39.

KANETO, H., SHARMA, A., SUZUMA, K., LAYBUTT, D. R., XU, G., BONNER-WEIR, S. & WEIR, G. C. 2002. Induction of c-Myc expression suppresses insulin gene transcription by inhibiting NeuroD/BETA2-mediated transcriptional activation. *J Biol Chem,* 277**,** 12998-3006.

KANETY, H., FEINSTEIN, R., PAPA, M. Z., HEMI, R. & KARASIK, A. 1995. Tumor necrosis factor alpha-induced phosphorylation of insulin receptor substrate-1 (IRS-1). Possible mechanism for suppression of insulin-stimulated tyrosine phosphorylation of IRS-1. *J Biol Chem,* 270**,** 23780-4.

KASHISHIAN, A., HOWARD, M., LOH, C., GALLATIN, W. M., HOEKSTRA, M. F. & LAI, Y. 1998. AKAP79 inhibits calcineurin through a site distinct from the immunophilin-binding region. *J Biol Chem,* 273**,** 27412-9.

KASHYAP, S., BELFORT, R., GASTALDELLI, A., PRATIPANAWATR, T., BERRIA, R., PRATIPANAWATR, W., BAJAJ, M., MANDARINO, L., DEFRONZO, R. & CUSI, K. 2003. A sustained increase in plasma free fatty acids impairs insulin secretion in nondiabetic subjects genetically predisposed to develop type 2 diabetes. *Diabetes,* 52**,** 2461-74.

KEANEY, J. F., JR., LARSON, M. G., VASAN, R. S., WILSON, P. W., LIPINSKA, I., COREY, D., MASSARO, J. M., SUTHERLAND, P., VITA, J. A., BENJAMIN, E. J. & FRAMINGHAM, S. 2003. Obesity and systemic oxidative stress: clinical correlates of oxidative stress in the Framingham Study. *Arterioscler Thromb Vasc Biol,* 23**,** 434-9.

KEATING, D. J., DUBACH, D., ZANIN, M. P., YU, Y., MARTIN, K., ZHAO, Y. F., CHEN, C., PORTA, S., ARBONES, M. L., MITTAZ, L. & PRITCHARD, M. A. 2008. DSCR1/RCAN1 regulates vesicle exocytosis and fusion pore kinetics: implications for Down syndrome and Alzheimer's disease. *Hum Mol Genet,* 17**,** 1020-30.

KELLER, M. P., CHOI, Y., WANG, P., DAVIS, D. B., RABAGLIA, M. E., OLER, A. T., STAPLETON, D. S., ARGMANN, C., SCHUELER, K. L., EDWARDS, S., STEINBERG, H. A., CHAIBUB NETO, E., KLEINHANZ, R., TURNER, S., HELLERSTEIN, M. K., SCHADT, E. E., YANDELL, B. S., KENDZIORSKI, C. & ATTIE, A. D. 2008. A gene expression network model of type 2 diabetes links cell cycle regulation in islets with diabetes susceptibility. *Genome Res,* 18**,** 706-16.

KERSTEN, S. 2001. Mechanisms of nutritional and hormonal regulation of lipogenesis. *EMBO Rep,* 2**,** 282-6.

KHAN, S. A., SATHYANARAYAN, A., MASHEK, M. T., ONG, K. T., WOLLASTON-HAYDEN, E. E. & MASHEK, D. G. 2015. ATGL-catalyzed lipolysis regulates SIRT1 to control PGC-1alpha/PPAR-alpha signaling. *Diabetes,* 64**,** 418-26.

KHO, D., MACDONALD, C., JOHNSON, R., UNSWORTH, C. P., O'CARROLL, S. J., DU MEZ, E., ANGEL, C. E. & GRAHAM, E. S. 2015. Application of xCELLigence RTCA Biosensor Technology for Revealing the Profile and Window of Drug Responsiveness in Real Time. *Biosensors (Basel),* 5**,** 199-222.

KIKUCHI, R., TSUJI, T., WATANABE, O., YAMAGUCHI, K., FURUKAWA, K., NAKAMURA, H. & AOSHIBA, K. 2017. Hypercapnia Accelerates Adipogenesis: A Novel Role of High CO2 in Exacerbating Obesity. *Am J Respir Cell Mol Biol,* 57**,** 570-580.

KIM, H. B., KIM, W. H., HAN, K. L., PARK, J. H., LEE, J., YEO, J. & JUNG, M. H. 2010. cAMP-response element binding protein (CREB) positively regulates mouse adiponectin gene expression in 3T3-L1 adipocytes. *Biochem Biophys Res Commun,* 391**,** 634-9.

KIM, H. B., KONG, M., KIM, T. M., SUH, Y. H., KIM, W. H., LIM, J. H., SONG, J. H. & JUNG, M. H. 2006a. NFATc4 and ATF3 negatively regulate adiponectin gene expression in 3T3-L1 adipocytes. *Diabetes,* 55**,** 1342-52.

KIM, I., KANG, E. S., YIM, Y. S., KO, S. J., JEONG, S. H., RIM, J. H., KIM, Y. S., AHN, C. W., CHA, B. S., LEE, H. C. & KIM, C. H. 2011. A low-risk ZnT-8 allele (W325) for post-transplantation diabetes mellitus is protective against cyclosporin A-induced impairment of insulin secretion. *Pharmacogenomics J,* 11**,** 191-8.

KIM, I. H. & NAM, T. J. 2017. Enzyme-treated Ecklonia cava extract inhibits adipogenesis through the downregulation of C/EBPalpha in 3T3-L1 adipocytes. *Int J Mol Med,* 39**,** 636-644.

KIM, J. B., SARRAF, P., WRIGHT, M., YAO, K. M., MUELLER, E., SOLANES, G., LOWELL, B. B. & SPIEGELMAN, B. M. 1998. Nutritional and insulin regulation of fatty acid synthetase and leptin gene expression through ADD1/SREBP1. *J Clin Invest,* 101**,** 1-9.

KIM, J. B. & SPIEGELMAN, B. M. 1996. ADD1/SREBP1 promotes adipocyte differentiation and gene expression linked to fatty acid metabolism. *Genes Dev,* 10**,** 1096-107.

KIM, K., OH, C. M., OHARA-IMAIZUMI, M., PARK, S., NAMKUNG, J., YADAV, V. K., TAMARINA, N. A., ROE, M. W., PHILIPSON, L. H., KARSENTY, G., NAGAMATSU, S., GERMAN, M. S. & KIM, H. 2015. Functional role of serotonin in insulin secretion in a diet-induced insulin-resistant state. *Endocrinology,* 156**,** 444-52.

KIM, S. J., TANG, T., ABBOTT, M., VISCARRA, J. A., WANG, Y. & SUL, H. S. 2016. AMPK Phosphorylates Desnutrin/ATGL and Hormone-Sensitive Lipase To Regulate Lipolysis and Fatty Acid Oxidation within Adipose Tissue. *Mol Cell Biol,* 36**,** 1961-76.

KIM, S. K. & HEBROK, M. 2001. Intercellular signals regulating pancreas development and function. *Genes Dev,* 15**,** 111-27.

KIM, S. S., JANG, S. A. & SEO, S. R. 2013. CREB-mediated Bcl-2 expression contributes to RCAN1 protection from hydrogen peroxide-induced neuronal death. *J Cell Biochem,* 114**,** 1115-23.

KIM, S. S., OH, Y., CHUNG, K. C. & SEO, S. R. 2012. Protein kinase A phosphorylates Down syndrome critical region 1 (RCAN1). *Biochem Biophys Res Commun,* 418**,** 657-61.

KIM, S. S. & SEO, S. R. 2011. The regulator of calcineurin 1 (RCAN1/DSCR1) activates the cAMP response element-binding protein (CREB) pathway. *J Biol Chem,* 286**,** 37841-8.

KIM, Y. S., CHO, K. O., LEE, H. J., KIM, S. Y., SATO, Y. & CHO, Y. J. 2006b. Down syndrome candidate region 1 increases the stability of the IkappaBalpha protein: implications for its anti-inflammatory effects. *J Biol Chem,* 281**,** 39051-61.

KINGSBURY, T. J. & CUNNINGHAM, K. W. 2000. A conserved family of calcineurin regulators. *Genes Dev,* 14**,** 1595-604.

KINOSHITA, M., ONO, K., HORIE, T., NAGAO, K., NISHI, H., KUWABARA, Y., TAKANABE-MORI, R., HASEGAWA, K., KITA, T. & KIMURA, T. 2010. Regulation of adipocyte differentiation by activation of serotonin (5-HT) receptors 5-HT2AR and 5-HT2CR and involvement of microRNA-448-mediated repression of KLF5. *Mol Endocrinol,* 24**,** 1978-87.

KITAMURA, T., KITAMURA, Y., KURODA, S., HINO, Y., ANDO, M., KOTANI, K., KONISHI, H., MATSUZAKI, H., KIKKAWA, U., OGAWA, W. & KASUGA, M. 1999. Insulin-induced phosphorylation and activation of cyclic nucleotide phosphodiesterase 3B by the serine-threonine kinase Akt. *Mol Cell Biol,* 19**,** 6286-96.

KLAUCK, T. M., FAUX, M. C., LABUDDA, K., LANGEBERG, L. K., JAKEN, S. & SCOTT, J. D. 1996. Coordination of three signaling enzymes by AKAP79, a mammalian scaffold protein. *Science,* 271**,** 1589-92.

KLEE, C. B., DRAETTA, G. F. & HUBBARD, M. J. 1988. Calcineurin. *Adv Enzymol Relat Areas Mol Biol,* 61**,** 149-200.

KLIONSKY, D. J., ABDELMOHSEN, K., ABE, A., ABEDIN, M. J., ABELIOVICH, H., ACEVEDO AROZENA, A., ADACHI, H., ADAMS, C. M., ADAMS, P. D., ADELI, K., ADHIHETTY, P. J., ADLER, S. G., AGAM, G., AGARWAL, R., AGHI, M. K., AGNELLO, M., AGOSTINIS, P., AGUILAR, P. V., AGUIRRE-GHISO, J., AIROLDI, E. M., AIT-SI-ALI, S., AKEMATSU, T., AKPORIAYE, E. T., AL-RUBEAI, M., ALBAICETA, G. M., ALBANESE, C., ALBANI, D., ALBERT, M. L., ALDUDO, J., ALGUL, H., ALIREZAEI, M., ALLOZA, I., ALMASAN, A., ALMONTE-BECERIL, M., ALNEMRI, E. S., ALONSO, C., ALTAN-BONNET, N., ALTIERI, D. C., ALVAREZ, S., ALVAREZ-ERVITI, L., ALVES, S., AMADORO, G., AMANO, A., AMANTINI, C., AMBROSIO, S., AMELIO, I., AMER, A. O., AMESSOU, M., AMON, A., AN, Z., ANANIA, F. A., ANDERSEN, S. U., ANDLEY, U. P., ANDREADI, C. K., ANDRIEU-ABADIE, N., ANEL, A., ANN, D. K., ANOOPKUMAR-DUKIE, S., ANTONIOLI, M., AOKI, H., APOSTOLOVA, N., AQUILA, S., AQUILANO, K., ARAKI, K., ARAMA, E., ARANDA, A., ARAYA, J., ARCARO, A., ARIAS, E., ARIMOTO, H., ARIOSA, A. R., ARMSTRONG, J. L., ARNOULD, T., ARSOV, I., ASANUMA, K., ASKANAS, V., ASSELIN, E., ATARASHI, R., ATHERTON, S. S., ATKIN, J. D., ATTARDI, L. D., AUBERGER, P., AUBURGER, G., AURELIAN, L., AUTELLI, R., AVAGLIANO, L., AVANTAGGIATI, M. L., AVRAHAMI, L., AWALE, S., AZAD, N., BACHETTI, T., BACKER, J. M., BAE, D. H., BAE, J. S., BAE, O. N., BAE, S. H., BAEHRECKE, E. H., BAEK, S. H., BAGHDIGUIAN, S., BAGNIEWSKA-ZADWORNA, A., et al. 2016. Guidelines for the use and interpretation of assays for monitoring autophagy (3rd edition). *Autophagy,* 12**,** 1-222.

KOCH, C. E., LOWE, C., PRETZ, D., STEGER, J., WILLIAMS, L. M. & TUPS, A. 2014. High-fat diet induces leptin resistance in leptin-deficient mice. *J Neuroendocrinol,* 26**,** 58-67.

KORENBERG, J. R., CHEN, X. N., SCHIPPER, R., SUN, Z., GONSKY, R., GERWEHR, S., CARPENTER, N., DAUMER, C., DIGNAN, P., DISTECHE, C. & ET AL. 1994. Down syndrome phenotypes: the consequences of chromosomal imbalance. *Proc Natl Acad Sci U S A,* 91**,** 4997-5001.

KOSTER, J. C., PERMUTT, M. A. & NICHOLS, C. G. 2005. Diabetes and insulin secretion: the ATP-sensitive K+ channel (K ATP) connection. *Diabetes,* 54**,** 3065-72.

KOUSSOUNADIS, A., LANGDON, S. P., UM, I. H., HARRISON, D. J. & SMITH, V. A. 2015. Relationship between differentially expressed mRNA and mRNA-protein correlations in a xenograft model system. *Sci Rep,* 5**,** 10775.

KRAUS, N. A., EHEBAUER, F., ZAPP, B., RUDOLPHI, B., KRAUS, B. J. & KRAUS, D. 2016. Quantitative assessment of adipocyte differentiation in cell culture. *Adipocyte,* 5**,** 351-358.

KREIER, F., FLIERS, E., VOSHOL, P. J., VAN EDEN, C. G., HAVEKES, L. M., KALSBEEK, A., VAN HEIJNINGEN, C. L., SLUITER, A. A., METTENLEITER, T. C., ROMIJN, J. A., SAUERWEIN, H. P. & BUIJS, R. M. 2002. Selective parasympathetic innervation of subcutaneous and intra-abdominal fat--functional implications. *J Clin Invest,* 110**,** 1243-50.

KRINTEL, C., OSMARK, P., LARSEN, M. R., RESJO, S., LOGAN, D. T. & HOLM, C. 2008. Ser649 and Ser650 are the major determinants of protein kinase A-mediated activation of human hormone-sensitive lipase against lipid substrates. *PLoS One,* 3**,** e3756.

KULMINSKAYA, N. & OBERER, M. 2019. Protein-protein interactions regulate the activity of Adipose Triglyceride Lipase in intracellular lipolysis. *Biochimie*.

KUMAR, V., ABBAS, A. K. & ASTER, J. C. 2014. *Robbins and Cotran pathologic basis of disease*, Philadelphia, PA Elsevier|Saunders.

KURABAYASHI, N. & SANADA, K. 2013. Increased dosage of DYRK1A and DSCR1 delays neuronal differentiation in neocortical progenitor cells. *Genes Dev,* 27**,** 2708-21.

KURI-HARCUCH, W., WISE, L. S. & GREEN, H. 1978. Interruption of the adipose conversion of 3T3 cells by biotin deficiency: differentiation without triglyceride accumulation. *Cell,* 14**,** 53-9.

KURSAWE, R., CAPRIO, S., GIANNINI, C., NARAYAN, D., LIN, A., D'ADAMO, E., SHAW, M., PIERPONT, B., CUSHMAN, S. W. & SHULMAN, G. I. 2013. Decreased transcription of ChREBP-alpha/beta isoforms in abdominal subcutaneous adipose tissue of obese adolescents with prediabetes or early type 2 diabetes: associations with insulin resistance and hyperglycemia. *Diabetes,* 62**,** 837-44.

KURSAWE, R., ESZLINGER, M., NARAYAN, D., LIU, T., BAZUINE, M., CALI, A. M., D'ADAMO, E., SHAW, M., PIERPONT, B., SHULMAN, G. I., CUSHMAN, S. W., SHERMAN, A. & CAPRIO, S. 2010. Cellularity and adipogenic profile of the abdominal subcutaneous adipose tissue from obese adolescents: association with insulin resistance and hepatic steatosis. *Diabetes,* 59**,** 2288-96.

KUSHNER, J. A., CIEMERYCH, M. A., SICINSKA, E., WARTSCHOW, L. M., TETA, M., LONG, S. Y., SICINSKI, P. & WHITE, M. F. 2005. Cyclins D2 and D1 are essential for postnatal pancreatic beta-cell growth. *Mol Cell Biol,* 25**,** 3752-62.

KUSMINSKI, C. M., SHETTY, S., ORCI, L., UNGER, R. H. & SCHERER, P. E. 2009. Diabetes and apoptosis: lipotoxicity. *Apoptosis,* 14**,** 1484-95.

LADNER, C. J., CZECH, J., MAURICE, J., LORENS, S. A. & LEE, J. M. 1996. Reduction of calcineurin enzymatic activity in Alzheimer's disease: correlation with neuropathologic changes. *J Neuropathol Exp Neurol,* 55**,** 924-31.

LAFONTAN, M. 2009. Advances in adipose tissue metabolism. *International Journal Of Obesity,* 32**,** S39.

LANGE, A. W., ROTHERMEL, B. A. & YUTZEY, K. E. 2005. Restoration of DSCR1 to disomy in the trisomy 16 mouse model of Down syndrome does not correct cardiac or craniofacial development anomalies. *Dev Dyn,* 233**,** 954-63.

LANGIN, D. 2006. Adipose tissue lipolysis as a metabolic pathway to define pharmacological strategies against obesity and the metabolic syndrome. *Pharmacol Res,* 53**,** 482-91.

LARGE, V., REYNISDOTTIR, S., LANGIN, D., FREDBY, K., KLANNEMARK, M., HOLM, C. & ARNER, P. 1999. Decreased expression and function of adipocyte hormone-sensitive lipase in subcutaneous fat cells of obese subjects. *J Lipid Res,* 40**,** 2059-66.

LASS, A., ZIMMERMANN, R., HAEMMERLE, G., RIEDERER, M., SCHOISWOHL, G., SCHWEIGER, M., KIENESBERGER, P., STRAUSS, J. G., GORKIEWICZ, G. & ZECHNER, R. 2006. Adipose triglyceride lipase-mediated lipolysis of cellular fat stores is activated by CGI-58 and defective in Chanarin-Dorfman Syndrome. *Cell Metab,* 3**,** 309-19.

LASS, A., ZIMMERMANN, R., OBERER, M. & ZECHNER, R. 2011. Lipolysis - a highly regulated multi-enzyme complex mediates the catabolism of cellular fat stores. *Prog Lipid Res,* 50**,** 14-27.

LAURANCE, M. E., KNAACK, D., FIORE, D. M. & HEGRE, O. D. 1998. Glucose responsive insulin secreting β-cell lines and method for producing same. Google Patents.

LAWRENCE, M. C., BHATT, H. S. & EASOM, R. A. 2002. NFAT regulates insulin gene promoter activity in response to synergistic pathways induced by glucose and glucagon-like peptide-1. *Diabetes,* 51**,** 691-8.

LE LAY, S., LEFRERE, I., TRAUTWEIN, C., DUGAIL, I. & KRIEF, S. 2002. Insulin and sterol-regulatory element-binding protein-1c (SREBP-1C) regulation of gene expression in 3T3-L1 adipocytes. Identification of CCAAT/enhancer-binding protein beta as an SREBP-1C target. *J Biol Chem,* 277**,** 35625-34.

LEAHY, J. L. 2005. Pathogenesis of type 2 diabetes mellitus. *Arch Med Res,* 36**,** 197-209.

LEAHY, K. P. & CRAWFORD, D. R. 2000. adapt78 protects cells against stress damage and suppresses cell growth. *Arch Biochem Biophys,* 379**,** 221-8.

LEAHY, K. P., DAVIES, K. J., DULL, M., KORT, J. J., LAWRENCE, K. W. & CRAWFORD, D. R. 1999. adapt78, a stress-inducible mRNA, is related to the glucose-regulated protein family of genes. *Arch Biochem Biophys,* 368**,** 67-74.

LEE, E. H., KIM, S. S., LEE, S., BAEK, K. H. & SEO, S. R. 2015. Pituitary Adenylate Cyclase-activating Polypeptide (PACAP) Targets Down Syndrome Candidate Region 1 (DSCR1/RCAN1) to control Neuronal Differentiation. *J Biol Chem,* 290**,** 21019-31.

LEE, H. J., KIM, Y. S., SATO, Y. & CHO, Y. J. 2009. RCAN1-4 knockdown attenuates cell growth through the inhibition of Ras signaling. *FEBS Lett,* 583**,** 2557-64.

LEE, M. J., WU, Y. & FRIED, S. K. 2013. Adipose tissue heterogeneity: implication of depot differences in adipose tissue for obesity complications. *Mol Aspects Med,* 34**,** 1-11.

LEE, Y. H., MOTTILLO, E. P. & GRANNEMAN, J. G. 2014. Adipose tissue plasticity from WAT to BAT and in between. *Biochim Biophys Acta,* 1842**,** 358-69.

LEFTEROVA, M. I. & LAZAR, M. A. 2009. New developments in adipogenesis. *Trends Endocrinol Metab,* 20**,** 107-14.

LENZEN, S. 2017. Chemistry and biology of reactive species with special reference to the antioxidative defence status in pancreatic beta-cells. *Biochim Biophys Acta Gen Subj,* 1861**,** 1929-1942.

LETEXIER, D., PINTEUR, C., LARGE, V., FRERING, V. & BEYLOT, M. 2003. Comparison of the expression and activity of the lipogenic pathway in human and rat adipose tissue. *J Lipid Res,* 44**,** 2127-34.

LEWIS, G. F., CARPENTIER, A., ADELI, K. & GIACCA, A. 2002. Disordered fat storage and mobilization in the pathogenesis of insulin resistance and type 2 diabetes. *Endocr Rev,* 23**,** 201-29.

LI, N., LI, B., BRUN, T., DEFFERT-DELBOUILLE, C., MAHIOUT, Z., DAALI, Y., MA, X. J., KRAUSE, K. H. & MAECHLER, P. 2012. NADPH oxidase NOX2 defines a new antagonistic role for reactive oxygen species and cAMP/PKA in the regulation of insulin secretion. *Diabetes,* 61**,** 2842-50.

LI, Q., HOSAKA, T., HARADA, N., NAKAYA, Y. & FUNAKI, M. 2013. Activation of Akt through 5-HT2A receptor ameliorates serotonin-induced degradation of insulin receptor substrate-1 in adipocytes. *Mol Cell Endocrinol,* 365**,** 25-35.

LI, X., CHAN, L. W. C., LI, X., LIU, C., YANG, G., GAO, J., DAI, M., WANG, Y., XIE, Z., LIU, J., ZHOU, F., ZHENG, T., FENG, D., GUO, S., LI, H., SUN, K. & YANG, S. 2020. Obesity-Induced Regulator of Calcineurin 1 Overexpression Leads to beta-Cell Failure Through Mitophagy Pathway Inhibition. *Antioxid Redox Signal,* 32**,** 413-428.

LIANG, Y., LI, C., GUZMAN, V. M., CHANG, W. W., EVINGER, A. J., PABLO, J. V. & WOODWARD, D. F. 2004. Upregulation of orphan nuclear receptor Nur77 following PGF(2alpha), Bimatoprost, and Butaprost treatments. Essential role of a protein kinase C pathway involved in EP(2) receptor activated Nur77 gene transcription. *Br J Pharmacol,* 142**,** 737-48.

LIN, F. T. & LANE, M. D. 1994. CCAAT/enhancer binding protein alpha is sufficient to initiate the 3T3-L1 adipocyte differentiation program. *Proc Natl Acad Sci U S A,* 91**,** 8757-61.

LIN, H. Y., MICHTALIK, H. J., ZHANG, S., ANDERSEN, T. T., VAN RIPER, D. A., DAVIES, K. K., ERMAK, G., PETTI, L. M., NACHOD, S., NARAYAN, A. V., BHATT, N. & CRAWFORD, D. R. 2003. Oxidative and calcium stress regulate DSCR1 (Adapt78/MCIP1) protein. *Free Radic Biol Med,* 35**,** 528-39.

LIPSKAIA, L. & LOMPRE, A. M. 2004. Alteration in temporal kinetics of Ca2+ signaling and control of growth and proliferation. *Biol Cell,* 96**,** 55-68.

LITOSCH, I., HUDSON, T. H., MILLS, I., LI, S. Y. & FAIN, J. N. 1982. Forskolin as an activator of cyclic AMP accumulation and lipolysis in rat adipocytes. *Mol Pharmacol,* 22**,** 109-15.

LITVIN, T. N., KAMENETSKY, M., ZARIFYAN, A., BUCK, J. & LEVIN, L. R. 2003. Kinetic properties of "soluble" adenylyl cyclase. Synergism between calcium and bicarbonate. *J Biol Chem,* 278**,** 15922-6.

LIU, F. T., NEWLAND, A. C. & JIA, L. 2003. Bax conformational change is a crucial step for PUMA-mediated apoptosis in human leukemia. *Biochem Biophys Res Commun,* 310**,** 956-62.

LIU, J. O. 2003. Endogenous protein inhibitors of calcineurin. *Biochem Biophys Res Commun,* 311**,** 1103-9.

LIU, L. & CLIPSTONE, N. A. 2007. Prostaglandin F2alpha inhibits adipocyte differentiation via a G alpha q-calcium-calcineurin-dependent signaling pathway. *J Cell Biochem,* 100**,** 161-73.

LIU, Y., PETERSON, D. A., KIMURA, H. & SCHUBERT, D. 1997. Mechanism of cellular 3-(4,5-dimethylthiazol-2-yl)-2,5-diphenyltetrazolium bromide (MTT) reduction. *J Neurochem,* 69**,** 581-93.

LOWELL, B. B. & SHULMAN, G. I. 2005. Mitochondrial dysfunction and type 2 diabetes. *Science,* 307**,** 384-7.

LU, X., ALTSHULER-KEYLIN, S., WANG, Q., CHEN, Y., HENRIQUE SPONTON, C., IKEDA, K., MARETICH, P., YONESHIRO, T. & KAJIMURA, S. 2018. Mitophagy controls beige adipocyte maintenance through a Parkin-dependent and UCP1-independent mechanism. *Sci Signal,* 11.

LU, X., YANG, X. & LIU, J. 2010. Differential control of ATGL-mediated lipid droplet degradation by CGI-58 and G0S2. *Cell Cycle,* 9**,** 2719-25.

MA, L., ROBINSON, L. N. & TOWLE, H. C. 2006. ChREBP*Mlx is the principal mediator of glucose-induced gene expression in the liver. *J Biol Chem,* 281**,** 28721-30.

MACDOUGALD, O. A. & LANE, M. D. 1995. Transcriptional regulation of gene expression during adipocyte differentiation. *Annu Rev Biochem,* 64**,** 345-73.

MACIAN, F. 2005. NFAT proteins: key regulators of T-cell development and function. *Nat Rev Immunol,* 5**,** 472-84.

MACKALL, J. C. & LANE, M. D. 1977. Role of pyruvate carboxylase in fatty acid synthesis: alterations during preadipocyte differentiation. *Biochem Biophys Res Commun,* 79**,** 720-5.

MACKALL, J. C., STUDENT, A. K., POLAKIS, S. E. & LANE, M. D. 1976. Induction of lipogenesis during differentiation in a "preadipocyte" cell line. *J Biol Chem,* 251**,** 6462-4.

MAECHLER, P. & WOLLHEIM, C. B. 2001. Mitochondrial function in normal and diabetic beta-cells. *Nature,* 414**,** 807-12.

MAEDA, T. & HORIUCHI, N. 2009. Simvastatin suppresses leptin expression in 3T3-L1 adipocytes via activation of the cyclic AMP-PKA pathway induced by inhibition of protein prenylation. *J Biochem,* 145**,** 771-81.

MAEDLER, K., FONTANA, A., RIS, F., SERGEEV, P., TOSO, C., OBERHOLZER, J., LEHMANN, R., BACHMANN, F., TASINATO, A., SPINAS, G. A., HALBAN, P. A. & DONATH, M. Y. 2002. FLIP switches Fas-mediated glucose signaling in human pancreatic beta cells from apoptosis to cell replication. *Proc Natl Acad Sci U S A,* 99**,** 8236-41.

MAEDLER, K., SPINAS, G. A., LEHMANN, R., SERGEEV, P., WEBER, M., FONTANA, A., KAISER, N. & DONATH, M. Y. 2001. Glucose induces beta-cell apoptosis via upregulation of the Fas receptor in human islets. *Diabetes,* 50**,** 1683-90.

MAIER, T., GUELL, M. & SERRANO, L. 2009. Correlation of mRNA and protein in complex biological samples. *FEBS Lett,* 583**,** 3966-73.

MAJKA, S. M., MILLER, H. L., HELM, K. M., ACOSTA, A. S., CHILDS, C. R., KONG, R. & KLEMM, D. J. 2014. Chapter Fifteen - Analysis and Isolation of Adipocytes by Flow Cytometry. *In:* MACDOUGALD, O. A. (ed.) *Methods in Enzymology.* Academic Press.

MAKKI, K., FROGUEL, P. & WOLOWCZUK, I. 2013. Adipose tissue in obesity-related inflammation and insulin resistance: cells, cytokines, and chemokines. *ISRN Inflamm,* 2013**,** 139239.

MAKOWSKI, L., BOORD, J. B., MAEDA, K., BABAEV, V. R., UYSAL, K. T., MORGAN, M. A., PARKER, R. A., SUTTLES, J., FAZIO, S., HOTAMISLIGIL, G. S. & LINTON, M. F. 2001. Lack of

macrophage fatty-acid-binding protein aP2 protects mice deficient in apolipoprotein E against atherosclerosis. *Nat Med,* 7**,** 699-705.

MALIN, S. K. & KASHYAP, S. R. 2016. Effects of various gastrointestinal procedures on beta-cell function in obesity and type 2 diabetes. *Surg Obes Relat Dis,* 12**,** 1213-9.

MANN, K. M., RAY, J. L., MOON, E. S., SASS, K. M. & BENSON, M. R. 2004. Calcineurin initiates smooth muscle differentiation in neural crest stem cells. *J Cell Biol,* 165**,** 483-91.

MAO, J., YANG, T., GU, Z., HEIRD, W. C., FINEGOLD, M. J., LEE, B. & WAKIL, S. J. 2009. aP2-Cre-mediated inactivation of acetyl-CoA carboxylase 1 causes growth retardation and reduced lipid accumulation in adipose tissues. *Proc Natl Acad Sci U S A,* 106**,** 17576-81.

MARCHETTI, P., DEL GUERRA, S., MARSELLI, L., LUPI, R., MASINI, M., POLLERA, M., BUGLIANI, M., BOGGI, U., VISTOLI, F., MOSCA, F. & DEL PRATO, S. 2004. Pancreatic islets from type 2 diabetic patients have functional defects and increased apoptosis that are ameliorated by metformin. *J Clin Endocrinol Metab,* 89**,** 5535-41.

MARIMAN, E. C. & WANG, P. 2010. Adipocyte extracellular matrix composition, dynamics and role in obesity. *Cell Mol Life Sci,* 67**,** 1277-92.

MARITIM, A. C., SANDERS, R. A. & WATKINS, J. B., 3RD 2003. Diabetes, oxidative stress, and antioxidants: a review. *J Biochem Mol Toxicol,* 17**,** 24-38.

MARSHAK, S., LEIBOWITZ, G., BERTUZZI, F., SOCCI, C., KAISER, N., GROSS, D. J., CERASI, E. & MELLOUL, D. 1999. Impaired beta-cell functions induced by chronic exposure of cultured human pancreatic islets to high glucose. *Diabetes,* 48**,** 1230-6.

MARTIN, K. R., CORLETT, A., DUBACH, D., MUSTAFA, T., COLEMAN, H. A., PARKINGTON, H. C., MERSON, T. D., BOURNE, J. A., PORTA, S., ARBONES, M. L., FINKELSTEIN, D. I. & PRITCHARD, M. A. 2012. Over-expression of RCAN1 causes Down syndrome-like hippocampal deficits that alter learning and memory. *Hum Mol Genet,* 21**,** 3025-41.

MARTINEZ, J. A. 2006. Mitochondrial oxidative stress and inflammation: an slalom to obesity and insulin resistance. *J Physiol Biochem,* 62**,** 303-6.

MARTINEZ-BOTAS, J., ANDERSON, J. B., TESSIER, D., LAPILLONNE, A., CHANG, B. H., QUAST, M. J., GORENSTEIN, D., CHEN, K. H. & CHAN, L. 2000. Absence of perilipin results in leanness and reverses obesity in Lepr(db/db) mice. *Nat Genet,* 26**,** 474-9.

MARTINEZ-MARTINEZ, S., GENESCA, L., RODRIGUEZ, A., RAYA, A., SALICHS, E., WERE, F., LOPEZ-MADERUELO, M. D., REDONDO, J. M. & DE LA LUNA, S. 2009. The RCAN carboxyl end mediates calcineurin docking-dependent inhibition via a site that dictates binding to substrates and regulators. *Proc Natl Acad Sci U S A,* 106**,** 6117-22.

MARTINEZ-MARTINEZ, S. & REDONDO, J. M. 2004. Inhibitors of the calcineurin/NFAT pathway. *Curr Med Chem,* 11**,** 997-1007.

MCCLAVE, S. A. & SNIDER, H. L. 2001. Dissecting the energy needs of the body. *Curr Opin Clin Nutr Metab Care,* 4**,** 143-7.

MCKENZIE, M. D., JAMIESON, E., JANSEN, E. S., SCOTT, C. L., HUANG, D. C., BOUILLET, P., ALLISON, J., KAY, T. W., STRASSER, A. & THOMAS, H. E. 2010. Glucose induces pancreatic islet cell apoptosis that requires the BH3-only proteins Bim and Puma and multi-BH domain protein Bax. *Diabetes,* 59**,** 644-52.

MCLAUGHLIN, T., CRAIG, C., LIU, L. F., PERELMAN, D., ALLISTER, C., SPIELMAN, D. & CUSHMAN, S. W. 2016. Adipose Cell Size and Regional Fat Deposition as Predictors of Metabolic Response to Overfeeding in Insulin-Resistant and Insulin-Sensitive Humans. *Diabetes,* 65**,** 1245-54.

MEHTA, S., LI, H., HOGAN, P. G. & CUNNINGHAM, K. W. 2009. Domain architecture of the regulators of calcineurin (RCANs) and identification of a divergent RCAN in yeast. *Mol Cell Biol,* 29**,** 2777-93.

MELDOLESI, J. & CHIEREGATTI, E. 2004. Fusion has found its calcium sensor. *Nat Cell Biol,* 6**,** 476-8.

MICHAEL, M. D., KULKARNI, R. N., POSTIC, C., PREVIS, S. F., SHULMAN, G. I., MAGNUSON, M. A. & KAHN, C. R. 2000. Loss of insulin signaling in hepatocytes leads to severe insulin resistance and progressive hepatic dysfunction. *Mol Cell,* 6**,** 87-97.

MILAGRO, F. I., CAMPION, J. & MARTINEZ, J. A. 2006. Weight gain induced by high-fat feeding involves increased liver oxidative stress. *Obesity (Silver Spring),* 14**,** 1118-23.

MILLER, C. N., YANG, J. Y., ENGLAND, E., YIN, A., BAILE, C. A. & RAYALAM, S. 2015. Isoproterenol Increases Uncoupling, Glycolysis, and Markers of Beiging in Mature 3T3-L1 Adipocytes. *PLoS One,* 10**,** e0138344.

MIYOSHI, H., PERFIELD, J. W., 2ND, OBIN, M. S. & GREENBERG, A. S. 2008. Adipose triglyceride lipase regulates basal lipolysis and lipid droplet size in adipocytes. *J Cell Biochem,* 105**,** 1430-6.

MIYOSHI, H., PERFIELD, J. W., 2ND, SOUZA, S. C., SHEN, W. J., ZHANG, H. H., STANCHEVA, Z. S., KRAEMER, F. B., OBIN, M. S. & GREENBERG, A. S. 2007. Control of adipose triglyceride lipase action by serine 517 of perilipin A globally regulates protein kinase A-stimulated lipolysis in adipocytes. *J Biol Chem,* 282**,** 996-1002.

MIYOSHI, H., SOUZA, S. C., ENDO, M., SAWADA, T., PERFIELD, J. W., 2ND, SHIMIZU, C., STANCHEVA, Z., NAGAI, S., STRISSEL, K. J., YOSHIOKA, N., OBIN, M. S., KOIKE, T. & GREENBERG, A. S. 2010. Perilipin overexpression in mice protects against diet-induced obesity. *J Lipid Res,* 51**,** 975-82.

MIYOSHI, H., SOUZA, S. C., ZHANG, H. H., STRISSEL, K. J., CHRISTOFFOLETE, M. A., KOVSAN, J., RUDICH, A., KRAEMER, F. B., BIANCO, A. C., OBIN, M. S. & GREENBERG, A. S. 2006. Perilipin promotes hormone-sensitive lipase-mediated adipocyte lipolysis via phosphorylation-dependent and -independent mechanisms. *J Biol Chem,* 281**,** 15837-44.

MODAK, M. A., PARAB, P. B. & GHASKADBI, S. S. 2009. Pancreatic islets are very poor in rectifying oxidative DNA damage. *Pancreas,* 38**,** 23-9.

MOGNOL, G. P., CARNEIRO, F. R., ROBBS, B. K., FAGET, D. V. & VIOLA, J. P. 2016. Cell cycle and apoptosis regulation by NFAT transcription factors: new roles for an old player. *Cell Death Dis,* 7**,** e2199.

MOHAMED-ALI, V., GOODRICK, S., RAWESH, A., KATZ, D. R., MILES, J. M., YUDKIN, J. S., KLEIN, S. & COPPACK, S. W. 1997. Subcutaneous adipose tissue releases interleukin-6, but not tumor necrosis factor-alpha, in vivo. *J Clin Endocrinol Metab,* 82**,** 4196-200.

MONTGOMERY, M. K. & TURNER, N. 2015. Mitochondrial dysfunction and insulin resistance: an update. *Endocr Connect,* 4**,** R1-R15.

MOODLEY, K., ANGEL, C. E., GLASS, M. & GRAHAM, E. S. 2011. Real-time profiling of NK cell killing of human astrocytes using xCELLigence technology. *J Neurosci Methods,* 200**,** 173-80.

MOORE, H. P., SILVER, R. B., MOTTILLO, E. P., BERNLOHR, D. A. & GRANNEMAN, J. G. 2005. Perilipin targets a novel pool of lipid droplets for lipolytic attack by hormone-sensitive lipase. *J Biol Chem,* 280**,** 43109-20.

MORAN, A., ZHANG, H. J., OLSON, L. K., HARMON, J. S., POITOUT, V. & ROBERTSON, R. P. 1997. Differentiation of glucose toxicity from beta cell exhaustion during the evolution of defective insulin gene expression in the pancreatic islet cell line, HIT-T15. *J Clin Invest,* 99**,** 534-9.

MORIGNY, P., HOUSSIER, M., MAIRAL, A., GHILAIN, C., MOUISEL, E., BENHAMED, F., MASRI, B., RECAZENS, E., DENECHAUD, P.-D., TAVERNIER, G., CASPAR-BAUGUIL, S., VIRTUE, S., SRAMKOVA, V., MONBRUN, L., MAZARS, A., ZANOUN, M., GUILMEAU, S., BARQUISSAU, V., BEUZELIN, D., BONNEL, S., MARQUES, M., MONGE-ROFFARELLO, B., LEFORT, C., FIELDING, B., SULPICE, T., ASTRUP, A., PAYRASTRE, B., BERTRAND-MICHEL, J., MEUGNIER, E., LIGAT, L., LOPEZ, F., GUILLOU, H., LING, C., HOLM, C., RABASA-LHORET, R., SARIS, W. H. M., STICH, V., ARNER, P., RYDÉN, M., MORO, C., VIGUERIE, N., HARMS, M., HALLÉN, S., VIDAL-PUIG, A., VIDAL, H., POSTIC, C. & LANGIN, D. 2019. Interaction between hormone-sensitive lipase and ChREBP in fat cells controls insulin sensitivity. *Nature Metabolism,* 1**,** 133-146.

MORIGNY, P., HOUSSIER, M., MOUISEL, E. & LANGIN, D. 2016. Adipocyte lipolysis and insulin resistance. *Biochimie,* 125**,** 259-66.

MOSETI, D., REGASSA, A. & KIM, W. K. 2016. Molecular Regulation of Adipogenesis and Potential Anti-Adipogenic Bioactive Molecules. *Int J Mol Sci,* 17.

MOSMANN, T. 1983. Rapid colorimetric assay for cellular growth and survival: application to proliferation and cytotoxicity assays. *J Immunol Methods,* 65**,** 55-63.

MULDER, H. & LING, C. 2009. Mitochondrial dysfunction in pancreatic beta-cells in Type 2 diabetes. *Mol Cell Endocrinol,* 297**,** 34-40.

MULLER, M. R. & RAO, A. 2010. NFAT, immunity and cancer: a transcription factor comes of age. *Nat Rev Immunol,* 10**,** 645-56.

MUSSON, R. E. A. & SMIT, N. P. M. 2011. Regulatory Mechanisms of Calcineurin Phosphatase Activity. *Current Medicinal Chemistry,* 18**,** 301-315.

NADLER, S. T., STOEHR, J. P., SCHUELER, K. L., TANIMOTO, G., YANDELL, B. S. & ATTIE, A. D. 2000. The expression of adipogenic genes is decreased in obesity and diabetes mellitus. *Proc Natl Acad Sci U S A,* 97**,** 11371-6.

NAGAO, K., IWAI, Y. & MIYASHITA, T. 2012. RCAN1 is an important mediator of glucocorticoid-induced apoptosis in human leukemic cells. *PLoS One,* 7**,** e49926.

NARENDRA, D., TANAKA, A., SUEN, D. F. & YOULE, R. J. 2008. Parkin is recruited selectively to impaired mitochondria and promotes their autophagy. *J Cell Biol,* 183**,** 795-803.

NATIONAL INSTITUTES OF HEALTH 1998. Clinical Guidelines on the Identification, Evaluation, and Treatment of Overweight and Obesity in Adults:The Evidence Report. *Obes Res,* 6 Suppl 2**,** 51S-209S.

NEAL, J. W. & CLIPSTONE, N. A. 2002. Calcineurin mediates the calcium-dependent inhibition of adipocyte differentiation in 3T3-L1 cells. *J Biol Chem,* 277**,** 49776-81.

NEDERGAARD, J., GOLOZOUBOVA, V., MATTHIAS, A., ASADI, A., JACOBSSON, A. & CANNON, B. 2001. UCP1: the only protein able to mediate adaptive non-shivering thermogenesis and metabolic inefficiency. *Biochim Biophys Acta,* 1504**,** 82-106.

NESS, J. M., HARVEY, C. A., STRASSER, A., BOUILLET, P., KLOCKE, B. J. & ROTH, K. A. 2006. Selective involvement of BH3-only Bcl-2 family members Bim and Bad in neonatal hypoxia-ischemia. *Brain Res,* 1099**,** 150-9.

NICHOLSON, A., REIFSNYDER, P. C., MALCOLM, R. D., LUCAS, C. A., MACGREGOR, G. R., ZHANG, W. & LEITER, E. H. 2010. Diet-induced obesity in two C57BL/6 substrains with intact or mutant nicotinamide nucleotide transhydrogenase (Nnt) gene. *Obesity (Silver Spring),* 18**,** 1902-5.

NIELSEN, T. S., JESSEN, N., JORGENSEN, J. O., MOLLER, N. & LUND, S. 2014. Dissecting adipose tissue lipolysis: molecular regulation and implications for metabolic disease. *J Mol Endocrinol,* 52**,** R199-222.

NIELSEN, T. S., KAMPMANN, U., NIELSEN, R. R., JESSEN, N., ORSKOV, L., PEDERSEN, S. B., JORGENSEN, J. O., LUND, S. & MOLLER, N. 2012. Reduced mRNA and protein expression of perilipin A and G0/G1 switch gene 2 (G0S2) in human adipose tissue in poorly controlled type 2 diabetes. *J Clin Endocrinol Metab,* 97**,** E1348-52.

NIELSEN, T. S., VENDELBO, M. H., JESSEN, N., PEDERSEN, S. B., JORGENSEN, J. O., LUND, S. & MOLLER, N. 2011. Fasting, but not exercise, increases adipose triglyceride lipase (ATGL) protein and reduces G(0)/G(1) switch gene 2 (G0S2) protein and mRNA content in human adipose tissue. *J Clin Endocrinol Metab,* 96**,** E1293-7.

NIQUET, J. & WASTERLAIN, C. G. 2004. Bim, Bad, and Bax: a deadly combination in epileptic seizures. *J Clin Invest,* 113**,** 960-2.

NOLAN, C. J., DAMM, P. & PRENTKI, M. 2011. Type 2 diabetes across generations: from pathophysiology to prevention and management. *Lancet,* 378**,** 169-81.

NOMURA, S., SHOUZU, A., OMOTO, S., NISHIKAWA, M. & IWASAKA, T. 2005. 5-HT2A receptor antagonist increases circulating adiponectin in patients with type 2 diabetes. *Blood Coagul Fibrinolysis,* 16**,** 423-8.

NOVIKOFF, A. B., NOVIKOFF, P. M., ROSEN, O. M. & RUBIN, C. S. 1980. Organelle relationships in cultured 3T3-L1 preadipocytes. *J Cell Biol,* 87**,** 180-96.

OBROWSKY, S., CHANDAK, P. G., PATANKAR, J. V., POVODEN, S., SCHLAGER, S., KERSHAW, E. E., BOGNER-STRAUSS, J. G., HOEFLER, G., LEVAK-FRANK, S. & KRATKY, D. 2013. Adipose triglyceride lipase is a TG hydrolase of the small intestine and regulates intestinal PPARalpha signaling. *J Lipid Res,* 54**,** 425-35.

OH, C. M., NAMKUNG, J., GO, Y., SHONG, K. E., KIM, K., KIM, H., PARK, B. Y., LEE, H. W., JEON, Y. H., SONG, J., SHONG, M., YADAV, V. K., KARSENTY, G., KAJIMURA, S., LEE, I. K., PARK, S. & KIM, H. 2015. Regulation of systemic energy homeostasis by serotonin in adipose tissues. *Nat Commun,* 6**,** 6794.

OHNO, H., MATSUZAKA, T., TANG, N., SHARMA, R., MOTOMURA, K., SHIMURA, T., SATOH, A., HAN, S. I., TAKEUCHI, Y., AITA, Y., IWASAKI, H., YATOH, S., SUZUKI, H., SEKIYA, M., NAKAGAWA, Y., SONE, H., YAHAGI, N., YAMADA, N., HIGAMI, Y. &

SHIMANO, H. 2018. Transgenic Mice Overexpressing SREBP-1a in Male ob/ob Mice Exhibit Lipodystrophy and Exacerbate Insulin Resistance. *Endocrinology,* 159**,** 2308-2323.

OIKONOMOU, E. K. & ANTONIADES, C. 2019. The role of adipose tissue in cardiovascular health and disease. *Nat Rev Cardiol,* 16**,** 83-99.

OLSON, E. N. & WILLIAMS, R. S. 2000. Calcineurin signaling and muscle remodeling. *Cell,* 101**,** 689-92.

OLSSON, H. & BELFRAGE, P. 1987. The regulatory and basal phosphorylation sites of hormone-sensitive lipase are dephosphorylated by protein phosphatase-1, 2A and 2C but not by protein phosphatase-2B. *Eur J Biochem,* 168**,** 399-405.

ONG, K. T., MASHEK, M. T., BU, S. Y., GREENBERG, A. S. & MASHEK, D. G. 2011. Adipose triglyceride lipase is a major hepatic lipase that regulates triacylglycerol turnover and fatty acid signaling and partitioning. *Hepatology,* 53**,** 116-26.

ORMAZABAL, V., NAIR, S., ELFEKY, O., AGUAYO, C., SALOMON, C. & ZUNIGA, F. A. 2018. Association between insulin resistance and the development of cardiovascular disease. *Cardiovasc Diabetol,* 17**,** 122.

ORRENIUS, S. 2004. Mitochondrial regulation of apoptotic cell death. *Toxicol Lett,* 149**,** 19-23.

OSTLUND, R. E., JR., YANG, J. W., KLEIN, S. & GINGERICH, R. 1996. Relation between plasma leptin concentration and body fat, gender, diet, age, and metabolic covariates. *J Clin Endocrinol Metab,* 81**,** 3909-13.

OSUGA, J., ISHIBASHI, S., OKA, T., YAGYU, H., TOZAWA, R., FUJIMOTO, A., SHIONOIRI, F., YAHAGI, N., KRAEMER, F. B., TSUTSUMI, O. & YAMADA, N. 2000. Targeted disruption of hormone-sensitive lipase results in male sterility and adipocyte hypertrophy, but not in obesity. *Proc Natl Acad Sci U S A,* 97**,** 787-92.

OTANI, T., MIZOKAMI, A., HAYASHI, Y., GAO, J., MORI, Y., NAKAMURA, S., TAKEUCHI, H. & HIRATA, M. 2015. Signaling pathway for adiponectin expression in adipocytes by osteocalcin. *Cell Signal,* 27**,** 532-44.

OU, Z., WANG, G., LI, Q., MA, Z., DAI, M. & ZOU, F. 2014. CRTC3 polymorphisms were associated with the plasma level of total cholesterol and the risks of overweight and hypertriglyceridemia in a Chinese Han population. *Mol Biol Rep,* 41**,** 125-30.

OUCHI, N., PARKER, J. L., LUGUS, J. J. & WALSH, K. 2011. Adipokines in inflammation and metabolic disease. *Nat Rev Immunol,* 11**,** 85-97.

PAGNON, J., MATZARIS, M., STARK, R., MEEX, R. C., MACAULAY, S. L., BROWN, W., O'BRIEN, P. E., TIGANIS, T. & WATT, M. J. 2012. Identification and functional characterization of protein kinase A phosphorylation sites in the major lipolytic protein, adipose triglyceride lipase. *Endocrinology,* 153**,** 4278-89.

PANTOJA, C., HUFF, J. T. & YAMAMOTO, K. R. 2008. Glucocorticoid signaling defines a novel commitment state during adipogenesis in vitro. *Mol Biol Cell,* 19**,** 4032-41.

PARKER, N., VIDAL-PUIG, A. J., AZZU, V. & BRAND, M. D. 2009. Dysregulation of glucose homeostasis in nicotinamide nucleotide transhydrogenase knockout mice is independent of uncoupling protein 2. *Biochim Biophys Acta,* 1787**,** 1451-7.

PARKER, T., WANG, K. W., MANNING, D. & DART, C. 2019. Soluble adenylyl cyclase links Ca(2+) entry to Ca(2+)/cAMP-response element binding protein (CREB) activation in vascular smooth muscle. *Sci Rep,* 9**,** 7317.

PARKS, B. W., SALLAM, T., MEHRABIAN, M., PSYCHOGIOS, N., HUI, S. T., NORHEIM, F., CASTELLANI, L. W., RAU, C. D., PAN, C., PHUN, J., ZHOU, Z., YANG, W. P., NEUHAUS, I., GARGALOVIC, P. S., KIRCHGESSNER, T. G., GRAHAM, M., LEE, R., TONTONOZ, P., GERSZTEN, R. E., HEVENER, A. L. & LUSIS, A. J. 2015. Genetic architecture of insulin resistance in the mouse. *Cell Metab,* 21**,** 334-347.

PASCAL, S. M., GUIOT, Y., PELENGARIS, S., KHAN, M. & JONAS, J. C. 2008. Effects of c-MYC activation on glucose stimulus-secretion coupling events in mouse pancreatic islets. *Am J Physiol Endocrinol Metab,* 295**,** E92-102.

PATH, G., BORNSTEIN, S. R., GURNIAK, M., CHROUSOS, G. P., SCHERBAUM, W. A. & HAUNER, H. 2001. Human breast adipocytes express interleukin-6 (IL-6) and its receptor system: increased IL-6 production by beta-adrenergic activation and effects of IL-6 on adipocyte function. *J Clin Endocrinol Metab,* 86**,** 2281-8.

PEIRIS, H., DUBACH, D., JESSUP, C. F., UNTERWEGER, P., RAGHUPATHI, R., MUYDERMAN, H., ZANIN, M. P., MACKENZIE, K., PRITCHARD, M. A. & KEATING, D. J. 2014. RCAN1 regulates mitochondrial function and increases susceptibility to oxidative stress in mammalian cells. *Oxid Med Cell Longev,* 2014**,** 520316.

PEIRIS, H., DUFFIELD, M. D., FADISTA, J., JESSUP, C. F., KASHMIR, V., GENDERS, A. J., MCGEE, S. L., MARTIN, A. M., SAIEDI, M., MORTON, N., CARTER, R., COUSIN, M. A., KOKOTOS, A. C., OSKOLKOV, N., VOLKOV, P., HOUGH, T. A., FISHER, E. M., TYBULEWICZ, V. L., BUSCIGLIO, J., COSKUN, P. E., BECKER, A., BELICHENKO, P. V., MOBLEY, W. C., RYAN, M. T., CHAN, J. Y., LAYBUTT, D. R., COATES, P. T., YANG, S., LING, C., GROOP, L., PRITCHARD, M. A. & KEATING, D. J. 2016. A Syntenic Cross Species Aneuploidy Genetic Screen Links RCAN1 Expression to beta-Cell Mitochondrial Dysfunction in Type 2 Diabetes. *PLoS Genet,* 12**,** e1006033.

PEIRIS, H. & KEATING, D. J. 2017. The neuronal and endocrine roles of RCAN1 in health and disease. *Clin Exp Pharmacol Physiol*.

PEIRIS, H., RAGHUPATHI, R., JESSUP, C. F., ZANIN, M. P., MOHANASUNDARAM, D., MACKENZIE, K. D., CHATAWAY, T., CLARKE, J. N., BREALEY, J., COATES, P. T., PRITCHARD, M. A. & KEATING, D. J. 2012. Increased expression of the glucose-responsive gene, RCAN1, causes hypoinsulinemia, beta-cell dysfunction, and diabetes. *Endocrinology,* 153**,** 5212-21.

PEREIRA, M. J., PALMING, J., RIZELL, M., AURELIANO, M., CARVALHO, E., SVENSSON, M. K. & ERIKSSON, J. W. 2013. The immunosuppressive agents rapamycin, cyclosporin A and tacrolimus increase lipolysis, inhibit lipid storage and alter expression of genes involved in lipid metabolism in human adipose tissue. *Mol Cell Endocrinol,* 365**,** 260-9.

PERLEY, M. J. & KIPNIS, D. M. 1967. Plasma insulin responses to oral and intravenous glucose: studies in normal and diabetic sujbjects. *J Clin Invest,* 46**,** 1954-62.

PETTINELLI, P. & VIDELA, L. A. 2011. Up-regulation of PPAR-gamma mRNA expression in the liver of obese patients: an additional reinforcing lipogenic mechanism to SREBP-1c induction. *J Clin Endocrinol Metab,* 96**,** 1424-30.

PFISTER, S. C., MACHADO-SANTELLI, G. M., HAN, S. W. & HENRIQUE-SILVA, F. 2002. Mutational analyses of the signals involved in the subcellular location of DSCR1. *BMC Cell Biol,* 3**,** 24.

PICK, A., CLARK, J., KUBSTRUP, C., LEVISETTI, M., PUGH, W., BONNER-WEIR, S. & POLONSKY, K. S. 1998. Role of apoptosis in failure of beta-cell mass compensation for insulin resistance and beta-cell defects in the male Zucker diabetic fatty rat. *Diabetes,* 47**,** 358-64.

PICKLES, S., VIGIE, P. & YOULE, R. J. 2018. Mitophagy and Quality Control Mechanisms in Mitochondrial Maintenance. *Curr Biol,* 28**,** R170-R185.

PLANTIER, L., BESNARD, V., XU, Y., IKEGAMI, M., WERT, S. E., HUNT, A. N., POSTLE, A. D. & WHITSETT, J. A. 2012. Activation of sterol-response element-binding proteins (SREBP) in alveolar type II cells enhances lipogenesis causing pulmonary lipotoxicity. *J Biol Chem,* 287**,** 10099-114.

POITOUT, V. & ROBERTSON, R. P. 2002. Minireview: Secondary beta-cell failure in type 2 diabetes--a convergence of glucotoxicity and lipotoxicity. *Endocrinology,* 143**,** 339-42.

PORTA, S., MARTI, E., DE LA LUNA, S. & ARBONES, M. L. 2007a. Differential expression of members of the RCAN family of calcineurin regulators suggests selective functions for these proteins in the brain. *Eur J Neurosci,* 26**,** 1213-26.

PORTA, S., SERRA, S. A., HUCH, M., VALVERDE, M. A., LLORENS, F., ESTIVILL, X., ARBONES, M. L. & MARTI, E. 2007b. RCAN1 (DSCR1) increases neuronal susceptibility to oxidative stress: a potential pathogenic process in neurodegeneration. *Hum Mol Genet,* 16**,** 1039-50.

PRAMME-STEINWACHS, I., JASTROCH, M. & USSAR, S. 2017. Extracellular calcium modulates brown adipocyte differentiation and identity. *Sci Rep,* 7**,** 8888.

PRASAD, R. B. & GROOP, L. 2015. Genetics of type 2 diabetes-pitfalls and possibilities. *Genes (Basel),* 6**,** 87-123.

PRENTKI, M., MATSCHINSKY, F. M. & MADIRAJU, S. R. 2013. Metabolic signaling in fuel-induced insulin secretion. *Cell Metab,* 18**,** 162-85.

PRENTKI, M. & NOLAN, C. J. 2006. Islet beta cell failure in type 2 diabetes. *J Clin Invest,* 116**,** 1802-12.

PUIGSERVER, P., WU, Z., PARK, C. W., GRAVES, R., WRIGHT, M. & SPIEGELMAN, B. M. 1998. A cold-inducible coactivator of nuclear receptors linked to adaptive thermogenesis. *Cell,* 92**,** 829-39.

QUTEINEH, L., BOCHUD, P. Y., GOLSHAYAN, D., CRETTOL, S., VENETZ, J. P., MANUEL, O., KUTALIK, Z., TREYER, A., LEHMANN, R., MUELLER, N. J., BINET, I., VAN DELDEN, C., STEIGER, J., MOHACSI, P., DUFOUR, J. F., SOCCAL, P. M., PASCUAL, M., EAP, C. B. & THE SWISS TRANSPLANT COHORT, S. 2017. CRTC2 polymorphism as a risk factor for the incidence of metabolic syndrome in patients with solid organ transplantation. *Pharmacogenomics J,* 17**,** 69-75.

RAHIER, J., GUIOT, Y., GOEBBELS, R. M., SEMPOUX, C. & HENQUIN, J. C. 2008. Pancreatic beta-cell mass in European subjects with type 2 diabetes. *Diabetes Obes Metab,* 10 Suppl 4**,** 32-42.

RAHMAN, N., BUCK, J. & LEVIN, L. R. 2013. pH sensing via bicarbonate-regulated "soluble" adenylyl cyclase (sAC). *Front Physiol,* 4**,** 343.

RAMIREZ-ZACARIAS, J. L., CASTRO-MUNOZLEDO, F. & KURI-HARCUCH, W. 1992. Quantitation of adipose conversion and triglycerides by staining intracytoplasmic lipids with Oil red O. *Histochemistry,* 97**,** 493-7.

RAMOS, E. M., HOFFMAN, D., JUNKINS, H. A., MAGLOTT, D., PHAN, L., SHERRY, S. T., FEOLO, M. & HINDORFF, L. A. 2014. Phenotype-Genotype Integrator (PheGenI): synthesizing genome-wide association study (GWAS) data with existing genomic resources. *Eur J Hum Genet,* 22**,** 144-7.

RAMSAY, T. G. 1996. Fat cells. *Endocrinol Metab Clin North Am,* 25**,** 847-70.

RANGANATHAN, G., UNAL, R., POKROVSKAYA, I., YAO-BORENGASSER, A., PHANAVANH, B., LECKA-CZERNIK, B., RASOULI, N. & KERN, P. A. 2006. The lipogenic enzymes DGAT1, FAS, and LPL in adipose tissue: effects of obesity, insulin resistance, and TZD treatment. *J Lipid Res,* 47**,** 2444-50.

RANTA, F., AVRAM, D., BERCHTOLD, S., DUFER, M., DREWS, G., LANG, F. & ULLRICH, S. 2006. Dexamethasone induces cell death in insulin-secreting cells, an effect reversed by exendin-4. *Diabetes,* 55**,** 1380-90.

RAO, A., LUO, C. & HOGAN, P. G. 1997. Transcription factors of the NFAT family: regulation and function. *Annu Rev Immunol,* 15**,** 707-47.

RAO, J. R., KEATING, D. J., CHEN, C. & PARKINGTON, H. C. 2012. Adiponectin increases insulin content and cell proliferation in MIN6 cells via PPARgamma-dependent and PPARgamma-independent mechanisms. *Diabetes Obes Metab,* 14**,** 983-9.

RAY, H., PINTEUR, C., FRERING, V., BEYLOT, M. & LARGE, V. 2009. Depot-specific differences in perilipin and hormone-sensitive lipase expression in lean and obese. *Lipids Health Dis,* 8**,** 58.

REAL DE ASUA, D., PARRA, P., COSTA, R., MOLDENHAUER, F. & SUAREZ, C. 2014. Evaluation of the impact of abdominal obesity on glucose and lipid metabolism disorders in adults with Down syndrome. *Res Dev Disabil,* 35**,** 2942-9.

REYNISDOTTIR, S., LANGIN, D., CARLSTROM, K., HOLM, C., ROSSNER, S. & ARNER, P. 1995. Effects of weight reduction on the regulation of lipolysis in adipocytes of women with upper-body obesity. *Clin Sci (Lond),* 89**,** 421-9.

RICCI, M. R. & FRIED, S. K. 1999. Isoproterenol decreases leptin expression in adipose tissue of obese humans. *Obes Res,* 7**,** 233-40.

RICCI, M. R., LEE, M. J., RUSSELL, C. D., WANG, Y., SULLIVAN, S., SCHNEIDER, S. H., BROLIN, R. E. & FRIED, S. K. 2005. Isoproterenol decreases leptin release from rat and human adipose tissue through posttranscriptional mechanisms. *Am J Physiol Endocrinol Metab,* 288**,** E798-804.

RICHARDS, P., OURABAH, S., MONTAGNE, J., BURNOL, A. F., POSTIC, C. & GUILMEAU, S. 2017. MondoA/ChREBP: The usual suspects of transcriptional glucose sensing; Implication in pathophysiology. *Metabolism,* 70**,** 133-151.

RIEMER, J., BULLEID, N. & HERRMANN, J. M. 2009. Disulfide formation in the ER and mitochondria: two solutions to a common process. *Science,* 324**,** 1284-7.

RINELLA, M. E., ELIAS, M. S., SMOLAK, R. R., FU, T., BORENSZTAJN, J. & GREEN, R. M. 2008. Mechanisms of hepatic steatosis in mice fed a lipogenic methionine choline-deficient diet. *J Lipid Res,* 49**,** 1068-76.

ROBERTS, R., HODSON, L., DENNIS, A. L., NEVILLE, M. J., HUMPHREYS, S. M., HARNDEN, K. E., MICKLEM, K. J. & FRAYN, K. N. 2009. Markers of de novo lipogenesis in adipose tissue: associations with small adipocytes and insulin sensitivity in humans. *Diabetologia,* 52**,** 882-90.

ROBERTSON, R. P. 2004. Chronic oxidative stress as a central mechanism for glucose toxicity in pancreatic islet beta cells in diabetes. *J Biol Chem,* 279**,** 42351-4.

ROBERTSON, R. P., HARMON, J., TRAN, P. O., TANAKA, Y. & TAKAHASHI, H. 2003. Glucose toxicity in beta-cells: type 2 diabetes, good radicals gone bad, and the glutathione connection. *Diabetes,* 52**,** 581-7.

ROBERTSON, R. P., OLSON, L. K. & ZHANG, H. J. 1994. Differentiating glucose toxicity from glucose desensitization: a new message from the insulin gene. *Diabetes,* 43**,** 1085-9.

ROBERTSON, R. P., ZHANG, H. J., PYZDROWSKI, K. L. & WALSETH, T. F. 1992. Preservation of insulin mRNA levels and insulin secretion in HIT cells by avoidance of chronic exposure to high glucose concentrations. *J Clin Invest,* 90**,** 320-5.

RODER, P. V., WU, B., LIU, Y. & HAN, W. 2016. Pancreatic regulation of glucose homeostasis. *Exp Mol Med,* 48**,** e219.

ROHRER, T. R., HENNES, P., THON, A., DOST, A., GRABERT, M., RAMI, B., WIEGAND, S., HOLL, R. W. & INITIATIVE, D. P. V. 2010. Down's syndrome in diabetic patients aged <20 years: an analysis of metabolic status, glycaemic control and autoimmunity in comparison with type 1 diabetes. *Diabetologia,* 53**,** 1070-5.

RORSMAN, P., ELIASSON, L., RENSTROM, E., GROMADA, J., BARG, S. & GOPEL, S. 2000. The Cell Physiology of Biphasic Insulin Secretion. *News Physiol Sci,* 15**,** 72-77.

RORSMAN, P. & RENSTROM, E. 2003. Insulin granule dynamics in pancreatic beta cells. *Diabetologia,* 46**,** 1029-45.

ROSELL, M., KAFOROU, M., FRONTINI, A., OKOLO, A., CHAN, Y. W., NIKOLOPOULOU, E., MILLERSHIP, S., FENECH, M. E., MACINTYRE, D., TURNER, J. O., MOORE, J. D., BLACKBURN, E., GULLICK, W. J., CINTI, S., MONTANA, G., PARKER, M. G. & CHRISTIAN, M. 2014. Brown and white adipose tissues: intrinsic differences in gene expression and response to cold exposure in mice. *Am J Physiol Endocrinol Metab,* 306**,** E945-64.

ROSEN, E. D., HSU, C. H., WANG, X., SAKAI, S., FREEMAN, M. W., GONZALEZ, F. J. & SPIEGELMAN, B. M. 2002. C/EBPalpha induces adipogenesis through PPARgamma: a unified pathway. *Genes Dev,* 16**,** 22-6.

ROSEN, E. D. & MACDOUGALD, O. A. 2006. Adipocyte differentiation from the inside out. *Nat Rev Mol Cell Biol,* 7**,** 885-96.

ROSEN, E. D. & SPIEGELMAN, B. M. 2006. Adipocytes as regulators of energy balance and glucose homeostasis. *Nature,* 444**,** 847-53.

ROSEN, E. D., WALKEY, C. J., PUIGSERVER, P. & SPIEGELMAN, B. M. 2000. Transcriptional regulation of adipogenesis. *Genes Dev,* 14**,** 1293-307.

ROTHERMEL, B., VEGA, R. B., YANG, J., WU, H., BASSEL-DUBY, R. & WILLIAMS, R. S. 2000. A protein encoded within the Down syndrome critical region is enriched in striated muscles and inhibits calcineurin signaling. *J Biol Chem,* 275**,** 8719-25.

ROTHERMEL, B. A., MCKINSEY, T. A., VEGA, R. B., NICOL, R. L., MAMMEN, P., YANG, J., ANTOS, C. L., SHELTON, J. M., BASSEL-DUBY, R., OLSON, E. N. & WILLIAMS, R. S. 2001. Myocyte-enriched calcineurin-interacting protein, MCIP1, inhibits cardiac hypertrophy in vivo. *Proc Natl Acad Sci U S A,* 98**,** 3328-33.

ROTHERMEL, B. A., VEGA, R. B. & WILLIAMS, R. S. 2003. The role of modulatory calcineurin-interacting proteins in calcineurin signaling. *Trends Cardiovasc Med,* 13**,** 15-21.

ROTTER, D., PEIRIS, H., GRINSFELDER, D. B., MARTIN, A. M., BURCHFIELD, J., PARRA, V., HULL, C., MORALES, C. R., JESSUP, C. F., MATUSICA, D., PARKS, B. W., LUSIS, A. J., NGUYEN, N. U. N., OH, M., IYOKE, I., JAKKAMPUDI, T., MCMILLAN, D. R., SADEK, H. A., WATT, M. J., GUPTA, R. K., PRITCHARD, M. A., KEATING, D. J. & ROTHERMEL, B. A. 2018. Regulator of Calcineurin 1 helps coordinate whole-body metabolism and thermogenesis. *EMBO Rep,* 19.

ROTTER, V., NAGAEV, I. & SMITH, U. 2003. Interleukin-6 (IL-6) induces insulin resistance in 3T3-L1 adipocytes and is, like IL-8 and tumor necrosis factor-alpha, overexpressed in human fat cells from insulin-resistant subjects. *J Biol Chem,* 278**,** 45777-84.

ROUST, L. R. & JENSEN, M. D. 1993. Postprandial free fatty acid kinetics are abnormal in upper body obesity. *Diabetes,* 42**,** 1567-73.

RUBIN, C. S., HIRSCH, A., FUNG, C. & ROSEN, O. M. 1978. Development of hormone receptors and hormonal responsiveness in vitro. Insulin receptors and insulin sensitivity in the preadipocyte and adipocyte forms of 3T3-L1 cells. *J Biol Chem,* 253**,** 7570-8.

RUIZ, R., JIDEONWO, V., AHN, M., SURENDRAN, S., TAGLIABRACCI, V. S., HOU, Y., GAMBLE, A., KERNER, J., IRIMIA-DOMINGUEZ, J. M., PUCHOWICZ, M. A., DEPAOLI-ROACH, A., HOPPEL, C., ROACH, P. & MORRAL, N. 2014. Sterol regulatory element-binding protein-1 (SREBP-1) is required to regulate glycogen synthesis and gluconeogenic gene expression in mouse liver. *J Biol Chem,* 289**,** 5510-7.

RULIFSON, I. C., KARNIK, S. K., HEISER, P. W., TEN BERGE, D., CHEN, H., GU, X., TAKETO, M. M., NUSSE, R., HEBROK, M. & KIM, S. K. 2007. Wnt signaling regulates pancreatic beta cell proliferation. *Proc Natl Acad Sci U S A,* 104**,** 6247-52.

RUSSELL, L. & FORSDYKE, D. R. 1991. A human putative lymphocyte G0/G1 switch gene containing a CpG-rich island encodes a small basic protein with the potential to be phosphorylated. *DNA Cell Biol,* 10**,** 581-91.

RUSSELL, T. R. & HO, R. 1976. Conversion of 3T3 fibroblasts into adipose cells: triggering of differentiation by prostaglandin F2alpha and 1-methyl-3-isobutyl xanthine. *Proc Natl Acad Sci U S A,* 73**,** 4516-20.

SABATINI, P. V., SPECKMANN, T. & LYNN, F. C. 2018. Friend and foe: beta-cell Ca(2+) signaling and the development of diabetes. *Mol Metab*.

SAENZ, G. J., HOVANESSIAN, R., GISIS, A. D. & MEDH, R. D. 2015. Glucocorticoid-mediated co-regulation of RCAN1-1, E4BP4 and BIM in human leukemia cells susceptible to apoptosis. *Biochem Biophys Res Commun,* 463**,** 1291-6.

SAKO, Y. & GRILL, V. E. 1990. Coupling of beta-cell desensitization by hyperglycemia to excessive stimulation and circulating insulin in glucose-infused rats. *Diabetes,* 39**,** 1580-3.

SAKSIDA, T., NIKOLIC, I., VUJICIC, M., NILSSON, U. J., LEFFLER, H., LUKIC, M. L., STOJANOVIC, I. & STOSIC-GRUJICIC, S. 2013. Galectin-3 deficiency protects pancreatic islet cells from cytokine-triggered apoptosis in vitro. *J Cell Physiol,* 228**,** 1568-76.

SALMA, N., XIAO, H. & IMBALZANO, A. N. 2006. Temporal recruitment of CCAAT/enhancer-binding proteins to early and late adipogenic promoters in vivo. *J Mol Endocrinol,* 36**,** 139-51.

SAMUEL, V. T. & SHULMAN, G. I. 2012. Mechanisms for insulin resistance: common threads and missing links. *Cell,* 148**,** 852-71.

SANDHIR, R. & BERMAN, N. E. 2010. Age-dependent response of CCAAT/enhancer binding proteins following traumatic brain injury in mice. *Neurochem Int,* 56**,** 188-93.

SARAVANAN, S. & PARI, L. 2016. Protective effect of thymol on high fat diet induced diabetic nephropathy in C57BL/6J mice. *Chem Biol Interact,* 245**,** 1-11.

SARJEANT, K. & STEPHENS, J. M. 2012. Adipogenesis. *Cold Spring Harb Perspect Biol,* 4**,** a008417.

SASSONE-CORSI, P. 2012. The cyclic AMP pathway. *Cold Spring Harb Perspect Biol,* 4.

SAVAGE, D. B., CHOI, C. S., SAMUEL, V. T., LIU, Z. X., ZHANG, D., WANG, A., ZHANG, X. M., CLINE, G. W., YU, X. X., GEISLER, J. G., BHANOT, S., MONIA, B. P. & SHULMAN, G. I. 2006. Reversal of diet-induced hepatic steatosis and hepatic insulin resistance by antisense oligonucleotide inhibitors of acetyl-CoA carboxylases 1 and 2. *J Clin Invest,* 116**,** 817-24.

SCHIMMEL, R. J. 1984. Stimulation of cAMP accumulation and lipolysis in hamster adipocytes with forskolin. *Am J Physiol,* 246**,** C63-8.

SCHIRMER, I., BUALEONG, T., BUDDE, H., CIMIOTTI, D., APPUKUTTAN, A., KLEIN, N., STEINWASCHER, P., REUSCH, P., MUGGE, A., MEYER, R., LADILOV, Y. & JAQUET, K. 2018. Soluble adenylyl cyclase: A novel player in cardiac hypertrophy induced by isoprenaline or pressure overload. *PLoS One,* 13**,** e0192322.

SCHIRRA, F., RICHARDS, S. M., LIU, M., SUZUKI, T., YAMAGAMI, H. & SULLIVAN, D. A. 2006. Androgen regulation of lipogenic pathways in the mouse meibomian gland. *Exp Eye Res,* 83**,** 291-6.

SCHWEIGER, M., LASS, A., ZIMMERMANN, R., EICHMANN, T. O. & ZECHNER, R. 2009. Neutral lipid storage disease: genetic disorders caused by mutations in adipose triglyceride lipase/PNPLA2 or CGI-58/ABHD5. *Am J Physiol Endocrinol Metab,* 297**,** E289-96.

SCHWEIGER, M., PAAR, M., EDER, C., BRANDIS, J., MOSER, E., GORKIEWICZ, G., GROND, S., RADNER, F. P., CERK, I., CORNACIU, I., OBERER, M., KERSTEN, S., ZECHNER, R., ZIMMERMANN, R. & LASS, A. 2012. G0/G1 switch gene-2 regulates human adipocyte lipolysis by affecting activity and localization of adipose triglyceride lipase. *J Lipid Res,* 53**,** 2307-17.

SCHWEIGER, M., SCHOISWOHL, G., LASS, A., RADNER, F. P., HAEMMERLE, G., MALLI, R., GRAIER, W., CORNACIU, I., OBERER, M., SALVAYRE, R., FISCHER, J., ZECHNER, R. & ZIMMERMANN, R. 2008. The C-terminal region of human adipose triglyceride lipase affects enzyme activity and lipid droplet binding. *J Biol Chem,* 283**,** 17211-20.

SEBIO, A., GERGER, A., MATSUSAKA, S., YANG, D., ZHANG, W., STREMITZER, S., STINTZING, S., SUNAKAWA, Y., YAMAUCHI, S., NING, Y., FUJIMOTO, Y., UENO, M. & LENZ, H. J. 2015. Genetic variants within obesity-related genes are associated with tumor recurrence in patients with stages II/III colon cancer. *Pharmacogenet Genomics,* 25**,** 30-7.

SEE, V. & LOEFFLER, J. P. 2001. Oxidative stress induces neuronal death by recruiting a protease and phosphatase-gated mechanism. *J Biol Chem,* 276**,** 35049-59.

SEKIYA, M., OSUGA, J., OKAZAKI, H., YAHAGI, N., HARADA, K., SHEN, W. J., TAMURA, Y., TOMITA, S., IIZUKA, Y., OHASHI, K., OKAZAKI, M., SATA, M., NAGAI, R., FUJITA, T., SHIMANO, H., KRAEMER, F. B., YAMADA, N. & ISHIBASHI, S. 2004. Absence of hormone-sensitive lipase inhibits obesity and adipogenesis in Lep ob/ob mice. *J Biol Chem,* 279**,** 15084-90.

SEO, S. R., KIM, S. S. & CHUNG, K. C. 2009. Activation of adenylate cyclase by forskolin increases the protein stability of RCAN1 (DSCR1 or Adapt78). *FEBS Lett,* 583**,** 3140-4.

SEWTER, C., BERGER, D., CONSIDINE, R. V., MEDINA, G., ROCHFORD, J., CIARALDI, T., HENRY, R., DOHM, L., FLIER, J. S., O'RAHILLY, S. & VIDAL-PUIG, A. J. 2002. Human obesity and type 2 diabetes are associated with alterations in SREBP1 isoform expression that are reproduced ex vivo by tumor necrosis factor-alpha. *Diabetes,* 51**,** 1035-41.

SHAO, D. & LAZAR, M. A. 1997. Peroxisome proliferator activated receptor gamma, CCAAT/enhancer-binding protein alpha, and cell cycle status regulate the commitment to adipocyte differentiation. *J Biol Chem,* 272**,** 21473-8.

SHAO, W. & ESPENSHADE, P. J. 2012. Expanding roles for SREBP in metabolism. *Cell Metab,* 16**,** 414-9.

SHARABI, K., TAVARES, C. D., RINES, A. K. & PUIGSERVER, P. 2015. Molecular pathophysiology of hepatic glucose production. *Mol Aspects Med,* 46**,** 21-33.

SHEN, W. J., YU, Z., PATEL, S., JUE, D., LIU, L. F. & KRAEMER, F. B. 2011. Hormone-sensitive lipase modulates adipose metabolism through PPARgamma. *Biochim Biophys Acta,* 1811**,** 9-16.

SHEPHERD, P. R. & KAHN, B. B. 1999. Glucose transporters and insulin action--implications for insulin resistance and diabetes mellitus. *N Engl J Med,* 341**,** 248-57.

SHIMANO, H. 2009. SREBPs: physiology and pathophysiology of the SREBP family. *FEBS J,* 276**,** 616-21.

SHIMANO, H., HORTON, J. D., HAMMER, R. E., SHIMOMURA, I., BROWN, M. S. & GOLDSTEIN, J. L. 1996. Overproduction of cholesterol and fatty acids causes massive liver enlargement in transgenic mice expressing truncated SREBP-1a. *J Clin Invest,* 98**,** 1575-84.

SHIMANO, H., SHIMOMURA, I., HAMMER, R. E., HERZ, J., GOLDSTEIN, J. L., BROWN, M. S. & HORTON, J. D. 1997. Elevated levels of SREBP-2 and cholesterol synthesis in livers of mice homozygous for a targeted disruption of the SREBP-1 gene. *J Clin Invest,* 100**,** 2115-24.

SHIMOMURA, I., SHIMANO, H., HORTON, J. D., GOLDSTEIN, J. L. & BROWN, M. S. 1997. Differential expression of exons 1a and 1c in mRNAs for sterol regulatory element binding protein-1 in human and mouse organs and cultured cells. *J Clin Invest,* 99**,** 838-45.

SHIMOMURA, I., SHIMANO, H., KORN, B. S., BASHMAKOV, Y. & HORTON, J. D. 1998. Nuclear sterol regulatory element-binding proteins activate genes responsible for the entire program of unsaturated fatty acid biosynthesis in transgenic mouse liver. *J Biol Chem,* 273**,** 35299-306.

SHIRANE, M. & NAKAYAMA, K. I. 2004. [Immunophilin FKBP38, an inherent inhibitor of calcineurin, targets Bcl-2 to mitochondria and inhibits apoptosis]. *Nihon Rinsho,* 62**,** 405-12.

SHOU, J., JING, J., XIE, J., YOU, L., JING, Z., YAO, J., HAN, W. & PAN, H. 2015. Nuclear factor of activated T cells in cancer development and treatment. *Cancer Lett,* 361**,** 174-84.

SHOU, Y., LI, L., PRABHAKARAN, K., BOROWITZ, J. L. & ISOM, G. E. 2004. Calcineurin-mediated Bad translocation regulates cyanide-induced neuronal apoptosis. *Biochem J,* 379**,** 805-13.

SIEGRIST-KAISER, C. A., PAULI, V., JUGE-AUBRY, C. E., BOSS, O., PERNIN, A., CHIN, W. W., CUSIN, I., ROHNER-JEANRENAUD, F., BURGER, A. G., ZAPF, J. & MEIER, C. A. 1997. Direct effects of leptin on brown and white adipose tissue. *J Clin Invest,* 100**,** 2858-64.

SILVA, J. P., KOHLER, M., GRAFF, C., OLDFORS, A., MAGNUSON, M. A., BERGGREN, P. O. & LARSSON, N. G. 2000. Impaired insulin secretion and beta-cell loss in tissue-specific knockout mice with mitochondrial diabetes. *Nat Genet,* 26**,** 336-40.

SINDHU, S., THOMAS, R., SHIHAB, P., SRIRAMAN, D., BEHBEHANI, K. & AHMAD, R. 2015. Obesity Is a Positive Modulator of IL-6R and IL-6 Expression in the Subcutaneous Adipose Tissue: Significance for Metabolic Inflammation. *PLoS One,* 10**,** e0133494.

SINET, P. M., THEOPHILE, D., RAHMANI, Z., CHETTOUH, Z., BLOUIN, J. L., PRIEUR, M., NOEL, B. & DELABAR, J. M. 1994. Mapping of the Down syndrome phenotype on chromosome 21 at the molecular level. *Biomed Pharmacother,* 48**,** 247-52.

SJOSTRAND, M. & ERIKSSON, J. W. 2009. Neuroendocrine mechanisms in insulin resistance. *Mol Cell Endocrinol,* 297**,** 104-11.

SKURK, T., ALBERTI-HUBER, C., HERDER, C. & HAUNER, H. 2007. Relationship between adipocyte size and adipokine expression and secretion. *J Clin Endocrinol Metab,* 92**,** 1023-33.

SOHN, J. H., LEE, Y. K., HAN, J. S., JEON, Y. G., KIM, J. I., CHOE, S. S., KIM, S. J., YOO, H. J. & KIM, J. B. 2018. Perilipin 1 (Plin1) deficiency promotes inflammatory responses in lean adipose tissue through lipid dysregulation. *J Biol Chem,* 293**,** 13974-13988.

SOLEIMANPOUR, S. A., CRUTCHLOW, M. F., FERRARI, A. M., RAUM, J. C., GROFF, D. N., RANKIN, M. M., LIU, C., DE LEON, D. D., NAJI, A., KUSHNER, J. A. & STOFFERS, D. A. 2010. Calcineurin signaling regulates human islet {beta}-cell survival. *J Biol Chem,* 285**,** 40050-9.

SOLINAS, G., VILCU, C., NEELS, J. G., BANDYOPADHYAY, G. K., LUO, J. L., NAUGLER, W., GRIVENNIKOV, S., WYNSHAW-BORIS, A., SCADENG, M., OLEFSKY, J. M. & KARIN, M. 2007. JNK1 in hematopoietically derived cells contributes to diet-induced inflammation and insulin resistance without affecting obesity. *Cell Metab,* 6**,** 386-97.

SONG, Y., ALTAREJOS, J., GOODARZI, M. O., INOUE, H., GUO, X., BERDEAUX, R., KIM, J. H., GOODE, J., IGATA, M., PAZ, J. C., HOGAN, M. F., SINGH, P. K., GOEBEL, N., VERA, L., MILLER, N., CUI, J., JONES, M. R., CONSORTIUM, C., CONSORTIUM, G., CHEN, Y. D., TAYLOR, K. D., HSUEH, W. A., ROTTER, J. I. & MONTMINY, M. 2010. CRTC3 links catecholamine signalling to energy balance. *Nature,* 468**,** 933-9.

SONG, Z., XIAOLI, A. M. & YANG, F. 2018. Regulation and Metabolic Significance of De Novo Lipogenesis in Adipose Tissues. *Nutrients,* 10.

SPIEGELMAN, B. M. & FLIER, J. S. 1996. Adipogenesis and obesity: rounding out the big picture. *Cell,* 87**,** 377-89.

SPIEGELMAN, B. M. & FLIER, J. S. 2001. Obesity and the regulation of energy balance. *Cell,* 104**,** 531-43.

STOCKERT, J. C., BLAZQUEZ-CASTRO, A., CANETE, M., HOROBIN, R. W. & VILLANUEVA, A. 2012. MTT assay for cell viability: Intracellular localization of the formazan product is in lipid droplets. *Acta Histochem,* 114**,** 785-96.

STOCKLI, J., ZADOORIAN, A., COOKE, K. C., DESHPANDE, V., YAU, B., HERRMANN, G., KEBEDE, M. A., HUMPHREY, S. J. & JAMES, D. E. 2019. ABHD15 regulates adipose tissue lipolysis and hepatic lipid accumulation. *Mol Metab,* 25**,** 83-94.

STRABLE, M. S. & NTAMBI, J. M. 2010. Genetic control of de novo lipogenesis: role in diet-induced obesity. *Crit Rev Biochem Mol Biol,* 45**,** 199-214.

STRALFORS, P. & BELFRAGE, P. 1983. Phosphorylation of hormone-sensitive lipase by cyclic AMP-dependent protein kinase. *J Biol Chem,* 258**,** 15146-52.

STRIPPOLI, P., LENZI, L., PETRINI, M., CARINCI, P. & ZANNOTTI, M. 2000. A new gene family including DSCR1 (Down Syndrome Candidate Region 1) and ZAKI-4: characterization from yeast to human and identification of DSCR1-like 2, a novel human member (DSCR1L2). *Genomics,* 64**,** 252-63.

STUNES, A. K., RESELAND, J. E., HAUSO, O., KIDD, M., TOMMERAS, K., WALDUM, H. L., SYVERSEN, U. & GUSTAFSSON, B. I. 2011. Adipocytes express a functional system for serotonin synthesis, reuptake and receptor activation. *Diabetes Obes Metab,* 13**,** 551-8.

SUDHOF, T. C. 1995. The synaptic vesicle cycle: a cascade of protein-protein interactions. *Nature,* 375**,** 645-53.

SUK, H. Y., ZHOU, C., YANG, T. T., ZHU, H., YU, R. Y., OLABISI, O., YANG, X., BRANCHO, D., KIM, J. Y., SCHERER, P. E., FRANK, P. G., LISANTI, M. P., CALVERT, J. W., LEFER, D. J., MOLKENTIN, J. D., GHIGO, A., HIRSCH, E., JIN, J. & CHOW, C. W. 2013. Ablation of calcineurin Abeta reveals hyperlipidemia and signaling cross-talks with phosphodiesterases. *J Biol Chem,* 288**,** 3477-88.

SULLIVAN, J. E., BROCKLEHURST, K. J., MARLEY, A. E., CAREY, F., CARLING, D. & BERI, R. K. 1994. Inhibition of lipolysis and lipogenesis in isolated rat adipocytes with AICAR, a cell-permeable activator of AMP-activated protein kinase. *FEBS Lett,* 353**,** 33-6.

SUMARA, G., SUMARA, O., KIM, J. K. & KARSENTY, G. 2012. Gut-derived serotonin is a multifunctional determinant to fasting adaptation. *Cell Metab,* 16**,** 588-600.

SUN, L., YOUN, H. D., LOH, C., STOLOW, M., HE, W. & LIU, J. O. 1998. Cabin 1, a negative regulator for calcineurin signaling in T lymphocytes. *Immunity,* 8**,** 703-11.

SUN, X., WU, Y., CHEN, B., ZHANG, Z., ZHOU, W., TONG, Y., YUAN, J., XIA, K., GRONEMEYER, H., FLAVELL, R. A. & SONG, W. 2011. Regulator of calcineurin 1 (RCAN1) facilitates neuronal apoptosis through caspase-3 activation. *J Biol Chem,* 286**,** 9049-62.

SZKUDELSKI, T., NOWICKA, E. & SZKUDELSKA, K. 2005. Leptin secretion and protein kinase A activity. *Physiol Res,* 54**,** 79-85.

TAGGART, L., COATES, V. & TRUESDALE-KENNEDY, M. 2013. Management and quality indicators of diabetes mellitus in people with intellectual disabilities. *J Intellect Disabil Res,* 57**,** 1152-63.

TAGI, V. M., GIANNINI, C. & CHIARELLI, F. 2019. Insulin Resistance in Children. *Front Endocrinol (Lausanne),* 10**,** 342.

TANAKA, Y., TRAN, P. O., HARMON, J. & ROBERTSON, R. P. 2002. A role for glutathione peroxidase in protecting pancreatic beta cells against oxidative stress in a model of glucose toxicity. *Proc Natl Acad Sci U S A,* 99**,** 12363-8.

TANEERA, J., FADISTA, J., AHLQVIST, E., ATAC, D., OTTOSSON-LAAKSO, E., WOLLHEIM, C. B. & GROOP, L. 2015. Identification of novel genes for glucose metabolism based upon expression pattern in human islets and effect on insulin secretion and glycemia. *Hum Mol Genet,* 24**,** 1945-55.

TANG, C., HAN, P., OPRESCU, A. I., LEE, S. C., GYULKHANDANYAN, A. V., CHAN, G. N., WHEELER, M. B. & GIACCA, A. 2007. Evidence for a role of superoxide generation in glucose-induced beta-cell dysfunction in vivo. *Diabetes,* 56**,** 2722-31.

TANG, Y., WALLACE, M., SANCHEZ-GURMACHES, J., HSIAO, W. Y., LI, H., LEE, P. L., VERNIA, S., METALLO, C. M. & GUERTIN, D. A. 2016. Adipose tissue mTORC2 regulates ChREBP-driven de novo lipogenesis and hepatic glucose metabolism. *Nat Commun,* 7**,** 11365.

TANSEY, J. T., SZTALRYD, C., GRUIA-GRAY, J., ROUSH, D. L., ZEE, J. V., GAVRILOVA, O., REITMAN, M. L., DENG, C. X., LI, C., KIMMEL, A. R. & LONDOS, C. 2001. Perilipin ablation results in a lean mouse with aberrant adipocyte lipolysis, enhanced leptin production, and resistance to diet-induced obesity. *Proc Natl Acad Sci U S A,* 98**,** 6494-9.

TASCHLER, U., RADNER, F. P., HEIER, C., SCHREIBER, R., SCHWEIGER, M., SCHOISWOHL, G., PREISS-LANDL, K., JAEGER, D., REITER, B., KOEFELER, H. C., WOJCIECHOWSKI, J., THEUSSL, C., PENNINGER, J. M., LASS, A., HAEMMERLE, G., ZECHNER, R. & ZIMMERMANN, R. 2011. Monoglyceride lipase deficiency in mice impairs lipolysis and attenuates diet-induced insulin resistance. *J Biol Chem,* 286**,** 17467-77.

TAYLOR, D. & GOTTLIEB, R. A. 2017. Parkin-mediated mitophagy is downregulated in browning of white adipose tissue. *Obesity (Silver Spring),* 25**,** 704-712.

THORNTON, B. & BASU, C. 2011. Real-time PCR (qPCR) primer design using free online software. *Biochem Mol Biol Educ,* 39**,** 145-54.

TILG, H. & MOSCHEN, A. R. 2008. Inflammatory mechanisms in the regulation of insulin resistance. *Mol Med,* 14**,** 222-31.

TOBE, K., SUZUKI, R., AOYAMA, M., YAMAUCHI, T., KAMON, J., KUBOTA, N., TERAUCHI, Y., MATSUI, J., AKANUMA, Y., KIMURA, S., TANAKA, J., ABE, M., OHSUMI, J., NAGAI, R. & KADOWAKI, T. 2001. Increased expression of the sterol regulatory element-binding protein-1 gene in insulin receptor substrate-2(-/-) mouse liver. *J Biol Chem,* 276**,** 38337-40.

TONOOKA, N., OSEID, E., ZHOU, H., HARMON, J. S. & ROBERTSON, R. P. 2007. Glutathione peroxidase protein expression and activity in human islets isolated for transplantation. *Clin Transplant,* 21**,** 767-72.

TONTONOZ, P. & SPIEGELMAN, B. M. 2008. Fat and beyond: the diverse biology of PPARgamma. *Annu Rev Biochem,* 77**,** 289-312.

TOWLE, H. C., KAYTOR, E. N. & SHIH, H. M. 1997. Regulation of the expression of lipogenic enzyme genes by carbohydrate. *Annu Rev Nutr,* 17**,** 405-33.

TRAYHURN, P. 2007. Adipocyte biology. *Obes Rev,* 8 Suppl 1**,** 41-4.

TRESGUERRES, M., LEVIN, L. R. & BUCK, J. 2011. Intracellular cAMP signaling by soluble adenylyl cyclase. *Kidney Int,* 79**,** 1277-88.

TRUJILLO, M. E. & SCHERER, P. E. 2006. Adipose tissue-derived factors: impact on health and disease. *Endocr Rev,* 27**,** 762-78.

TSUBAI, T., YOSHIMI, A., HAMADA, Y., NAKAO, M., ARIMA, H., OISO, Y. & NODA, Y. 2017. Effects of clozapine on adipokine secretions/productions and lipid droplets in 3T3-L1 adipocytes. *J Pharmacol Sci,* 133**,** 79-87.

TURRENS, J. F. 2003. Mitochondrial formation of reactive oxygen species. *J Physiol,* 552**,** 335-44.

UCHIDA-KITAJIMA, S., YAMAUCHI, T., TAKASHINA, Y., OKADA-IWABU, M., IWABU, M., UEKI, K. & KADOWAKI, T. 2008. 5-Hydroxytryptamine 2A receptor signaling cascade modulates adiponectin and plasminogen activator inhibitor 1 expression in adipose tissue. *FEBS Lett,* 582**,** 3037-44.

UENO, M., SHEN, W. J., PATEL, S., GREENBERG, A. S., AZHAR, S. & KRAEMER, F. B. 2013. Fat-specific protein 27 modulates nuclear factor of activated T cells 5 and the cellular response to stress. *J Lipid Res,* 54**,** 734-43.

UNGER, R. H. 2002. Lipotoxic diseases. *Annu Rev Med,* 53**,** 319-36.

UNGER, R. H., ZHOU, Y. T. & ORCI, L. 1999. Regulation of fatty acid homeostasis in cells: novel role of leptin. *Proc Natl Acad Sci U S A,* 96**,** 2327-32.

UYEDA, K., YAMASHITA, H. & KAWAGUCHI, T. 2002. Carbohydrate responsive element-binding protein (ChREBP): a key regulator of glucose metabolism and fat storage. *Biochem Pharmacol,* 63**,** 2075-80.

UYSAL, K. T., WIESBROCK, S. M., MARINO, M. W. & HOTAMISLIGIL, G. S. 1997. Protection from obesity-induced insulin resistance in mice lacking TNF-alpha function. *Nature,* 389**,** 610-4.

VAN DIJK, S. J., MOLLOY, P. L., VARINLI, H., MORRISON, J. L., MUHLHAUSLER, B. S. & MEMBERS OF EPI, S. 2015. Epigenetics and human obesity. *Int J Obes (Lond),* 39**,** 85-97.

VARGA, A. & JAMES, D. 2006. Real-time RT-PCR and SYBR Green I melting curve analysis for the identification of Plum pox virus strains C, EA, and W: effect of amplicon size, melt rate, and dye translocation. *J Virol Methods,* 132**,** 146-53.

VARINLI, H., OSMOND-MCLEOD, M. J., MOLLOY, P. L. & VALLOTTON, P. 2015. LipiD-QuanT: a novel method to quantify lipid accumulation in live cells. *J Lipid Res,* 56**,** 2206-16.

VARMA, V. R., VARMA, S., AN, Y., HOHMAN, T. J., SEDDIGHI, S., CASANOVA, R., BERI, A., DAMMER, E. B., SEYFRIED, N. T., PLETNIKOVA, O., MOGHEKAR, A., WILSON, M. R., LAH, J. J., O'BRIEN, R. J., LEVEY, A. I., TRONCOSO, J. C., ALBERT, M. S. & THAMBISETTY, M. 2017. Alpha-2 macroglobulin in Alzheimer's disease: a marker of neuronal injury through the RCAN1 pathway. *Mol Psychiatry,* 22**,** 13-23.

VEGA, R. B., ROTHERMEL, B. A., WEINHEIMER, C. J., KOVACS, A., NASEEM, R. H., BASSEL-DUBY, R., WILLIAMS, R. S. & OLSON, E. N. 2003. Dual roles of modulatory calcineurin-interacting protein 1 in cardiac hypertrophy. *Proc Natl Acad Sci U S A,* 100**,** 669-74.

VEGA, R. B., YANG, J., ROTHERMEL, B. A., BASSEL-DUBY, R. & WILLIAMS, R. S. 2002. Multiple domains of MCIP1 contribute to inhibition of calcineurin activity. *J Biol Chem,* 277**,** 30401-7.

VERBOVEN, K., WOUTERS, K., GAENS, K., HANSEN, D., BIJNEN, M., WETZELS, S., STEHOUWER, C. D., GOOSSENS, G. H., SCHALKWIJK, C. G., BLAAK, E. E. & JOCKEN, J. W. 2018. Abdominal subcutaneous and visceral adipocyte size, lipolysis and inflammation relate to insulin resistance in male obese humans. *Sci Rep,* 8**,** 4677.

VERNOCHET, C., MOURIER, A., BEZY, O., MACOTELA, Y., BOUCHER, J., RARDIN, M. J., AN, D., LEE, K. Y., ILKAYEVA, O. R., ZINGARETTI, C. M., EMANUELLI, B., SMYTH, G., CINTI, S., NEWGARD, C. B., GIBSON, B. W., LARSSON, N. G. & KAHN, C. R. 2012. Adipose-specific deletion of TFAM increases mitochondrial oxidation and protects mice against obesity and insulin resistance. *Cell Metab,* 16**,** 765-76.

VIJAYAKUMAR, A., ARYAL, P., WEN, J., SYED, I., VAZIRANI, R. P., MORAES-VIEIRA, P. M., CAMPOREZ, J. P., GALLOP, M. R., PERRY, R. J., PERONI, O. D., SHULMAN, G. I., SAGHATELIAN, A., MCGRAW, T. E. & KAHN, B. B. 2017. Absence of Carbohydrate Response Element Binding Protein in Adipocytes Causes Systemic Insulin Resistance and Impairs Glucose Transport. *Cell Rep,* 21**,** 1021-1035.

VISHWANATH, D., SRINIVASAN, H., PATIL, M. S., SEETARAMA, S., AGRAWAL, S. K., DIXIT, M. N. & DHAR, K. 2013. Novel method to differentiate 3T3 L1 cells in vitro to produce highly sensitive adipocytes for a GLUT4 mediated glucose uptake using fluorescent glucose analog. *J Cell Commun Signal,* 7**,** 129-40.

VISTICA, D. T., SKEHAN, P., SCUDIERO, D., MONKS, A., PITTMAN, A. & BOYD, M. R. 1991. Tetrazolium-based assays for cellular viability: a critical examination of selected parameters affecting formazan production. *Cancer Res,* 51**,** 2515-20.

VOGEL, C. & MARCOTTE, E. M. 2012. Insights into the regulation of protein abundance from proteomic and transcriptomic analyses. *Nat Rev Genet,* 13**,** 227-32.

VROEGRIJK, I. O., VAN KLINKEN, J. B., VAN DIEPEN, J. A., VAN DEN BERG, S. A., FEBBRAIO, M., STEINBUSCH, L. K., GLATZ, J. F., HAVEKES, L. M., VOSHOL, P. J., RENSEN, P. C., VAN DIJK, K. W. & VAN HARMELEN, V. 2013. CD36 is important for adipocyte recruitment and affects lipolysis. *Obesity (Silver Spring),* 21**,** 2037-45.

WAKIL, S. J. & ABU-ELHEIGA, L. A. 2009. Fatty acid metabolism: target for metabolic syndrome. *J Lipid Res,* 50 Suppl**,** S138-43.

WANG, H., MAECHLER, P., ANTINOZZI, P. A., HERRERO, L., HAGENFELDT-JOHANSSON, K. A., BJORKLUND, A. & WOLLHEIM, C. B. 2003. The transcription factor SREBP-1c is instrumental in the development of beta-cell dysfunction. *J Biol Chem,* 278**,** 16622-9.

WANG, H. G., PATHAN, N., ETHELL, I. M., KRAJEWSKI, S., YAMAGUCHI, Y., SHIBASAKI, F., MCKEON, F., BOBO, T., FRANKE, T. F. & REED, J. C. 1999. Ca2+-induced apoptosis through calcineurin dephosphorylation of BAD. *Science,* 284**,** 339-43.

WANG, Y., DE KEULENAER, G. W., WEINBERG, E. O., MUANGMAN, S., GUALBERTO, A., LANDSCHULZ, K. T., TURI, T. G., THOMPSON, J. F. & LEE, R. T. 2002. Direct biomechanical induction of endogenous calcineurin inhibitor Down Syndrome Critical Region-1 in cardiac myocytes. *Am J Physiol Heart Circ Physiol,* 283**,** H533-9.

WANG, Y., WANG, H., HEGDE, V., DUBUISSON, O., GAO, Z., DHURANDHAR, N. V. & YE, J. 2013. Interplay of pro- and anti-inflammatory cytokines to determine lipid accretion in adipocytes. *Int J Obes (Lond),* 37**,** 1490-8.

WEIR, M. 2001. Impact of immunosuppressive regimes on posttransplant diabetes mellitus. *Transplant Proc,* 33**,** 23S-26S.

WEIR, M. R. & FINK, J. C. 1999. Risk for posttransplant Diabetes mellitus with current immunosuppressive medications. *Am J Kidney Dis,* 34**,** 1-13.

WHEELER, M. B., SHEU, L., GHAI, M., BOUQUILLON, A., GRONDIN, G., WELLER, U., BEAUDOIN, A. R., BENNETT, M. K., TRIMBLE, W. S. & GAISANO, H. Y. 1996. Characterization of SNARE protein expression in beta cell lines and pancreatic islets. *Endocrinology,* 137**,** 1340-8.

WILKINS, B. J. & MOLKENTIN, J. D. 2002. Calcineurin and cardiac hypertrophy: where have we been? Where are we going? *J Physiol,* 541**,** 1-8.

WITTE, N., MUENZNER, M., RIETSCHER, J., KNAUER, M., HEIDENREICH, S., NUOTIO-ANTAR, A. M., GRAEF, F. A., FEDDERS, R., TOLKACHOV, A., GOEHRING, I. & SCHUPP, M. 2015. The Glucose Sensor ChREBP Links De Novo Lipogenesis to PPARgamma Activity and Adipocyte Differentiation. *Endocrinology,* 156**,** 4008-19.

WOLLHEIM, C. B. 2000. Beta-cell mitochondria in the regulation of insulin secretion: a new culprit in type II diabetes. *Diabetologia,* 43**,** 265-77.

WORLD HEALTH ORGANISATION 2000, *Obesity: preventing and managing the global epidemic*, World Health Organisation, Geneva, viewed on 20 February 2018, <https://www.who.int/nutrition/publications/obesity/WHO_TRS_894/en/>

WORLD HEALTH ORGANISATION 2016, *Global Report on Diabetes*, World Health Organisation, Geneva, viewed on 20 February 2018, <https://apps.who.int/iris/bitstream/handle/10665/204871/9789241565257_eng.pdf;jsessionid=A7FC2C0B49B406AE6DC54C1AD036C5AA?sequence=1>.

WU, H., KAO, S. C., BARRIENTOS, T., BALDWIN, S. H., OLSON, E. N., CRABTREE, G. R., ZHOU, B. & CHANG, C. P. 2007. Down syndrome critical region-1 is a transcriptional target of nuclear factor of activated T cells-c1 within the endocardium during heart development. *J Biol Chem,* 282**,** 30673-9.

WU, Y. & SONG, W. 2013. Regulation of RCAN1 translation and its role in oxidative stress-induced apoptosis. *FASEB J,* 27**,** 208-21.

WUEEST, S., RAPOLD, R. A., RYTKA, J. M., SCHOENLE, E. J. & KONRAD, D. 2009. Basal lipolysis, not the degree of insulin resistance, differentiates large from small isolated adipocytes in high-fat fed mice. *Diabetologia,* 52**,** 541-6.

WUEEST, S., YANG, X., LIU, J., SCHOENLE, E. J. & KONRAD, D. 2012. Inverse regulation of basal lipolysis in perigonadal and mesenteric fat depots in mice. *Am J Physiol Endocrinol Metab,* 302**,** E153-60.

WYLER, S. C., LORD, C. C., LEE, S., ELMQUIST, J. K. & LIU, C. 2017. Serotonergic Control of Metabolic Homeostasis. *Front Cell Neurosci,* 11**,** 277.

XIE, H. Q. & JOHNSON, G. V. 1998. Calcineurin inhibition prevents calpain-mediated proteolysis of tau in differentiated PC12 cells. *J Neurosci Res,* 53**,** 153-64.

YADAV, A., KATARIA, M. A., SAINI, V. & YADAV, A. 2013. Role of leptin and adiponectin in insulin resistance. *Clin Chim Acta,* 417**,** 80-4.

YAHIA, S., EL-FARAHATY, R. M., EL-HAWARY, A. K., EL-HUSSINY, M. A., ABDEL-MASEIH, H., EL-DAHTORY, F. & EL-GILANY, A. H. 2012. Leptin, insulin and thyroid hormones in a cohort of Egyptian obese Down syndrome children: a comparative study. *BMC Endocr Disord,* 12**,** 22.

YANG, J., ROTHERMEL, B., VEGA, R. B., FREY, N., MCKINSEY, T. A., OLSON, E. N., BASSEL-DUBY, R. & WILLIAMS, R. S. 2000. Independent signals control expression of the calcineurin inhibitory proteins MCIP1 and MCIP2 in striated muscles. *Circ Res,* 87**,** E61-8.

YANG, T. T., SUK, H. Y., YANG, X., OLABISI, O., YU, R. Y., DURAND, J., JELICKS, L. A., KIM, J. Y., SCHERER, P. E., WANG, Y., FENG, Y., ROSSETTI, L., GRAEF, I. A., CRABTREE, G. R. & CHOW, C. W. 2006a. Role of transcription factor NFAT in glucose and insulin homeostasis. *Mol Cell Biol,* 26**,** 7372-87.

YANG, T. T., UNG, P. M., RINCON, M. & CHOW, C. W. 2006b. Role of the CCAAT/enhancer-binding protein NFATc2 transcription factor cascade in the induction of secretory phospholipase A2. *J Biol Chem,* 281**,** 11541-52.

YANG, X., LU, X., LOMBES, M., RHA, G. B., CHI, Y. I., GUERIN, T. M., SMART, E. J. & LIU, J. 2010. The G(0)/G(1) switch gene 2 regulates adipose lipolysis through association with adipose triglyceride lipase. *Cell Metab,* 11**,** 194-205.

YANG, X., ZHANG, X., HECKMANN, B. L., LU, X. & LIU, J. 2011. Relative contribution of adipose triglyceride lipase and hormone-sensitive lipase to tumor necrosis factor-alpha (TNF-alpha)-induced lipolysis in adipocytes. *J Biol Chem,* 286**,** 40477-85.

YAO, Y. G. & DUH, E. J. 2004. VEGF selectively induces Down syndrome critical region 1 gene expression in endothelial cells: a mechanism for feedback regulation of angiogenesis? *Biochem Biophys Res Commun,* 321**,** 648-56.

YE, J., COULOURIS, G., ZARETSKAYA, I., CUTCUTACHE, I., ROZEN, S. & MADDEN, T. L. 2012. Primer-BLAST: a tool to design target-specific primers for polymerase chain reaction. *BMC Bioinformatics,* 13**,** 134.

YOULE, R. J. & NARENDRA, D. P. 2011. Mechanisms of mitophagy. *Nat Rev Mol Cell Biol,* 12**,** 9-14.

YOULE, R. J. & VAN DER BLIEK, A. M. 2012. Mitochondrial fission, fusion, and stress. *Science,* 337**,** 1062-5.

YOUNG, R. L., LUMSDEN, A. L., MARTIN, A. M., SCHOBER, G., PEZOS, N., THAZHATH, S. S., ISAACS, N. J., CVIJANOVIC, N., SUN, E. W. L., WU, T., RAYNER, C. K., NGUYEN, N. Q., FONTGALLAND, D., RABBITT, P., HOLLINGTON, P., SPOSATO, L., DUE, S. L., WATTCHOW, D. A., LIOU, A. P., JACKSON, V. M. & KEATING, D. J. 2018. Augmented capacity for peripheral serotonin release in human obesity. *Int J Obes (Lond),* 42**,** 1880-1889.

YOUNGREN, J. F. 2007. Regulation of insulin receptor function. *Cell Mol Life Sci,* 64**,** 873-91.

YU, S. P., CANZONIERO, L. M. & CHOI, D. W. 2001. Ion homeostasis and apoptosis. *Curr Opin Cell Biol,* 13**,** 405-11.

ZANDBERGEN, F., MANDARD, S., ESCHER, P., TAN, N. S., PATSOURIS, D., JATKOE, T., ROJAS-CARO, S., MADORE, S., WAHLI, W., TAFURI, S., MULLER, M. & KERSTEN, S. 2005. The G0/G1 switch gene 2 is a novel PPAR target gene. *Biochem J,* 392**,** 313-24.

ZEBISCH, K., VOIGT, V., WABITSCH, M. & BRANDSCH, M. 2012. Protocol for effective differentiation of 3T3-L1 cells to adipocytes. *Anal Biochem,* 425**,** 88-90.

ZECHNER, R., ZIMMERMANN, R., EICHMANN, T. O., KOHLWEIN, S. D., HAEMMERLE, G., LASS, A. & MADEO, F. 2012. FAT SIGNALS--lipases and lipolysis in lipid metabolism and signaling. *Cell Metab,* 15**,** 279-91.

ZHANG, Y., PROENCA, R., MAFFEI, M., BARONE, M., LEOPOLD, L. & FRIEDMAN, J. M. 1994. Positional cloning of the mouse obese gene and its human homologue. *Nature,* 372**,** 425-32.

ZHOU, L., WANG, X., YANG, Y., WU, L., LI, F., ZHANG, R., YUAN, G., WANG, N., CHEN, M. & NING, G. 2011. Berberine attenuates cAMP-induced lipolysis via reducing the inhibition of phosphodiesterase in 3T3-L1 adipocytes. *Biochim Biophys Acta,* 1812**,** 527-35.

ZIERLER, K. A., JAEGER, D., POLLAK, N. M., EDER, S., RECHBERGER, G. N., RADNER, F. P., WOELKART, G., KOLB, D., SCHMIDT, A., KUMARI, M., PREISS-LANDL, K., PIESKE, B., MAYER, B., ZIMMERMANN, R., LASS, A., ZECHNER, R. & HAEMMERLE, G. 2013. Functional cardiac lipolysis in mice critically depends on comparative gene identification-58. *J Biol Chem,* 288**,** 9892-904.

ZIMMERMANN, R., STRAUSS, J. G., HAEMMERLE, G., SCHOISWOHL, G., BIRNER-GRUENBERGER, R., RIEDERER, M., LASS, A., NEUBERGER, G., EISENHABER, F., HERMETTER, A. & ZECHNER, R. 2004. Fat mobilization in adipose tissue is promoted by adipose triglyceride lipase. *Science,* 306**,** 1383-6.

ZIPPIN, J. H., CHEN, Y., NAHIRNEY, P., KAMENETSKY, M., WUTTKE, M. S., FISCHMAN, D. A., LEVIN, L. R. & BUCK, J. 2003. Compartmentalization of bicarbonate-sensitive adenylyl cyclase in distinct signaling microdomains. *FASEB J,* 17**,** 82-4.

ZIPPIN, J. H., CHEN, Y., STRAUB, S. G., HESS, K. C., DIAZ, A., LEE, D., TSO, P., HOLZ, G. G., SHARP, G. W., LEVIN, L. R. & BUCK, J. 2013. CO2/HCO3(-)- and calcium-regulated soluble adenylyl cyclase as a physiological ATP sensor. *J Biol Chem,* 288**,** 33283-91.

APPENDICES

Appendix A. Validating IRCA drug results

The results in section 3.3 were reconfirmed with drugs that were made by me compared to preliminary results (Figure 1.28).

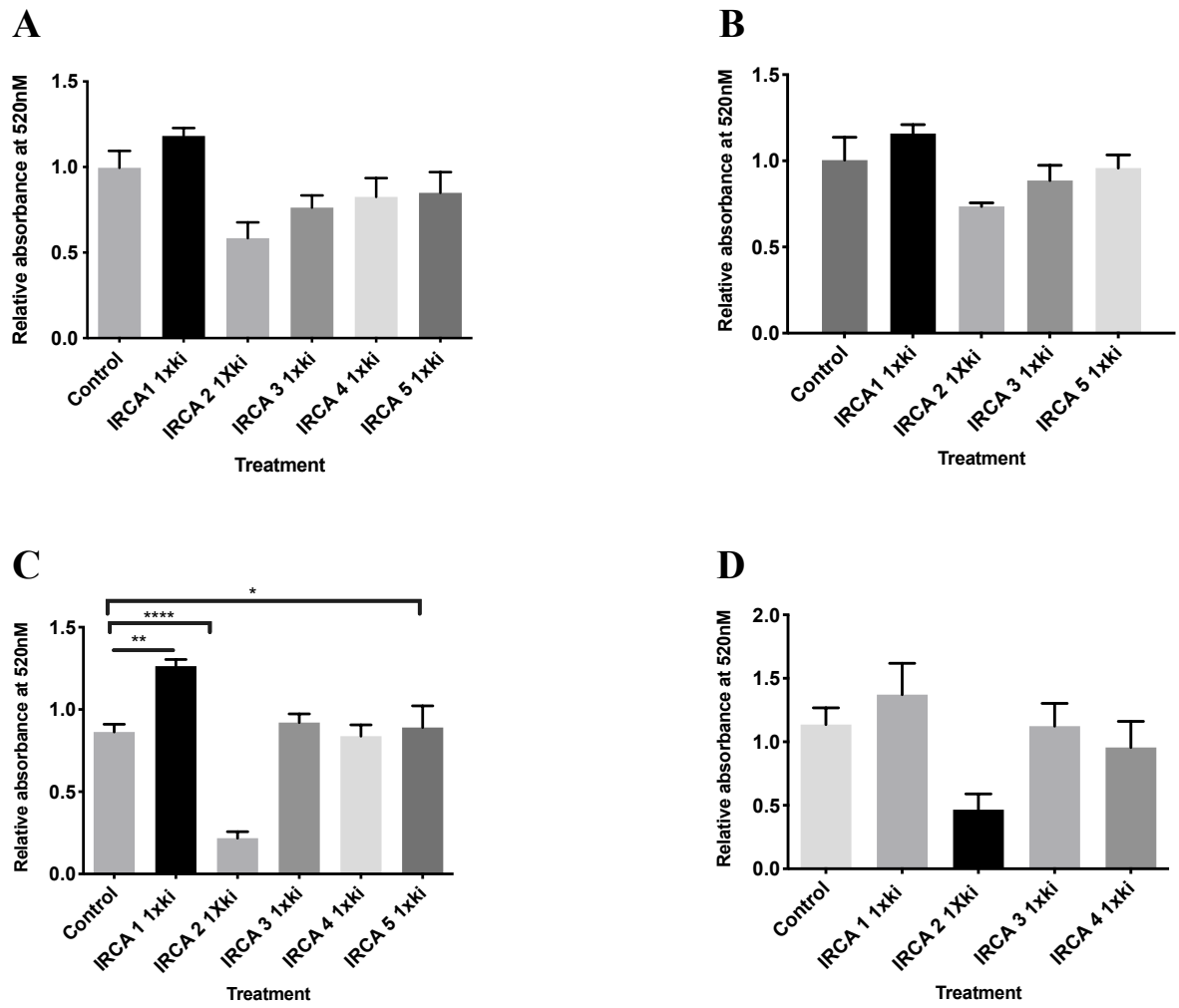

Appendix A-1. Comparison of drugs used in main experiments and drugs used in preliminary experiments (n=4). **(A)** My MTT assay with 1xki drugs compared to **(B)** drugs used for preliminary results 1xki drugs. **(C)** My Oil Red-O assay with 1xki drugs compared to **(D)** 1xki drugs used for preliminary results. Asterisks show where one-way ANOVA with Dunnett *post-hoc* test indicate difference (One-way ANOVA with Dunnett *post-hoc* analysis, *p<0.05, **** p<0.0001).

Appendix B. Sample melt curves and quantitation curves for qPCR gene targets

Appendix B.1. Markers of proliferation and apoptosis genes used in Chapter 4

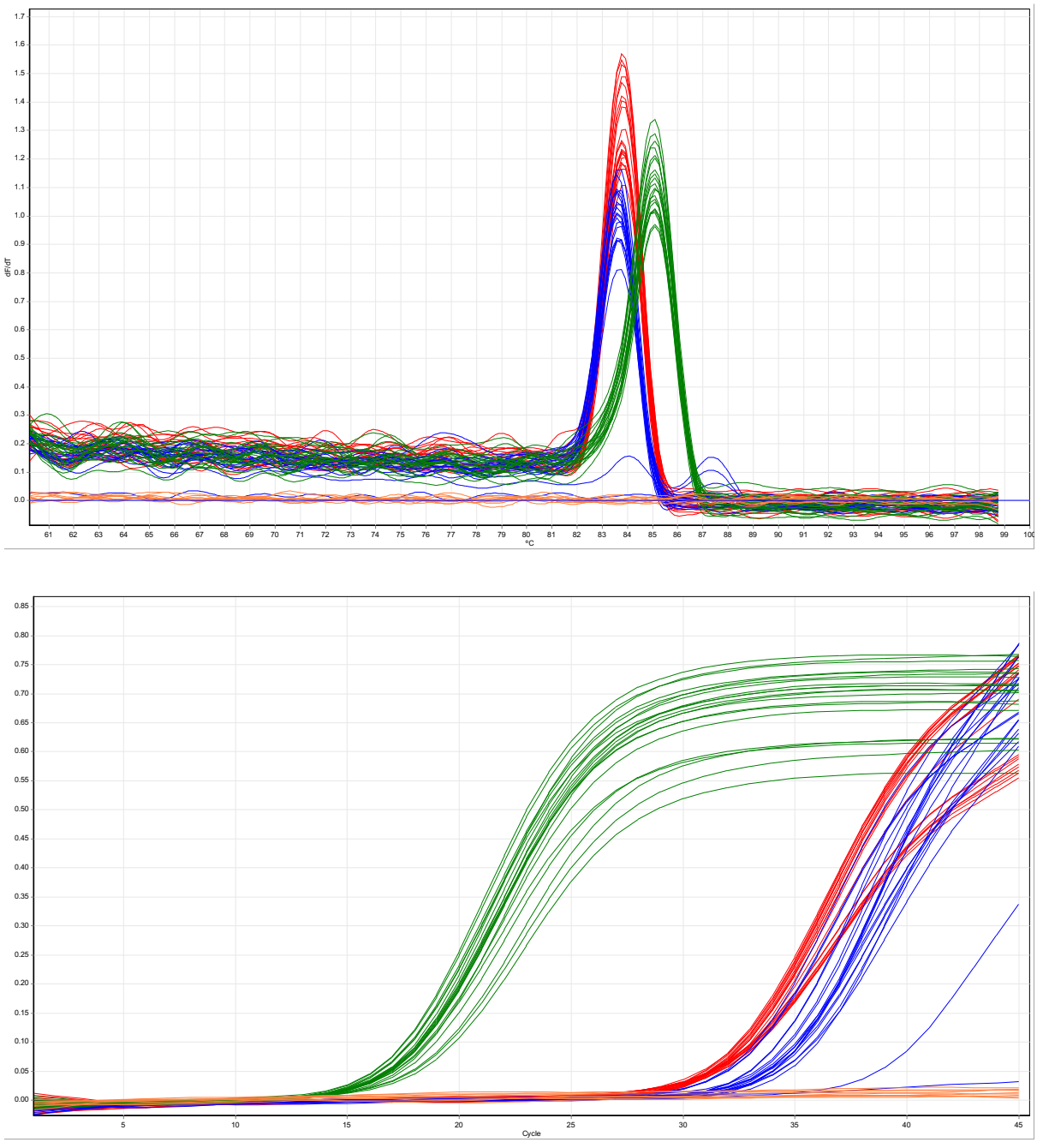

Appendix B-1. (A) Melt curve and (B) quantitation curve showing orange: no template control, green: β-actin housekeeper gene, red: *Bim* and blue: *Ccnd1* of IRCA drugs at the minimum effective concentration on β-TC6 cell line.

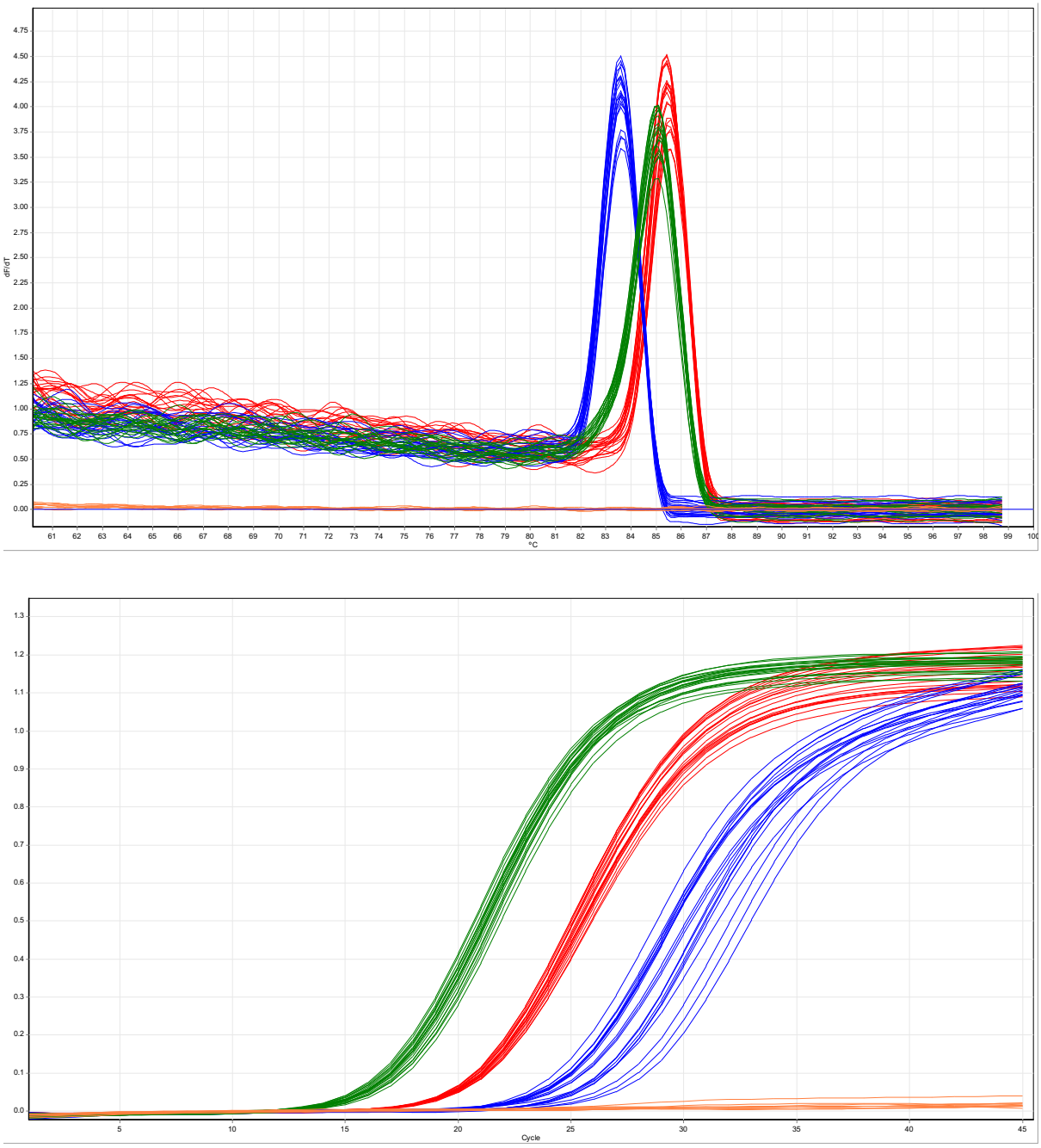

Appendix B-2. (A) Melt curve and (B) quantitation curve showing orange: no template control, green: β-*actin* housekeeper gene, red: *Bax* and blue: *Ccnd2*(2) of IRCA drugs at the minimum effective concentration on β-TC6 cell line.

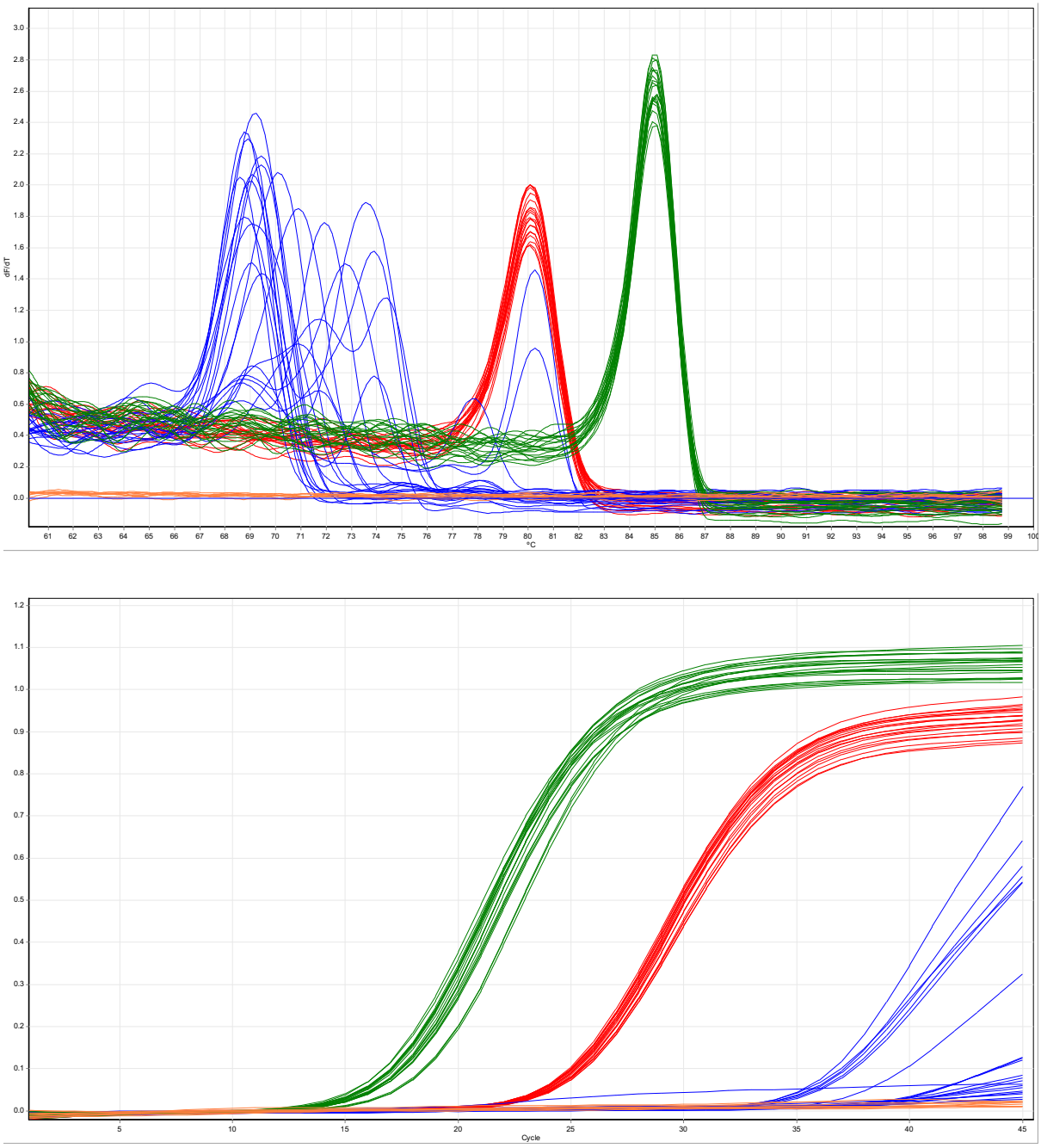

Appendix B-3. (A) Melt curve and (B) quantitation curve showing orange: no template control, green: β-actin housekeeper gene, red: *Puma* and blue: *Ccnd2*(1) of IRCA drugs at the minimum effective concentration on β-TC6 cell line.

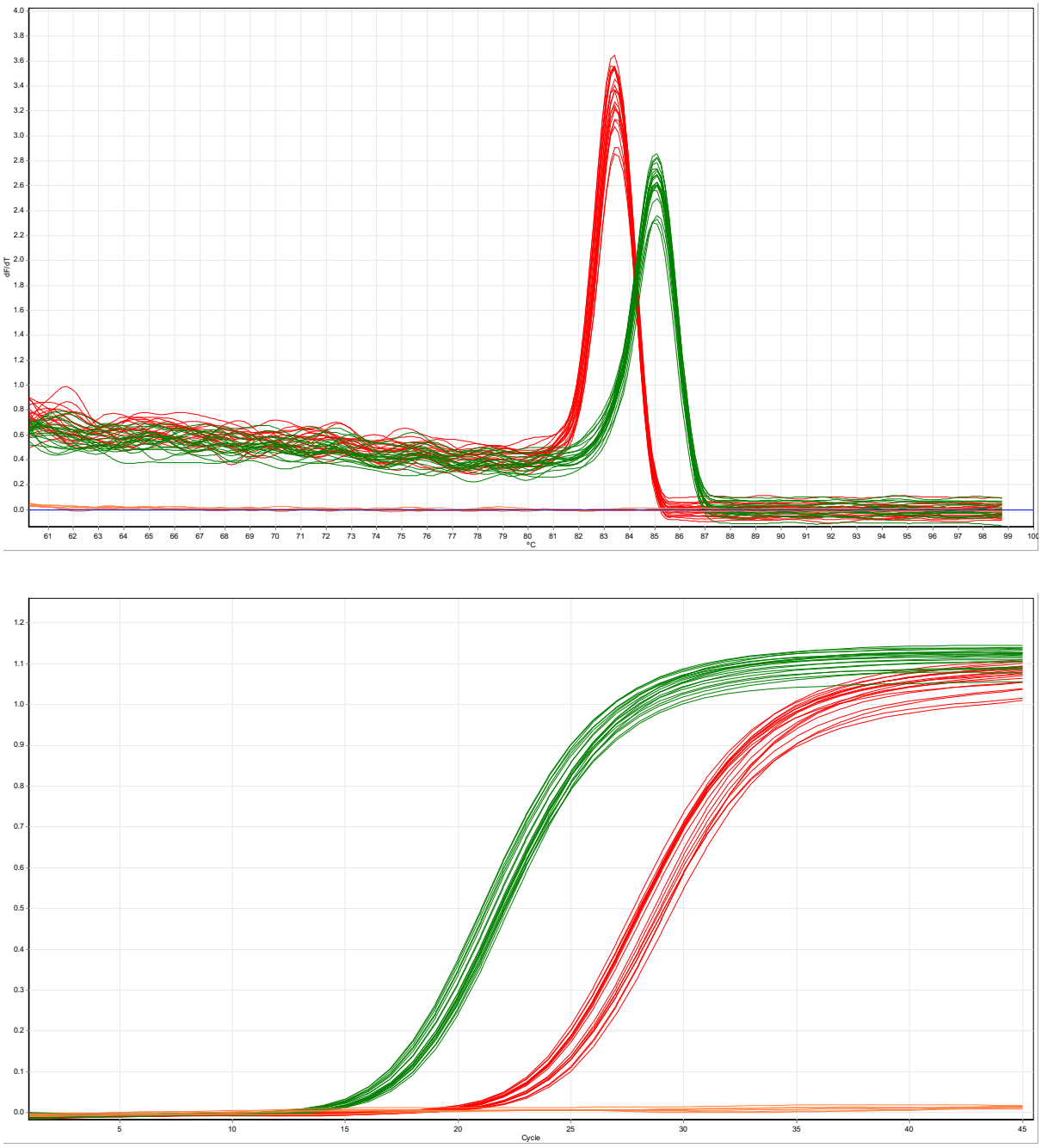

Appendix B-4. (A) Melt curve and (B) quantitation curve showing orange: no template control, green: β-actin housekeeper gene, red: *Caspase3* of IRCA drugs at the minimum effective concentration on β-TC6 cell line.

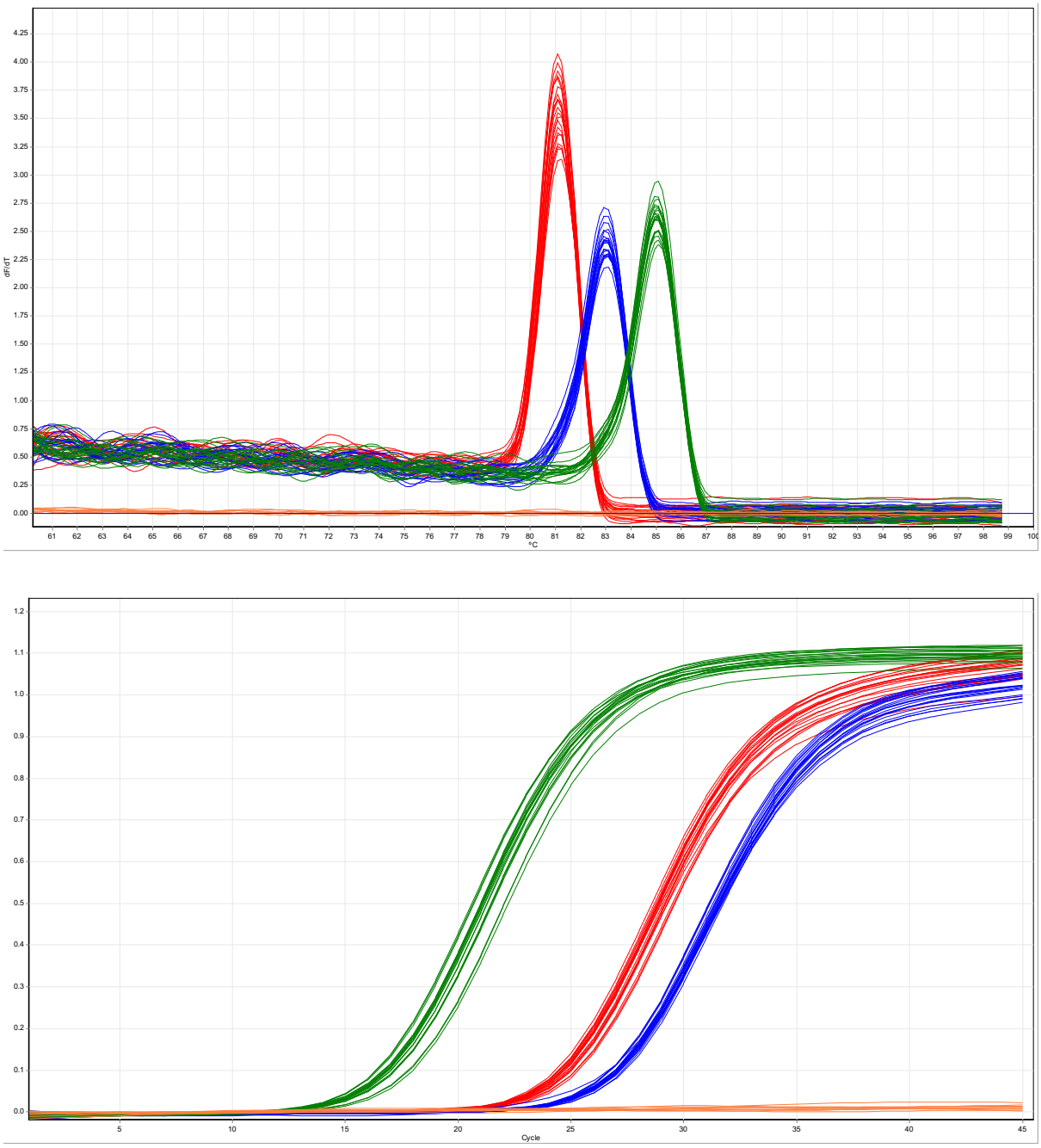

Appendix B-5. (A) Melt curve and (B) quantitation curve showing orange: no template control, green: β-actin housekeeper gene, red: *Caspase 8*, blue: *Caspase 9* of IRCA drugs at the minimum effective concentration on β-TC6 cell line.

Appendix B.2. Gene targets for lipolysis, lipogenesis and adipogenesis genes

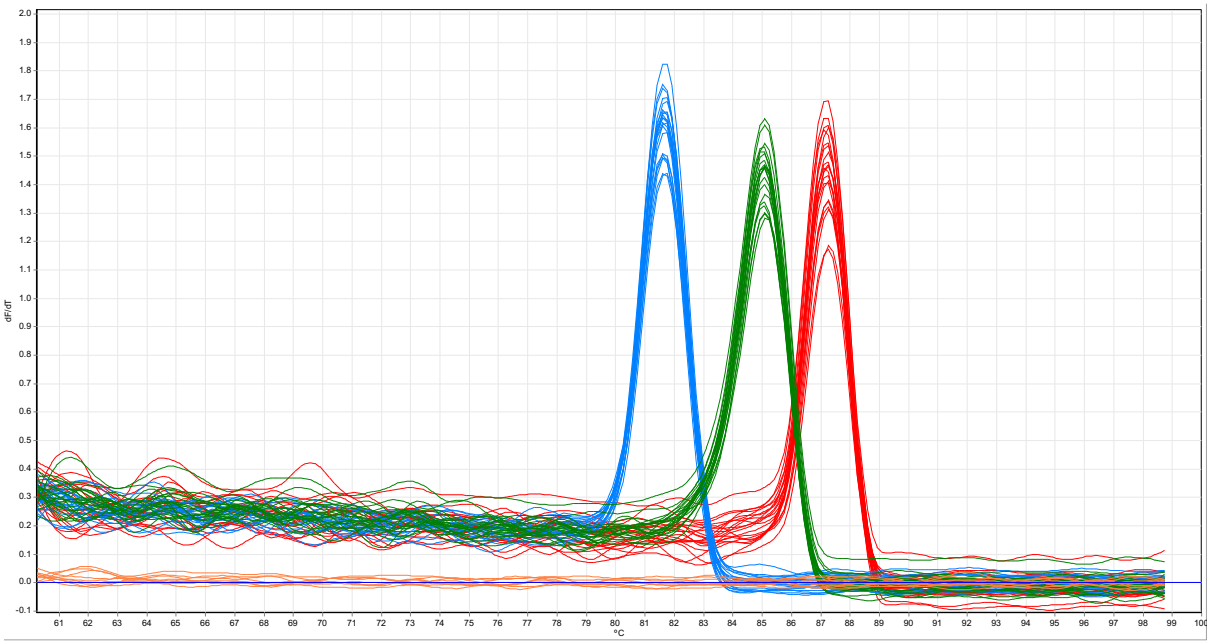

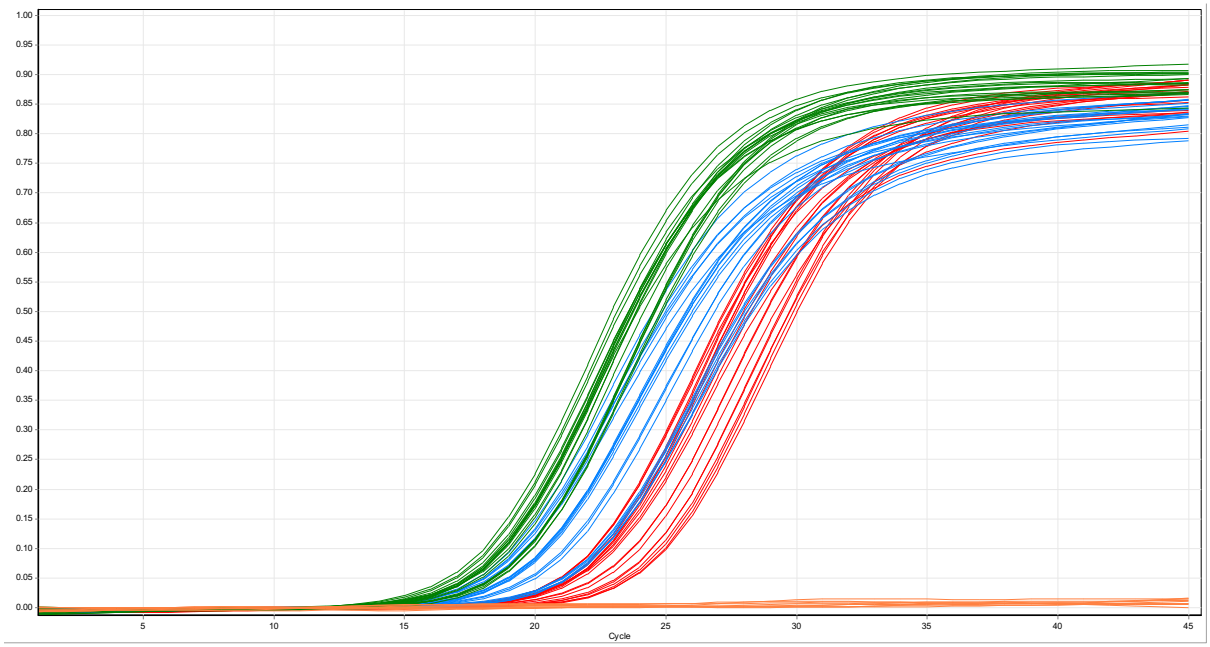

Appendix B-6. (A) Melt curve and (B) quantitation curve showing orange: no template control, green: β-actin housekeeper gene, red: *Plin1*, blue: *Atgl* of eWAT of RCAN1 WT and *Rcan1*$^{-/-}$ on a HFD

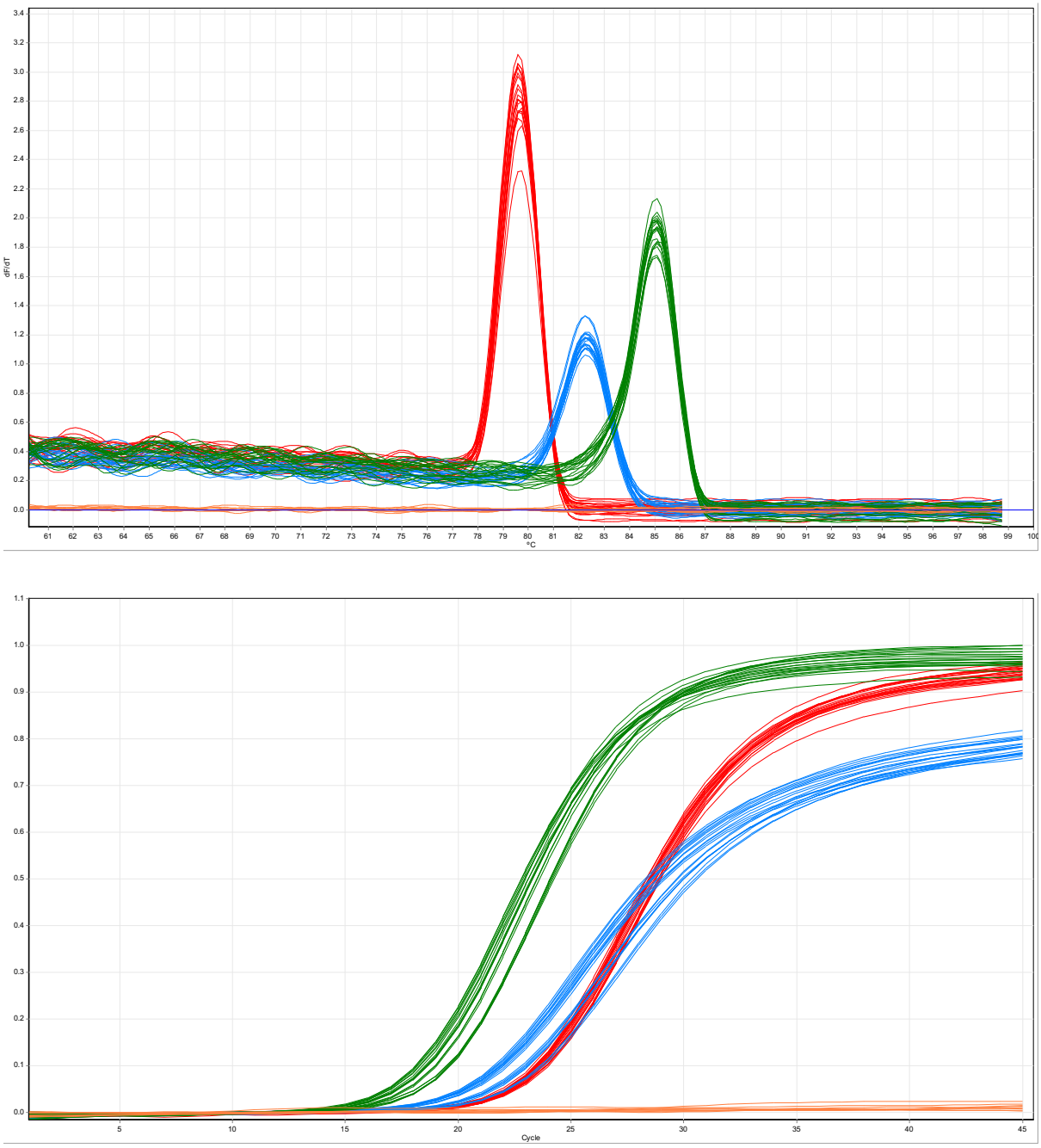

Appendix B-7. (A) Melt curve and (B) quantitation curve showing orange: no template control, green: β-actin housekeeper gene, red: *Cgi-58*, blue: *G0s2* of eWAT of RCAN1 WT and *Rcan1*$^{-/-}$ on a HFD

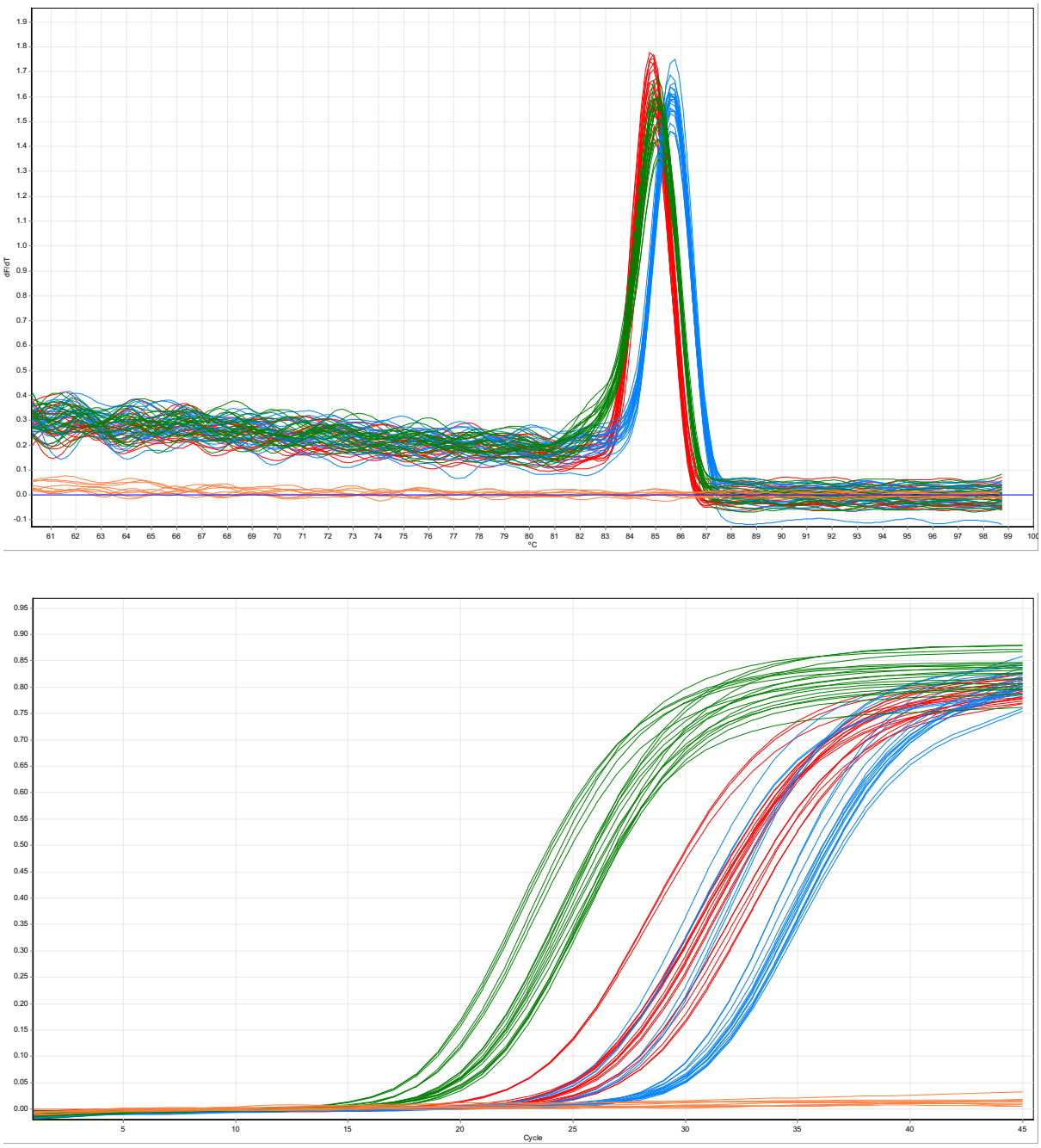

Appendix B-8. (A) Melt curve and (B) quantitation curve showing orange: no template control, green: β-actin housekeeper gene, red: *Hsl*, blue: *Srebp1*-total of eWAT of RCAN1 WT and *Rcan1*$^{-/-}$ on a LFD

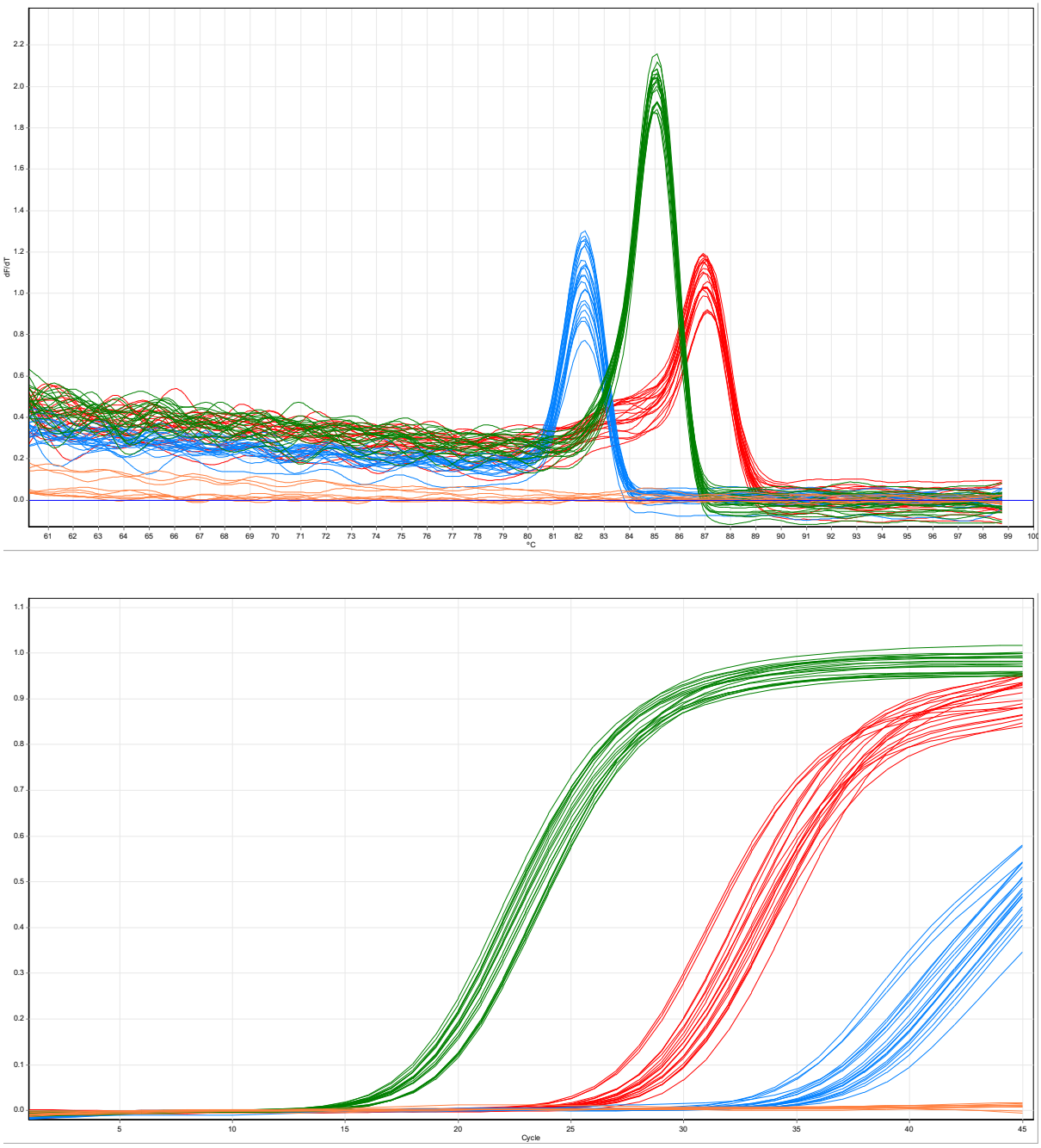

Appendix B-9. (A) Melt curve and (B) quantitation curve showing orange: no template control, green: β-actin housekeeper gene, red: *Srebp1c*, blue: *Srebp1a* of eWAT of RCAN1 WT and *Rcan1*$^{-/-}$ on a HFD

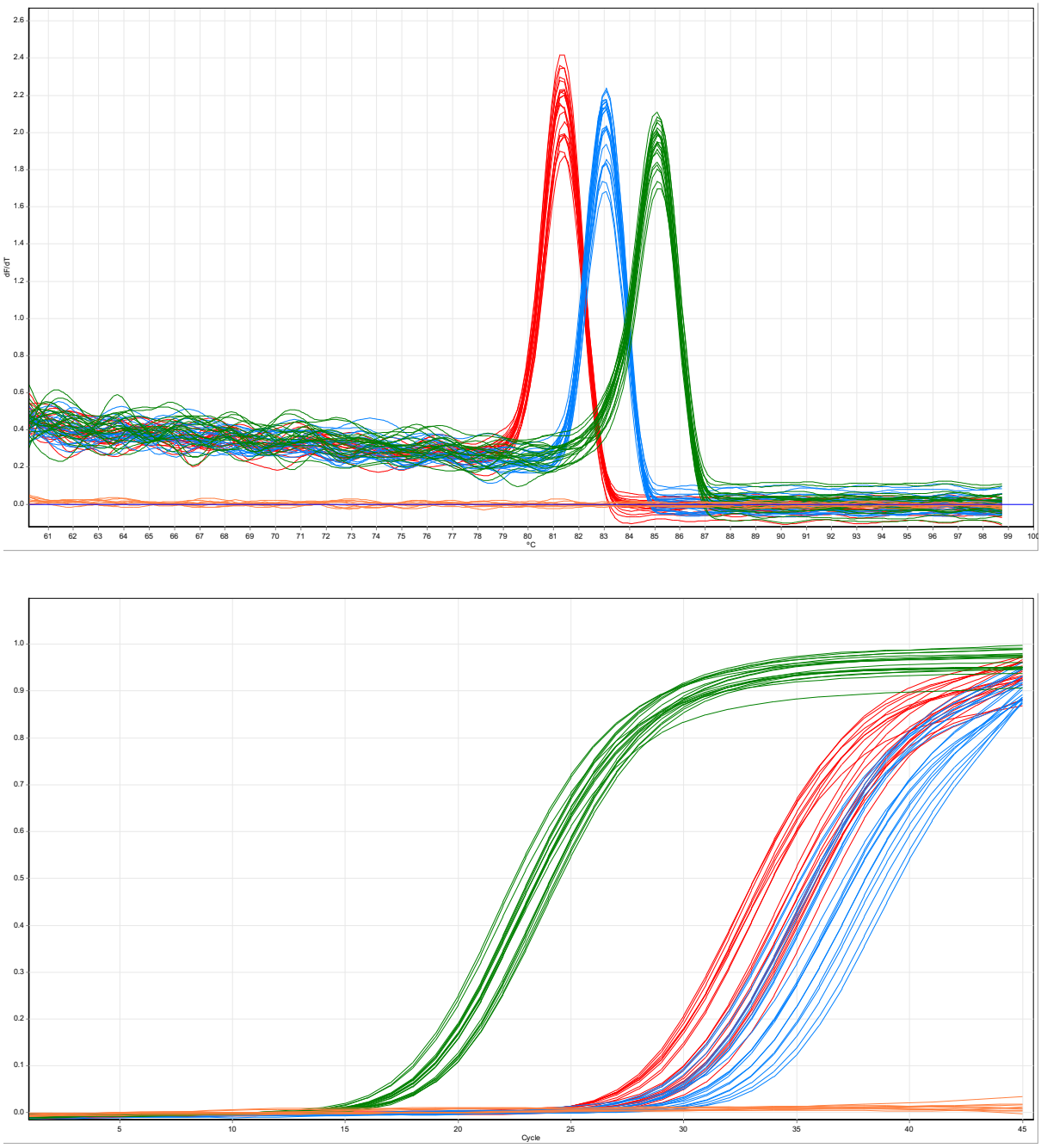

Appendix B-10. (A) Melt curve and (B) quantitation curve showing orange: no template control, green: β-actin housekeeper gene, red: *Chrebp*-total, blue: *Chrebp-α* of eWAT of RCAN1 WT and *Rcan1*$^{-/-}$ on a HFD

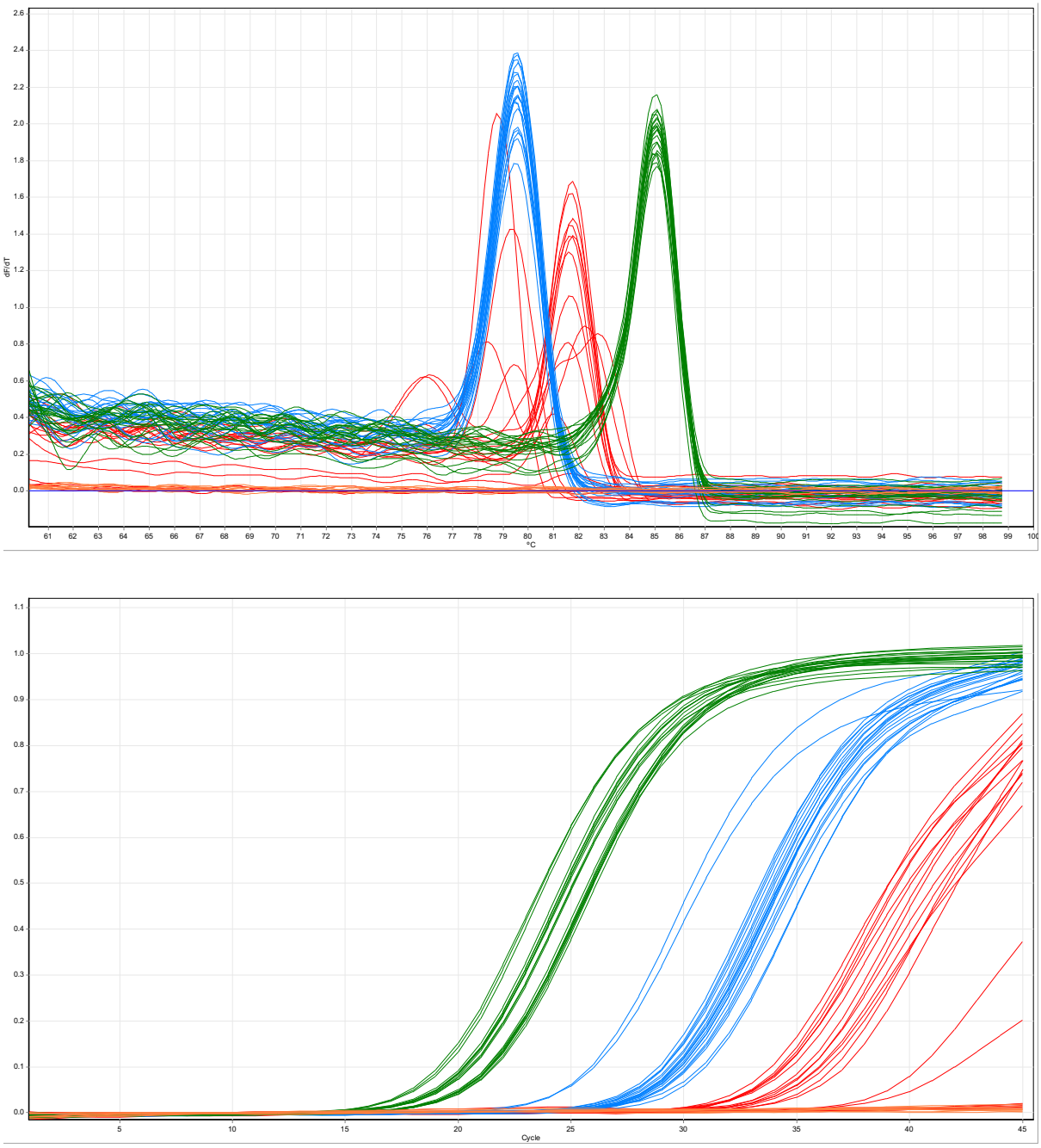

Appendix B-11. (A) Melt curve and (B) quantitation curve showing orange: no template control, green: β-actin housekeeper gene, red: *Chrebp-β*, blue: *Acc1* of eWAT of RCAN1 WT and *Rcan1*$^{-/-}$ on a HFD

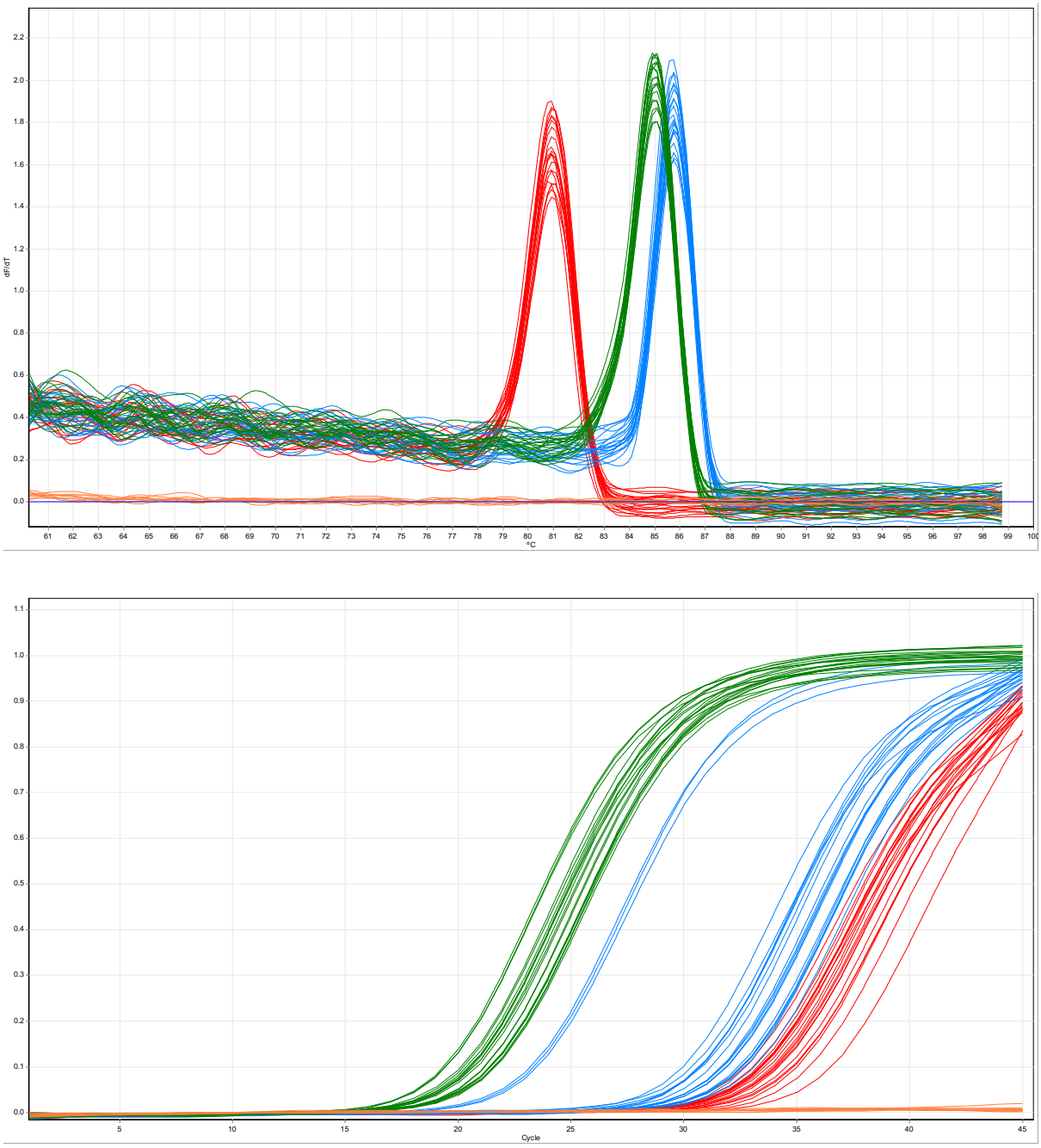

Appendix B-12. (A) Melt curve and (B) quantitation curve showing orange: no template control, green: β-actin housekeeper gene, red: *Acc2*, blue: *Acl* of eWAT of RCAN1 WT and *Rcan1*$^{-/-}$ on a LFD

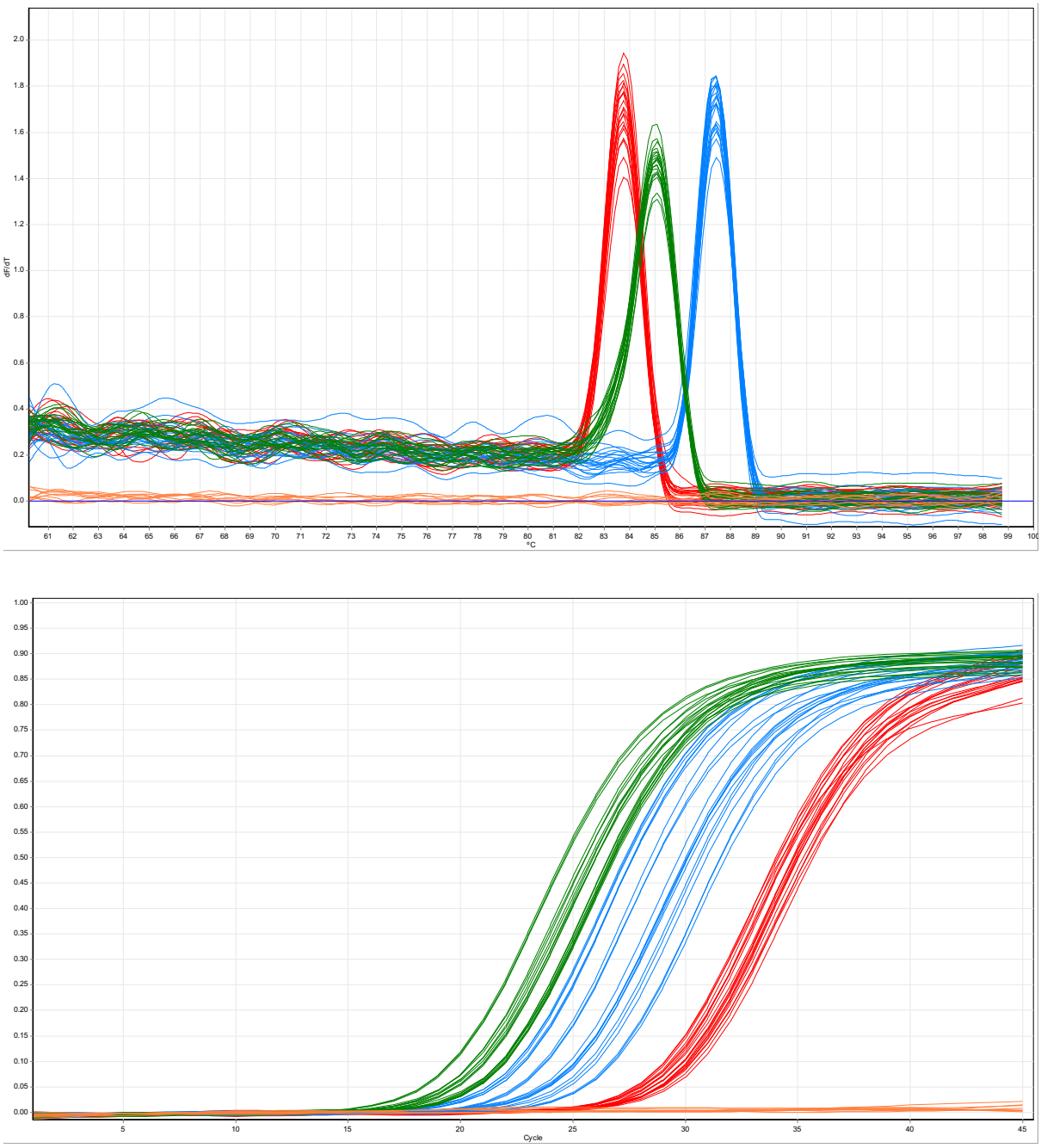

Appendix B-13. (A) Melt curve and (B) quantitation curve showing orange: no template control, green: β-actin housekeeper gene, red: *Fas*, blue: *Cebp-α* of eWAT of RCAN1 WT and *Rcan1*$^{-/-}$ on a LFD

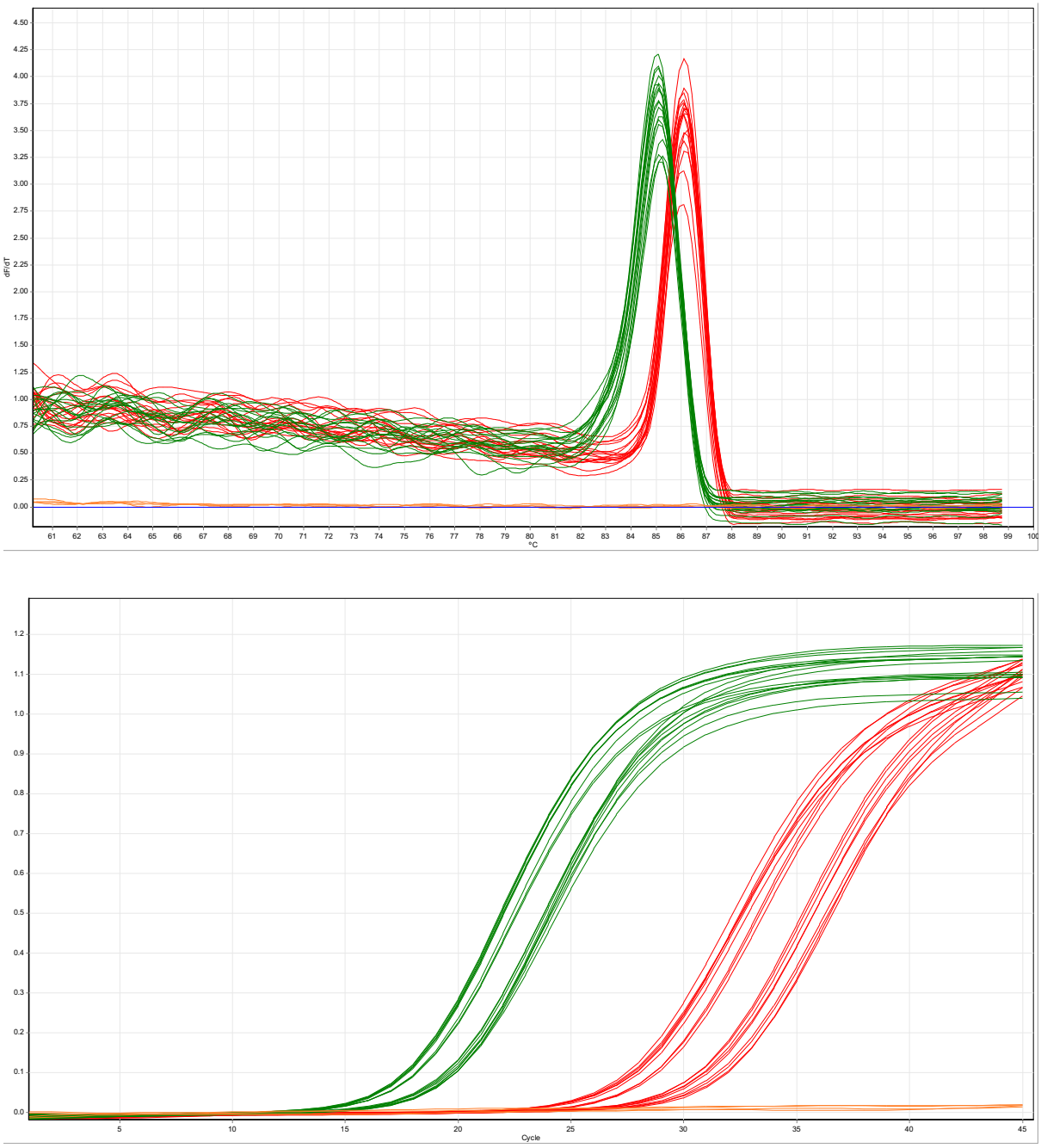

Appendix B-14. (A) Melt curve and (B) quantitation curve showing orange: no template control, green: β-actin housekeeper gene, red: *leptin* of eWAT of RCAN1 WT and *Rcan1*$^{-/-}$ on a HFD

Appendix B.3. Adipocyte expression of *Rcan1.1* and *Rcan1.4* after incubation with various factors

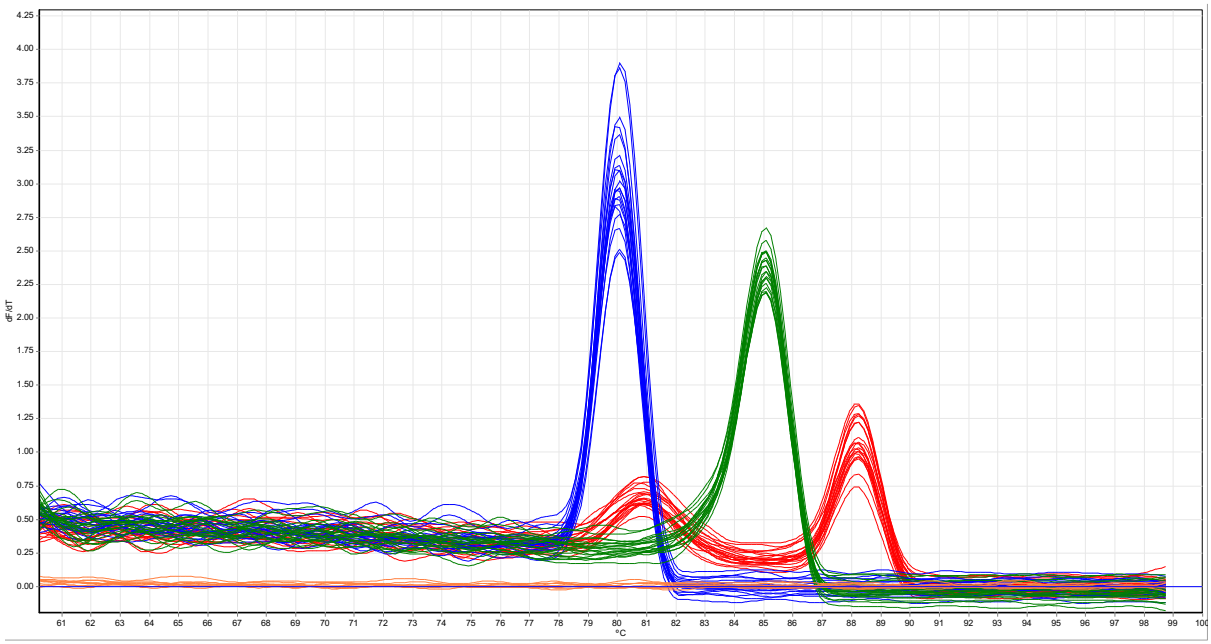

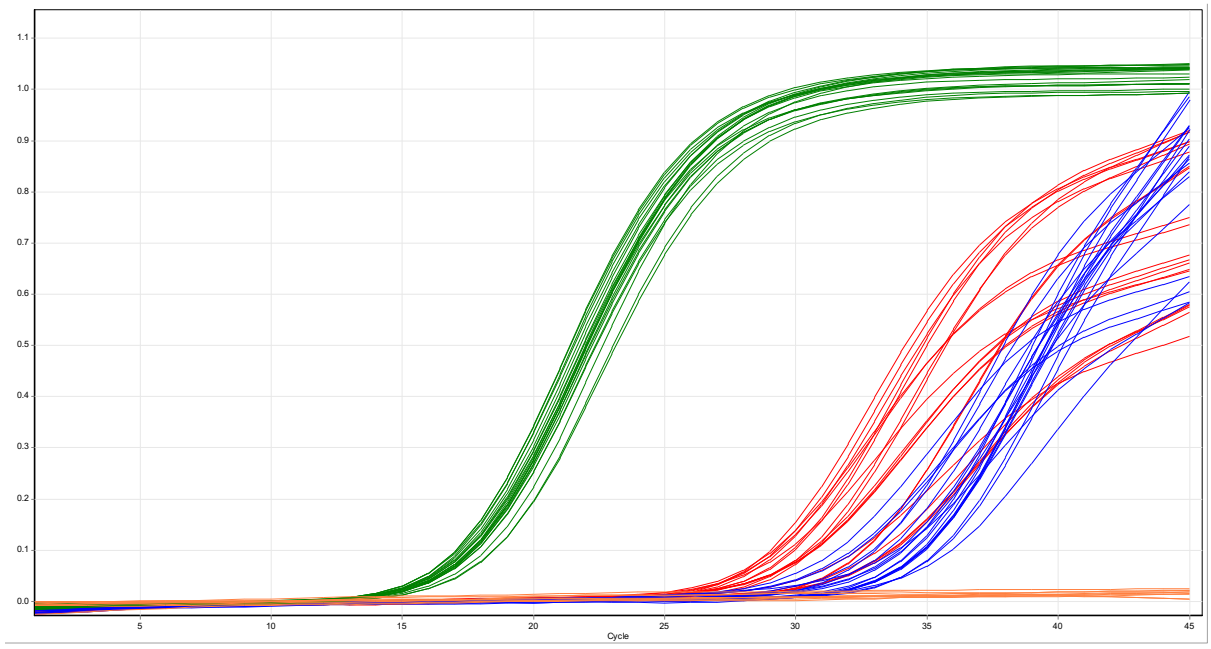

Appendix B-15. (A) Melt curve and (B) quantitation curve showing orange: no template control, green: β-actin housekeeper gene, red: *Rcan1.1*, Blue: *Rcan1.4* on 3T3-L1 developed adipocytes.

Appendix C. Sample image of gel

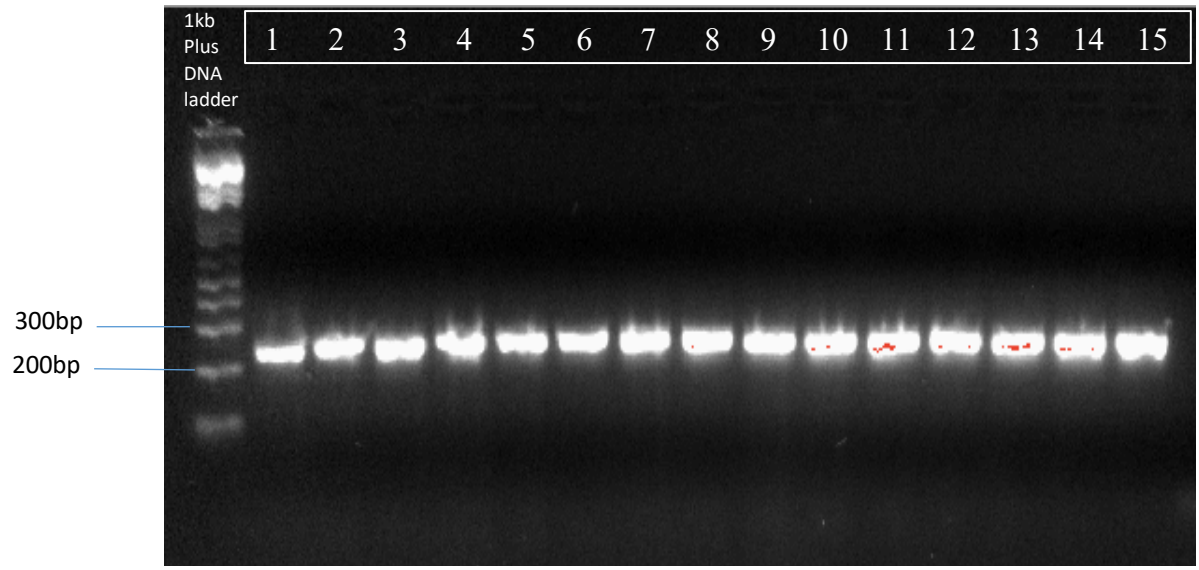

Appendix C-1. Sample of gel electrophoresis. On the left shows the 1Kb Plus DNA ladder in 3% agarose gel (Invitrogen, Australia). A volume of 5µl of the prepared ladder (200ng/ul) was mixed with 2µl of the 6x loading dye (Sigma). After loading samples, the 3% agarose gel was run at 80V for 45 minutes. The gel was imaged using Image Lab™ Software (Bio-Rad) under ultra-violet light utilising the Gel Doc EZ imager (Bio-Rad) at the exposure time of 0.5 seconds. Lane 1 to 15 contain the products of the housekeeper β-actin when RT-PCR was conducted on β-TC6 cell line that had no treatment (237 bp PCR product).